AD_____

Award Number: W81XWH-06-1-0363

TITLE: The Role of Osteoblast-Derived Cytokines in Bone Metastatic Breast Cancer

PRINCIPAL INVESTIGATOR: Karen M. Bussard

CONTRACTING ORGANIZATION: The Pennsylvania State University
University Park, PA 16802

REPORT DATE: January 2009

TYPE OF REPORT: Annual Summary

PREPARED FOR: U.S. Army Medical Research and Materiel Command
Fort Detrick, Maryland 21702-5012

REPORT DOCUMENTATION PAGE

Form Approved
OMB No. 0704-0188

1. REPORT DATE	2. REPORT TYPE	3. DATES COVERED
1 Jan 2009	Annual Summary	1 Mar 2006 – 31 Dec 2008

4. TITLE AND SUBTITLE

The Role of Osteoblast-Derived Cytokines in Bone Metastatic Breast Cancer

5a. CONTRACT NUMBER

5b. GRANT NUMBER
W81XWH-06-1-0363

5c. PROGRAM ELEMENT NUMBER

6. AUTHOR(S)

Karen M. Bussard

E-Mail: kmb337@psu.edu

5d. PROJECT NUMBER

5e. TASK NUMBER

5f. WORK UNIT NUMBER

7. PERFORMING ORGANIZATION NAME(S) AND ADDRESS(ES)

The Pennsylvania State University
University Park, PA 16802

8. PERFORMING ORGANIZATION REPORT NUMBER

9. SPONSORING / MONITORING AGENCY NAME(S) AND ADDRESS(ES)
U.S. Army Medical Research and Materiel Command
Fort Detrick, Maryland 21702-5012

10. SPONSOR/MONITOR'S ACRONYM(S)

11. SPONSOR/MONITOR'S REPORT NUMBER(S)

12. DISTRIBUTION / AVAILABILITY STATEMENT
Approved for Public Release; Distribution Unlimited

13. SUPPLEMENTARY NOTES

14. ABSTRACT
Breast cancer (BC) metastasizes to bone. While the mechanism for directed metastasis is unknown, the bone microenvironment likely provides a fertile soil for metastatic BC cells. Our purpose is to determine how OB-derived cytokines influence BC metastases to bone. Goals include investigating the production of OB-derived cytokines in response to BC cells or their conditioned medium (CM), the production of bone-derived cytokines in response to BC cells in vivo, the presence of functional cytokine receptors on OBs and BC cells, and the chemoattractant effect of OB-derived cytokines on BC metastasis. OB and BC cells expressed IL-6, KC/GRO-α, MIP-2/IL-8, and VEGF, but only OBs produced MCP-1. OB-derived cytokine production increased with direct co-culture of BC cells or CM treatment. OB CM was a chemoattractant for BC cells. BC cells cultured with OBs enhanced TRAP positive multi-nucleated OC formation in vitro. Concentrations of IL-6, VEGF, and MCP-1 increased in cancer-bearing mice, but MIP-2 and KC were expressed in negligible amounts. MCP-1 and VEGF were localized in the trabecular bone matrix, while IL-6 was expressed in the bone marrow. MCP-1 and VEGF were not detected adjacent to BC cells. Human VEGF expression increased with increasing tumor size. Megakaryocyte numbers in the bone marrow cavity were increased in cancer-bearing mice. These data suggest that OBs are an important source of cytokines in bone metastatic breast cancer. These findings implicate the importance of the bone microenvironment and cancer cell modulation in facilitating metastatic tumor cell colonization and survival.

15. SUBJECT TERMS
osteoblast, metastasis, MDA-MB-231, IL-6, MCP-1, KC, VEGF, MIP-2

16. SECURITY CLASSIFICATION OF:			17. LIMITATION OF ABSTRACT	18. NUMBER OF PAGES	19a. NAME OF RESPONSIBLE PERSON
a. REPORT	b. ABSTRACT	c. THIS PAGE			USAMRMC
U	U	U	UU	208	19b. TELEPHONE NUMBER *(include area code)*

Table of Contents

Part 1: INTRODUCTION

Breast cancer preferentially metastasizes to the ends of long bones in humans [1]. The mechanism for preferential metastasis is unknown, but it is likely that bone provides a hospitable environment for breast cancer cell colonization and survival [2].

Bone resorbing osteoclasts and bone depositing osteoblasts remodel bone with no net bone gain or bone loss [3]. Bone metastatic breast cancer cells disrupt bone remodeling to favor of bone resorption. Osteoclasts are constitutively activated, resulting in osteolytic lesions that cause bone pain and hypercalcemia [4]. Osteoblasts cease depositing bone and undergo apoptosis [5]. Current therapies utilize bisphosphonates to block osteoclast function and slow osteolytic lesion progression [6]. Lesions already present, however, do not heal [7]. Research has focused on breast cancer cell-derived cytokine production as key to understanding preferential bone metastasis [8]. While they may have a supporting role, we have evidence that bone metastatic breast cancer cells direct *osteoblasts* to produce inflammatory cytokines that may indirectly be chemoattractants, growth, or maintenance factors for the cancer cells.

It has been reported that in addition to exhibiting an inability to mineralize bone martix and the suppression of bone matrix proteins [5, 9, 10], osteoblasts exposed to metastatic breast cancer cells or their conditioned media switch into an inflammatory mode and produce cytokines that can attract not only leukocytes, but also osteoclast precursors [11]. Expanding on the work of Kinder, et al., we sought to identify additional key factors that were unique to an osteoblast-derived inflammatory response to bone metastatic breast cancer cells or their conditioned medium [11]. **We hypothesized that osteoblast-derived inflammatory cytokines, specifically IL-6, MCP-1, KC / GRO-α, MIP-2 / IL-8, and VEGF, increased in the presence of human metastatic breast cancer cells and acted as chemoattractants, growth, and maintenance factors for cancer cells or for osteoclasts. We also hypothesized that the osteoblast-derived cytokine expression would increase the most with treatment of a bone-seeking cancer variant.** Using an *in vitro* culture or xenograft model of human metastatic or non-metastatic breast cancer cell variants, we found that osteoblasts undergo a stress response (irrespective of cancer cell variant), substantially increasing their production of inflammatory cytokines, that not only aid in bone metastatic breast cancer colonization and survival, but also enhance the formation of mature osteoclasts. The aims of this proposal are: 1) To determine how *osteoblast*-derived inflammatory cytokine production by MC3T3-E1 osteoblasts is altered in response to co-culture or conditioned media of bone metastatic MDA-MB-231 breast cancer cell variants. 2) To determine how bone-derived inflammatory cytokine production is altered in response to breast cancer cells *in vivo*. 3) To determine if osteoblasts and breast cancer cells have receptors and can respond to *osteoblast*-derived inflammatory cytokines.

Parts 2-6: BODY

Part 2: MATERIALS AND METHODS

2.1: Cells

2.1.1: Osteoblasts

MC3T3-E1 cells, a murine pre-osteoblast line capable of differentiation and mineralization in culture [12], were a gift from Dr. Norman Karin, Pacific Northwest National Laboratory. MC3T3-E1 cells were maintained in MC3T3-E1 growth medium consisting of alpha Minimum Essential Medium (αMEM) (Mediatech, Manassas, VA), 10% neonatal FBS (Cansera, Roxdale, Ontario), and penicillin 100 U/ml/streptomycin 100 µg/ml (Sigma, St. Louis, MO). The osteoblasts were not used above passage 20. For experiments as indicated, MC3T3-E1 cells were plated at 1 x 10^5 cells / ml in MC3T3-E1 growth medium. Twenty-four hours later, the medium was removed, cells rinsed with phosphate buffered saline (PBS), and medium replaced with a MC3T3-E1 differentiation medium (αMEM, 10% neonatal FBS, penicillin 100 U/ml/streptomycin 100 µg/ml, 50 µg/ml ascorbic acid (Sigma, St. Louis, MO), and 10 mM β-glycerophosphate (Sigma, St. Louis, MO)). According to Lian and Stein, bone cell differentiation is characterized by three principle periods distinguished by markers indicative of each stage: proliferation (1~9 days), extracellular matrix maturation (~12 days), and extracellular matrix mineralization (~25 days) [13]. For experiments as indicated, MC3T3-E1 cells were grown to these three stages: growth (4 days), early differentiation (10 days), or late differentiation (20 days). The stage of osteoblast differentiation was verified by alkaline phosphatase expression (Materials and Methods 2.3, Figure 2.2, Figure 3.4) and Von Kossa expression (Materials and Methods 2.4, Figure 3.3, Figure 3.4). MC3T3-E1 differentiation medium was exchanged every third day. Cells were cultured in a humidified chamber of 5% CO_2 and 95% air at 37˚C and tested negative for *Mycoplasma* spp. infection using a PCR Mycoplasma Detection Set (TaKaRa Bio, Inc., Shiga, Japan).

2.1.2: Breast cancer cell variants

MDA-MB-231W cells are a human metastatic breast cancer line derived from a pleural effusion of an adenocarcinoma [14]. MDA-MB-231BRMS cells are the isologous line in which metastasis was suppressed to bone as well as to other organs by transfection of the BRMS1 gene [15, 16]. MDA-MB-435 cells are a highly metastatic human breast cancer cell line derived from a malignant pleural effusion of an infiltrating ductal carcinoma [14, 17]. While there has been some speculation that MDA-MB-435 cells are derived from melanoma origin [18], Sellappan, et al., showed that MDA-MB-435 cells expressed epithelial markers and secrete milk lipids; two properties of breast cells [19]. Therefore, it is likely that MDA-MB-435 cells are of breast origin. MDA-MB-435BRMS cells are human non-metastatic breast cancer cells that form locally invasive tumors when injected into mammary fat pads but are significantly less metastatic to bone and other organs [15, 16]. MDA-MB-468P cells are a non-metastatic human breast cancer cell line derived from the pleural effusion of a metastatic breast adenocarcinoma [14]. All cells were a gift from Dr. Danny Welch, University of Alabama, Birmingham. MDA-MB-231PY cells are a human metastatic breast cancer cell line derived from a pleural effusion [14] and were grown from the same original isolate as MDA-MB-231W. MDA-MB-

231PY cells were used to make MDA-MB-231BO bone-seeking and MDA-MB-231BR brain-seeking metastatic breast cancer cells by repeated sequential passaging in nude mice, and in culture of metastatic cells obtained from bone and brain metastases, respectively [20]. All three cell lines were a gift from Dr. Toshiyuki Yoneda, University of Texas Health Science Center, San Antonio, Texas. Table 2.1 is a summary of the characteristics of MDA-MB-231 breast cancer cell variants and MDA-MB-468P non-metastatic breast cancer cells.

For intracardiac inoculations, cell lines expressing green fluorescent protein (GFP) were utilized. MDA-MB-231W-GFP and MDA-MB-231BRMS-GFP cells are analogous to MDA-MB-231W and MDA-MB-231BRMS cells, respectively, but have been engineered to express GFP [14]. Both cell lines were a gift from Dr. Danny Welch, University of Alabama, Birmingham. MDA-MB-231PY-GFP and MDA-MB-231BO-GFP cells are the GFP variants of MDA-MB-231PY and MDA-MB-231BO metastatic breast cancer cells, respectively [20]. Both cell lines were a gift from Dr. Patricia Steeg, National Cancer Institute at the National Institutes of Health, Bethesda, Maryland, with explicit approval from the originator of the cell lines, Dr. Toshiyuki Yoneda, University of Texas Health Science Center, San Antonio, Texas. Cells for intracardiac inoculation were maintained in an antibiotic-free environment for at least three passages immediately prior to use and tested negative for *Mycoplasma* spp. infection using a PCR Mycoplasma Detection Set (TaKaRa Bio, Inc., Shiga, Japan). All cells were maintained in a breast cancer growth medium of DMEM (Mediatech, Manassas, VA), 5% neonatal FBS, and 1% penicillin 100 U/ml/streptomycin 100 µg/ml, except for MDA-MB-231PY, MDA-MB-231BO, and MDA-MB-231BR, and their GFP counterparts, which were maintained in 10% neonatal FBS. Cells were cultured in a humidified chamber of 5% CO_2 and 95% air at 37˚C.

2.1.3: Epithelial and Mesenchymal Non-Cancer Cells

hTERT-HME1 human mammary epithelial cells were obtained from normal breast tissue and were immortalized by infection with the retrovirus pBabepuro+hTERT vector [21, 22]. These cells were a gift from Dr. Henry Donahue, The Pennsylvania State University, Hershey, PA. MCF-10A non-tumorigenic human epithelial cells were derived from a fibrocystic nodule of the breast [23]. NIH/3T3 murine fibroblasts are a mesenchymal cell line established from NIH Swiss mouse primary embryo cultures [24]. These cells were a gift from Dr. Danny Welch, University of Alabama, Birmingham. HBL-100 human epithelial cells were derived from an early lactation sample of breast milk with no evidence of breast lesions found in the donor [25]. HC11 clonal murine mammary epithelial cells were derived from immortalized Comma-D1 epithelial cells [26]. Comma-D1 murine epithelial cells were isolated from the mammary gland of midpregnant BALB/c mice [26]. These three cell lines were a gift from Dr. Craig Baumrucker, The Pennsylvania State University, University Park, PA. Primary fibroblasts are human mesenchymal cells isolated from human foreskin (a gift from Dr. Samina Alam, The Pennsylvania State University, Hershey, PA). 3T3-L1 fibroblasts are a clonal murine mesenchymal cell line developed from 3T3 (Swiss albino) that can be made to differentiate in culture to adipocytes in the presence of high serum [27]. The cells were used in the adipose-like state [27]. These cells were a gift from Benjamin Belda, The Pennsylvania State University, University Park, PA. All cells were cultured

in a humidified chamber of 5% CO_2 and 95% air at 37˚C. Table 2.1 is a summary of the characteristics of epithelial and mesenchymal non-cancer cells.

2.1.4: Primary mammary epithelial and fibroblast cell isolation

Primary mammary epithelial and primary mammary fibroblasts were obtained from the mammary tissue of C57BL/6 mice following an established protocol [28, 29]. Briefly, all plastics utilized were pre-coated with 5% bovine serum albumin (Sigma) in PBS. Mammary glands from lactating mice were removed, homogenized, and incubated in a sterile, pre-warmed collagenase solution (23.5 ml DMEM, 23.5 ml Ham's F12 [Mediatech], 500 µl Fungizone® [1:100; Gibco, Carlsbad, CA], 0.1 g Collagenase 1A [0.2 g / 100 ml; Sigma], and 2 ml Gentamycin [5 µg/ml; Sigma]) for 1 hour at 37˚C with shaking (100 rpm). The homogenate was centrifuged at 680 xg for 30 seconds, top and bottom layers were collected and resuspended seperately in DMEM/F12. Both cellular fractions were centrifuged for 10 minutes at 680 xg, supernatants removed, and pellets combined in DMEM/F12. DNase (40 µl at 2 U/ml; Qiagen, Valencia, CA) was added; pellets manually shaken for 5 minutes; DMEM/F12 (6 ml) added; and the mixture centrifuged at 680 xg rpm for 10 minutes. The supernatant was discarded, and the pellet resuspended in DMEM/F12 (10 ml), and centrifuged briefly at 300 xg. The supernatant was removed and placed in a culture dish to obtain primary mammary fibroblasts. The pellet was resuspended in DMEM/F12 (10 ml), followed by a short centrifugation (to 680 xg). The supernatant was discard, and the pellet resuspended. This was repeated 10 times to obtain a primary mammary epithelial cell pellet. After each resuspension, the pellet composition was monitored by examining 10 µl of the resuspended pellet via light microscopy. Single cells of the suspension were identified by morphology as fibroblasts and groups of organiod-like cells in the suspension were identified by morphology as primary mammary epithelial cells [28, 29]. The cells were cultured in a growth medium consisting of 1000x insulin transferrin selenium (100 µl; Gibco), epidermal growth factor (5 µl of 100 µg/ml; Gibco), 5% neonatal FBS, Gentamycin (100 µl of 50 mg/ml), 1% penicillin 100 U/ml/streptomycin 100 µg/ml, 1% Fungizone®, and DMEM/F12 in a total volume of 100 mls. Cells were cultured in a humidified chamber of 5% CO_2 and 95% air at 37˚C.

2.1.5: Osteoclast Precursors

RAW264.7 murine osteoclast precursors were a gift from Dr. Pamela Hankey, The Pennsylvania State University [30]. The cells were maintained in a growth medium of DMEM and 5% FBS (Sigma).

Bone marrow monocytes were obtained from the femoral and tibial bone marrow of C57BL/6 mice. Briefly, femurs and tibiae from euthanized mice were harvested and cleaned free of soft tissue. Bone ends were removed, and the bone marrow in the bone shaft flushed using αMEM. A total of 6 femurs and 6 tibiae were used. Bone marrow was combined, homogenized, and centrifuged. The bone marrow pellet was washed three times in αMEM plus 1% penicillin 100 U/ml/streptomycin 100 µg/ml, and finally resuspended in a total volume of 2 mls growth medium (αMEM, 10% FBS, and 1% penicillin 100 U/ml/streptomycin 100 µg/ml). Cells were cultured in a humidified chamber of 5% CO_2 and 95% air at 37˚C.

2.2: Osteoblast Morphology

In order to assay for alterations in osteoblast morphology, a commercial stain (LeukoStat™, Fisher Scientific, Pittsburg, PA) was used. MC3T3-E1 osteoblasts were plated at 1 x 10^5 cells / ml in 35 x 10 mm dishes. Twenty-four hours later, growth medium was replaced with either 50 or 75% MDA-MB-231 human metastatic breast cancer cell variant conditioned medium. Cells were cultured for an additional four days and stained using a LeukoStat™ stain kit to visualize cellular morphology. To use the LeukoStat™ stain, osteoblast medium was removed, cells rinsed with PBS, and cells fixed for 10 minutes using 10% formalin (VWR, Bridgeport, NJ). Formalin was removed, cell layer covered with LeukoStat™ solution I, and cells stained for 1 minute. The solution was removed, cell layer covered with LeukoStat™ solution II, and cells stained for an additional minute. Solution II was removed, cells rinsed 5 times with PBS, and photographed.

2.3: Alkaline Phosphatase Staining

Bone alkaline phosphatase is a biochemical marker of osteoblast differentiation *in vitro* and bone turnover *in vivo* [31]. Two methods were utilized to assay for osteoblast differentiation state: alkaline phosphatase expression via a stain, and alkaline phosphatase enzymatic activity. MC3T3-E1 cells were plated at 1x10^5 cells / cm^2 in a MC3T3-E1 growth medium. Twenty-four hours later, medium was exchanged for MC3T3-E1 differentiation medium. Cells were grown for 4 (growth), 10 (early differentiation), or 20 days (late differentiation). The medium was exchanged every third day. To stain for alkaline phosphatase, on day 4, 10, or 20, differentiation medium was removed, cells washed with PBS, and fixed with 10% formalin (VWR). The cells were rinsed with PBS in three sequential washes, and cells covered with alkaline phosphatase stain (0.0013 g Napthol AS-BI Phosphate (Sigma), 0.2M Tris, pH 8.5 (Sigma), and 0.0075 g Fast Blue RR Salt (Sigma) in a total volume of 13 ml). The stain was filtered and cells incubated for 30 minutes at 37˚C. Cells were rinsed and photographed.

In order to determine alkaline phosphatase enzymatic activity, a QuantiChrom™ Alkaline Phosphatase Assay Kit (BioAssay Systems, Hayward, CA) was used. On day 4, 10, or 20, differentiation medium was removed, cells washed with PBS, and detached using 1ml lysis buffer consisting of 100 mM glycine (Sigma), 1 mM magnesium chloride (Sigma), and 0.1% Triton X-100, pH 10.0 (Sigma) in dH_2O for 15 minutes at 4˚C. Twenty microliters of the homogenized sample was added to the alkaline phosphatase working solution, which consists of 1 ml assay buffer (BioAssay Systems), 25 µl 0.2 M magnesium acetate (BioAssay Systems), and 10 µl 1 M *p*-Nitrophenyl phosphate (BioAssay Systems). The solution was mixed, and read on a UV spectrophotometer (Beckman-Coulter, Fullerton, CA) at 405 nm at 0, 2, and 4 minutes after mixing. The alkaline phosphatase activity (IU/L) was calculated through a manufacturer-provided equation which takes into account the rate of change in optical density between 0 and 2, and 2 and 4 minutes as read at 405 nm.

2.4: Mineralization

To assay for the state of osteoblast mineralization, MC3T3-E1 cells were stained for Von Kossa, a biochemical marker of bone mineralization [32, 33]. Some studies have

suggested, however, that Von Kossa staining alone is not sufficient to confirm the presence of mineralization *in vitro*. Bonewald, et al. found that while cultures of differentiating MC3T3-E1 cells stained positive for mineralization by Von Kossa, they did not contain the calcium phosphate material hydroxyapatite as determined by electron microscopy and Fourier transform infrared microspectroscopy [34]. The MC3T3-E1 cultures, however, contained material of an unknown origin that represented dystrophic mineralization [34]. However, a number of other investigators have successfully cultured MC3T3-E1 cells to produce hydroxyapatite and bone-like mineralized material that is not dystrophic, as was characterized by electron microscopy [35, 36]. Furthermore, in this laboratory, MC3T3-E1 cells have been found to successfully mineralize *in vitro*, as determined by alizarin red staining, using the same cell differentiation protocol as that followed for Von Kossa staining [37]. Therefore, here Von Kossa staining was used as an indicator of bone mineralization. MC3T3-E1 cells were cultured and fixed as described for alkaline phosphatase activity. Cells were incubated with 5% silver nitrate (Sigma) for 30 minutes at room temperature in the dark. Cells were rinsed with dH_2O and photographed.

2.5: Flow Cytometry

In order to assay for GFP expression in cancer cells, flow cytometry was used. MDA-MB-231-GFP human breast cancer cell variants at ~90% confluency, were detached, washed, and fixed with 2% paraformaldehyde in PBS (VWR). It has been reported that use of as much as 4% paraformaldehyde maintains fluorescence during cell and tissue fixation [38]. GFP expression per cell was analyzed by flow cytometry (Beckman-Coulter FC500). Standardized fluorescent beads (5.05 μm; Sphero Accucount Ultra Rainbow Fluorescent particles, Spherotech, Libertyville, IL) were used to estimate GFP expression. Dead cells and debris were eliminated by forward and side scatter gating. GFP was excited by a 488 nm argon ion laser and fluorescence was detected using a 510-530 nm filter in the FL1 channel.

2.6: Conditioned media preparation

MC3T3-E1 cells were plated in MC3T3-E1 growth medium. Twenty-four hours later, medium was removed, cells rinsed with PBS, and medium replaced with MC3T3-E1 differentiation medium. MC3T3-E1 cells were grown to either 4, 10, or 20 days. Differentiation media was exchanged every third day. On either day 4, 10, or 20, differentiation medium was removed and the cultures rinsed with PBS. αMEM was added to the osteoblasts (20 ml in a T-150 flask where there are ~9.1×10^4 cells / cm^2) for 24 hours. MC3T3-E1 cell conditioned medium (OBCM) was collected, centrifuged to remove cellular debris, and stored at -20^o C.

MDA-MB-231 breast cancer cell variants were grown to 90% confluency. Breast cancer growth medium was removed and the cultures rinsed with PBS. αMEM was added to the cancer cells (20 ml in a T-150 flask where there are ~1.3×10^5 cells/cm^2). Cultures were incubated for 24 hours. Breast cancer cell conditioned medium (BCCM) was collected, centrifuged at 300 xg to remove cellular debris, and stored at -20^o C (Figure 2.1). In one experiment, BCCM was collected, centrifuged at 100,000 xg to remove any insoluble material, such as exosomes, and stored at -20^o C.

2.7: Conditioned media treatments of osteoblasts

Vehicle media (VM) consisted of MC3T3-E1 differentiation media. A 2X differentiation medium was formulated for MC3T3-E1 cell treatments using 50% BCCM (αMEM, 20% neonatal FBS, 100 μg/ml ascorbic acid, 20 mM β-glycerophosphate, 200 IU/ml penicillin, and 200 μg/ml streptomycin). Conditioned medium (CM) for treatment of cells was comprised of one half volume BCCM and one half volume 2X MC3T3-E1 differentiation medium. This scheme ensured that concentrations of serum and differentiation factors were identical for VM and CM.

MC3T3-E1 cells were treated with CM for twenty-four hours, after which the culture medium supernatant was collected, centrifuged to remove cellular debris, and stored at -20^{o}C. Figure 2.2 is a flow chart of the MC3T3-E1 cell *in vitro* experimental assay design where MC3T3-E1 cells were grown to 4, 10, or 20 days, and treated as previously described.

2.8: Osteoblast indirect co-culture transwell assay system with human cell variants

In order to determine the appropriate pore size to use in a transwell assay system of metastatic breast cancer cells and osteoblasts, pilot studies were carried out to determine which sized pore, 0.4 or 3 μm, would best meet the following criteria: 1) breast cancer cells did not invade the osteoblast cell layer beneath the insert and, 2) MC3T3-E1 cells expressed alkaline phosphatase while in the transwell system. From these experiments, a 3 μm pore size was determined to be the best suited for future experiments (Appendix, Section 7.1; Figure 7.1-7.2, Table 7.1).

MC3T3-E1 cells were plated at 5 x 10^4 cells / well and cultured for 10 or 20 days in MC3T3-E1 differentiation medium in 24 well plates. On day 9 or 19, human metastatic breast cancer or human epithelial cell variants were plated on the inserts of a transwell assay system (BD Falcon™, Franklin Lakes, NJ) in their respective growth medium at osteoblast : human cell ratios of either "10:1" (5 x 10^4 osteoblasts to 1,890 human cells), "1:1" (5 x 10^4 osteoblasts to 18,900 human cells), and "1:2" (5 x 10^4 osteoblasts to 37,800 human cells) and allowed to adhere overnight. These cell numbers were determined based on culture dish and insert surface area (manufacturer recommended 1.89 x 10^4 cells / 33 mm^2 for a 24 well insert). For hTERT-HME1 and MDA-MB-468P cells, cells were plated in inserts 3 days earlier to allow for the cells to proliferate to the same numbers as MDA-MB-231BRMS. MDA-MB-468P cells were additionally plated at double the density in order to obtain comparable cell numbers as MDA-MB-231BRMS: "10:1" (5 x 10^4 osteoblasts : 0.378 x 10^4 MDA-468P cells), "1:1" (5 x 10^4 osteoblasts : 3.78 x 10^4 MDA-468P cells), and "1:2" (5 x 10^4 osteoblasts : 7.56 x 10^4 MDA-468P cells). Twenty-four hours later, the growth medium from human cell was removed, cells rinsed with PBS, and differentiation medium of the osteoblasts exchanged. Seven hundred and fifty microliters differentiation medium was placed in the lower chamber and 0.3 ml media placed in the upper chamber. Inserts containing human cells were placed into the transwell system with MC3T3-E1 differentiation medium. Seventy-two hours later, the culture supernatant was removed, centrifuged to remove cellular debris, and stored at -20˚C (Figure 2.3). Media from both top and bottom chambers were assayed independently for cytokine concentration.

2.9: Osteoblast co-culture with human metastatic breast cancer cells

MC3T3-E1 cells were plated at 1 x 10^5 cells / cm^2 in MC3T3-E1 growth medium. Twenty-four hours later, the medium was removed, cells rinsed with PBS, and medium replaced with MC3T3-E1 differentiation medium. MC3T3-E1 cells were grown to either 10 or 20 days. Differentiation media was exchanged every third day. On day 10 or 20 of MC3T3-E1 cell differentiation, MDA-MB-231W human metastatic breast cancer cells were added at an osteoblast : breast cancer cell ratio of 10:1. Two days later, the co-culture supernatant was collected, centrifuged to remove cellular debris, and stored at -20^{o}C.

2.10: Intracardiac Inoculations

MDA-MB-231 human metastatic breast cancer cell variants at ~90% confluency, were detached, washed with three sequential rounds of centrifugation and resuspension, and finally resuspended in sterile PBS to 15 x 10^5 cells / ml. Female athymic mice aged 6 weeks (Harlan Sprague-Dawley, Indianapolis, IN), were anesthetized via an intraperitoneal injection of a mixture of ketamine (129 mg/kg) and xylazine (4 mg/kg). One MDA-MB-231-GFP metastatic breast cancer cell variant per mouse was injected at 3 x 10^5 cells / 200 μl into the left cardiac ventricle. This site is typically located between the third and fourth, or fourth and fifth intracostal space of the ribs, lateral to the sternum. The presence of pulsating bright red colored blood, as opposed to a dark burgundy color, at the beginning and end of each inoculation confirmed the site of injection and delivery of cells into the arterial portion of the circulatory system. This type of injection minimizes first-pass filtration through the pulmonary capillaries (lungs) and allows the maximal number of metastatic breast cancer cells to reach the bone. Six mice were utilized per experimental group (Figure 2.4). Three weeks post-inoculation, it was attempted to inoculate half of the mice via tail vein injection with 500 μl of 0.5 mg/ml Brefeldin A in PBS, further diluted from a stock concentration of 20 mg/ml Brefeldin A in DMSO as per Liu, et al [39]. However, successful inoculation of this volume was only achieved with 2 mice. Brefeldin A is a lactone antibiotic that interferes with cytokine secretion and blocks protein transport from the endoplasmic recticulum to the Golgi apparatus. Proteins accumulate inside the endoplasmic recticulum and thus remain inside the cell [39]. Six hours post-Brefeldin A inoculation, all mice were euthanized via CO_2 inhalation. No changes in cytokine localization were found when mice were inoculated with Brefeldin A. Mice were maintained under the guidelines of the NIH and The Pennsylvania State University. All protocols were approved and monitored by the Institutional Animal Care and Use Committee.

In preparation for the study of bone architecture, densitometry, and magnetic resonance imaging (MRI), whole femurs and tibiae cleaned free of soft tissue were wrapped in PBS soaked gauze and stored at -20˚C. For use, bones were thawed at room temperature and removed from the gauze wraps.

2.11: Blood and bone marrow serum collection

To obtain blood serum, immediately post-euthanization, mouse carcasses were inverted, fine tweezers utilized to remove an eye from the eye socket, and mouse blood obtained via eye bleed. The mouse carcass was gently massaged from tail to head in

order to aid blood flow. Whole blood was collected in a non-anticoagulant, sterile tube and stored 4˚C overnight. The following day, clotted blood was centrifuged at 300 xg for 3-5 minutes and the top serum fraction collected. Blood serum was assayed for cytokine expression.

Bone marrow plasma was collected from murine femurs. Bone marrow from cut bones (ends versus shaft) was flushed from bone sections with 1 ml DMEM. Bone marrow from both ends (proximal and distal to the hip) were combined. Flushed bone marrow was centrifuged and the top plasma fraction collected and assayed for murine cytokine expression.

2.12: Fluorescence stereo-microscopy

Femurs and tibiae were harvested, dissected free of soft tissue, and examined by fluorescence stereo-microscopy using a Nikon SMZ 1500 Fluorescence Stereoscope (Nikon Instruments, Inc., Melville, NY) with a P-HR PLAN APO 1X objective and 10X eyepiece, allowing for magnification in the range of 12-120X, and an ENDOW GFP Longpass GFP fluorescence filter ($\lambda_{excitation}$ = 488 nm; $\lambda_{emission}$ = 515 nm; Chroma Technology Corporation, Rockingham, VT). Photographs were taken using a Nikon CoolPix 8400 digital camera with a 24-85 mm zoom lens (Nikon Instruments, Inc., Melville, NY).

2.13: Retrieval of human breast cancer cells

Breast cancer cells were retrieved from murine femurs. Bone marrow from cut bones (ends versus shaft) was flushed separately from bone sections with DMEM. Bone marrow from both ends (proximal and distal to the hip) were combined. Flushed bone marrow was centrifuged and the pellet resuspended and cultured in 1 ml of the respective breast cancer growth medium (i.e. flushed bone marrow from a mouse inoculated with MDA-MB-231BRMS-GFP cells was plated with MDA-MB-231BRMS-GFP growth medium). Cancer cells present in the marrow were grown and expanded to no more than 2 passages post-recovery, and BCCM collected. Retrieved BCCM was stored at -20^{o}C.

2.14: Femur Cultures

Femurs were photographed and cut into ends (proximal and distal to the hip) and shaft. Bone marrow was separately flushed and collected for a different use. Isolated bone pieces were crushed and cultured separately in 1 ml α-MEM. Twenty-four hours later, culture supernatants were obtained and assayed for cytokine expression.

2.15: Cytokine analyses

Cytokines in culture medium were detected with a RayBio® Murine Cytokine Antibody Array III System for MC3T3-E1 (Norcross, GA) and later quantified with Murine Bio-Plex™ Cytokine Assay Systems (Bio-Rad, Hercules, California) or sandwich ELISAs, where indicated, following the protocols recommended by R&D Systems. Cytokines in BCCM were detected and quantified using Human Bio-Plex™ Cytokine Assay Systems (Bio-Rad). Cytokine concentrations were normalized to one million cells; however, the cell numbers in various conditioned medium preparations showed less than 15% variation. Cytokines in femur cultures were detected and quantified using Murine or Human Bio-Plex™ Cytokine Assay Systems. Cytokines in blood and bone marrow

serum were detected and quantified using Murine Bio-Plex™ Cytokine Assay System for serum samples. Cytokine protein levels were verified using species-specific sandwich ELISAs (R & D Systems, Minneapolis, MN) following R & D Systems recommended protocols. Intra-assay variation was typically less than 15%.

2.16: Cytokines and growth factors

Murine IL-6, murine KC, human IL-6 recombinant proteins, and anti-IL-6 murine, and anti-KC murine neutralizing antibody were obtained from R & D Systems. Murine and human VEGF recombinant protein and anti-VEGF murine neutralizing antibody were obtained from PeproTech (Rocky Hill, NJ). Anti-IL-6, anti-KC, and anti-VEGF murine neutralizing antibodies were all used at concentrations of 5 ng/ml, a concentration in excess to adequately neutralize the amount of murine IL-6, KC, and VEGF found in 10 or 20 day old osteoblast conditioned medium as determined by a Murine Bio-Rad Bio-Plex™ Cytokine Assay System. Murine IL-6, murine VEGF, and human VEGF recombinant proteins were used at concentrations of 1 ng/ml. Murine KC recombinant protein was used at a concentration of 0.1 ng/ml. These cytokine concentrations were similar to IL-6, KC, and VEGF concentrations found in osteoblast conditioned medium from 10 or 20 day old osteoblasts as determined by a Murine Bio-Plex™ Cytokine Assay System. Human anti-TGF-$\beta_{1,2,3}$ neutralizing antibody (R & D Systems), was used at a concentration of 5 μg/ml (sufficient to neutralize 25 ng/ml TGF-β).

2.17: Bone preparation for immunohistochemistry

Dissected femurs and tibiae were fixed for 24-48 hours at 4˚C in 4% paraformaldehyde (VWR) in PBS, and decalcified for an additional 24-48 hours at 4˚C with 0.5 mole/L EDTA in dH_2O (Sigma) [38, 40].

For embedding, bones were soaked in 30% sucrose (Sigma) in PBS for 24 hours, placed in Shandon Cryomatrix™ embedding medium (Thermo Shandon, Waltham, MA), and snap frozen in liquid nitrogen using the Gentle-Jane® SnapFreezing technique (Instrumedics Inc., Hackensack, NJ). Frozen samples were wrapped in aluminum foil, and stored at -20˚C.

2.18: CryoJane Frozen Section Preparation

Cryosectioning was performed on a Leica CM1900 Cryostat (Leica, Inc., Nussloch, Germany) equipped with the CryoJane Frozen Sectioning Kit (Instrumedics Inc.). For sectioning, femurs were oriented with the end proximal to the hip pointed toward the blade. Ten micron thick longitudinal sections were cut using a Diamond High Profile Knife (C.L. Sturkey, Lebanon, PA). Pre-chilled adhesive transfer tape windows (Instrumedics Inc.) were used to transfer cut sections onto pre-chilled adhesive coated slides (CJ4X adhesive coated slides; Instrumedics Inc.). Three to four bone sections were placed onto each slide. Bone sections were permanently bonded to slides with three flashes of ultraviolet light. Transfer tape windows were removed, and slides stored in slide boxes at -20˚C. In some cases, poly-L-lysine (VWR) coated slides were also utilized.

2.19: Immunohistochemistry

Bone sections were allowed to equilibrate to room temperature for at least 30 minutes prior to use. Sections were circled with an ImmEdge Hydrophobic Barrier Pen (Vector Laboratories, Burlingame, CA), permealized for 10 minutes using 0.2% Triton-X (Sigma) in PBS, and washed three times for five minutes each with Tris-buffered saline (TBS; Sigma). Sections were treated with hyaluronidase (1 mg/ml in TBS; Sigma) for 30 minutes at 37˚C for antigen retrieval and washed three times for five minutes each with TBS. Endogenous peroxidase activity was blocked using PEROXIDAZED (Biocare Medical, Concord, CA) for 10 minutes at room temperature, sections washed three times for 5 minutes each with TBS, and blocked with 10% donkey serum in TBS-X (Sigma) for 1 hour. Slides were incubated for one hour with either primary rabbit polyclonal anti-GFP IgG (1:1500; Molecular Probes, Eugene, OR), rabbit polyclonal anti-mouse MCP-1 (30 μg/ml; Abcam, Cambridge, MA), rabbit polyclonal anti-mouse CD41 (1:100; Abcam), goat polyclonal anti-mouse VEGF (25 μg/ml; R & D Systems), goat polyclonal anti-human VEGF (10 μg/ml; R & D Systems), or goat polyclonal anti-mouse IL-6 (30 μg/ml; R & D Systems) and washed three times for 5 minutes each with TBS. A secondary antibody of either biotinylated donkey anti-rabbit (1:750; Abcam) or biotinylated donkey anti-goat (1:2500; Abcam) was applied for one hour and sections washed three times for 5 minutes each with TBS. Both primary and secondary antibodies were diluted in TBS-X for use. Sections were incubated with avidin-horse radish peroxidase for 20 minutes (Covance, Dedham, MA), washed three times for 5 minutes each with TBS, and visualized using either a Biogenex liquid 3,3' Diaminobenzidine (DAB) kit (Biogenex, San Ramon, CA) or a liquid DAB kit (Sigma). The DAB reaction was stopped by immersing slides in dH_2O. Slides were counterstained using Gill's Hematoxylin (Vector Laboratories, Burlingame, CA), washed with dH_2O, and mounted with VectaMount (Vector Laboratories). Sections with the primary antibody deleted and non-cancer bearing murine bones served as negative controls. Images were viewed using a Leitz Dialux 20 light microscope (Leitz), which includes a 10X eyepiece, with either a 6.3X NPI Leitz (Leitz) or 25X Ph2 Plan Carl Zeiss (Carl Zeiss MicroImaging, Inc., Thronwood, NY) objective allowing for magnification in the range of 63-250X. A Leitz GFP fluorescence filter was fitted to the microscope ($\lambda_{excitation}$ = 488 nm; $\lambda_{emission}$ = 515 nm, Leitz). The Leitz Dialux 20 microscope was fitted to mount a Nikon CoolPix 8400 digital camera with a 24-85 mm zoom lens (Nikon Instruments, Inc.).

2.20: Bone architecture / densitometry / MRI

For bone architecture studies, and with the help of Dr. Neil Sharkey and Noriaki Okita, thawed bones were arranged in a 30 mm sample holder of a μCT40 Desktop MicroCT Scanner (SCANCO Medical AG, Zürich, Switzerland) and their entire lengths scanned. Slices were acquired using machine settings of 55 KVp, 145 μA and 200 ms integration times. Images were reconstructed in 2048 x 2048 pixel matrices and stored in 3D arrays with an isotropic voxel size of 15.4 μm. A threshold value equivalent to 25% of the maximal gray scale was chosen to identify bone tissue from background. Company-provided software and custom scripts were utilized to view images, create 3-dimensional models of the bones and determine trabecular bone volumes in the metaphyseal regions harboring tumors.

For bone densitometry, thawed bones were arranged on the sample tray of a Lunar PIXImus II x-ray densitometer (GE Medical Systems, Fitchburg, WI) and scanned via a Dual Energy X-ray Absorptiometry (DEXA) scan. Company-provided software that utilizes a ratio of attenuation of the high and low energies allowed for the generation of images. Bone mineral density (BMD), which is a ratio of bone mineral composition (BMC) to area, was calculated from these images.

For MRI analyses, with the help of Dr. Andrew Webb and Dr. Thomas Neuberger, whole femurs were removed from decalcification solution and immersed in a PBS solution containing 1% v/v gadoteridol (279.3 mg/ml) contrast agent (ProHance®, Bracco Diagnostics, Inc., Princeton, NJ) for at least three days. Images were acquired on a 14.1 tesla vertical bore MRI system (Varian Inc, Palo Alto, CA). The T_1 and T_2 relaxation times of PBS with contrast agent were determined with standard inversion recovery and spin echo methods, giving values of 250 ms and 17 ms, respectively. The short T_1 enabled a short repetition time of 200 ms to be used for the three dimensional spin echo imaging sequence. Using a field of view of 16 x 5 x 5 mm^3 and matrix size of 512 x 142 x 142, a resolution of 29 x 35 x 35 μm^3 was obtained. The total scan time was 13.5 h with 12 signal averages. By choosing an echo time of 19.3 ms, the T_2 contrast was high enough to clearly delineate clearly cancerous regions from healthy tissue. After zero filling the raw data by a factor of two and reconstructing the images in MATLAB (The Mathworks, Bolder, CO, USA) via an inverse three-dimensional Fourier transform, the dataset was imported into AMIRA (Mercury Computer Systems Inc., Chelmsford, MA, USA) and segmentation of the bone and infiltrated area performed based on intensity levels. Finally, the ratio of total bone volume to cancerous volume was calculated based on the segmentation.

2.21: Chemoattraction

For assay of breast cancer cell chemoattraction, MDA-MB-231W human metastatic breast cancer cells were resuspended in DMEM at a concentration 1 x 10^6 cells/ml. Vybrant DiI (5 µl/ml of cell suspension; Molecular Probes, Eugene, OR) was added to the cancer cells per manufacturers instructions. MDA-MB-231W human metastatic breast cancer cells were resuspended and plated at a density of 5 x 10^4 cells in BD™ Falcon FluoroBlok™ inserts with 8 µm pores (Becton Dickinson, Franklin Lakes, NJ). MDA-MB-231W human metastatic breast cancer cells, stained with Vybrant DiI, were placed in a transwell assay system in 24 well plates with *one of the following* treatments in the bottom chamber (Figure 2.5): a) osteoblast conditioned medium prepared from MC3T3-E1 cells grown to either 10 or 20 days, b) osteoblast conditioned medium from MC3T3-E1 cells grown to either 10 or 20 days plus 5 ng/ml anti-IL-6 *and* anti-KC mouse neutralizing antibody, c) osteoblast conditioned medium from MC3T3-E1 cells grown to either 10 or 20 days plus 5 ng/ml anti-IL-6, anti-KC, *and* anti-VEGF mouse neutralizing antibody, d) 0.1 ng/ml murine KC, 1 ng/ml murine IL-6, *and* 1 ng/ml murine VEGF recombinant protein that were previously dried to the underside of the membrane inserts, e) 0.1 ng/ml murine KC, 1 ng/ml murine IL-6, *and* 1 ng/ml murine VEGF *soluble* recombinant protein, f) 1 ng/ml human IL-6 *and* 1 ng/ml human VEGF, g) 25 ng/ml human IL-6 *and* 100 ng/ml human VEGF *soluble* recombinant protein, *or* h) osteoblast conditioned medium from 10 day old osteoblasts plus 5 µg/ml anti-TGF-$\beta_{1,2,3}$

neutralizing antibody. MDA-MB-231W human metastatic breast cancer cells incubated for 24 hours (Figure 2.5). FluoroBlok™ transwell membrane inserts were cut free from the insert using a No. 11 blade scalpel and mounted using Fluoromount-G™ (Southern Biotechnology Associates, Birmingham, AL). The number of Vybrant DiI stained MDA-MB-231W human metastatic breast cancer cells that migrated to the opposite side of the membrane (toward the chemoattractant) were counted on a Leitz Dialux 20 light microscope (Leitz), which includes a 10X eyepiece, with either a 6.3X NPI Leitz (Leitz) or 25X Ph2 Plan Carl Zeiss (Carl Zeiss MicroImaging, Inc.) objective allowing for magnification in the range of 63-250X. A Leitz fluorescence filter was fitted to the microscope ($\lambda_{absorption}$ = 549 nm; $\lambda_{emission}$ = 565 nm, Leitz). The Leitz Dialux 20 microscope was fitted to mount a Nikon CoolPix 8400 digital camera with a 24-85 mm zoom lens (Nikon Instruments, Inc.) which was used to acquire the images.

2.22: Osteoclast formation

RAW264.7 cells were plated in 24-well dishes at 5 x 10^3 cells/ml. Twenty-four hours later, cells were treated with either 50 ng/ml recombinant murine soluble RANK-L (PeproTech, Rocky Hills, NJ) or a) the culture supernatant of MC3T3-E1 cells, grown to 10 or 20 days, treated with MDA-MB-231W CM for 24 hours, b) the culture supernatant of MC3T3-E1 cells, grown to 10 or 20 days, co-cultured with MDA-MB-231W human metastatic breast cancer cells for 48 hours, or c) either 1, 10, or 100 ng/ml murine IL-6 recombinant protein.

For bone marrow monocyte cell preparation, 10 µl of the bone marrow cell suspension : 1 ml growth medium was added to the wells of a 24-well dish. Twenty-four hours later, cells were treated with either 100 ng/ml recombinant murine M-CSF (PeproTech) and 50 ng/ml recombinant human RANK-L or a) the culture supernatant of MC3T3-E1 cells, grown to 10 or 20 days, treated with MDA-MB-231W CM for 24 hours, b) the culture supernatant of MC3T3-E1 cells, grown to 10 or 20 days, co-cultured with MDA-MB-231W human metastatic breast cancer cells for 48 hours, or c) either 1, 10, or 100 ng/ml murine IL-6 recombinant protein.

Conditioned medium was prepared from either MC3T3-E1 cells grown to 10 or 20 days (OBCM) as indicated, or MDA-MB-231W human metastatic breast cancer cells (BCCM). CM solution was comprised of one half volume OBCM or BCCM, as indicated, and one half volume 2X osteoclast growth medium (αMEM, 20% neonatal FBS, 200 IU/ml penicillin, and 200 µg/ml streptomycin for bone marrow monocytes. Or, for RAW264.6 cells, DMEM and 20% FBS.). This scheme ensured that concentrations of serum and growth factors were identical for all treatments. The medium was exchanged every third day. Two weeks later, osteoclasts were stained for tartrate-resistant acid phosphatase (TRAP).

2.23: TRAP Staining

Osteoclasts were evaluated by TRAP staining (Sigma). Cells were fixed with 10% formalin (VWR), and incubated for one hour at 37˚C in the dark, with a filtered solution of water, acetate, naphthol AS-BI phosphoric acid, tartrate, and Fast Garnet GBC salt. The cells were subsequently stained with an acid hematoxylin solution for 5 minutes. TRAP positive, multinucleated osteoclasts were counted using light microscopy.

2.24: Data Analysis

Alterations in cytokine concentrations were measured using species-specific standard ELISAs or Bio-Rad Bio-Plex™ cytokine assays. Three biological replicates were cultured per experiment, and the experiments performed twice for a total of six biological replicates per condition. Each replicate was assayed by ELISA in duplicate. Intra-assay variation was typically less than 15%. Due to space constraints, it was not possible to assay the biological replicates on the same ELISA plate. Inter-assay (plate-to-plate) variation was high (50% or greater). Since the inter-assay variation was high, the results were not averaged. Instead, results were displayed from one representative experiment, which illustrated the change in cytokine concentration from a culture treated with breast cancer cells or their conditioned media and a control treated with vehicle medium. The range of cytokine expression, or fold increase/decrease of cytokine concentration, that pertains to the illustrated representative graph, is listed. Raw data pertaining to additional biological replicates is contained in the Appendix, Section 7.4.

Task 1. **To determine how *osteoblast*-derived inflammatory cytokine production by MC3T3-E1 osteoblasts is altered in response to co-culture or CM of bone metastatic MDA-MB-231 breast cancer cell variants. (Months 1-12)**

Part 3: RESULTS: THE EFFECT OF HUMAN METASTATIC AND NON-METASTATIC BREAST CANCER CELLS, AND HUMAN EPITHELIAL CELLS, ON OSTEOBLASTS

3.1: Rationale

Previous studies conducted in this laboratory have shown that metastatic breast cancer cells brought about altered adhesion and loss of differentiation capabilities [41]. Instead, the osteoblasts were found to undergo an inflammatory stress response and produce inflammatory cytokines that may be chemoattractants for metastatic breast cancer cells: interleukin-6 (IL-6), IL-8 (macrophage inflammatory protein-2 [MIP-2]), and monocyte chemoattractant protein-1 (MCP-1) [11]. From these observations, it is proposed that osteoblast-derived factors are as integral, if not more important, than breast cancer-derived factors in cancer metastases. In addition, it is thought that inflammatory cytokines contribute to osteoblast autocrine and osteoblast-breast cancer cell paracrine mechanisms resulting in significant cross-talk between the two cell types. Experiments described here focus on understanding the effect of metastatic breast cancer cells on osteoblasts.

3.2: Osteoblasts, while in the presence of metastatic breast cancer cell conditioned medium for up to 4 days, have normal morphology, differentiate, and deposit calcium

Previous studies conducted in this laboratory have shown that metastatic breast cancer cells profoundly affect osteoblasts through increased osteoblast apoptosis, altered osteoblast morphology and adhesion, and suppressed osteoblast differentiation and mineralization as evidenced by a lack of expression of alkaline phosphatase, bone sialoprotein, and osteocalcin [9, 42, 43]. These effects were found when osteoblasts were

cultured for extended periods of time (5 to 35 days) with metastatic breast cancer conditioned medium. In order to determine how metastatic breast cancer cells effect osteoblasts when cultured for shortened times (24 hours to 4 days), osteoblast morphology, differentiation, protein expression, and ability to deposit calcium were assessed when osteoblasts were treated with the conditioned medium from metastatic breast cancer cell variants.

3.2.1: Metastatic breast cancer variant conditioned media did not alter MC3T3-E1 cell morphology

In pilot experiments, the effects of conditioned medium on the morphology of proliferating osteoblasts was tested. MC3T3-E1 cells were plated at 1 x 10^5 cells / ml in 35 x 10 mm dishes. Twenty-four hours later, growth medium was replaced with either 50 or 75% conditioned medium from MDA-MB-231 human metastatic breast cancer cell variants. Cells were cultured for an additional four days prior to staining with a LeukoStat™ stain kit to visualize cellular morphology. When examined by light microscopy, MC3T3-E1 cells treated with conditioned medium from MDA-MB-231 human metastatic breast cancer cell variants retained a rounded shape, as opposed to a thin, spindle-like shape (Figure 3.1) [5]. Thus, were no gross differences seen in MC3T3-E1 morphology amongst cells treated with MDA-MB-231 human metastatic breast cancer variant conditioned medium or vehicle medium (Figure 3.1).

3.2.2: Differentiated MC3T3-E1 cells, treated with metastatic breast cancer variant conditioned media for 24 hours, expressed alkaline phosphatase and deposited calcium

In further experiments, MC3T3-E1 cells were grown to differentiation (12 or 16 days) and treated with either vehicle medium (VM) or MDA-MB-231 human metastatic breast cancer variant conditioned medium. Twenty-four hours later, MC3T3-E1 cells were stained for alkaline phosphatase expression or Von Kossa for deposition of calcium. Alkaline phosphatase and Von Kossa staining were used to define bone turnover and mineralization, respectively [31-33]. Some studies have suggested that Von Kossa staining alone is not sufficient to confirm the presence of mineralization *in vitro* [34]. Other investigators, however, have successfully cultured MC3T3-E1 cells to produce hydroxyapatite and bone-like mineralized material characterized by electron microscopy [35, 36]. In this laboratory, MC3T3-E1 cells have been shown to successfully mineralize *in vitro*, as determined by alizarin red staining, using the same cell differentiation protocol as that followed for Von Kossa staining [37]. Therefore, here the Von Kossa stain was used to demonstrate calcium deposition, and was also used as a possible indicator of bone mineralization. No visual changes were seen in the expression of alkaline phosphatase (Figure 3.2) or Von Kossa (Figure 3.3) in osteoblasts treated with MDA-MB-231 human metastatic variant conditioned medium treatment or vehicle medium. MC3T3-E1 cells were also assayed for changes in alkaline phosphatase enzyme activity (Table 3.1A-B) after treatment with metastatic breast cancer variant conditioned medium. Small differences in the quantitative expression of alkaline phosphatase activity were found between cancer variant conditioned medium treatment and vehicle medium

(Table 3.1A-B). These differences were considered to be negligible. No differences in the expression of alkaline phosphatase activity were found amongst cancer cell variant conditioned medium treatment under these conditions (Table 3.1A-B).

3.3: Untreated osteoblasts express alkaline phosphatase, deposit calcium, and express inflammatory cytokines

Current models suggest that cytokines and chemokines are keys to understanding bone metastatic breast cancer [8, 44-46]. Osteoblasts, in particular, have been reported to produce proteins such as RANK-L and PTHrP that contribute to the "vicious cycle of breast cancer metastasis" [8, 47, 48]. It is possible that the osteoblasts themselves naturally produce cytokines or chemokines which may be involved in bone metastatic breast cancer. Therefore, untreated MC3T3-E1 cells were assayed for their ability to differentiate, deposit calcium, and produce cytokines.

In order to characterize the differentiation status of normal MC3T3-E1 cells at times surveyed in this study, the osteoblasts were assayed for alkaline phosphatase expression and ability to deposit calcium. MC3T3-E1 cells were grown to three different stages of development: 4 days (growth), 10 days (early differentiation), or 20 days (late differentiation) and stained for alkaline phosphatase or Von Kossa. MC3T3-E1 cells expressed alkaline phosphatase at both 10 and 20 days, but Von Kossa at 20 days (Figure 3.4).

To determine the cytokines expressed by osteoblasts, the conditioned medium from MC3T3-E1 cells cultured alone was collected and assayed for the presence of murine cytokines by a murine Bio-Rad Bio-Plex™. In particular, MC3T3-E1 cells produced various quantities of murine IL-6, VEGF, KC, MIP-2, and MCP-1 as represented by + (little: 0.01-0.08 ng/ml), ++ (modest amount: 0.09-0.4 ng/ml), and +++ (substantial amount: >0.05 ng/ml)(Table 3.2). MCP-1, specifically, was producted by MC3T3-E1 cells in substantial amounts (>2 ng/ml). Thus, MC3T3-E1 cells naturally produce IL-6, VEGF, KC, MIP-2, and MCP-1 in various concentrations.

3.4: Osteoblasts produce inflammatory cytokines in the presence of metastatic breast cancer cells or their conditioned medium

According to current models, chemokines and cytokines produced by breast cancer cells are key to understanding breast cancer cell metastasis [8, 44-46]. In addition, it has been reported that chronic inflammation following exposure to cancer cells, foreign materials, or micro-organisms, may lead to changes in cytokine expression; specifically IL-6, IL-8, and MCP-1 [49-52]. Therefore, MC3T3-E1 cell cytokine production was assessed following treatment with MDA-MB-231 breast cancer cell variants or their conditioned medium.

3.4.1: Osteoblast-derived cytokine production was increased in the presence of metastatic breast cancer conditioned medium

Culture supernatants from 10 day old MC3T3-E1 cells treated with either 50% VM or MDA-MB-231W CM for 24 hours were assayed using a RayBio® Murine Cytokine Array III system. Of the 62 various cytokines on the array, increases in IL-6, MCP-1, and VEGF were seen when osteoblasts were treated with MDA-MB-231W CM (Figure 3.5). Osteoblast-derived murine cytokine production appeared to be both

induced (VEGF) and increased (IL-6 and MCP-1) with treatment. Small changes were also seen in MIP-1γ, LIX, and RANTES. Kinder, et al. additionally noted an increase in murine IL-6 and MCP-1 when 25 day old osteoblasts were treated with MDA-MB-231W CM [11]. IL-6, VEGF, and MCP-1 have been reported in the literature to be involved in inflammation [53-57]. Since IL-6, MCP-1, and VEGF exhibited the largest change in expression with treatment of metastatic breast cancer conditioned medium, these cytokines were selected for future experimentation.

3.5: Osteoblasts increased inflammatory cytokine production in response to conditioned medium from human metastatic breast cancer variants, and epithelial or mesenchymal variants *in vitro*

IL-6, MCP-1, and VEGF are cytokines involved in inflammation [53-57]. To assay for and quantitate additional inflammatory cytokines that might be involved in the MC3T3-E1 cell response to metastatic breast cancer cells, a Bio-Rad Bio-Plex™ Murine Cytokine Assay was carried out. The Bio-Plex included 32 cytokines involved in inflammation (Mouse Group I, 23-plex plus Mouse Group II, 9-plex)(Table 3.3). MC3T3-E1 cells grown to 4, 10, or 20 days were treated with VM or conditioned medium from MDA-MB-231 metastatic variants for 24 hours. Osteoblast-derived cytokine production increased with metastatic breast cancer CM treatment; however, the change was independent of the variant (Figure 3.6). Trends in osteoblast-derived cytokine expression were similar amongst osteoblast stages of differentiation; however, differences were most dramatic with 10 (Figure 3.6A) or 20 day old (Figure 3.6B) osteoblasts. Therefore, we chose to concentrate on these more mature osteoblasts.

MIP-2 and VEGF cytokine expression were seen to increase minimally in 10 day osteoblasts (Figure 3.6A)(Table 3.4A). MCP-1 and KC expression increased >1.5 fold (Table 3.3A). IL-6 expression increased from 85 pg/ml (VM) to 885-3286 pg/ml (CM); a 10-39 fold increase over VM (Figure 3.6A)(Table 3.4A). No trends were found amongst treatment with breast cancer cell variants; CM variant treatments yielded similar results. Increases in osteoblast-derived cytokine expression were more pronounced in 20 day old osteoblasts than 10 day (Figure 3.6B)(Table 3.4B). VEGF expression increased minimally; MIP-2 and MCP-1 expression increased 2 fold or greater; KC expression increased 3-57 fold; and IL-6 expression increased 12.5-76.8 fold (Table 3.4B). No differences were found amongst treatments with MDA-MB-231 breast cancer variants. In summary, it was found that osteoblast-derived cytokine production was increased in the presence of breast cancer CM. Furthermore, effects were more pronounced in late stage osteoblasts. Thus, these results suggest that stages of osteoblast differentiation play an important role in determining their cytokine response to breast cancer CM.

The increases in cytokines with metastatic CM treatment were also dose-dependent (Figure 3.7). MC3T3-E1 cells grown to 4 (Figure 3.7A)(Table 3.5A), 10 (Figure 3.7B)(Table 3.5B), or 20 days (Figure 3.7C)(Table 3.5C) were treated with VM or 10, 25, or 50% MDA-MB-231 metastatic breast cancer variant conditioned medium. Twenty-four hours later, murine IL-6 expression (a representative murine cytokine) was assayed via standard murine sandwich ELISAs. Osteoblast-derived cytokine production increased in a dose-dependent manner with metastatic breast cancer CM treatment. This change was similar for all variants. IL-6 expression increased minimally when osteoblasts were grown to 4 days (Figure 3.7A)(Table 3.5A). When

osteoblasts were grown to 10 days, IL-6 expression increased 2.5-50 fold (Figure 3.7B)(Table 3.5B). Finally, when osteoblasts were grown to 20 days, IL-6 expression increased 2-69 fold (Figure 3.7C)(Table 3.5C). Since effects were more pronounced in late stage osteoblasts, these data additionally suggested that osteoblast differentiation played an important role in determining osteoblast-derived cytokine response to breast cancer CM.

Furthermore, to determine if soluble materials or membrane-derived vesicles in the conditioned medium caused MC3T3-E1 cells to elicit an inflammatory response, 10 day old osteoblasts (representative differentiation stage) were treated for 24 hours with MDA-MB-231W human metastatic breast cancer conditioned medium that was ultracentrifuged at 100,000 xg in order to remove any insoluble material. Osteoblast-derived cytokine production increased with ultracentrifuged CM (Figure 3.8). The osteoblast-derived cytokine response to ultracentrifuged CM was, on average, 8.4 fold greater than VM (Figure 3.8)(Table 3.6). It was interesting to note, however, that the increase in cytokine production when osteoblasts were treated with ultracentrifuged MDA-MB-231W human metastatic breast cancer conditioned medium was nearly 3 fold greater than that seen with treatment of the non-centrifuged metastatic variant CM (Figure 3.8)(Table 3.6). This increase may be due to the removal of some form of inhibitor by ultracentrifugation, which was membrane vesicle bound in conditioned medium. Thus, ultracentrifugation of human metastatic breast cancer conditioned medium did not remove the material causing an osteoblast inflammatory response.

3.5.1: Osteoblast-derived cytokines were increased in the presence of MDA-231-GFP variant conditioned medium

To confirm that osteoblast-derived cytokines also increased in the presence of conditioned medium from MDA-231-GFP variants to be used for *in vivo* intracardiac inoculations, 10 day old MC3T3-E1 cells (representative differentiation stage) were treated for 24 hours with CM from MDA-231-GFP variants. Osteoblast-derived cytokine production increased following treatment with conditioned medium from MDA-231-GFP variants (Figure 3.9)(Table 3.7). When osteoblasts were grown to 10 days, the change in murine KC and MIP-2 expression increased up to 3 fold over VM (Figure 3.9)(Table 3.7). MCP-1 expression increased up to 13 fold (Figure 3.9)(Table 3.7). And VEGF and IL-6 expression increased up to 52 fold (Figure 3.9)(Table 3.7). Thus, osteoblast-derived cytokines were similarly increased when osteoblasts were treated with MDA-231-GFP variant CM as they were when treated with CM from MDA-231 metastatic variants.

3.5.2: Osteoblasts increased inflammatory cytokine production in response to human epithelial cell conditioned medium

In order to determine if the increase in osteoblast-derived inflammatory cytokine production was unique to metastatic breast cancer cells, osteoblasts were treated with CM from MDA-MB-231BRMS (a non-metastatic breast cancer cell variant of the MDA-MB-231 cell line), MDA-MB-468P (a non-metastatic breast cancer cell variant of a cell line other than MDA-MB-231 derivation), or hTERT-HME1 (a non-metastatic, 'normal' mammary epithelial cell line) human epithelial, non-metastatic cell variants and assayed for cytokine expression. *For the remainder of the study, these three cell lines will be*

collectively referred to as "human epithelial cell variants." MC3T3-E1 cells grown to 4, 10, or 20 days were treated with VM or human epithelial cell variant CM for 24 hours.

It was found that osteoblast-derived cytokine production increased with human epithelial cell variant CM treatment; in fact, the response was greater, in some cases, than that found with treatment of metastatic variant CM as a whole (Figure 3.10). When osteoblasts were grown to 10 days, the change in murine MIP-2 and VEGF expression increased up to 13 fold (Figure 3.10A)(Table 3.8A) compared to minimal increases seen with treatment of metastatic variant CM (Figure 3.6A)(Table 3.4A). KC expression increased 2.4-238 fold (compared to a 1.5 fold increase with treatment of metastatic variant CM [Figure 3.6A][Table 3.4A]); and IL-6 expression increased 0.3-92 fold (Figure 3.10A)(Table 3.8A) compared to 10-39 fold increases found with treatment of metastatic variant CM (Figure 3.6A)(Table 3.4A).

Increases were more pronounced when osteoblasts were grown to 20 days. MIP-2, VEGF, compared to increases between 2-57 fold with treatment of metastatic variant CM (Figure 3.6B)(Table 3.4B). KC expression increased nearly 335 fold over VM (Figure 3.10B)(Table 3.8B) compared to increases of between 12.5-76.8 fold over VM with treatment of metastatic variant CM (Figure 3.6B)(Table 3.4B). The change in osteoblast-derived cytokine expression was similar for all human epithelial cell variants (Figure 3.10). Trends in osteoblast-derived cytokine expression, as seen with metastatic breast cancer variant CM treatment, were similar amongst osteoblast stage of differentiation; however differences were most dramatic with 20 day old (Figure 3.10B) osteoblasts.

Interestingly, there was not an increase in osteoblast-derived MCP-1 in both osteoblasts grown to 10 or 20 days when osteoblasts were treated with CM from human epithelial variants (Figure 3.10A-B). This was compared to increases of between 2-11.5 fold over VM when osteoblasts were treated with metastatic variant CM (Figure 3.6)(Table 3.4). In fact, decreases between 50-100% occurred in osteoblast-derived MCP-1 when MC3T3-E1 cells were grown to 10 or 20 days and treated with CM from human epithelial cell variants. These changes were generally consistent amongst additional biological replicates assayed, and were in contrast to 2-9 fold increases seen with osteoblast treatment of metastatic breast cancer variant CM. Thus, while osteoblast-derived MCP-1 was substantially increased when MC3T3-E1 cells are treated with CM from metastatic cancer cells, MCP-1 was not increased but was instead *decreased* when osteoblasts are treated with CM from human epithelial cells. Therefore, the induction, or lack thereof, of MCP-1 in osteoblasts may be the distinguishing feature between the activity of metastatic and non-metastatic breast cancer cell variants in the process of breast cancer cell colonization of the bone microenvironment. These data suggested that osteoblast-derived MCP-1 expression was increased by metastatic breast cancer variant CM but not CM from human epithelial cell variants.

Furthermore, increases in osteoblast-derived cytokine production were more pronounced (fold increases over VM of up to 238) when osteoblasts were treated with human epithelial variant CM compared to increases in osteoblast-derived cytokine production when osteoblasts were treated with metastatic variant CM (fold increases over VM of up to 76.8). It has been reported that bone metastatic human breast cancer cells mimic the skeletal phenotype of osteoblasts [58]. It is possible that human metastatic breast cancer conditioned media, because of cancer cell mimicry of osteoblasts, results in

a lessened inflammatory response by MC3T3-E1 cells (Figure 3.6). This lessened inflammatory response to human metastatic breast cancer conditioned media by MC3T3-E1 cells may be a protective function, specifically to evade immune surveillance, for the cancer cells. In addition, the lessened inflammatory response to human metastatic breast cancer conditioned media by MC3T3-E1 cells is in contrast to a generalized inflammatory response to epithelial cells that do not express an osteoblast phenotype (such as human epithelial cell variants)(Figure 3.10). Therefore, these data suggested that osteoblast treatment with human metastatic breast cancer cells or their conditioned media (MDA-MB-231 metastatic breast cancer cell variants; cells which mimic an osteoblast phenotype) resulted in an osteoblast inflammatory response that was not as great as that expressed by osteoblasts treated with human epithelial cells (MDA-MB-231BRMS, MDA-MB-468P, hTERT-HME1; cells that do not express an osteoblast phenotype.). Thus, tumor cell presence in the bone microenvironment may be sufficient, but not necessary, to elicit an inflammatory response by osteoblasts.

3.5.3: Osteoblasts increased inflammatory cytokine production in response to epithelial and mesechymal cell conditioned medium

Contrary to the hypothesis that osteoblast-derived cytokines are increased only in the presence of metastatic breast cancer cells or their CM, when MC3T3-E1 cells were treated with human epithelial cell CM, their production of inflammatory cytokines was larger than that seen with treatment of human metastatic breast cancer CM. It may be the case that the osteoblast cytokine response to human epithelial CM is a generalized response to epithelial cells. It has been reported that osteoblasts express the mRNA to Toll-like Receptor (TLR) 2, TLR 4, and TLR 9 [59-61]. TLR 2 binds to Heat Shock Protein 70 (HSP 70), among others [62]. Interestingly, HSP 70 has been found to be overexpressed in malignant melanoma [62]. However, no evidence has been found in this study to suggest that lipopolysaccharide, HSP 70, or CpG DNA, ligands to TLR 2, 4, and 9, respectively [59-62], are secreted by the human metastatic breast cancer cells or human epithelial cells utilized. Therefore, it cannot be concluded that the inflammatory response elicited by osteoblasts treated with metastatic breast cancer or human epithelial cell CM is due to signaling from a TLR cascade.

Since a larger response was seen when osteoblasts were treated with human epithelial cell CM than when osteoblasts were treated with metastatic variant CM, this begs the question, do osteoblasts increase their production of inflammatory cytokines when treated with CM from non-cancer cells? Therefore, in order to determine if the increase in osteoblast-derived inflammatory cytokine production to CM from human epithelial variants was due to epithelial cells that were not necessarily of cancer origin, osteoblasts were treated with CM from additional human or murine epithelial or mesechymal cells. MC3T3-E1 cells grown to 10 days (representative differentiation stage) were treated with VM or CM from a) human metastatic breast cancer (MDA-231, MDA-435), b) human non-metastatic breast cancer (MDA-231BRMS, MDA-435BRMS, MCF-10A), c) human epithelial (HBL-100), d) murine epithelial (HC11, Comma-D1, Primary Mammary Epithelial, Primary human foreskin), or e) murine mesenchymal CM (NIH/3T3 fibroblasts, 3T3-L1 fibroblasts, adipocytes, primary murine fibroblasts) for 24 hours (Table 2.1). It was found that osteoblast-derived IL-6 and MCP-1 production

(representative murine cytokines) increased after treatment with human or murine metastatic, epithelial, or mesenchymal cell variant CM treatment (Figure 3.11).

Osteoblast-derived IL-6 and MCP-1 production increased 17.2-215 or 1.7-13.5 fold, respectively following treatment with either MDA-MB-231 or MDA-MB-435 human metastatic breast cancer CM and their non-metastatic–BRMS variants (Figure 3.11A-B); however, treatment with CM from MDA-MB-231 variants yielded a substantially greater cytokine increase (IL-6: 16 fold; MCP-1: 10 fold increase over MDA-435 CM)(Table 3.9). Osteoblast treatment with non-metastatic MCF-10A breast cancer cells resulted in a 250 or 26 fold increase in murine IL-6 and MCP-1 expression, respectively, which was 1.2 fold greater than that seen with metastatic BCCM (Figure 3.11A-B)(Table 3.9). Osteoblast treatment with murine NIH/3T3 or primary human foreskin CM led to increased IL-6 and MCP-1 production up to 8.5 fold over VM, which was similar to treatment with MDA-MB-435 breast cancer CM variants (Figure 3.11A-B)(Table 3.9).

Osteoblast-derived IL-6 and MCP-1 expression increased substantially with treatment with CM from other epithelial or mesenchymal variants (Figure 3.11C-D). In particular, IL-6 expression increased up to 155 fold over VM (Figure 3.11C)(Table 3.9). MCP-1 expression increased up to 74 fold over VM (Figure 3.11D)(Table 3.9). MC3T3-E1 cell treatment of HC11, Comma-D1, HBL-100, primary mammary fibroblast, primary mammary epithelial, adipocyte, and murine fibroblast CM resulted in increases of murine IL-6 and MCP-1 65 and 2.7 fold greater, respectively, than treatment with metastatic breast cancer CM (Figure 3.11C-D)(Table 3.9). These data suggested that osteoblasts elicited an inflammatory response when in the presence of CM from epithelial or mesenchymal cell variants. The inflammatory response was similar amongst metastatic or non-metastatic variant. Furthermore, the osteoblast-derived inflammatory cytokine response to metastatic variant breast cancer CM was less than CM from epithelial or mesenchymal variants. Therefore, these data further suggested that osteoblast treatment with human metastatic breast cancer cell conditioned media (MDA-MB-231 metastatic breast cancer cell variants, cells that mimic an osteoblast phenotype) resulted in an osteoblast inflammatory response that was not as great as treatment with the conditioned medium from epithelial or mesenchymal cell variants (MDA-MB-231BRMS, MDA-MB-435BRMS, MCF-10A, NIH/3T3, primary human foreskin, HC11, Comma-D1, HBL-100, primary mammary fibroblast, primary mammary epithelial, adipocyte, or murine fibroblast; cells that do not resemble an osteoblast phenotype.).

3.5.4: *Osteoblast-derived cytokine production was not increased following treatment of CM from osteoblasts*

In order to determine if the osteoblast-derived inflammatory cytokine response was due to treatment with any CM, MC3T3-E1 cells grown to 10 days were treated with their own CM. The response to osteoblast CM was very small. At most, osteoblast-derived IL-6 expression increased 3 fold over VM (Figure 3.12A)(Table 3.10). MCP-1 expression increases were also minimal. They increased no more than 1.3 fold over VM (Figure 3.12B)(Table 3.10). These data suggested that osteoblasts did not increase cytokine expression following treatment with osteoblast CM.

3.6: Osteoblast-derived cytokines did not increase when MC3T3-E1 cells were co-cultured indirectly with MDA-MB-231 metastatic breast cancer or human epithelial cell variants in a transwell system

When MC3T3-E1 cells were treated with the conditioned medium from MDA-MB-231 human metastatic breast cancer or human epithelial cell variants, osteoblast cytokine production was substantially increased from VM (Figures 3.6, 3.10). In addition, it was found that factors secreted by metastatic breast cancer cells which act on osteoblasts were soluble and not associated with membranes (Figure 3.8). However, osteoblast treated with the CM from metastatic breast cancer cells does not fully recapitulate events *in vivo* where the interaction of both cell types would occur. Therefore, in order to determine if the co-culture of osteoblasts with metastatic breast cancer or epithelial cells would increase osteoblast cytokine production, osteoblasts were co-cultured indirectly in a transwell system (Figure 2.3) with human metastatic breast cancer or epithelial cells. In order to avoid the possibility that human metastatic breast cancer cells would overgrow an osteoblast cell layer, an indirect transwell system co-culture method was utilized that keeps the co-cultivated cells separated and not in direct contact (Figure 2.3).

3.6.1: *Osteoblast-derived cytokines did not increase when MC3T3-E1 cells were co-cultured indirectly with MDA-MB-231 metastatic breast cancer cell variants in a transwell system*

An indirect, co-culture transwell system model was utilized to examine changes in osteoblast-derived cytokine production. In addition, a model in which the co-cultivated murine osteoblasts and human breast cancer cells were not in direct contact was utilized to ensure that the breast cancer cells would not overgrow the osteoblast cell layer. MDA-MB-231 human metastatic breast cancer cell variants were added to a tranwell assay system containing 10 or 20 day old osteoblasts at a ratio of 1 osteoblast : 1 human epithelial cell. MC3T3-E1 cells cultured separately, as well as MC3T3-E1 cells cultured with MC3T3-E1 cells were cultured as controls. After 72 hours, culture supernatants were assayed for cytokine expression via Murine Bio-Rad Bio-Plex™ Cytokine Assays. Culture supernatants from the top insert and bottom well were independently analyzed for cytokine expression. There were no differences between culture supernatant from the top insert compared to the bottom well.

When osteoblasts were grown to 10 days, there were no increases in osteoblast-derived cytokine expression in the presence of human metastatic breast cancer cells, change. In fact, murine VEGF expression decreased between 60-95% in an indirect co-culture of MC3T3-E1 cells and MDA-MB-231 metastatic breast cancer cell variants in a transwell system. These data suggested that osteoblast-derived cytokines, except for MCP-1 were not increased when 10 day old MC3T3-E1 cells were co-cultured indirectly in a transwell system with MDA-MB-231 human metastatic breast cancer cell variants under conditions of this study.

Interestingly, when 10 day old MC3T3-E1 cells were co-cultured indirectly with human metastatic breast cancer cells, osteoblast-derived MCP-1 production increased (Figure 3.13A)(Table 3.11A). The increase in osteoblast-derived MCP-1 production was small (12-47% increase when compared to VM) compared to larger increases seen (42-116% compared to VM) when 10 day old osteoblasts were treated with human metastatic

breast cancer cell CM (Figure 3.6A, Table 3.4A). The increase (12-47% compared to VM) in osteoblast-derived MCP-1 when 10 day old MC3T3-E1 cells were co-cultured indirectly with human metastatic breast cancer cells was consistent amongst biological replicates assayed. Thus, osteoblast-derived MCP-1 expression increased minimally (12-47% compared to VM; compared to 42-116% when 10 day old osteoblasts were treated with human metastatic breast cancer CM) when 10 day old MC3T3-E1 cells were co-cultured indirectly with human metastatic breast cancer cells.

MC3T3-E1 cells were co-cultured indirectly in a transwell system with MC3T3-E1 cells as a control. There were no differences between osteoblasts cultured alone (VM) and osteoblasts cultured with osteoblasts (Figure 3.13A)(Table 3.11A).

When osteoblasts were grown to 20 days, there were no differences in IL-6, KC, or MIP-2 expression (Figure 3.13B)(Table 3.11B). MCP-1 and VEGF cytokine expression, however, decreased between 64.2-71.5% from VM (Figure 3.13B)(Table 3.11B). These data suggested that VEGF and MCP-1 were slightly decreased when 20 day old MC3T3-E1 cells were co-cultured indirectly in a transwell system with MDA-MB-231 human metastatic breast cancer cell variants. These data additionally suggested that effects of human metastatic breast cancer cells on osteoblasts in an indirect, co-culture transwell system are more pronounced when osteoblasts are most mature (20 days) compared to when osteoblasts are grown to 10 days.

Twenty day old osteoblasts were co-cultured indirectly in a transwell system with osteoblasts as a control (Figure 3.13B)(Table 3.11B). No changes were seen in osteoblast-derived cytokine expression (Figure 3.13B)(Table 3.11B).

3.6.2: *Osteoblast-derived cytokines were not increased when MC3T3-E1 cells were co-cultured indirectly in a transwell system with human epithelial cell variants, except for indirect co-culture with hTERT-HME1 cells*

In order to assay for changes in osteoblast-derived cytokine production when osteoblasts were cultured in the presence of non-metastatic cells, MC3T3-E1 cells were co-cultured indirectly in a transwell system at a ratio of 1 osteoblast : 1 human epithelial cell with MDA-MB-231BRMS, MDA-MB-468P, or hTERT-HME1 cells. MC3T3-E1 cells, and MC3T3-E1 cells co-cultured indirectly in a transwell system with MC3T3-E1 cells were cultured as controls. After 72 hours, culture supernatants were assayed for cytokine expression via Murine Bio-Rad Bio-Plex™ Cytokine Assays.

When osteoblasts were grown to 10 days, their cytokine expression when co-cultured indirectly in a transwell system with MDA-231BRMS or MDA-468P cells did not change (Figure 3.14A)(Table 3.12A). In fact, VEGF expression decreased ~77.5% from VM (Figure 3.14A)(Table 3.12A). On the other hand, cytokine expression of osteoblasts co-cultured indirectly in a transwell system with hTERT-HME1 cells increased as much as 50 times compared to VM (Figure 3.14A)(Table 3.12A). No change from VM was observed when 10 day old osteoblasts were co-cultured indirectly in a transwell system with osteoblasts (Figure 3.14A)(Table 3.12A). These data suggested that osteoblast-derived cytokines did not increase when 10 day old osteoblasts were co-cultured indirectly in a transwells system with MDA-MB-231BRMS or MDA-MB-468P human non-metastatic breast cancer cells, but do increase when co-cultured indirectly in a transwell system with hTERT-HME1 human mammary epithelial cells.

When 20 day old osteoblasts were co-cultured indirectly in a transwell system

with MDA-231BRMS or MDA-468P cells, osteoblast-derived KC, MIP-2, and IL-6 did not increase (Figure 3.14B)(Table 3.12B). In fact, VEGF and MCP-1 osteoblast-derived expression decreased (57-79% compared to VM) when MC3T3-E1 cells were co-cultured indirectly in a transwell system with MDA-231BRMS or MDA-468P cells (Figure 3.14B)(Table 3.12B). On the other hand, cytokine expression of osteoblasts co-cultured indirectly in a transwell system with hTERT-HME1 cells was variable. Osteoblast-derived MIP-2 did not change; there was a decrease in osteoblast-derived MCP-1 and VEGF expression (19-57.2% compared to VM); but there was between a 2.5-6.5 fold increase compared to VM in osteoblast-derived IL-6 or KC expression (Figure 3.14B)(Table 3.12B). No differences in osteoblast-derived cytokine expression were observed when 20 day old osteoblasts were co-cultured indirectly in a transwell system with osteoblasts (Figure 3.14B)(Table 3.12B). These data suggested that osteoblast-derived cytokines from 20 day old MC3T3-E1 cells were not increased in response to the human non-metastatic breast cancer cell variants MDA-231BRMS or MDA-468P, but were variable in response to hTERT-HME1 cells, under conditions of this experiment.

In order to determine if osteoblast-derived cytokine expression would be altered with increased numbers of cancer cells, MC3T3-E1 cells were grown to either 10 or 20 days and co-cultured indirectly in a transwell system with MDA-MB-231W human metastatic breast cancer cells (used as a representative metastatic breast cancer cell line) at osteoblast : breast cancer cell ratios of 10:1, 1:1, and 1:2. MC3T3-E1 cells as well as MC3T3-E1 cells co-cultured indirectly in a transwell system with MC3T3-E1 cells (OB+OB) were cultured as controls. After 72 hours, culture supernatants were assayed for cytokine expression via Murine Bio-Rad Bio-Plex^{TM} Cytokine Assays. When MC3T3-E1 cells were co-cultured indirectly in a transwell system with other MDA-MB-231 metastatic breast cancer cell variants or human epithelial cells, results were similar amongst the cell lines assayed.

When osteoblasts were grown to 10 days, osteoblasts expression of KC, MIP-2, and IL-6 did not change (Figure 3.15A)(Table 3.13A). Osteoblast-derived VEGF expression slightly decreased (8-50%) from VM (Figure 3.15A)(Table 3.13A), and murine MCP-1 expression increased 20-30% over VM (Figure 3.15A)(Table 3.13A). Neither of the changes in osteoblast-derived cytokine expression occurred in a dose-dependent manner. These data suggested that when co-cultured indirectly in a transwell system with human metastatic breast cancer cells, osteoblast-derived cytokine expression of 10 day old osteoblasts was not altered in a dose-dependent manner under conditions of this experiment.

When MC3T3-E1 cells were grown to 20 days and co-cultured indirectly in a transwell system with MDA-MB-231W cells at osteoblast : human metastatic breast cancer cell ratios of 10:1, 1:1, and 1:2, osteoblast-derived cytokine expression of KC and MIP-2 did not change (Figure 3.15B)(Table 3.13B). Osteoblast-derived MCP-1 expression decreased 30-33% compared to VM (Figure 3.15B)(Table 3.13B), but osteoblast-derived IL-6 and VEGF expression increased up to 13 fold over VM (Figure 3.15B)(Table 3.13B). Neither the changes in murine MCP-1 nor IL-6 cytokine expression were dose-dependent. However, when MC3T3-E1 cells were co-cultured indirectly in a transwell system with MDA-MB-231W human metastatic breast cancer cells, osteoblast-derived VEGF expression increased with increasing quantity of human metastatic breast cancer cells. These data suggested that osteoblast-derived VEGF

expression of 20 day old osteoblasts co-cultured indirectly in a transwell system with MDA-MB-231W human metastatic breast cancer cells increased with increasing quantity of metastatic breast cancer cells, but osteoblast-derived cytokine production of KC, MIP-2, MCP-1, and IL-6 did not.

3.7: Osteoblast-derived cytokines were altered in a direct co-culture of MC3T3-E1 cells and MDA-MB-231W human metastatic breast cancer cells

It seemed unreasonable that CM from metastatic breast cancer cells should affect osteoblasts, while an indirect culture did not. Therefore, a direct cell culture was used. Zhang, et al. reported that direct cellular coupling between normal and cancerous cells resulted in an altered phenotype of the normal cells [63]. With direct cellular communication lacking in an indirect transwell co-culture system, perhaps direct cellular communication between osteoblasts and human cells, in addition to conditioned medium treatment, will also elicit a change in MC3T3-E1 cytokine expression.

A direct co-culture model was tested to examine for changes in osteoblast-derived cytokine concentration. MDA-MB-231W human metastatic breast cancer *cells* were added to 10 or 20 day old MC3T3-E1 cells at a ratio of 10 MC3T3-E1 cells : 1 MDA-MB-231W metastatic breast cancer cell. MC3T3-E1 cells were cultured separately as controls. After 48 hours, culture supernatants were assayed for cytokine expression via Murine Bio-Rad Bio-Plex™ Cytokine Assays. Examination by standard light microscopy revealed that breast cancer cells had attached to the osteoblast cell layer and proliferated. No cellular debris were observed.

Trends in osteoblast-derived cytokine response to breast cancer cells were similar between 10 or 20 day osteoblasts; however, cytokine increases were more pronounced in osteoblasts of the later differentiation stage, similar to that found with osteoblast responses to conditioned medium (Figure 3.6A-B). MIP-2 cytokine expression did not increase in 10 day osteoblasts (Figure 3.16A)(Table 3.14A). However, there was at least a two fold increase in KC, VEGF, IL-6, and MCP-1 expression compared to VM (Figure 3.16A)(Table 3.14A). A similar effect was seen with 20 day osteoblasts (Figure 3.16B). MIP-2 cytokine expression did not increase; however, there was at least a two fold increase in VEGF, IL-6, and MCP-1 expression (Figure 3.16B)(Table 3.14B). KC cytokine expression increased substantially, from undetectable amounts to 0.40 ng/ml (Figure 3.16B)(Table 3.14B). Thus, breast cancer cells exerted a direct effect on osteoblast cytokine production. Since metastatic breast cancer cells preferentially traffic to the femur metaphyses [40], which includes the growth plate, a direct affect on osteoblasts may have a profound effect on the bone microenvironment which may favor breast cancer cell colonization.

3.8: Summary

MC3T3-E1 cells, grown to various stages of growth as verified by alkaline phosphatase activity and calcium deposition (Figure 3.4), expressed the inflammatory cytokines IL-6, KC, MIP-2, VEGF, and MCP-1 in various concentrations (Table 3.2). When MC3T3-E1 cells were in the presence of human metastatic breast cancer cells or their conditioned medium for no more than 4 days, osteoblasts had normal morphology, differentiated, and deposited calcium (Figures 3.1-3.3). MC3T3-E1 cells additionally increased their production of inflammatory cytokines when in the presence of human

metastatic breast cancer cells or their conditioned medium (Figures 3.5-3.6)(Table 3.3-3.4). This increase was seen when osteoblasts were treated with human metastatic breast cancer CM (Figure 3.6)(Table 3.4) or in direct co-culture with human metastatic breast cancer cells (Figure 3.16)(Table 3.14). No differences were seen amongst human metastatic breast cancer cell variants assayed (Figure 3.6)(Table 3.4). Additionally, the increase in osteoblast-derived inflammatory cytokine production was dose-dependent (Figure 3.7)(Table 3.5). Furthermore, the factors causing MC3T3-E1 cells to increase their cytokine production when in the presence of metastatic breast cancer cells or their CM were not removed by ultracentrifugation (Figure 3.8)(Table 3.6). Finally, osteoblasts did not increase their production of inflammatory cytokines when treated with the CM from osteoblasts (Figure 3.12)(Table 3.10). MC3T3-E1 cytokine expression was not substantially altered, however, when osteoblasts were co-cultured indirectly with human metastatic breast cancer cells in a transwell assay (Figure 3.13, Figure 3.15)(Table 3.11, Table 3.13). This lack of increase in osteoblast-derived cytokine production may be due to technical problems (time of indirect co-culture, secreted protein binding to the membrane) of the indirect co-culture transwell assay. These data suggest that osteoblasts increase their production of inflammatory cytokines in a direct co-culture of human metastatic breast cancer cells or when treated with their conditioned media.

Part 4: RESULTS: THE EFFECT OF OSTEOBLASTS ON HUMAN BREAST CANCER AND HUMAN EPITHELIAL CELLS

4.1: Rationale

Osteoblasts increased their production of the inflammatory cytokines IL-6, KC, VEGF, MCP-1, and MIP-2 when treated with human metastatic breast cancer cells or their conditioned media (Figures 3.6, 3.16)(Tables 3.4, 3.14). In addition, it has been reported that cytokines and chemokines derived from human metastatic breast cancer cells, such as IL-8, are keys to understanding bone metastatic breast cancer [8, 44-46]. While it is evident that metastatic breast cancer cells affect osteoblast cytokine production, it is not known whether osteoblasts affect human metastatic breast cancer cytokine expression. Therefore, it was asked if there were changes in human-derived cytokine production when human metastatic breast cancer cells were co-cultured with osteoblasts. Thus, experiments described here focus on understanding the effect of osteoblasts on human metastatic breast cancer cells.

4.2: Untreated osteoblasts, metastatic breast cancer cells, and human epithelial cell variants expressed inflammatory cytokines

MC3T3-E1 production of inflammatory cytokines was increased when they were treated with conditioned medium from MDA-MB-231 human metastatic breast cancer or human epithelial cell variants compared to VM. In order to determine the cytokine production of untreated osteoblasts, metastatic breast cancer cells, and human epithelial cell variants, each cell type was cultured alone and assayed for cytokine expression.

To determine the cytokines expressed by each cell type, MC3T3-E1 cells, MDA-MB-231 variant breast cancer CM and human epithelial cell variant CM alone were assayed on a murine or human Bio-Rad Bio-Plex™. While all cell types expressed IL-6, VEGF, murine KC / human GRO-α, and murine MIP-2 / human IL-8 in various

quantities as represented by + (little: 0.01-0.08 ng/ml), ++ (modest amount: 0.09-0.4 ng/ml), and +++ (substantial amount: >0.5 ng/ml), MCP-1 was expressed in negligible amounts (<0.01 ng/ml) in the CM of all human epithelial cell variants assayed (Table 4.1). MC3T3-E1 cells expressed MCP-1 in comparatively substantial amounts (>2 ng/ml). Thus, MCP-1 was expressed by osteoblasts, but was not expressed by the human metastatic breast cancer or epithelial cell variants tested.

To determine the cytokines present in conditioned medium from breast cancer cell variants, conditioned medim from MDA-MB-231 variants were assayed (Human Bio-Rad Bio-Plex^{TM})(Figure 4.1). To correct for batch-to-batch variation, BCCM cytokine concentrations were normalized per one million cells. In the MDA-MB-231 variants examined, where at least three different batches of BCCM per variant was prepared and assayed, cell variation was typically less than 15%. Human IL-6 expression ranged from 0.01-0.26 ng/ml and human VEGF expression ranged from 0.36-13 ng/ml (Figure 4.1). Since human cells do not express murine MIP-2 or KC, we assayed for their human counterparts, IL-8 and GRO-α, respectively [55]. Human IL-8 expression ranged from 0.07-0.13 ng/ml and human GRO-α expression ranged from 0.03-0.13 ng/ml (Figure 4.1A). Human metastatic breast cancer cell variants produced negligible amounts of MCP-1; 0.009-0.016 ng/ml (Figure 4.1A). These concentrations were in sharp contrast to comparatively large amounts (~3 ng/ml) of murine-derived MCP-1 produced by untreated MC3T3-E1 cells (Figure 3.6A-B). Thus, MCP-1 was produced by MC3T3-E1 cells but *not* by human metastatic breast cancer cells.

Human epithelial cell variant conditioned medium was additionally assayed alone for cytokine expression (MDA-231BRMS, MDA-468P, and hTERT-HME1)(Figure 4.1B). In the human epithelial cell variants examined, at least three different batches of conditioned medium per variant were assessed, and intra-assay variation was typically less than 15%. Human epithelial cell variant conditioned medium expressed the same cytokines expressed by metastatic breast cancer conditioned medium; however, cytokine levels were much greater in conditioned medium from human epithelial cell variants (MDA-231BRMS, MDA-468P, and hTERT-HME1)(Figure 4.1B). Human IL-6 expression ranged from 0.026 – 0.04 ng/ml and human VEGF expression ranged from 0.54 – 0.87 ng/ml. Human IL-8 and GRO-α were assessed since cancer cells do not express MIP-2 or KC, respectively [55]. Human IL-8 expression ranged from 0.024 – 0.16 ng/ml and human GRO-α expression ranged from 0.007 – 0.82 ng/ml.

Human MCP-1 was produced by human epithelial cell conditioned medium alone in comparatively small amounts to MC3T3-E1 cells (Figure 4.1B). Human MCP-1 expression by human epithelial cell variant conditioned medium ranged from 0.001 – 0.02 ng/ml compared to ~3 ng/ml produced by osteoblasts (Figure 3.6A-B). Thus, MCP-1 was produced by MC3T3-E1 cells and *not* by the human epithelial cell variants, MDA-MB-231BRMS, MDA-MB-468P, or hTERT-HME1.

Finally, in order to determine if breast cancer cell-GFP variants expressed cytokines similar to non-GFP variants, MDA-MB-231-GFP variant BCCM were assayed (Human Bio-Rad Bio-Plex^{TM})(Figure 4.2). To correct for batch-to-batch variation, BCCM cytokine concentrations were normalized per one million cells. In the MDA-MB-231-GFP variants examined, where three different batches of BCCM per variant was assessed, cell variation was typically less than 15%. Human IL-6 expression ranged from 0.008-0.04 ng/ml and human VEGF expression ranged from 0.04-0.07 ng/ml (Figure

4.2). The human counterparts to murine MIP-2 and KC, IL-8 and GRO-α, respectively, were assayed [55]. Human IL-8 expression ranged from 0.02-0.12 ng/ml and human GRO-α expression ranged from 0.01-0.12 ng/ml (Figure 4.2). Human breast cancer cell-GFP variants produced negligible amounts of MCP-1; 0.001-0.002 ng/ml (Figure 4.2), which was comparable to that seen with metastatic breast cancer and human epithelial cell variant MCP-1 expression (Figure 4.1A-B). These concentrations were in contrast to comparatively large amounts (~3 ng/ml) of murine-derived MCP-1 produced by untreated MC3T3-E1 cells (Figure 3.6A-B). Thus, MCP-1 was produced by MC3T3-E1 murine cells but *not* by human breast cancer cells that express GFP.

4.2.1: *Cancer cell-derived cytokines were expressed in the soluble fraction of MDA-MB-231W conditioned medium*

To determine if the cytokines in breast cancer conditioned medium were found in the soluble fraction or associated with membranes, breast cancer conditioned medium that was ultracentrifuged at 100,000 xg was assayed for cytokine expression via Human Bio-Rad Bio-Plex™ (Figure 4.3). There was no difference in human IL-6 expression between BCCM and ultracentrifuged BCCM (0.002 ng/ml)(Figure 4.3)(Table 4.2). Furthermore, differences in human IL-8, MCP-1, and GRO-α expression were negligible (Figure 4.3)(Table 4.2). A 0.7 fold change was noted in human VEGF expression between BCCM and ultracentrifuged BCCM (Figure 4.3)(Table 4.2). Thus there were little to no differences in the cytokines tested between BCCM and ultracentrifuged BCCM.

Similar to human metastatic breast cancer and human epithelial cell variants, ultracentrifuged BCCM contained small amounts of MCP-1; 0.0004 ng/ml (box, Figure 4.3)(Table 4.2). Comparable to the relatively large amounts of MCP-1 produced by untreated osteoblasts (~3 ng/ml, Figure 3.6A-B), these amounts were negligible. Thus, MCP-1 was produced by MC3T3-E1 cells but *not* by human metastatic breast cancer cells.

4.3: Human-derived cytokines decreased when human metastatic breast cancer or human epithelial cell variants were co-cultured indirectly in a transwell system with murine osteoblasts

Contrary to the increase in osteoblast-derived cytokines observed when MC3T3-E1 cells were co-cultured directly with human metastatic breast cancer cells or treated with their CM (Figure 3.6-3.10, Figure 3.16), osteoblast-derived cytokines, except for MCP-1, were not increased when human metastatic breast cancer or human epithelial cells were co-cultured indirectly in a transwell system with MC3T3-E1 cells (Figure 3.13). As described in Section 3.6, this finding may indicate a possible technical problem with the assay. In particular, it may be the case that the seventy-two hour time frame between when the two cell populations were co-cultured indirectly with each other was not long enough to fully recapitulate events that may occur in an *in vivo* setting. The seventy-two hour time frame was utilized to avoid cancer cell migration into the underlying osteoblast cell layer, but was a limitation of the assay. However, it was asked if there were changes in human-derived cytokine production when the cancer cells were co-cultured indirectly with osteoblasts in a transwell system.

MDA-MB-231 human metastatic breast cancer cell variants were added to a transwell assay system containing 10 or 20 day old osteoblasts at an osteoblast : breast cancer cell ratio of 1:1. MDA-MB-231 metastatic breast cancer cell variants were cultured separately as controls. After 72 hours, culture supernatants were assayed for the expression of breast cancer cell cytokines via Human Bio-Rad Bio-Plex™ Cytokine Assays.

Human cancer-cell derived cytokine production substantially decreased up to 100% compared to VM, when cancer cells were co-cultured indirectly in a transwell system with 10 day old MC3T3-E1 cells (Figure 4.4A-D)(Table 4.3A). In addition, MCP-1 was not expressed by cancer cells alone or in an indirect transwell co-culture system with osteoblasts (box, Figure 4.4A-D). These data suggested that breast cancer cells decreased their production of certain cancer-cell derived cytokines when co-cultured indirectly in a transwell system with 10 day old osteoblasts.

Similar trends were found when osteoblasts were grown to 20 days. When human metastatic breast cancer cell variants were co-cultured indirectly in a transwell system with 20 day old MC3T3-E1 cells, human cancer cell-derived cytokine production decreased up to 100% (Figure 4.5A-D)(Table 4.3B). In either case, MCP-1 was not expressed by either the cancer cells alone or when co-cultured indirectly in a transwell system with osteoblasts (box, Figure 4.5A-D).

Interestingly, when MDA-MB-231BO human bone-seeking metastatic breast cancer cells were co-cultured indirectly in a transwell system with 10 day old MC3T3-E1 cells, human cancer cell-derived IL-8 production decreased only by 17% compared to decreases of up to 100% with other metastatic breast cancer cell variants (Figure 4.4C)(Table 4.3A). While this trend was only seen with cancer cell-derived IL-8 expression in an indirect co-culture of MC3T3-E1 cells and MDA-MB-231BO human metastatic breast cancer cells, similar trends were also seen when MDA-MB-231BRMS and MDA-MB-468P human non-metastatic breast cancer cells were co-cultured indirectly with 20 day old MC3T3-E1 cells (Figure 4.5A,B)(Table 4.4B). Therefore, it may be the case that cancer cell-derived IL-8 is particularly important in the metastatic progression of MDA-MB-231BO bone-seeking cancer cells.

Furthermore, human epithelial cell-derived cytokine production decreased as much as 100% compared to VM when MDA-MB-231BRMS, MDA-MB-468P, or hTERT-HME1 cells were co-cultured indirectly in a transwell system with 10 day old MC3T3-E1 cells (Figure 4.6A-C). Additionally, MCP-1 was not expressed by MDA-MB-231BRMS or hTERT-HME1 cells (box, Figure 4.6A,C)(Table 4.4A). MCP-1 was, however expressed by MDA-MB-468P cells alone (0.6 ng/ml), but decreased 95% to 0.03 ng/ml when these cells were in the presence of MC3T3-E1 cells (Figure 4.6B). These data suggested that human epithelial cell variants decreased their production of human epithelial cell-derived cytokines when co-cultured indirectly in a transwell system with 10 day old osteoblasts.

Furthermore, when human epithelial cell variants were co-cultured indirectly in a transwell system with 20 day old MC3T3-E1cells, human epithelial cell-derived cytokine production decreased up to 100% over VM (Figure 4.7A-C)(Table 4.4B). Additionally, MCP-1 was not expressed by MDA-MB-231BRMS or hTERT-HME1 cells either alone or when co-cultured indirectly in a transwell system with osteoblasts (box, Figure 4.7A,C). MCP-1 was expressed by MDA-MB-468P cells alone (0.6 ng/ml) and

increased slightly (50%) when co-cultured indirectly in a transwell system with MC3T3-E1 cells (0.9 ng/ml)(Figure 4.7B). IL-6 was also expressed by MDA-MB-468P or MDA-MB-231BRMS cells alone (0.08; 0.002 ng/ml, respectively) and slightly increased when these cells were co-cultured indirectly in a transwell system with MC3T3-E1 cells (0.5; 0.01 ng/ml, respetively)(Figure 4.7). Finally, IL-8 and GRO-α were also expressed by hTERT-HME1 cells alone (1.0; 1.5 ng/ml, respectively), but slightly increased when these cells were co-cultured indirectly in a transwell system with MC3T3-E1 cells (1.2; 1.7 ng/ml, respectively)(Figure 4.7B). However, these increases were small compared to the substantial decreases (up to 100%) seen in both human metastatic and non-metastatic breast cancer cell-derived cytokines when co-cultured indirectly in a transwell system with osteoblasts (Figure 4.4A-D, Figure 4.5A-D, Figure 4.6A-C). These data suggested human epithelial cell variants decreased their cytokine production when co-cultured indirectly in a transwell system with 20 day old osteoblasts.

In order to verify the substantial decreases seen in cancer cell-derived cytokine expression when cancer cells were co-cultured indirectly in a transwell system with osteoblasts (Figure 4.4-4.7), a control of cancer cells co-cultured indirectly in a transwell system with cancer cells was carried out. MDA-MB-231W human metastatic breast cancer cells were co-cultured indirectly in a transwell system with MDA-MB-231W human metastatic breast cancer cells at a cancer cell : cancer cell ratio of 1:1. Seventy-two hours later, the resultant culture supernatants were collected and assayed for cancer cell-derived cytokine expression via a Bio-Rad Bio-Plex™ Human Cytokine Assay. Cancer cell-derived cytokine expression of human metastatic breast cancer cells was substantially decreased (up to 100%) compared with breast cancer cells co-cultured in a transwell system with breast cancer cells (Figure 4.8)(Table 4.3-4.4).

4.3.1: *Human-derived cytokine expression was dose-dependent*

In order to determine if human-derived cytokine production increased with increasing quantity of human cells, human metastatic breast cancer or human epithelial cell variants were cultured in a transwell system *alone* in two different quantities: 1) Dose #1 (representing the indirect transwell co-culture of osteoblast : human cell ratio of 1:1) or 2) Dose #2 (representing the indirect transwell co-culture of osteoblast : human cell ratio of 1:2). Seventy-two hours later, culture supernatants were assayed for human cytokine expression via Human Bio-Rad Bio-Plex™ Cytokine Assays.

Human-derived IL-6 expression increased with increasing human cell number (Figure 4.9). IL-6 expression increased up to 4.5 fold when a 1:1 metastatic cell ratio was compared to a 1:2 ratio (Figure 4.9)(Table 4.5). Furthermore, IL-6 expression increased up to 4 fold when a 1:1 human epithelial cell ratio was compared to a 1:2 ratio (Figure 4.9). Similar trends were found with the expression of human IL-8, VEGF, and MIP-2 (Appendix 7.4). Thus, when increased numbers of human cells were cultured *alone* in a transwell system, human-derived cytokines similarly increased in a dose-dependent manner.

4.4: Cancer-derived cytokines were altered in a direct co-culture of MC3T3-E1 cells and MDA-MB-231W human metastatic breast cancer cells

It seemed unreasonable that CM from metastatic breast cancer cells should affect osteoblasts, while an indirect co-culture did not. Therefore, a direct cell culture was used.

Zhang, et al. reported that direct cellular coupling between normal and cancerous cells resulted in an altered phenotype of the normal cells [63]. With direct cellular communication lacking in an indirect transwell co-culture system, perhaps direct cellular communication between osteoblasts and human cells, in addition to conditioned medium treatment, will also elicit a change in MC3T3-E1 cytokine expression.

In order to determine if cancer cell-derived cytokine production was altered in direct co-culture with osteoblasts as it was in the transwell system, MDA-MB-231W human metastatic breast cancer cells (used as a representative metastatic breast cancer cell line) were directly co-cultured with MC3T3-E1 cells grown to 10 or 20 days. MDA-MB-231W human metastatic breast cancer *cells* were added to 10 or 20 day old MC3T3-E1 osteoblasts at a ratio of 10 MC3T3-E1 cells : 1 MDA-MB-231W metastatic breast cancer cell. MDA-MB-231W metastatic breast cancer cells were cultured separately as controls. Examination by standard light microscopy revealed that breast cancer cells had attached to the osteoblast cell layer and proliferated. No cellular debris were observed. After 48 hours, culture supernatants were assayed for cytokine expression via Human Bio-Rad Bio-Plex^{TM} Cytokine Assays.

Trends in cancer cell-derived cytokine expression were similar between 10 and 20 day old osteoblasts (Figure 4.10A-B)(Table 4.6). However similarly to that seen in the transwell system (Figure 4.4-4.7), cancer cell-derived cytokine production *decreased* up to 100% from breast cancer cells cultured alone, in a direct co-culture with osteoblasts (Figure 4.10)(Table 4.6). Cancer cell-derived MCP-1 and VEGF expression decreased by 100%, IL-8 expression deceased 93%, IL-6 expression decreased 90%, and GRO-α expression decreased 89% from VM (Figure 4.10)(Table 4.6). Thus, osteoblasts exerted a direct effect on metastatic breast cancer cells *in vitro*.

4.5: Summary

Human metastatic breast cancer cells cultured alone expressed the inflammatory cytokines IL-8, VEGF, IL-6, and GRO-α in various concentrations (Figure 4.1)(Table 4.1). However, human metastatic breast cancer cells did NOT express MCP-1, which was expressed in comparatively large amounts (~3 ng/ml) by MC3T3-E1 osteoblast (Figure 3.6, Figure 4.1)(Table 4.1). Furthermore, the cancer cell-derived cytokines IL-6, VEGF, IL-8, and GRO-α were expressed in the soluble fraction of MDA-MB-231W conditioned medium (Figure 4.2). When MDA-MB-231 human metastatic breast cancer cell variants were co-cultured indirectly with MC3T3-E1 cells, osteoblast-derived cytokine expression of MC3T3-E1 cells did not increase (Figure 3.13). To the contrary, human-derived cytokine production *decreased* (Figures 4.4-4.7, 4.10). Furthermore, human-derived cytokine expression was dose-dependent when human metastatic breast cancer or human epithelial cells were cultured alone in increasing quantities in a transwell system (Figure 4.9). These data suggest that osteoblasts exerted a direct effect on metastatic breast cancer cells *in vitro.*

Task 2. **To determine how bone-derived inflammatory cytokine production is altered in response to breast cancer cells *in vivo*. (Months 13-17)**

Part 5: RESULTS: BONE-DERIVED CYTOKINES WERE ALTERED IN THE PRESENCE OF HUMAN BREAST CANCER CELLS IN AN *IN VIVO* MURINE MODEL

5.1: Rationale:

Osteoblast-derived cytokines increased when MC3T3-E1 cells were treated with human metastatic breast cancer cell conditioned medium and when directly co-cultured with human metastatic breast cancer cells *in vitro*. In order to assess osteoblast-derived cytokine production *in vivo*, human breast cancer cell variants were inoculated via intracardiac injection into athymic nude mice. Three or four weeks post-inoculation, mice were euthanized and cytokine expression in the bone microenvironment was assessed via cytokine arrays and immunohistochemistry.

5.2: Human breast cancer cells traffic to the ends of the long bones of mice

In order to assay bone-derived cytokine production in cancer-bearing mice, an *in vivo* model was used. Three weeks post-inoculation, femurs from mice injected with metastatic or non-metastatic human breast cancer cells were harvested, cleaned free of soft tissue, and photographed using light and fluorescent stereo-microscopes. MDA-MB-231W-GFP (Figure 5.1A), MDA-MB-231PY-GFP (circle, Figure 5.1B), and MDA-MB-231BO-GFP (circle, Figure 5.1C) human breast cancer cells had metastasized to the bone, colonizing areas which include the ends of long bones. MDA-MB-231BRMS-GFP (circle, Figure 5.1D) cells additionally disseminated to ends of long bones of mice. It has been reported that MDA-MB-231BRMS-GFP cells disseminate to the ends of long bones of mice, but do not form locally invasive tumors [15]. Therefore, both human metastatic and the non-metastatic BRMS breast cancer cell variants trafficked to the ends of long bones of mice. As seen by fluorescence stereo-microscopy, both MDA-MB-231PY-GFP (circle, Figure 5.1B) and MDA-MB-231BO-GFP (circle, Figure 5.1C) human metastatic breast cancer cell variants appeared less bright than MDA-MB-231W-GFP (Figure 5.1A). In order to determine if MDA-MB-231PY-GFP and MDA-MB-231BO-GFP human metastatic breast cancer cell variants also were less fluorescent pre-inoculation, flow cytometry was carried out. GFP fluorescence intensity pre-inoculation was ~1.5 log less in both MDA-MB-231PY-GFP (grey peak) and MDA-MB-231BO-GFP (blue peak) compared to MDA-MB-231W-GFP (red peak)(Figure 5.2A-B). The fluorescence intensity of MDA-MB-231PY-GFP (grey peak, foreground) and MDA-MB-231BO-GFP (blue peak, background) were comparable (Figure 5.2C). Therefore, the fluorescence intensity of MDA-MB-231PY-GFP and MDA-MB-231BO-GFP human metastatic breast cancer cell variants were less, pre-inoculation, than MDA-MB-231W-GFP.

5.3: Bone-derived cytokine production was increased in cancer-bearing mice

To assay for bone-derived cytokine production in cancer-bearing mice, femurs were harvested, cut into bone metaphyses (ends) and bone diaphysis (shaft), bone marrow flushed, and bone pieces independently crushed and cultured. Twenty-four hours later, culture supernatants were assayed for cytokine expression (Murine Bio-Rad Bio-

Plex™ Cytokine Assays). A xenograft model system (human cancer cells inoculated into athymic mice) permitted species-specific cytokine detection. Changes in the murine-derived cytokine expression from individual mice were treated separately and not averaged to avoid the confounding of data by any potential outlier mice (due to illness or unexplained inflammation).

Bone-derived cytokine expression was increased in the metaphyses of MDA-MB-231W-GFP cancer-bearing mice (Figure 5.3A-C). In particular, the largest increase, compared to non-cancer-bearing mice, was found in the region distal to the hip (Figure 5.3C)(Table 5.1). These results were in agreement with Phadke, et al., who had found that metastatic breast cancer cells preferentially traffic to bone ends and first seed the region distal to the hip, followed by the area proximal to the hip [40]. The largest change in bone-derived cytokine production of cancer-bearing femurs was also found in the region distal to the hip (Figure 5.3C)(Table 5.1), followed by proximal to the hip (Figure 5.3A)(Table 5.1). Little change was seen in bone-derived cytokine production of the bone diaphysis compared to non-cancer-bearing mice (Figure 5.3B)(Table 5.1).

These same trends were found in femurs harvested from mice inoculated with MDA-MB-231PY-GFP, MDA-MB-231BO-GFP bone-seeking, and MDA-MB-231BRMS-GFP human breast cancer cell variants. The largest increase in bone-derived cytokine production was found in the region distal to the hip (Figure 5.4-5.6A)(Table 5.1), followed by the region proximal to the hip (Figure 5.4-5.6C)(Table 5.1). Less substantial increases in bone-derived cytokine production were seen in the shaft (Figure 5.4-5.6B)(Table 5.1). While no major differences were found in cytokine expression amongst breast cancer cell variants, bone-derived cytokine expression was increased the most in mice inoculated with MDA-MB-231BO-GFP bone-seeking cells (Figure 5.5A-C). The metastatically suppressed MDA-MB-231BRMS-GFP cells disseminated to murine bone (Figure 5.1D); however, changes in bone-derived cytokine expression were larger in the femurs of mice inoculated with human metastatic breast cancer cell variant (Table 5.1). Thus, bone-derived cytokines were increased in the presence of human breast cancer cells *in vivo*.

5.4: The bone microenvironment minimally altered cancer cell-derived cytokine production

To determine if the bone microenvironment altered cytokine production of inoculated cancer cells, the cells were retrieved from the bone marrow of femurs of mice. Post-inoculation cancer cells were expanded to no more than 2 passages post-recovery, where alterations in cytokine expression due to proliferation have been previously found to be minimal, and BCCM subjected to Human Bio-Rad Bio-Plex™ Cytokine Assays. While additional murine cells may have been present in the retrieved cells, the Bio-Rad Bio-Plex™ Cytokine Assay was specific for human cytokines, and was used to measure cytokines produced by the cancer cells.

All breast cancer cell lines were recovered from bone marrow except MDA-MB-231BRMS-GFP cells which did not grow in culture. BCCM from retrieved cells from mice inoculated with MDA-MB-231W-GFP, MDA-MB-231PY-GFP, and MDA-MB-231BO-GFP human metastatic breast cancer cells did not exhibit substantial differences in human cancer cell-derived cytokine expression compared with the same cells pre-inoculation (Figure 5.7A-C)(Table 5.2A). In fact, the conditioned medium of some

retrieved cells expressed a smaller amount of cytokines than pre-inoculated cells (Figure 5.7A-C)(Table 5.2B). While in some instances the cytokine expression was decreased 100%, the cytokine concentration in these cancer cells prior to exposure to the bone microevvironment (control) initially was small (~0.013 ng/ml)(Figure 5.7A-C). These concentrations are small in comparison to bone-derived cytokine production (up to ~15 ng/ml)(Figures 5.3-5.6). Thus, the bone microenvironment did not substantially alter cancer cell-derived cytokine production under conditions of this study.

5.5: Murine-derived cytokine expression was minimally altered in the bone marrow plasma of cancer-bearing mice

Because bone-derived cytokines were increased in the presence of human breast cancer cells (Figure 5.3-5.6), the bone marrow plasma of cancer-bearing mice was assessed for changes in cytokine expression. Bone marrow plasma was collected from the femoral ends and shaft of mice inoculated with MDA-MB-231-GFP breast cancer cell variants and subjected to a Murine Bio-Rad Bio-Plex™ Serum Cytokine Assay. In order to conduct the Bio-Rad Bio-Plex™ Serum Cytokine Assay, serum samples were diluted 4 fold with serum diluent as per manufacturer's instructions. In addition, the bone marrow itself was flushed in a volume of 1 ml, further diluting cytokines present. Therefore, upon conducting the assay, samples, and the cytokines present within them, were diluted 5 fold. Some changes in the murine-derived cytokine expression in the bone marrow plasma from murine femur ends were found (Figure 5.8A-D)(Table 5.3A). In some cases, murine-derived cytokine production increased; however, these increases (to 0.006-0.035 ng/ml) were between 0-7 fold that of the murine-derived cytokine production in the bone marrow plasma of the control mouse (0.001–0.04 ng/ml)(Figure 5.8A-D)(Table 5.3A). In addition, the murine-derived cytokine expression of murine cytokines found in the bone marrow plasma of control- and cancer-bearing mice was small (0.001-0.04 ng/ml)(Figure 5.8A-D)(Table 5.3A), compared to cytokine concentrations present in the femurs of control- and cancer- bearing mice (0.01-11.5 ng/ml)(Figures 5.3-5.6). In other cases, murine-derived cytokine production deceased (Figure 5.8A-D)(Table 5.3B). Even though some decreases were 100% that of the murine-derived cytokine expression of the control mouse, in these cases the control mouse bone marrow plasma cytokine expression was small (0.004 ng/ml). Since the limit of detection of the Bio-Rad Bio-Plex™ is between 0.002-0.005 ng/ml, these small changes in murine-derived cytokine expression of bone marrow plasma may be function of sampling error by the assay. Therefore, the differences in the murine-derived cytokine expression of the bone marrow plasma from the metaphyses of control- and cancer-bearing mice were considered minimal. Murine-derived KC expression was not detected in bone marrow plasma from femoral ends (Figure 5.8). It is possible that changes in cytokine expression of the bone marrow plasma were beyond the limits of detection (0.002-0.005 ng/ml) of the Bio-Rad Bio-Plex™ Serum Cytokine Assay due to the 5 fold dilution of the samples necessary to carry out this assay.

Furthermore, small changes in the murine-derived cytokine expression in the bone marrow plasma from murine femur shafts were found (Figure 5.9A-D). Again, in certain cases, murine-derived cytokine production increased; however, these increases (to 0.001-0.029 ng/ml) were between 0-29 fold that of the murine-derived cytokine production in the bone marrow plasma of the control mouse (0–0.003 ng/ml)(Figure 5.9A-D)(Table

5.3A). In addition, the murine-derived cytokine expression of murine cytokines found in the bone marrow plasma of control- and cancer-bearing mice was small (0-0.067 ng/ml)(Figure 5.9A-D)(Table 5.3A), compared to cytokine concentrations present in the femurs of control- and cancer-bearing mice (0.01-11.5 ng/ml)(Figures 5.3-5.6). In other cases, murine-derived cytokine production deceased (Figure 5.9A-D)(Table 5.3B). Even though some decreases were up to 92% that of the murine-derived cytokine expression of the control mouse, in these cases the control mouse bone marrow plasma cytokine expression was small (0.067 ng/ml)(Figure 5.9A-D)(Table 5.3B). These differences were considered minor. Additionally, murine-derived KC expression was not detected in bone marrow plasma from the femoral shaft of cancer-bearing or non-cancer-bearing mice (Figure 5.9). Again, it may be possible that changes in cytokine expression of the bone marrow plasma were beyond the limits of detection of the Bio- Rad Bio-Plex™ Serum Cytokine Assay due to the 5 fold dilution of samples. Thus, under conditions of this experiment, inflammatory cytokine production of bone marrow plasma of the femoral ends or shaft was minimally altered in cancer-bearing mice.

5.6: Murine-derived cytokines were minimally altered in the blood serum of cancer-bearing mice

To determine if the murine-derived cytokines were altered in the blood serum of cancer-bearing mice, blood serum was collected from mice inoculated with MDA-MB-231-GFP breast cancer cell variants as described in the Materials and Methods and subjected to a Murine Bio-Rad Bio-Plex™ Serum Cytokine Assay. Similar to the processing of bone marrow plasma samples, blood serum samples were diluted 4 fold with serum diluent as per manufacturer's instructions in order to conduct the Bio-Rad Bio-Plex™ Serum Cytokine Assay. Small changes in the murine-derived cytokine expression were found (Figure 5.10A-D)(Table 5.4). In some cases, there appeared to be small increases in murine-derived cytokine production (Figure 5.10)(Table 5.4A). However, these increases were minor in comparison to the small concentrations of murine-derived cytokines present in the blood of control- and cancer-bearing mice (1.2-10 fold of 0-0.067 ng/ml)(Figure 5.10)(Table 5.4A). In other cases, murine-derived cytokine expression appeared to decease (Figure 5.10)(Table 5.4B). However, these differences were considered as minor variations around the baseline (0.005 ng/ml to 0 ng/ml)(Figure 5.10).

Murine-derived KC expression was not detected in any blood serum sample (Figure 5.10). Again, it may be possible that changes in cytokine expression of the blood serum were beyond the limits of detection of the Bio- Rad Bio-Plex™ Serum Cytokine Assay due to the 5 fold dilution of samples. Thus, there were no substantial changes in the production of inflammatory cytokines of the blood serum from cancer-bearing mice under the conditions of this experiment.

5.7: Metastastic breast cancer cells were localized to the trabecular bone

Three approaches were used to determine tumor cell localization within bone: 1) μCT, 2) MRI, and 3) densitometry. In order to assess cancer- and non-cancer-bearing bones using μCT, tibia from non-cancer-bearing and cancer-bearing mice three weeks post-inoculation were photographed and scanned using a μCT40 Desktop Cone-Beam MicroCT Scanner. Three dimensional models of the bone, trabeculae, and tumor, if

present, were constructed and quantitated. Tumors in cancer-bearing tibia were found in bone metaphyses as opposed to the bone diaphysis. A tumor in the bone metaphysis, as indicated by arrows and fluorescence, is illustrated in a representative tibia (posterior view, Figure 5.11A-B). The tumor was localized to the trabecular bone (arrow, Figure 5.11C-D). Interestingly, trabecular bone volume as calculated in the cancer-bearing tibia, was 75% less (inset, Figure 5.11C) than non-cancer-bearing mice (inset, Figure 5.11E). Results were similar amongst tibiae assayed from mice inoculated with MDA-MB-231-GFP variants. This indicates that trabecular bone volume was decreased in cancer-bearing mice.

5.8: Tumor volume was estimated via MRI

MRI was used to confirm tumor location and determine the tumor volume of which was highly heterogenous. Femurs were photographed using light microscopy (Figure 5.12A, E) and fluorescence stereo-microscopy (Figure 5.12B, F) to initially detect tumors. In this example, a non-cancer-bearing (Figure 5.12A-D) and cancer-bearing (Figure 5.12E-H) femur were shown. A tumor was detected in the bone metaphysis distal to the hip of an MDA-MB-231W-GFP cancer-bearing mouse four weeks post-inoculation. The signal from the tumor, shown as white mass in the region distal to the hip (Figure 5.12G), was segmented (Figure 5.12H) and bone volume calculated. In this example, tumor to bone volume was estimated to be 2.7%, with the absolute volume of tumor estimated to be 1.32 mm^3. Tumor localization within the bone was similar among assayed femurs from mice inoculated with cancer cell variants. Control femurs were from non-cancer-bearing mice (e.g. Figure 5.12A-D).

5.9: Bone mineral density was estimated via densitometry

Densitometry was used to estimate bone mineral density of cancer-bearing and non-cancer-bearing mice. In this example, tibiae from non-cancer-bearing and cancer-bearing mice that were also assessed for tumor localization via μCT (Figure 5.11E-F, Figure 5.11A-D, respectively) were utilized. The bone mineral density of the non-cancer-bearing tibia as a whole was estimated to be 0.046 g/cm^2. This measurement is in contrast to the estimated bone mineral density of the cancer-bearing tibia as a whole, which was 0.043 g/cm^2. Therefore, there was an ~7% decrease in the bone mineral density of the cancer-bearing tibia as a whole, compared to the non-cancer-bearing tibia as a whole. Thus, the overall bone mineral density of a cancer-bearing tibia was less than a non-cancer-bearing tibia. Results were similar amongst other cancer- and non-cancer-bearing bones assayed.

5.10: Murine MCP-1 and VEGF were localized to the trabecular bone matrix and murine IL-6 to the bone marrow in both non-cancer-bearing and cancer-bearing mice

Immunohistochemistry was used to localize murine VEGF and MCP-1 in the femur. A xenograft model system (human cancer cells inoculated into mice) permitted species-specific cytokine detection. Both murine VEGF and MCP-1 were detected in the trabecular bone matrix of femur metaphyses near the growth plate, in defined regions in both the areas proximal (Figure 5.13A-B) and distal (Figure 5.13C-D) to the hip. These

regions of cytokine expression were found in both cancer-bearing and non-cancer-bearing mice. Neither MCP-1 nor VEGF were found in the bone marrow (Figure 5.13E-F). No qualitative differences were detected via immunohistochemistry with cytokine expression between non-cancer-bearing and cancer-bearing mice or amongst femurs containing metastatic or non-metastatic MDA-MB-231-GFP variants.

The cortical bone of control and cancer-bearing femurs was also examined for the presence of murine MCP-1 and VEGF via immunohistochemistry. Both murine MCP-1 and VEGF were detected in a 10-50 μm wide strip in cortical bone of the metaphyseal periphery (arrows, Figure 5.14A-D). These cytokines were seen in both regions proximal (murine VEGF, Figure 5.14A; murine MCP-1, Figure 5.14B) and distal to the hip (murine VEGF, Figure 5.14C; murine MCP-1, Figure 5.14D) of murine femurs. Neither murine MCP-1 nor VEGF were localized in the diaphysis (murine MCP-1, Figure 5.14E; murine VEGF, Figure 5.14F). Murine MCP-1 and VEGF were not detected in the bone marrow (Figure 5.13E-F). No visual differences in cytokine expression of murine MCP-1 or VEGF were apparent between non-cancer-bearing or cancer-bearing femur sections or amongst MDA-MB-231-GFP breast cancer cell variants.

Femur sections were also stained for murine IL-6 via immunohistochemistry. Interestingly, murine IL-6 was not present in the matrix or localized to the metaphyseal regions of the femur. Instead, ~100-110 small clumps of cells per field of view, staining positive for murine IL-6, were found throughout the bone marrow (Figure 5.15); there was no specific area of localization. No differences were found between non-cancer-bearing or cancer-bearing mice, nor metastatic breast cancer cell variants.

5.11: Cytokine expression was detected in an area ~150 μm beyond the tumor

While no differences in the expression of murine cytokines in the trabecular bone or cortical bone were detected in cancer-bearing mice compared to non-cancer-bearing mice, it was possible that cytokine expression was altered in areas of the bone adjacent to the tumor. In order to assay for the production of cytokines nearby tumor cells, MDA-MB-231W-GFP cells were detected via fluorescence stereo-microscopy in trabecular bone of the region distal to the hip (Figure 5.16A, box). In the corresponding immunohistochemistry image (Figure 5.16B), cancer cells were localized by staining with anti-GFP IgG. Tumor cells were seen adjacent to cortical bone, slightly superior to trabecular bone (Figure 5.16A-B). Tumor cells were also found in the marrow cavity, but not in the cortical bone matrix (Figure 5.16B). When murine MCP-1 (Figure 5.16C), murine VEGF (Figure 5.16D), and human VEGF (Figure 5.16E) presence were assayed via immunohistochemistry in cancer-bearing sections, none were detected directly adjacent to the tumor. However, murine MCP-1 and VEGF presence was detected in areas about 150 μm beyond the tumor. In a representative femur (Figure 5.17A-D), in which a tumor was detected in the region distal to the hip (rectangle), both murine VEGF and MCP-1 were detected in cortical bone (circle). Interestingly, both cytokines wereexpressed in a gradient, i.e. regions superior to the tumor expressed more cytokine than adjacent to the tumor (murine MCP-1, Figure 5.17A; murine VEGF, Figure 5.17B).

Furthermore, the cytokine gradient was only observed in the area beyond the tumor. When cortical bone on the opposite side of the femur was examined (triangle), both murine MCP-1 (Figure 5.17C) and murine VEGF (Figure 5.17D) were present in defined strips. No differences were seen between cancer-bearing or non-cancer-bearing

mice. Additionally, no differences were seen between cancer cell variants.

5.12: Human VEGF expression increased with increased tumor size

Human VEGF tumor-derived cytokine expression was also assayed. Human breast cancer cells do not express MCP-1 (Figure 4.1-4.3); therefore, human MCP-1 expression was not assessed. The presence of human VEGF in the bone microenvironment increased with increasing tumor size. It was found that in instances of low tumor to bone volume, where murine bone marrow tissue was infiltrated with human cancer cells, human VEGF expression was low (comparatively small number of human cancer cells (circles) to large number of murine bone marrow cells (arrows))(Figure 5.18A). However, in instances where there was high tumor to bone volume, whereby cancer cells encompassed the region and little to no murine tissue remained, human VEGF expression from tumor cells was detected in copious amounts (comparatively large number of human cancer cells to small number of murine bone marrow cells) (Figure 5.18B). This variation was observed in mice inoculated with MDA-MB-231W-GFP and MDA-MB-231PY-GFP metastatic breast cancer cells. Under the conditions used in this study, increases in tumor-derived VEGF were not seen in femurs from MDA-MB-231BO-GFP or MDA-MB-231BRMS-GFP inoculated mice.

5.13: Megakaryocyte numbers increased in cancer-bearing femur sections

As femur sections were examined for cytokine presence, it was noticed that there were more megakaryocytes (morphologically distinguishable via Gill's hematoxylin stain) in the bone marrow of cancer-bearing mice than non-cancer-bearing mice. When quantitated per field of view, the bone marrow of femurs from non-cancer-bearing mice contained approximately 3 megakaryocytes per field (Figure 5.19A) while bone marrow from mice inoculated with cancer cells contained approximately 6-20 megakaryocytes (MDA-MB-231W-GFP, 8-10 (Figure 5.19B); MDA-MB-231PY-GFP, 16-20 (Figure 5.19C); MDA-MB-231BO-GFP, 7-9 (Figure 5.19D); MDA-MB-231BRMS-GFP, 6-8 (Figure 5.19E)). The identification of megakaryocytes was verified independently by 2 cytologists and a Diplomate of the American College of Laboratory Animal Medicine with experience in rodent pathology. In addition, femurs were stained for CD41/gpIIb/IIIa, a major integrin on platelets and megakaryocytes, via immunohistochemistry [65]. Interestingly, megakaryocytes on femur sections from non-cancer-bearing mice stained positive for CD41 antigen (Figure 5.20A), whereas sections from cancer-bearing mice did not (Figure 5.20B).

5.14: Brefeldin A altered the color of murine femurs

Brefeldin A, a lactone antibiotic that results in protein accumulation within the cell [39], was utilized for immunohistochemistry to attempt to determine the cellular origin of secreted inflammatory cytokines. Six hours post-Brefeldin A inoculation, mice were euthanized, femurs harvested, cleaned free of soft tissue, and photographed using a light microscope. It was very difficult to 1) get the Brefeldin A to go into solution and 2) inoculate the full volume via tail vein injection as per the protocol described by Liu, et al. [39]. Regardless, the femurs of mice receiving the Brefeldin A injection were different in color than mice that had not received the injection (Figure 5.21). The femurs of mice

receiving the Brefeldin A injection were a green – grey color (Figure 5.21, right), compared to the femurs of mice that had not received Brefeldin A, which were bright red (Figure 5.21, left). Therefore, Brefeldin A alters the color of murine femurs.

5.15: Summary

When inoculated into the left cardiac ventricle of female athymic nude mice, human metastatic and non-metastatic breast cancer cells trafficked to the femur metaphyses of cancer-bearing mice (Figure 5.1). Furthermore, human metastatic breast cancer cells, in particular, colonized the trabecular bone of cancer-bearing tibiae as detected by μCT (Figure 5.11). The trabecular bone volume was decreased in cancer-bearing tibia compared with non-cancer-bearing tibia (Figure 5.11C, D inset). Tumor volume was additionally estimated via MRI and densitometry (Figure 5.12).

In addition, the bone-derived cytokines IL-6, MCP-1, VEGF, MIP-2, and KC were increased in the femur metaphyses of cancer-bearing mice (Figures 5.3-5.6)(Table 5.1). Specifically, the largest increase in bone-derived cytokine expression was found in the region distal to the hip, followed by the region proximal to the hip (Figures 5.3-5.6). Increases in bone-derived cytokine expression in the bone diaphysis were minimal (Figures 5.3-5.6). The bone microenvironment minimally altered cancer cell-derived cytokine production (Figure 5.7)(Table 5.2), and murine-derived cytokine expression was minimally altered in the bone marrow plasma as well as the blood serum of cancer-bearing mice (Figures 5.8-5.9)(Tables 5.3-5.4). It may have been possible, however, that changes in cytokine expression of the bone marrow plasma or blood serum were beyond the limits of detection of the Bio- Rad Bio-Plex^{TM} Serum Cytokine Assay due to the necessary 5 fold dilution of the serum-based samples as recommended by the manufacturer's protocol. Murine MCP-1 and VEGF were detected via immunohistochemistry in the trabecular bone matrix, but were not found in the bone shaft, in both non-cancer-bearing and cancer-bearing mice (Figures 5.13-5.14). Murine IL-6 was found throughout the bone marrow in both non-cancer-bearing and cancer-bearing mice (Figure 5.15). When tumor cells were present in the bone microenvironment, cytokine expression was not detected immediately adjacent to the tumor (Figure 5.16), but was present in an area ~150 μm beyond the tumor (Figure 5.17). In addition, murine MCP-1 and murine VEGF were present in a gradient that increased away from the tumor cells (Figure 5.17), and human VEGF expression increased with increasing tumor size (Figure 5.18). Futhermore, the number of megakaryocytes increased in femur sections from cancer-bearing mice (Figure 5.19). And femur sections from non-cancer-bearing mice stained positive for the CD41 antigen while femur sections from cancer-bearing mice did not (Figure 5.20). These data, as a whole, suggested that bone metastatic breast cancer cells influenced the bone microenvironment by decreasing trabecular bone volume, altering murine-derived cytokine production, as well as causing a recruitment of megakaryocytes to the site of cancer metastases.

Task 3. **To determine if osteoblasts and breast cancer cells have receptors and can respond to *osteoblast*-derived inflammatory cytokines. (Months 18-33)**

Part 6: RESULTS: THE EFFECT OF OSTEOBLAST-DERIVED CYTOKINES ON HUMAN METASTATIC BREAST CANCER CELLS AND OSTEOBLASTS

6.1: Rationale

Metastatic breast cancer cells alter osteoblast adhesion, differentiation, and increase osteoblast apoptosis [41]. Futhermore, in the presence of metastatic breast cancer cells, osteoblasts underwent an inflammatory stress response and produced inflammatory cytokines: IL-6, MIP-2/IL-8, MCP-1, VEGF, and KC/GRO-α. It may be the case that osteoblast-derived cytokines facilitate cancer metastases. In addition, it is thought that inflammatory cytokines contribute to osteoblast autocrine and osteoblast-breast cancer cell paracrine mechanisms resulting in significant cross-talk between the two cell types. Experiments described here focus on determining if osteoblast-derived cytokines are chemoattractants for metastatic breast cancer cells, determining if osteoblast-derived factors will elicit the formation of TRAP positive multi-nucleated osteoclasts, determining whether osteoblasts produce IL-6 when indirectly co-cultured with metastatic breast cancer cells, or examining whether anti-TGF-β or PTHrP block the inflammatory stress response elicited by osteoblasts in response to metastatic breast cancer cells.

6.2: Osteoblast conditioned medium was a chemoattractant for MDA-MB-231W human metastatic breast cancer cells *in vitro*

It was hypothesized that osteoblasts produced cytokines that may be chemoattractants for metastatic breast cancer cells. Therefore, osteoblast conditioned medium was assessed for its ability to chemoattract metastatic breast cancer cells. As a positive control, osteoblast conditioned medium from MC3T3-E1 cells grown to 10 or 20 days was used as a chemoattractant. Both osteoblast conditioned medium from 10 (Figure 6.1A)(Table 6.1) and 20 day old osteoblasts (Figure 6.1B)(Table 6.1) were potent chemoattractants for MDA-MB-231W human metastatic breast cancer cells. MDA-MB-231W human metastatic breast cancer cells were used as a representative cell population because no differences were seen amongst other cancer cell variants utilized in other assays. It was determined that ~860 MDA-MB-231 human metastatic breast cancer cells per field of view were chemoattracted toward the osteoblast conditioned medium from 10 day osteoblasts (Figure 6.1A)(Table 6.1) and ~980 MDA-MB-231 human metastatic breast cancer cells per field of view were chemoattracted toward the osteoblast conditioned medium from 20 day osteoblasts (Figure 6.1B)(Table 6.1). Approximately 12% more MDA-MB-231W human metastatic breast cancer cells per field of view were chemoattracted toward osteoblast conditioned medium from 20 day old osteoblasts than the number of cancer cells that were chemoattracted toward osteoblast conditioned medium from 10 day old osteoblasts. However, with consideration of the standard deviation (Table 6.1), these data suggested that there were no differences in the migration of human metastatic breast cancer cells toward the conditioned medium of osteoblasts grown to 10 or 20 days.

Mierke, et al. identified IL-8, but not MCP-1, as a chemoattractant for MDA-MB-231W human metastatic breast cancer cells [64]. A survey of the literature suggested that the chemoattractant capabilities of IL-6, KC, and VEGF on MDA-MB-231W human metastatic breast cancer cells were unknown. Thus, IL-6, KC, and VEGF components of the osteoblast conditioned medium were assessed for chemoattraction of MDA-MB-231W human breast cancer cells. MDA-MB-231W human metastatic breast cancer cells, however, were not chemoattracted to human or murine IL-6, KC, and VEGF (Figure 6.1B)(Table 6.1). Furthermore, cancer cell migration was not decreased when murine IL-6, KC, and VEGF were neutralized in osteoblast conditioned medium alone or in combination (~860 MDA-MB-231W human metastatic breast cancer cells per field of view were chemoattracted toward the conditioned medium from osteoblasts grown to 10 days compared to ~970 MDA-MB-231W human metastatic breast cancer cells per field of view that were chemoattracted toward conditioned medium from osteoblasts grown to 10 days incubated with anti-IL-6, KC, and VEGF(Figure 6.1C)(Table 6.1). In fact, ~12% more MDA-MB-231W human metastatic breast cancer cells migrated toward conditioned medium from osteoblasts grown to 10 days incubated with anti-IL-6, KC, and VEGF compared to the conditioned medium from osteoblasts grown to 10 days (Table 6.1). Thus, neither IL-6, KC, nor VEGF appeared to chemoattract, alone or in combination, MDA-MB-231W human metastatic breast cancer cells. Therefore, osteoblasts secrete other materials, besides IL-6, KC, or VEGF, that were chemoattractants for metastatic breast cancer cells.

Kinder, et al. identified TGF-β as a possible mediator of an osteoblast-derived inflammatory stress response in the presence of metastatic breast cancer cells [11]. Therefore, TGF-β was assessed to determine its ability to chemoattract metastatic breast cancer cells. A neutralizing antibody to TGF-$\beta_{1,2,3}$ was used to assess for alterations in MDA-MB-231 human metastatic breast cancer migration. Osteoblast conditioned medium from 10 day osteoblasts was used as a chemoattractant and positive control (Figure 6.2A)(Table 6.1). Osteoblast conditioned medium from 10 day old osteoblasts was additionally incubated with 5 μg/ml anti-TGF-$\beta_{1,2,3}$ to determine if breast cancer cell migration was halted. There was little change in MDA-MB-231W metastatic breast cancer cell migration towards osteoblast conditioned medium with the use of the TGF-$\beta_{1,2,3}$ neutralizing antibody (Figure 6.2B)(Table 6.1). Breast cancer migration was similar to (within 10%) cancer cell migration towards osteoblast conditioned medium from 10 day old osteoblasts (~860 MDA-MB-231W human metastatic breast cancer cells per field of view were chemoattracted to the conditioned medium from osteoblasts grown to 10 days compared to ~950 MDA-MB-231W human metastatic breast cancer cells per field of view that were chemoattracted to the conditioned medium from osteoblasts grown to 10 days incubated with anti- TGF-$\beta_{1,2,3}$)(Figure 6.2B)(Table 6.1). Therefore, the neutralization of TGF-$\beta_{1,2,3}$ did not alter MDA-MB-231W human metastatic breast cancer cell migration towards osteoblast conditioned medium. Thus, osteoblasts secrete other material besides TGF-β that were chemoattractants for metastatic breast cancer cells.

6.3: Supernatants from osteoblasts cultured with breast cancer cells or their conditioned medium elicited the formation of TRAP positive osteoclasts *in vitro*

It was hypothesized that rather than acting as chemoattractants for human metastatic breast cancer cells, osteoblast conditioned medium, containing IL-6, MCP-1,

VEGF, KC/GRO-α, and MIP-2/IL-8, facilitated osteoclastogenesis. To investigate the contribution of MC3T3-E1 osteoblast-derived cytokine production on osteoclastogenesis, RAW264.7 cells and bone marrow monocytes were treated for 14 days with culture supernatant of MC3T3-E1 cells that had been treated with breast cancer conditioned medium or co-cultured with cancer cells. Osteoclast formation was assessed by TRAP stain. TRAP positive multi-nucleated osteoclasts (4; Figure 6.3A) formed from bone marrow monocytes following treatment of the culture supernatant from 10 day old osteoblasts treated with breast cancer conditioned medium. TRAP positive multi-nucleated osteoclasts additionally formed when 10 or 20 day old osteoblasts were co-cultured with MDA-MB-231W human metastatic breast cancer cells (Day 10, 2 colonies; day 20, 3 colonies)(Table 6.2). No TRAP positive cells were found with any treatment of RAW264.7 cells. Thus, the culture supernatants of osteoblasts in the presence of breast cancer cells or their conditioned medium elicited TRAP positive osteoclast formation from bone marrow monocytes.

Murine IL-6 was additionally utilized to assess for TRAP positive multi-nucleate osteoclast formation from both RAW264.7 cells and bone marrow monocytes. Murine IL-6 was added to both cells types at concentrations of 1, 10, and 100 ng/ml; concentrations representative of IL-6 expression in both MC3T3-E1 cells as well as MDA-MB-231 metastatic breast cancer cells (Figure 3.6A-B, Figure 4.1A). Neither mono-nucleated nor multi-nucleated TRAP positive cells were detected in cultures from RAW264.7 cells. Mono-nucleated TRAP positive cells were found in bone marrow monocyte cultures treated with 1 ng/ml murine IL-6 (0 - 473 cells)(Figure 6.3B). No additional mono- or multi-nucleated TRAP positive cells were found in bone marrowmonocyte cultures treated with 10 or 100 ng/ml murine IL-6. These data suggested that 1 ng/ml murine IL-6 was sufficient to elicit TRAP positive cell formation in bone marrowmonocytes, but did not lead to multi-nucleated cell formation. Thus, murine IL-6 alone was not sufficient for multi-nucleated, TRAP positive osteoclast formation from bone marrow monocytes.

6.4: Osteoblasts produced alkaline phosphatase and IL-6 when co-cultured indirectly in a transwell system with human metastatic breast cancer cells

In pilot studies, osteoblasts were co-cultured indirectly in a transwell system with human metastatic breast cancer cells changes in cytokine expression. First, the pore size of the transwell system was tested. MDA-231W or MDA-231GFP cells were plated in either 0.4 μm or 3 μm pore size inserts and added to wells containing 11 day old MC3T3-E1 cells. Four days later, culture media were collected, centrifuged to remove any debris, and stored at -20°C.

Alkaline phosphatase enzyme activity of MC3T3-E1 cells was assessed for alkaline phosphatase enzyme activity. While results were not consistent, a few trends were seen (Table 6.3). Osteoblasts grown in wells of a transwell system containing 0.4 μm pore size inserts with cancer cells produced more alkaline phosphatase activity at 4 minutes than those containing grown in wells of a transwell system containing 3 μm pore size inserts. These data suggest that metastatic breast cancer cells in the 3 μm pore size inserts altered the alkaline phosphatase expression of MC3T3-E1 cells.

Images were taken using light and fluorescent microscopy of: a) MC3T3-E1 cells and b) the insert containing MDA-MB-231GFP cells. Images obtained via fluorescence

microscopy suggest that although few human breast cancer cells migrated through pores to the underside of the insert (Figure 6.4B), none migrated into the MC3T3-E1 cell layer (Figure 6.4A). Thus, the four day incubation period after the breast cancer cells were plated resulted in no cancer cell invasion into the osteoblast layer.

Finally, a murine IL-6 ELISA was conducted on culture supernatants obtained from an indirect co-culture in a transwell system of osteoblasts and metastatic breast cancer cells. An indirect co-culture transwell system consisting of inserts with 3 μm pores resulted in the largest response in osteoblast-derived IL-6 (Figure 6.5). The IL-6 response elicited by MC3T3-E1 cells grown in a transwell system with 0.4 μm pore size inserts was not detected or greatly reduced (Figure 6.5). Based on these results, transwell inserts with a 3 μm pore size were chosen for future experiments.

6.5: Neither PTHrP nor anti-TGF-β effectively block the osteoblast-derived inflammatory stress response elicited by human metastatic breast cancer cells

Kinder, et al. identified PTHrP and TGF-β as possible mediators of an osteoblast-derived inflammatory stress response in the presence of metastatic breast cancer cells [11]. Both PTHrP and TGF-β are present in breast cancer conditioned media and are known to induce at least one cytokine of interest (IL-6, IL-8, or MCP-1) [114, 115]. To determine if PTHrP and/or TGF-β in the conditioned medium were directly responsible for the increase in osteoblast-derived cytokines, an antagonist to PTHrP ([Asn^{10}, Leu^{11}, $dTrp^{12}$] PTHrP (7-34)) and a neutralizing antibody to TGF-β_{1-2} were used. MC3T3-E1 cells were grown for 16 days in MC3T3-E1 differentiation medium containing 2% Serum Replacement (Sigma; utilized to eliminate FBS as a possible source of TGF-β or PTHrP). MC3T3-E1 cells were treated with either VM or CM as described in the Materials and Methods and assayed for murine IL-6 (representative cytokine) via standard sandwich ELISAs.

The addition of TGF-β to VM elicited an increase in osteoblast-derived IL-6 and treatment with TGF-β antibody effectively blocked this response (Figure 6.6). Addition of PTH (1-34) also caused an increase in murine IL-6 while treatment with the PTHrP antagonist (7-34) did not (Figure 6.6). In sharp contrast to the expected results, the combination of both PTH and the antagonist PTHrP (7-34) generated a greater murine IL-6 response than PTH alone (Figure 6.6).

When CM was treated with neutralizing antibody to TGF-β before the addition to the MC3T3-E1 cells, the antibody did not block IL-6 production; in fact, more murine IL- 6 was produced (Figure 6.6). Osteoblast-derived IL-6 was also increased when CM was treated with the antagonist PTHrP (7-34) (Figure 6.6). Neutralizing antibody to TGF-β and PTHrP antagonist (7-34) were additionally used to determine if blocking both molecules would prevent the increase in murine IL-6. There was a 40 percent decrease in the amount of IL-6 produced by MC3T3-E1 cells when blocking agents were added to the CM (osteoblast + CM + anti-TGFβ + PTHrP (7-34) treatment = 0.110 ng/ml murine IL-6; osteoblast + CM treatment = 0.187 ng/ml murine IL-6) (Figure 6.6). However, neutralizing both molecules did not reduce osteoblast-derived IL-6 concentrations to VM levels (Figure 6.6). Thus, PTHrP nor anti-TGF-β, either alone or in combination, do not effectively block the osteoblast-derived inflammatory stress response elicited by human metastatic breast cancer cells.

6.6: Summary

The conditioned medium from osteoblasts grown to 10 or 20 days was a potent chemoattractant for metastatic breast cancer cells (Figure 6.1)(Table 6.1). However, when a neutralizing antibody to murine IL-6, KC, or VEGF, either alone or in combination incubated with the osteoblast conditioned medium, metastatic breast cancer cell migration was not altered (Figure 6.1)(Table 6.1). Furthermore, when a neutralizing antibody to TGF-$\beta_{1,2,3}$ was incubated with the osteoblast conditioned medium, metastatic breast cancer cell migration was also not altered (Figure 6.2)(Table 6.2). MDA-MB-231W human metastatic breast cancer cells were also not chemoattracted to human or murine IL-6, KC, or VEGF (Figure 6.1)(Table 6.1). These data suggest that osteoblasts secrete other materials, besides IL-6, KC, or VEGF, that affect human metastatic breast cancer cell migration.

In addition, supernatants from osteoblasts cultured with metastatic breast cancer cells or their CM elicited the formation of TRAP positive, multi-nucleated osteoclasts (Figure 6.3)(Table 6.3). In addition to multi-nucleated osteoclasts, mono-nucleated osteoclasts were also formed (Figure 6.3)(Table 6.2). Murine IL-6 elicited the formation of TRAP positive, mono-nucleated osteoclasts, but did not elicit the formation of TRAP positive, multi-nucleated osteoclasts (Figure 6.3)(Table 6.2). These data suggest that murine IL-6 alone is not sufficient to elicit the formation of TRAP positive, multi-nucleated osteoclasts, but that the culture supernatants from osteoblasts cultured with metastatic breast cancer cells or their CM were sufficient to elicit the formation of TRAP positive, multi-nucleated osteoclasts.

Furthermore, the alkaline phosphatase enzyme activity of osteoblasts was altered when they were indirectly co-cultured with metastatic breast cancer cells in a transwell system with 3 μm pore size inserts (Table 6.3). Osteoblasts indirectly co-cultured with metastatic breast cancer cells in a transwell system with 3 μm pore size inserts additionally produced the largest amount of murine IL-6 (Figure 6.5).

Finally, an increase in osteoblast-derived IL-6 was observed when TGF-β was added to VM. This response, however, was blocked with treatment of anti-TGF-β. Treatment with a combination of both PTH and PTHrP (7-34), contrary to the expected results, generated an increase in murine IL-6, which was larger than the addition of PTH alone (Figure 6.6). When anti-TGF-β was added to CM prior to the addition to osteoblasts, an increase in murine IL-6 was seen (Figure 6.6). Murine IL-6 was also increased when CM was treated with PTHrP (7-34) prior to addition to osteoblasts (Figure 6.6). When added to CM in combination, a reduction in the osteoblast-derived inflammatory response was also not observed (Figure 6.6). Therefore, PTHrP nor anti-TGF-β, either alone or in combination, do not effectively block the osteoblast-derived inflammatory stress response elicited by human metastatic breast cancer cells.

Part 7: KEY RESEARCH ACCOMPLISHMENTS

- Osteoblasts are an important source of KC, MCP-1, IL-6, and VEGF in the vicious cycle of breast cancer bone metastasis.
- Osteoblasts naturally produce large amounts of MCP-1.
- Breast cancer cell variants and their GFP counterparts do NOT produce MCP-1, but DO produce IL-8.

- Osteoblast maturation state is important in determining the osteoblast response to metastatic breast cancer cells.
- Osteoblast-derived cytokine expression is increased with treatment of CM from non-osteoblast cells. This effect is cell-type dependent (i.e. osteoblast-derived cytokine production did not increase when osteoblasts were treated with osteoblast CM).
- Osteoblast-derived cytokine production with treatment of non-metastatic cells or their CM is over and above that seen with treatment of metastatic breast cancer cell variants.
- The increase in osteoblast-derived cytokine production is independent of treatment cell species, origin, or tumorigenicity.
- Maximum induction of osteoblast-derived cytokine secretion at day 10 occurred with treatment of a brain-seeking variant. This effect was not seen at day 20.
- No difference among metastatic breast cancer cell variants was seen when osteoblasts and human cancer cell variants were placed in a "co-culture" system together.
- Osteoblast-derived MCP-1 decreased with treatment of MDA-MB-231 breast cancer cell variants and MDA-MB-468P non-metastatic cancer cells at day 20 in a "co-culture" transwell system.
- A limited dose response in osteoblast-derived cytokine production was seen with increasing amounts of non-osteoblasts in a "co-culture" transwell system.
- A distinct dose response was seen in human-derived cytokine production with increasing amounts of non-osteoblasts by themselves in a "co-culture" transwell system.
- Zero to low amounts of MCP-1 are produced by human non-osteoblast cells in a "co-culture" transwell system with murine osteoblasts.
- Human non-osteoblast-derived cytokine production decreased significantly when human non-osteoblasts were in a "co-culture" transwell system with murine osteoblasts.
- Brefeldin A induces a color change in murine bones.
- Retrieved human breast cancer cells had decreased cytokine production compared with non-injected human cancer cells.
- Zero to low amounts of MCP-1 are produced by human cancer cells ex-vivo.
- The metaphyses (ends) of bone in normal mice produce KC, MIP-2, IL-6, VEGF, and MCP-1.
- In cancer-bearing mice, the metaphyses (ends) of bone produce signficantly higher amounts of KC, MIP-2, IL-6, and VEGF than control or the bone diaphysis (shaft). Breast cancer cells predominantly traffic to the bone ends.
- No differences were seen amongst human cancer cell variants and their tumor formation or cytokine production in a murine model of breast cancer bone metastasis.
- Murine MCP-1 and murine VEGF were localized to the trabecular bone and surrounding area in control and cancer-bearing mice.
- Murine MCP-1 and murine VEGF production was not apparent within ~150 μm of the tumor in the 4 week murine model.
- Human VEGF production increased with tumor volume.
- Megakaryocyte presence increased in certain femur sections. Megakaryocytes may prime the bone niche for cancer cell arrival.
- Osteoblast conditioned medium was a potent chemoattractant for MDA-231 cells.
- KC, IL-6, or VEGF were not chemoattractants for MDA-231 cells.

- Neutralizing KC, IL-6, or VEGF in osteoblast conditioned medium did not alter MDA-231 cancer cell migration.
- Osteoblasts are an important source of cytokines, specifically MCP-1, in breast cancer bone metastasis.
- Cancer cell manipulation of the bone microenvironment facilitates tumor cell colonization and survival.

Part 8: REPORTABLE OUTCOMES

Degrees Obtained Support by this Award:

2008 **Bussard, KM.** Doctor of Philosophy in Pathobiology. Awarded by The Pennsylvania State University, December 20, 2008.

Publications:

2006 Phadke, PA; Mercer, RR; Harms JF; Jia, Y; Kappes, JC; Frost, AR; Jewell, JL; **Bussard, KM;** Nelson, S; Moore, C; Gay, CV; Mastro, AM; Welch, DR. "Kinetics of Metastatic Breast Cancer Cell Trafficking in Bone." Clinical Cancer Research. 12: (5) 1431.

2008 Kinder, M; Chislock, EM; **Bussard, KM;** Shuman, LA; Mastro, AM. Metastatic Breast Cancer Induces an Osteoblast Inflammatory Response. Experimental Cell Research. 314: (1), 173.

2008 **Bussard, KM;** Gay, CV; Mastro, AM. The Microenvironment in Metastasis: What is Special About Bone? Cancer Metastasis Reviews. 27: (1), 41.

2009 **Bussard, KM;** Okita, N; Sharkey, N; Neuberger, T; Webb, A; Mastro, AM. IL-6, MCP-1, and VEGF are Localized in the Bone Microenvironment of Metastatic Breast Cancer-Bearing Mice. Submitted to Cancer Cell.

2009 **Bussard, KM**; Mastro, AM. Osteoblast-derived Cytokines Facilitate Bone Metastatic Breast Cancer. (working title) Manuscript in preparation.

Oral Presentations:

2006 **Bussard, KM;** Phadke, PA; Mercer, RR; Harms JF; Jia, Y; Kappes, JC; Frost, AR; Jewell, JL; Nelson, S; Moore, C; Gay, CV; Mastro, AM; Welch, DR. "Kinetics of Metastatic Breast Cancer Cell Trafficking in Bone." Presented at the American Association for Cancer Research Annual Meeting's Tumor Biology Minisymposium, April 1-5, 2006.

2008 **Bussard, KM;** Mastro, AM. "Osteoblast-Derived Cytokines are Major Mediators in Facilitating Bone Metastatic Breast Cancer." Presented at the American Association

for Cancer Research Annual Meeting's Tumor Biology Minisymposium, April 12-16, 2008.

Abstracts / Poster Presentations:

2005 **Bussard, KM;** Shuman, LS; Mercer, RR; Phadke, PA; Nelson, SM; Jewell, JL; Chislock, EM; Kinder, M; Welch, DR; Gay, CV; Mastro, AM. "The Interaction of Metastatic Breast Cancer Cells with Osteoblasts." Presented at the CrossOver 2005 Meeting sponsored by The Huck Institutes of The Life Sciences and The Materials Research Institute, The Pennsylvania State University, October 13-14, 2005.

2006 **Bussard, KM;** Chislock, EM; Kinder, M; Gay, CV; Mastro, AM. "A Classic Set of Osteoblast-Derived Inflammatory Cytokines is Produced in Response to Bone Metastatic Breast Cancer." The 11th International Congress of the Metastasis Research Society, Tokushima, Japan, September 3-6, 2006 .

2007 **Bussard, KM;** Mastro, AM. "Osteoblast-derived Inflammatory Cytokines are Produced in Response to Human Metastatic Breast Cancer Cells." The 100th Annual American Association for Cancer Research Annual Meeting, Los Angeles, CA, April 14-18, 2007. Proceedings of the 97th Annual Meeting for American Association for Cancer Research.

2007 **Bussard, KM**; Mastro, AM. "Osteoblasts Naturally Produce Cytokines that Influence the Tumor Microenvironment in Bone Metastatic Breast Cancer." Skeletal Complications of Malignancy V, The Paget Foundation. October 25-27, 2007.

2008 **Bussard, KM**; Mastro, AM. "The Role of Osteoblast-Derived Cytokines in Bone Metastatic Breast Cancer." Era of Hope Meeting, Baltimore, MD, June 25-28, 2008.

Research Opportunities Attended Based on this Research:

- American Association for Cancer Research – Edward A. Smuckler "Pathobiology of Cancer" Workshop selected attendee. Snowmass, CO: July 15-22, 2007.

Awards / Grants / Fellowships Won Based on this Research:

- American Association for Cancer Research – Scholar-In-Training Award: 2008
- The Pennsylvania State University College of Agricultural Sciences Travel Award: 2008.
- American Association for Cancer Research – Women in Cancer Research Brigid G. Leventhal Scholar Award in Cancer Research: 2006.
- Department of Defense Predoctoral Traineeship Award in Breast Cancer (Fellowship): 2006-2009.
- The Pennsylvania Space Grant Consortium NASA Space Grant Fellowship: 2005-2007, 2007-2009.
- Sigma Xi Grants-in-Aid of Research Award, 2005-2006

Part 9: CONCLUSION

Despite the prevalence of bone metastatic breast cancer, little is known as to why bone is a preferred site of metastasis [2, 4, 47]. Besides breast, primary cancers that frequently metastasize to bone include prostate, lung, thyroid, and kidney [47]. In contrast, cancers of the gastrointestinal tract seldom do [47]. There are many reasons why bone, specifically the metaphysis, is a particularly attractive site for preferential metastasis. One reason may be that the metaphyseal bone is a highly vascularized, metabolically active region of long bone composed of many bone trabeculae [2]. Volumous vascular sinusoids with lumen diameters much larger than the cancer cells are present within a few microns of the trabecular bone [66, 67]. Blood flow within the sinusoids is sluggish, being described as more "in a lake than in a stream" [66]. Vascular sinusoids are also specifically designed to allow for easy movement of cells into and out of the bone marrow [2, 66]. Sinusoidal walls are trilaminar and are lined by stromal endothelial cells that lack tight junctions. These interdigitating cells rest on an irregular, discontinuous basement membrane [47]. Therefore, metastatic cancer cells could easily interact with vascular components, adhere to underlying endothelium, and invade secondary locations.

Bone-depositing osteoblasts and bone-resorbing osteoclasts contribute to bone remodeling and, in conjunction with cells of the bone marrow, secrete cytokines, chemokines, and growth factors that are used by tumor cells in the metastatic process. Cancer cell-secreted IL-8 and IL-6 have been implicated in increased bone metastasis and stimulation of osteoclast differentiation, leading to increased bone resorption and release from the bone matrix of cancer cell survival factors such as TGF-β [44, 68]. Furthermore, Kinder, et al. demonstrated metastatic breast cancer cells co-opt osteoblasts into producing increased quantities of IL-6 and MCP-1 [11], which are involved in breast cancer cell migration, survival, and osteoclast activation [69, 70]. To determine whether additional cytokines were involved in the osteoblast response to breast cancer cells, an expanded cytokine screen that included a larger array of inflammatory cytokines was carried out. This panel additionally identified VEGF as a cytokine of interest (Figure 3.5).

Previous experiments by Mercer, et al. suggested that MDA-MB-231 human metastatic breast cancer cell conditioned medium altered MC3T3-E1 cell morphology, differentiation, and mineralization under conditions of chronic, long-term (5-35 days) exposure [5]. In order to more fully characterize the effects of human metastatic breast cancer cells on osteoblasts, preliminary experiments were carried out in which MC3T3-E1 cells were treated with conditioned medium from MDA-MB-231 human metastatic breast cancer cell variants for 24 hours–4 days (acute, short-term treatment). Osteoblast morphology, differentiation, and mineralization were assessed. Data suggested that, under conditions of this study, MC3T3-E1 cell morphology, differentiation, and mineralization were not altered by MDA-MB-231 human metastatic breast cancer cell variants after short-term treatment (Figures 3.1-3.3). While no morphological or physical effects of human metastatic breast cancer cells were seen during this short exposure, it may be possible that molecular events were more prominent.

The interactions of osteoblasts and metastatic breast cancer cells were tested in three ways: 1) with breast cancer conditioned medium, 2) in an indirect transwell co-

culture system, and 2) with direct co-culture. Both the conditioned medium and the direct co-culture led to an increased cytokine response by the osteoblasts (Figure 3.6, Figure 3.16). The transwell system did not (Figure 3.13). This lack of response may be due to the system parameters, i.e. the co-culture was only able to be carried out for 3 days due to the high proliferation rate of the cancer cells. Furthermore, any cancer cell secretions would have had to pass through the transwell filter, where they may have bound to the membrane. Since direct co-culture with metastatic breast cancer cells and metastatic breast cancer conditioned medium elicited a response by the osteoblasts, it seems reasonable to conclude that cancer cells secreted some soluble factors that activated the osteoblasts.

In contrast to the osteoblast response, a different result was found for cancer cell secretion of cytokines. In the two systems in which cancer cells were present, indirect transwell co-culture and direct co-culture, the secretion of the cancer cell cytokines IL-8, GRO-α, IL-6, and VEGF decreased compared to secretion of cancer cells in the absence of osteoblasts (Figures 4.4-4.7, Figure 4.10). The decrease was up to 100% in both the indirect transwell co-culture system and direct co-culture system. These data suggested that soluble factors secreted by the osteoblasts, as well as factors exchanged through direct cell contact, exerted an effect on human metastatic breast cancer cells under conditions of this study. Furthermore, MDA-MB-231W metastatic breast cancer cells express receptors to cytokines identified in this study, IL-6, IL-8/MIP-2, GRO-α/KC, and VEGF (Table 6.1)[71-74]. It seems reasonable to conclude that breast cancer cells decreased their cytokine production due to an inhibitory protein, which may be IL-6, MIP-2, KC, VEGF, or MCP-1, secreted by the osteoblasts.

One of the central goals of this study was to determine if treatment with a bone-seeking metastatic breast cancer cell variant increased osteoblast-derived cytokine production more than the less metastasis-specific parental lines. No differences were found amongst osteoblasts treated with conditioned medium from metastatic breast cancer variants (Figure 3.6). Thus, the osteoblast response to metastatic breast cancer cells appeared to be a generalized inflammatory response to metastatic breast cancer cells.

Human metastatic breast cancer cells and osteoblasts were assayed for their production of cytokines alone (Tables 3.2, 4.1; Figures 3.6, 4.1). Interestingly, human metastatic breast cancer cells expressed negligible quantities of MCP-1 (Figure 4.1). In contrast, MCP-1 was expressed in large quantities by MC3T3-E1 cells (~3 ng/ml)(Figure 3.6). When osteoblasts were treated with human metastatic breast cancer cells or their conditioned medium, MCP-1 expression increased 1-9 fold over vehicle medium (Figure 3.6). Therefore, osteoblast-derived MCP-1 production may be important in the tumor microenvironment.

Bone-derived cytokine production was also examined *ex vivo*. A xenograft model system of human cancer cells inoculated into athymic mice allowed for independent determination of breast cancer-derived (human) and bone-derived (murine) cytokines. Similar to finding from the *in vitro* model, bone-derived cytokine production was increased in cultures of femurs harvested from cancer-bearing mice (Figures 5.3-5.6). Results were similar amongst the breast cancer cell variants tested. Femur-derived cytokine production increased to a larger extent in bone metaphyses compared to the diaphysis (Figures 5.3-5.6). In a previous study using the same *in vivo* model, metastatic

breast cancer cells preferentially metastasized to bone ends, particularly the region distal to the hip first, and proximal to the hip second, as opposed to bone shaft [40]. The increase in bone-derived cytokine production, as investigated in this study, closely mimicked trafficking patterns of metastatic breast cancer cells. There was little difference in bone-derived cytokine production in the bone shaft of non-cancer-bearing mice compared to cancer-bearing mice (Figures 5.3-5.6). In addition, it was found by immunohistochemistry that MCP-1 and VEGF were localized to trabecular bone matrix, as opposed to bone shaft, in both non-cancer-bearing and cancer-bearing mice (Figure 5.13). Thus, bone matrix-associated cytokines may play a role in cancer cell localization within the femur.

In previous studies, it was found that the culture supernatants of the bone metaphyses flushed free of marrow expressed cytokines that were different from those in the diaphysis. In addition, these cytokines were strongly observed in the bone metaphyses instead of the marrow from the metaphyses (Table 6.2). These cytokines included IL-6, MCP-1, VEGF, MIP-2, and KC. Furthermore, it has been reported that cells of the bone (e.g. osteoblasts, osteoclasts, bone marrow cells) naturally produce MCP-1, IL-6, and VEGF mRNA [54, 57, 75], and osteoblasts produce MCP-1 and IL-6 in murine models of osteomyelitis and infected human bone tissue [76, 77]. Taken together, these data suggest that these cytokines were specifically produced by osteoblasts and not cells of the bone stroma or bone marrow.

While it is clear that metastatic breast cancer cells exert profound effects on bone cells, the cancer cells recovered from bone only showed minimal changes in the production of VEGF, IL-6, IL-8, or GRO-α when compared to cells pre-inoculation (Figure 5.7). However, it may be that study conditions, including time post-inoculation, passage number *ex vivo*, and small sample size, were not conducive for detecting an effect of bone on cancer cells. Furthermore, it could be argued that murine cytokines do not bind to human receptors. While human cells do not express murine MIP-2 or KC, they do express the human counterparts IL-8 and GRO-α, respectively [55, 78]. In addition, metastatic breast cancer cells express receptors to cytokines identified in this study (IL-6, MIP-2/IL-8, KC/GRO-α, VEGF, and MCP-1)[71-74]. There is high homology in the amino acid sequences of these murine and human ligands and their receptors [55, 78]. Therefore, is seems reasonable to conclude that osteoblast-derived murine IL-6, MIP-2, KC, VEGF, and MCP-1 bind to their respective receptors that are present on human cancer cells.

Osteoblast-derived cytokines may provide a favorable environment to facilitate tumor cell colonization and survival. In particular, MCP-1 and VEGF were present in the trabeculae of bone metaphyses (an area to which breast cancer cells preferentially traffic [40]) and not the cortical bone shaft as detected by immunohistochemistry (Figures 5.13-5.14). Furthermore, utilizing a μCT scan, it was found that metastatic breast cancer cells specifically localized within the trabecular bone of the metaphyseal region of the femur or tibia (Figure 5.11). Interestingly, and contrary to the hypothesis that bone-derived cytokines would be increased in cancer-bearing mice compared to non-cancer-bearing mice, no visual differences in cytokine expression via immunohistochemistry were observed between non-cancer-bearing or cancer-bearing mice. However, a quantitative *in vivo* analysis conducted with a sensitive (as little as 2 pg/ml) cytokine array revealed that bone-derived KC, MIP-2, IL-6, MCP-1, and VEGF were increased in the presence of

MDA-MB-231 human metastatic breast cancer cells (Figure 5.3-5.6). Thus, quantitative changes in bone microenvironment cytokine expression may be beyond the detection limits of the immunohistochemistry assay used in this study. Or, alternatively, it is likely that soluble cytokines in the bone microenvironment were lost or washed away during bone fixation and processing. However, immunohistochemistry allowed us to visualize cytokine localization within the bone. It was found that IL-6 was present in the bone marrow, while MCP-1 and VEGF were present in the matrix of the bone metaphyses (Figures 5.13-5.15). While the exact reason for the presence of IL-6 in the bone marrow, as opposed to the bone metaphyses, is unknown (IL-6, MCP-1, and VEGF are all produced by cells of the bone including osteoblasts and osteoclasts [55], and thus should all be present in the bone metaphyses), the short half life of IL-6 (2-3 hours)[79] may have played a role in its detection. It is possible that an increase in IL-6 in the metaphyseal regions of the femur may have occurred due to the presence of metastatic breast cancer cells. However, it may also be possible that when femurs from cancer-bearing mice were examined three weeks post-inoculation, the increase in IL-6 expression had subsequently decreased, and was therefore not detected. Thus, the examination of femurs from mice inoculated with metastatic breast cancer cells by immunohistochemistry at earlier times (1 hour), utilizing the same protocols described in the Materials and Methods and Results sections, may identify alterations in cytokine expression that were not evident at later times. VEGF and MCP-1, on the other hand, were located in the bone matrix (Figures 5.13-5.14), and VEGF is matrix-bound [80]. Therefore, these cytokines would not degrade quickly, and they may aid in tumor cell colonization and survival at secondary sites. These data as a whole suggested that bone metastatic breast cancer cells were attracted to regions of high bone turnover that express IL-6, MCP-1, and VEGF. Furthermore, VEGF, MCP-1, and IL-6, may aid in 'priming' the metaphyseal bone microenvironment for cancer cell arrival. This idea has been postulated in recent literature as the formation of a 'pre-metastatic niche [81, 82].'

As reviewed by Kaplan, et al. [82], and Wels, et al. [81], the possibility that tumor cells are capable of priming distant sites has been debated for over a century. When Stephen Paget first described the 'seed and soil' hypothesis, he stated "When a plant goes to seed, its seeds are carried in all directions; but they can only grow if they fall on congenial soil [83]." One could argue whether Paget was referring to cancer cell priming of a secondary site; but, clearly the microenvironment of secondary locations are crucial in determining whether 1) cancer cells will metastasize to that site and 2) if cancer cell proliferation is supported. If cancer cells can prime a distant, secondary site for colonization, bone, rich in growth factors, cell adhesion molecules, cytokines, and chemokines, will be a prime location for cancer cell settlement. In addition to bone marrow derived-cytokines that exist before tumor cell arrival and create a congenial soil, an increase in the number of megakaryocytes prior to cancer cell arrival in the bone microenvironment, was observed in mice that were inoculated with breast cancer cells (Figure 5.19). It is possible that megakaryocytes help prime the metaphyseal bone for cancer cell arrival and colonization.

In fact, similar to breast cancer cells co-opting osteoblasts into altering their cytokine expression [11], metastatic breast cancer cells may impose the same change upon other cells of the bone microenvironment. It was found that, in the presence of metastatic breast cancer cells, expression of both bone-derived and cancer cell-derived

cytokines was altered (Figures 5.16, 5.18). Neither the matrix-bound murine MCP-1, nor matrix-bound murine VEGF were detected adjacent to tumor cells, but were found ~150 μm away (Figure 5.16-5.17). In addition, megakaryocytes did not stain positive for CD41 (a marker for mature megakaryocytes) in mice inoculated with breast cancer cells, whereas megakaryocytes in sections from non-cancer-bearing mice did (Figure 5.20). While it could be argued that a lack of positive stain for CD41 may be due to the differentiation state of megakaryocytes (immature vs. mature), it has been reported that CD41 appears very early in the differentiation of megakaryocytes [65]. A test to assay for an increased production of megakaryocytes, is to assay for thrombopoietin. Thrombopoietin is a a glycoprotein hormone that stimulates the production and differentiation of megakaryocytes [84]. An experiment describing how to assay for thrombopoietin concentrations in the blood of both cancer- and non-cancer-bearing mice is found in section 9.1: future directions. These findings support the idea that cancer cells co-opt cells of the bone microenvironment into creating a unique niche for cancer cell survival.

It was found that osteoblast conditioned medium was a potent chemoattractant for metastatic breast cancer cells (Figure 6.1). This finding was previously reported by Giunciuglio, et al. [85]. However, cytokines identified in this study, specifically IL-6, KC, and VEGF, either alone or in combination, were not chemoattractants for the cancer cells (Figure 6.1). It has been reported that IL-8 (human; MIP-2, murine) is a chemoattractant for MDA-MB-231W metastatic breast cancer cells, but MCP-1 is not [64]. Combinations of human and murine IL-6, KC, and VEGF were tested as chemoattractants for metastatic breast cancer cells. Neutralizing antibodies to IL-6, KC, and VEGF were also added to osteoblast conditioned medium either separately, or in combination, and assessed for cancer cell migration. None of these cytokines altered human metastatic breast cancer cell migration in a transwell system (Figure 6.1).

If not chemoattractants, what might be the role of osteoblast-derived cytokines in bone metastatic breast cancer? It was reported that MDA-MB-231W metastatic breast cancer cells express receptors to all cytokines identified in this study (Table 9.1)[71-74]. It was also reported that these cytokines, IL-6, IL-8, and VEGF in particular, are maintenance factors for metastatic breast cancer cells (Table 9.1)[46, 71, 86]. Furthermore, it has been reported that these factors, in addition to MCP-1, stimulate osteoclastogenesis, leading to increased bone resorption and release from bone of other breast cancer maintenance factors such as TGF-β (Table 9.1)[4, 44, 87-89]. Thus, these cytokines may be indirectly involved in osteoclastogenesis as well as breast cancer cell maintenance and survival.

To further investigate the possibility that cytokines are involved in osteoclastogenesis, the effect of osteoblast-derived cytokines on osteoclast formation was examined. TRAP positive multi-nucleated osteoclasts formed when bone marrow cells were incubated with the culture supernatant of osteoblasts treated with breast cancer cells or their conditioned medium (Figure 6.3). No TRAP positive multi-nucleated osteoclasts were formed when bone marrow cells were treated with the conditioned medium from osteoblasts or breast cancer cells alone (Figure 6.3). Thus, the interaction of osteoblasts and breast cancer cells or their conditioned medium resulted in the production of or increase in a factor(s) that facilitates osteoclastogenesis, such as MCP-1. MCP-1 was produced in large quantities by osteoblasts alone (~3 ng/ml)(Figure 3.6), and its

expression increased substantially when osteoblasts were cultured with the conditioned medium from metastatic breast cancer cells (up to 18 ng/ml)(Figure 3.6). However, MCP-1 was expressed in negligible quantities by metastatic breast cancer cells. Furthermore, MCP-1, in concentrations of between 5-25 ng/ml, is known to stimulate osteoclastogenesis *in vitro* [89-91]. Therefore, metastatic breast cancer cells may indirectly stimulate osteoclastogenesis by enhancing osteoblast production of MCP-1. Osteoclastogenesis would lead to increased bone resorption and the release from bone of known breast cancer maintenance factors like TGF-β [68]. Conversely, the interaction of osteoblasts and breast cancer cells or their conditioned medium may also result in the production of an inhibitory factor or decrease in factor expression that leads to osteoclastogenesis. In order to determine if the interaction of osteoblasts and breast cancer cells produced a factor that facilitated osteoclastogenesis, IL-6, utilized as a representative cytokine, was added to bone marrow cells. TRAP positive multi-nucleated osteoclasts were not formed when bone marrow cells were treated with IL-6, under conditions of this study (Figure 6.3). Thus, cytokines in the culture supernatant of osteoblasts cultured with metastatic breast cancer cells or their conditioned medium other than *or* in addition to IL-6 are necessary for osteoclast formation.

In this study, the role of osteoblast-derived cytokines in bone metastatic breast cancer was assessed using various tests. It was found that osteoblast-derived cytokines were 1) increased in the presence of metastatic breast cancer cells or their conditioned medium *in vitro* (Figures 3.6, 3.16, 5.3-5.6), 2) were present in the femur metaphyses of cancer-bearing and non-cancer-bearing mice *in vivo* (Figure 5.13-5.14), but 3) did not facilitate osteoclastogenesis (IL-6)(Figure 6.3), or 4) were not chemoattractants for metastatic breast cancer cells *in vitro* (Figure 6.1). However, even though osteoblast-derived cytokines were not identified as chemoattractants, their role in bone metastatic breast cancer may be just as sinister. In addition to RANK, osteoclast precursors express receptors for IL-6, IL-8/MIP-2, GRO-α/KC, MCP-1, and VEGF [44, 87-89, 92]. In the absence of the RANK-RANKL pathway, these cytokines can stimulate osteoclastogenesis [44, 87-89]. With this knowledge, the following model of cytokine involvement in bone metastatic breast cancer is proposed (Figure 9.1): Osteoblast-derived IL-6, KC, MCP-1, MIP-2, and VEGF are produced during normal bone remodeling, which occurs in the metaphyseal region of long bones. Metastatic breast cancer cells are attracted to the bone microenvironment through a yet unidentified chemoattractant. Here osteoblasts are induced to increase their production of the inflammatory cytokines IL-6, KC, MCP-1, MIP-2, and VEGF, leading to increased osteoclastogenesis and bone resorption, independent of the RANK-RANKL pathway of osteoclastogenesis. Additional breast cancer maintenance factors, such as TGF-β [4], are released from bone, which facilitate breast cancer cell colonization and survival. Furthermore, MCP-1 is specifically produced by the cells of the bone [55, 70], including osteoblasts [93], but not by metastatic breast cancer cells. Metastatic breast cancer cells do, however, express the receptor to MCP-1, CCR1/2 [4, 72, 73]. MCP-1 stimulates osteoclastogenesis, but also may be a maintenance factor for metastatic breast cancer cells. Furthermore, Takashita, et al. reported that TGF-β increased the expression of MCP-1 in osteoblasts [94]. Therefore, the presence of metastatic breast cancer cells ultimately leads to the release of the breast cancer maintenance factor TGF-β, which subsequently induces the expression of MCP-1, that leads to osteoclastogenesis as well as facilitating tumor cell colonization

and survival. Furthermore, elevated serum levels of MCP-1 are an indicator of poor prognosis in a patient [95, 96]. Lebrecht, et al. conducted a study that examined the MCP-1 serum levels in patients with breast cancer, ductal carcinoma in situ, benign breast lesions, as well as healthy women [95]. It was found that physiological levels of serum MCP-1 in healthy patients or women with benign breast lesions was 175 pg/ml, whereas MCP-1 serum concentrations were higher in patients with advanced stages of breast cancer (194-200 pg/ml)[95]. It was additionally determined that the concentration of serum MCP-1 correlated with advanced tumor stage as well as lymph node involvement in the disease [95]. Therefore, it is possible that MCP-1 may also influence tumorigenesis by facilitating tumor growth and metastatic spread.

If osteoblast-derived MCP-1, MIP-2, KC, VEGF, and IL-6 are not chemoattractants for human metastatic breast cancer cells, what factors are? First, there is the possibility that the transwell system *in vitro* (Figure 2.3) did not fully recapitulate events *in vivo*. In addition to osteoblasts and osteoblast cell secretions, the bone microenvironment *in vivo* consists of cells of the bone stroma, such as endothelial cells, that have been shown to increase breast cancer cell invasion [64]. It may be possible that interaction with these cells *in vivo*, in addition to the osteoblast-derived cytokines identified in this study, facilitate breast cancer cell migration. Second, there has been considerable evidence in the literature that chemokines, specifically CXCL12 (stromal cell-derived factor 1; SDF-1) and its respective receptor, CXCR4, are involved in attracting breast cancer cells to the bone microenvironment (SDF-1 is the only known ligand for CXCR4 [72, 97, 98]). Muller, et al. reported that MDA-MB-231W human metastatic breast cancer cells express CXCR4. In addition, it was reported that the ligand to CXCR4, SDF-1, is expressed in high concentrations in bone and bone marrow [72]. Furthermore, exogenous SDF-1 was found to induce the directional migration and directional invasion of MDA-MB-231W human metastatic breast cancer cells through a reconstituted basement membrane [72]. Additionally, metastatic breast cancer cells migrated towards bone marrow conditioned medium, while neutralization of CXCR4 significantly reduced metastasis *in vivo* [72]. Finally, Sun, et al. reported that high levels of SDF- 1 were present in the femur metaphyses and epiphyses (areas to which breast cancer cells preferentially traffic [40]) as opposed to the diaphysis [99]. The blockade of CXCR4 reduced bone metastases *in vivo*, as well as limited intratibial tumor growth [99]. These findings indicate that the SDF-1/CXCR4 axis plays an important role in the directional metastasis of metastatic breast cancer cells to bone.

In further studies, Kang, et al. reported that a multigenic program, which includes CXCR4, mediates breast cancer metastases to bone [100]. Overexpression of CXCR4 in MDA-MB-231W human metastatic breast cancer cells, resulted in a significant increase in cancer cell metastases to the skeleton [100]. Furthermore, when CXCR4 was overexpressed with IL-11 and osteopontin, there was a dramatic increase in both the rate and incidence of bone metastases [100]. In addition, high expression of CXCR4 has been clinically correlated with bone metastases [72, 101, 102]. Furthermore, inhibition of CXCR4 by the selective synthetic polypeptide TN14003 or by small interfering RNA effectively blocks breast cancer cell metastases [103] or growth *in vivo* [104], respectively. Thus, as an addition to the proposed model of breast cancer metastases to the bone (Figure 9.1), SDF-1 could serve as the chemoattractant. Metastatic breast cancer cells, expressing the CXCR4 receptor, are attracted to SDF-1 in the bone

microenvironment. The presence of breast cancer cells in the bone causes a substantial increase in the osteoblast-derived cytokines IL-6, MIP-2, KC, MCP-1, and VEGF, which are already present, and leads to increased osteoclastogenesis, the release from bone of additional breast cancer maintenance factors like TGF-β [4], and enhancement of the vicious cycle of bone metastatic breast cancer (Figure 9.2). In the model proposed in Figure 9.2, osteoclastogenesis may occur independent of the RANK-RANKL pathway. (The SDF-1/CXCR4 axis, and its interaction with osteoblast-derived cytokines, was not tested in the study described here. Future studies may incorporate SDF-1/CXCR4 and osteoblast-derived cytokines when attempting to decipher mechanisms of bone metastatic breast cancer.)

In addition to the SDF-1/CXCR4 axis, macrophage-stimulating protein (MSP) and its receptor RON may also been involved in breast cancer metastases to the bone microenvironment. It has been reported that MSP facilitates the growth and dissemination of tumors in mice [105]. Welm, et al. reported that tumors that expressed MSP were more locally invasive and metastasized earlier than tumors that did not express the ligand [105]. Furthermore, it was found that tumor cells that expressed MSP were able to stimulate the activation of osteoclast-like cells, which resulted in bone resorption [105]. In addition, altered expression of the receptor to MSP, RON, on epithelial cells have been found to lead to neoplastic transformation in athymic nude mice, and promote tumor metastases [106]. Therefore, the expression of the MSP/RON axis may play a role in accentuating tumor cell migration to secondary sites.

While many unanswered questions remain, the probability of a pre-metastatic niche and/or metastatic signature is likely. Both bone- and tumor-derived MCP-1, VEGF, IL-8/MIP-2, GRO-α/KC, and IL-6, as examined in this study, have a variety of known targets including osteoclast precursors, osteoclasts, endothelial cells, cancer cells, and osteoblasts [55, 107, 108]. Each of these cells contribute to making the metaphyseal region of bone attractive for metastatic breast cancer cell colonization. Furthermore, the arrival of increased numbers of megakaryocytes (Figure 5.19) may additionally prepare the bone metaphysis for cancer cell colonization. Schick, et al. reported that megakaryocytes synthesize and secrete von Willebrand factor and fibronectin, two proteins involved in cellular adhesion, during their maturation [109]. It is possible that these adhesive proteins may facilitate breast cancer cell adhesion to and colonization in the bone. In addition, VEGF and IL-6 induce megakaryocytopoiesis [110, 111]. Therefore, an increase in these osteoblast-derived cytokines due to the presence of metastatic breast cancer cells may facilitate megakaryocyte development and the subsequent fertilization of a congenial soil for metastatic breast cancer cell colonization and survival. Given evidence of the impact of IL-6, MIP-2, KC, MCP-1, and VEGF on the bone microenvironment, there is little doubt that they are key mediators in bone metastatic breast cancer.

9.1: Future directions

Through a serendipitous observation, it was seen that the number of megakaryocytes increased in the femurs of cancer-bearing mice (Figure 5.19). These mice had not yet developed clinically detectable tumors; yet the increase in the number of megakaryocytes present was substantial when compared to non-cancer-bearing mice. The presence of megakaryocytes in cancer progression presents several interesting

questions: 1) are concentrations of thrombopoietin, a glycoprotein hormone that stimulates the production and differentiation of megakaryocytes [84], elevated in the blood of cancer-bearing mice? 2) At what time do megakaryocytes increase their presence in cancer-bearing mice? 3) How long after an increase in megakaryocyte numbers will metastatic cancer cells, and ultimately, tumor formation occur? 4) Do megakaryocytes indicate the site of bone metastatic breast cancer cell colonization? 5) At what point do megakaryocytes lose the antigen for CD41 in cancer-bearing mice. 6) Is the increase in megakaryocytes due to an increase in osteoblast-derived cytokines? And, 7) do megakaryocytes indeed prime the bone 'soil' for cancer cell arrival and colonization? These questions can be addressed in a series of experiments examining megakaryocyte arrival in the bone microenvironment and subsequent tumor formation *in vivo*. First, athymic nude mice inoculated via intracardiac injection with MDA-MB-231W-GFP human metastatic breast cancer cells could be euthanized at various times from 1 hour to 4 weeks post-inoculation, and their blood collected via an eye bleed. Serum or plasma thrompoietin concentrations could then be determined via an ELISA [112]. Conducting the ELISA for the determination of thrombopoietin concentrations would answer question 1 listed above, and additionally show if megakaryocytes were stimulated to differentiate in bone metastatic breast cancer. In addition, the murine femurs could be harvested, and examined for the presence of megakaryocytes via immunohistochemical staining of CD41, hematoxylin and eosin stain, as well as fluorescence stereo-microscopy for the presence of metastatic tumor cells. The comparison of results derived from this experiment, which would show megakaryocyte presence over time, the formation and location of tumor cells with respect to megakaryocyte presence, as well as loss of CD41 by the megakaryocytes, would answer questions 2-5 listed above. Is the increase in megakaryocytes due to an increase in osteoblast-derived cytokines? This situation is unlikely. First, osteoblast-derived cytokines are normally produced in the bone microenvironment. Megakaryocytes were not present in large numbers in non-cancer-bearing mice, where minor fluctuations of cytokine expression may occur during bone turnover. Second, osteoblast-derived cytokines increased in quantity *after* cancer cell arrival. Third, megakaryocyte arrival and increase in number was seen *before* the arrival of metastatic tumor formation. Thus, it seems reasonable to conclude that the increase in numbers of megakaryocytes in the bone microenvironment was not due to an increase in osteoblast-derived cytokines. In order to determine whether megakaryocytes prime the bone microenvironment for cancer cell arrival and colonization, one could repeat the proposed experiment, but use mice rendered severely deficient in megakaryocytes through the targeted gene deletion of the thrombopoietin receptor c-Mpl [113]. If cancer cells continue to seed the bone microenvironment, then megakaryocytes are sufficient, but not necessary for metastatic tumor formation at a secondary site.

Interestingly, and contrary to the hypothesis that bone-derived cytokines would be elevated in cancer-bearing mice compared to non-cancer-bearing mice, there were no visual differences in the expression of murine-derived cytokines in the femurs of cancer-bearing and non-cancer-bearing mice as detected by immunohistochemistry (Figures 5.13-5.15). It may be the case that, upon tumor formation, maximal changes in cytokine expression in the bone marrow had already occurred. Therefore, it may be beneficial to examine murine-derived cytokine expression over the course of time to determine

whether they are altered early in cancer progression. Again, athymic nude mice inoculated via intracardiac injection with MDA-MB-231W-GFP human metastatic breast cancer cells could be euthanized over various times from 1 hour to 4 weeks, their femurs harvested, and examined for the presence of murine-derived cytokines via immunohistochemistry, culturing of femur pieces, as well as for tumor formation via fluorescence stereo-microscopy. The alteration of murine cytokine levels at early stages of cancer progression, would suggest that metastatic breast cancer cells, whether or not present in the bone microenvironment, exert substantial effects on the bone cells, possibly co-opting those cells to prepare the bone microenvironment for metastatic cancer cell colonization and survival. It may be that at an earlier stage of cancer progression that anti-cancer therapies such as bisphosphonates, chemotherapy, and radiation therapy, would be most effective clinically.

Finally, contrary to the hypothesis that osteoblast-derived cytokines are increased only in the presence of bone-seeking, metastatic breast cancer cells, no differences were observed in cytokine expression between metastatic, bone-seeking, or non-metastatic human breast cancer cells when inoculated via intracardiac injection into athymic nude mice *in vivo* (Figures 5.3-5.6). These results were also observed with *in vitro* studies (Figure 3.6). Furthermore, osteoblast-derived cytokine expression increased the most when osteoblasts were treated with conditioned media from human epithelial cells *in vitro* (Figure 3.10). These results pose three interesting questions: 1) do changes in cytokine expression occur earlier in cancer progression with a bone-seeking variant? 2) Do changes in cytokine expression occur earlier in cancer progression with a non-metastatic BRMS variant? 3) What changes in cytokine expression occur when athymic nude mice are inoculated with a cell line other than metastatic or non-metastatic breast cancer cells? Once again, these questions can be answered via *in vivo* experimentation. Athymic nude mice independently inoculated via intracardiac injection with a) MDA-MB-231W-GFP, b) MDA-MB-231PY-GFP, c) MDA-MB-231BO-GFP, d) MDA-MB-231BRMS-GFP, or e) hTERT-HME1 cells engineered to express GFP (non-cancerous cell) could be euthanized at various times from 1 hour to six weeks post-inoculation, their femurs harvested, and examined for the presence of murine-derived cytokines via immunohistochemical staining, culturing of cut femur pieces, as well as fluorescence stereo-microscopy for tumor formation. Increases in murine-derived cytokine expression may occur earlier than three weeks in both bone-seeking and non-metastatic breast cancer cell variants, suggesting that breast cancer cells exert an effect on osteoblasts early in cancer progression, irrespective of tumor formation. Additionally, the inoculation of hTERT-HME1 cells engineered to express GFP may more clearly indicate the magnitude of the inflammatory response elicited by murine cells. Specifically, it may be the case that murine-derived cytokines are substantially increased in mice inoculated with hTERT-HME1 cells, and that these increases will be above and beyond that seen with inoculation of human metastatic breast cancer cells. These results would suggest that the resultant increase in murine-derived cytokines is a generalized inflammatory response due to the inoculation of non-cancerous cells, which is similar to the inflammatory response seen with the implant of foreign particles such as titanium transplants [52]. Furthermore, these data would then suggest that human metastatic breast cancer cells mimic an osteoblast phenotype *in vivo*, resulting in a murine-derived inflammatory response that is not as large as inoculation with non-cancerous cells, such hTERT-HME1.

Anti-cancer or anti-inflammatory drugs may then be better tailored to the response induced by metastatic breast cancer cells as opposed to that induced by non-cancerous cells, in order to more effectively combat bone metastatic breast cancer.

9.2: Summary

The findings presented in this study support the idea that breast cancer metastases create a unique bone niche by co-opting the normal cells of the bone to favor tumor cell colonization and survival. While other cells types are undoubtedly involved in metastatic and tumorigenic processes, here, a direct effect of metastatic breast cancer cells on osteoblasts is demonstrated.

Part 10: REFERENCES

1. Roodman, GD. "Mechanisms of bone metastasis." N Engl J Med. 350: 2004. 1655-1664.
2. Mastro, AM, CV Gay, DR Welch. "The skeleton as a unique environment for breast cancer cells." Clin & Exp Metas. 20: 2003. 275-284.
3. Kanis, JA, EV McCloskey. "Bone turnover and biochemical markers in malignancy." Cancer. 80: 1997. 1538-1545.
4. Mundy, GR. "Metastasis to bone: causes, consequences and therapeutic opportunities." Nat Rev Cancer. 2: 2002. 584-593.
5. Mercer, R, C Miyasaka, AM Mastro. "Metastatic breast cancer cells suppress osteoblast adhesion and differentiation." Clin & Exp Metas. 21: 2004. 427-435.
6. Hiraga, T, PJ Williams, GR Mundy. "The bisphosphonate ibandronate promotes apoptosis in MDA-MB-231 human breast cancer cells in bone metastases." Cancer Res. 61: 2001. 4418-4424.
7. Taube, T, I Elomaa, C Blomqvist, NC Benton, JA Kanis. "Histomorphometric evidence for osteoclast-mediated bone resorption in metastatic breast cancer." Bone. 15: 1994. 161-166.
8. Guise, TA. "Molecular mechanisms of osteolytic bone metastases." Cancer. 88: 2000. 2892-2898.
9. Mastro, AM, CV Gay, DR Welch, HJ Donahue, J Jewell, R Mercer, D DiGirolamo, EM Chislock, K Guttridge. "Breast cancer cells induce osteoblast apoptosis: a possible contributor to bone degradation." J Cell Biochem. 91: 2004. 265-276.
10. Mercer, R, AM Mastro. "Cytokines secreted by bone-metastatic breast cancer cells alter the expression pattern of f-actin and reduce focal adhesion plaques in osteoblasts through PI3K." Exp Cell Res. 310: 2005. 270-281.
11. Kinder, M, EM Chislock, KM Bussard, LA Shuman, AM Mastro. "Metastatic breast cancer induces an osteoblast inflammatory response." Exp Cell Res. 314: 2008. 173-183.
12. Sudo, H, HA Kodama, Y Amagai, S Yamamoto, S Kasai. "In vitro differentiation and calcification in a new clonal osteogenic cell line derived from newborn mouse calvaria." J Cell Biol. 96(1): 1983. 191-198.
13. Lian, JB, GS Stein. "Concepts of osteoblast growth and differentiation: basis for modulation of bone cell development and tissue formation." Crit Rev Oral Biol Med. 3: 1992. 269-305.

14. Cailleau, R, M Olive, QV Cruciger. "Long-term human breast carcinoma cell lines of metastatic origin: preliminary characterization." In Vitro. 14: 1978. 911-915.
15. Phadke, PA, KS Vaidya, KT Nash, DR Hurst, DR Welch. "BRMS1 suppresses breast cancer experimental metastasis to multiple organs by inhibiting several steps of the metastatic process." Am J Pathol. 172: 2008. 809-817.
16. Seraj, MJ, RS Samant, MF Verderame, DR Welch. "Functional evidence for a novel human breast carcinoma metastasis suppressor, BRMS1, encoded at chromosome 11q13[1]." Cancer Res. 60: 2000. 2764-2769.
17. Price, JE. "Metastasis from human breast cancer cell lines." Breast Cancer Res Treat. 39: 1996. 93-102.
18. Ross, DT, U Scherf, MB Eisen, CM Perou, C Rees, P Spellman, V Iyer, SS Jeffrey, M Van de Rijn, M Waltham, A Pergamenschikov, JC Lee, D Lashkari, D Shalon, TG Myers, JN Weinstein, D Botstein, PO Brown. "Systematic variation in gene expression patterns in human cancer cell lines." Nature Genet. 24: 2000. 208-209.
19. Sellappan, S, R Grijalva, X Zhou, W Wang, MB Eli, GB Mills, D Yu. "Lineage infidelity of MDA-MB-435 Cells: Expression of melanocyte proteins in a breast cancer cell line
." Cancer Res. 64: 2004. 3479-3485.
20. Yoneda, T, PJ Williams, T Hiraga, M Niewolna, R Nishimura. "A bone-seeking clone exhibits different biological properties from the MDA-MD-231 parental human breast cancer cells and a brain-seeking clone in vivo and in vitro." J Bone Miner Res. 16: 2001. 1486-1495.
21. Shay, JW, WE Wright, D Brasiskyte, BA Van der Haegen. "E6 of human papillomavirus type 16 can overcome the M1 stage of immortalization in human mammary epithelial cells but not in human fibroblasts." Oncogene. 8: 1993. 1407-1413.
22. Clontech. "Infinity human mammary epithelial cell line." CLONTECHniques. 15: 2000. 12-13.
23. Soule, H, CM McGrath, Soule, H, CM McGrathSoule, H, CM McGraths; Immortal human mammary epithelial cell lines. United States patent 5,026,637. 1991.
24. Jainchill, JL, SA Aaronson, GJ Todaro. "Murine sarcoma and leukemia viruses: assay using clonal lines of contact-inhibited mouse cells." J Virol. 4: 1969. 549-553.
25. Gaffney, EV. "A cell line (HBL-100) established from human breast milk." Cell Tissue Res. 227: 1982. 563-568.
26. Ball, R, RR Friis, CA Schoenenberger, W Doppler, B Groner. "Prolactin regulation of beta-casein gene expression and of a cytosolic 120-kd protein in a cloned mouse mammary epithelial cell line." J EMBO. 7: 1988. 2089-2095.
27. Green, H, M Meuth. "An established pre-adipose cell line and its differentiation in culture." Cell. 3: 1974. 127-133.
28. Hirai, Y, A Lochter, S Galosy, S Koshida, MJ Bissell. "Epimorphin functions as a key morphoregulator for mammary epithelial cells." J Cell Biol. 140: 1998. 159-169.
29. Fata, JE, H Mori, AJ Ewald, H Zhang, E Yao, Z Werb, MJ Bissell. "The MAPKERK-1,2 pathway integrates distinct and antagonistic signals from TGFb and FGF7 in morphogenesis of mouse mammary epithelium." Dev Biol. 306: 2007. 193-207.
30. Raschke, WC, S Baird, P Ralph, I Nakoinz. "Functional macrophage cell lines transformed by Abelson leukemia virus." Cell. 15: 1978. 261-267.

31. Price, CP. "Multiple forms of human serum alkaline phosphatase: detection and quantitation." Ann Clin Biochem. 30: 1993. 355-372.
32. Sheehan, D, B Hrapchak. Theory and practice of histotechnology. 2nd ed. Ohio: Battelle Press, 1980.
33. Rungby, J, M Kassem, EF Eriksen, G Danscher. "The von Kossa reaction for calcium deposits: silver lactate staining increases sensitivity and reduces background." Histochem J. 25: 1993. 446-451.
34. Bonewald, LF, SE Harris, J Rosser, MR Dallas, SL Dallas, NP Camacho, B Boyan, A Boskey. "von Kossa staining alone is not sufficient to confirm that mineralization in vitro represents bone formation." Calcif Tissue Int. 72: 2003. 537-547.
35. Sudo, H, HA Kodama, Y Amagai, S Yamamoto, S Kasai. "In vitro differentiation and calcification in a new clonal osteogenic cell line derived from newborn mouse calvaria." J Cell Biol. 96: 1983. 191-198.
36. Franceschi, RT, BS Iyer. "Relationship between collagen synthesis and expression of the osteoblast phenotype in MC3T3-E1 cells." J Bone Miner Res. 7: 1992. 235-246.
37. Dhurjati, R, X Liu, CV Gay, AM Mastro, EA Vogler. "Extended-term culture of bone cells in a compartmentalized bioreactor." Tissue Eng. 12: 2006. 3045-3054.
38. Harms, JF, LR Budgeon, ND Christensen, DR Welch. "Maintaining GFP tissue fluorescence through bone decalcification and long-term storage." BioTechniques. 33: 2002. 1197-1200.
39. Liu, F, JL Whitton. "Cutting edge: re-evaluating the in vivo cytokine responses of CD8+ T cells during primary and secondary viral infections." J Immunol. 174: 2005. 5936-5940.
40. Phadke, PA, RR Mercer, JF Harms, J Yujiang, AR Frost, JL Jewell, KM Bussard, S Nelson, C Moore, JC Kappes, CV Gay, AM Mastro, DR Welch. "Kinetics of metastatic breast cancer cell trafficking in bone." Clin Cancer Res. 12: 2006. 1431-1440.
41. Mercer, R, C Miyasaka, AM Mastro. "Metastatic breast cancer cells suppress osteoblast adhesion and differentiation." Clin & Exp Metas. 21(5): 2004. 427-435.
42. Mercer, R, C Miyasaka, AM Mastro. "Metastatic breast cancer cells suppress osteoblast adhesion and differentiation." Clin Exp Metastasis. 21: 2004. 427-435.
43. Mercer, RM, AM Mastro. "Cytokines secreted by bone-metastatic breast cancer cells alter the expression pattern of f-actin and reduce focal adhesion plaques in osteoblasts through PI3K." Exp Cell Res. 310: 2005. 270-281.
44. Bendre, M, DC Montague, T Peery, NS Akel, D Gaddy, LJ Suva. "Interleukin-8 stimulation of osteoclastogenesis and bone resorption is a mechanism for the increased osteolysis of metastatic bone disease." Bone. 33: 2003. 28-37.
45. Bendre, M, D Gaddy, RW Nicholas, LJ Suva. "Breast cancer metastasis to bone." Clin Ortho Rel Res. 415S: 2003. S39-S45.
46. Bendre, M, D Gaddy-Kurten, T Foote-Mon, NS Akel, RA Skinner, RW Nicholas, LJ Suva. "Expression of interleukin 8 and not parathyroid hormone-related protein by human breast cancer cells correlates with bone metastasis in vivo." Cancer Res. 62: 2002. 5571-5579.
47. Bussard, KM, CV Gay, AM Mastro. "The bone microenvironment in metastasis; what is special about bone?" Cancer Metastasis Rev. 27: 2008. 41-55.
48. Guise, TA, JJ Yin, SD Taylor, Y Kumagai, MR Dallas, BF Boyce, T Yoneda, GR Mundy. "Evidence for a causal role of parathyroid-hormone-related protein in the

pathogenesis of human breast cancer-mediated osteolysis." J Clin Invest. 98: 1996. 1544-1549.
49. de Visser, K, LM Coussens. "The inflammatory tumor microenvironment and its impact on cancer development." Contrib Microbiol. 13: 2006. 118-137.
50. Marriott, I. "Osteoblast responses to bacterial pathogens: a previously unappreciated role for bone-forming cells in host defense and disease progression." Immunol Res. 30: 2004. 291-308.
51. Wright, KM, JS Friedland. "Regulation of chemokine gene expression and secretion in Staphylococcus aureus-infected osteoblasts." Microbes Infect. 6: 2004. 844-852.
52. Fritz, EA, TT Glant, C Vermes, JJ Jacobs, KA Roebuck. "Titanium particles induce the immediate early stress responsive chemokines IL-8 and MCP-1 in osteoblasts." J Orthop Res. 20: 2002. 490-498.
53. Kurihara, N, D Bertolini, T Suda, Y Akiyama, GD Roodman. "IL-6 stimulates osteoclast-like multinucleated cell formation in long term human marrow cultures by inducing IL-1 release." J Immunol. 144(11): 1990. 4226-4230.
54. Black, K, IR Garrett, GR Mundy. "Chinese hamster ovarian cells transfected with the murine interleukin-6 gene cause hypercalcemia as well as cachexia, leukocytosis and thrombocytosis in tumor-bearing nude mice." Endocrinology. 128: 1991. 2657-2659.
55. Fitzgerald, KA, LAJ O'Neill, AJH Gearing, RE Callard. The cytokine facts book. New York: Academic Press, 2001.
56. Carmeliet, P, V Ferreira, G Breier, S Pollefeyt, L Kieckens, M Gertsenstein, M Fahrig, A Vandenhoeck, K Harpal, C Eberhardt, C Declercq, J Pawling, L Moons, D Collen, W Risau, A Nagy. "Abnormal blood vessel development and lethality in embryos lacking a single VEGF allele." Nature. 380: 1996. 435-439.
57. Ferrara, N, K Carver-Moore, H Chen, M Dowd, L Lu, KS O'Shea, L Powell-Braxton, KJ Hillan, MW Moore. "Heterozygous embryonic lethality induced by targeted inactivation of the VEGF gene." Nature. 380: 1996. 439-442.
58. Barnes, GL, A Javed, SM Waller, MH Kamal, KE Hebert, MQ Hassan, A Bellahcene, AJ Van Wijnen, MF Young, JB Lian, GS Stein, LC Gerstenfeld. "Osteoblast-related transcription factors Runx2 (Cbfa1/AML3) and Msx2 mediate the expression of bone sialoprotein in human metastatic breast cancer cells." Cancer Res. 15: 2003. 2631-2637.
59. Tetsuya, M. "Toll-like receptor signals and periodontitis." Annals of Kagoshima University Dental School. 24: 2004. 21-32.
60. Bar-Shavit, Z. "Taking a toll on the bones: regulation of bone metabolism by innate immune regulators " Autoimmunity. 41: 2008. 195-203.
61. Zou, W, A Amcheslavsky, Z Bar-Shavit. "CpG oligodeoxynucleotides modulate the osteoclastogenic activity of osteoblasts via toll-like receptor 9." J Biol Chem. 278: 2003. 16732-16740.
62. Tavaria, M, T Gabriele, I Kola, RL Anderson. "A hitchhiker's guide to the human Hsp70 family." Cell Stress Chaperones. 1: 1996. 23-28.
63. Zhang, W, WT Couldwell, MF Simard, H Song, JH-C Lin, M Nedergaard. "Direct gap junction communication between malignant glioma cells and astrocytes." Cancer Res. 59: 1999. 1994-2003.

64. Mierke, CT, DP Zitterbart, P Kollmannsberger, C Raupach, U Schlotzer-Schrehardt, TW Goecke, J Behrens, B Fabry. "Breakdown of the endothelial barrier function in tumor cell transmigration." Biophys J. 94: 2007. 2832-2846.
65. Olthof, SG, S Fatrai, AL Drayer, M Tyl, E Vellenga, JJ Schuringa. "Downregulation of STAT5 in CD34+ Cells Promotes Megakaryocytic Development while Activation of STAT5 Drives Erythropoiesis." Stem cells. 26: 2008. 1732-1742.
66. Mazo, IB, UH von Andrian. "Adhesion and homing of blood-borne cells in bone marrow microvessels." J Leukoc Biol. 66: 1999. 25-32.
67. Buckwalter, JA. "Pharmacological treatment of soft-tissue injuries." J Bone Joint Surg Am. 77: 1995. 1902-1914.
68. Guise, TA, JM Chirgwin. "Transforming growth factor-beta in osteolytic breast cancer bone metastases." Clin Ortho Rel Res. 4155: 2003. 532-538.
69. Badache, A, NE Hynes. "Interleukin 6 inhibits proliferation and, in cooperation with epidermal growth factor receptor autocrine loop, increases migration of T47D breast cancer cells." Cancer Res. 61: 2001. 383-391.
70. Goede, V, L Brogelli, M Ziche, HG Augustin. "Induction of inflammatory angiogenesis by monocyte chemoattractant protein-1." Int J Cancer. 82: 1999. 765-770.
71. Underhill, N, JK Heath. "Oncostatin M (OSM) cytostasis of breast tumor cells: characterization of an OSM receptor beta-specific kernel." Cancer Res. 66: 2006. 10891-10901.
72. Muller, A, B Homey, H Soto, N Ge, D Catron, ME Buchanan, T McClanahan, E Murphy, W Yuan, SN Wagner, JL Barrera, A Mohar, E Verastegui, A Zlotnik. "Involvement of chemokine receptors in breast cancer metastasis." Nature. 410: 2001. 50-56.
73. Raman, D, PJ Baugher, YM Thu, A Richmond. "Role of chemokines in tumor growth." Cancer Letters. 256: 2007. 137-165.
74. Wu, Y, AT Hooper, Z Zhong, L Witte, P Bohlen, S Rafii, DJ Hicklin. "The vascular endothelial growth factor receptor (VEGFR-1) supports growth and survivial of human breast carcinoma." Int J Cancer. 119: 2006. 1519-1529.
75. Horowitz, MC, JA Lorenzo. Principles of bone biology. 2 ed. San Diego: Academic Press, 2002.
76. Marriott, I, DL Gray, SL Tranguch, VG Fowler Jr., M Stryjewski, LS Levin, MC Hudson, KL Bost. "Osteoblasts express the inflammatory cytokine interleukin-6 in a murine model of *Staphylococcus aureus* osteomyelitis and infected human bone tissue." Am J Pathol. 164: 2004. 1399-1406.
77. Marriott, I, DL Gray, D Rati, VG Fowler Jr., M Stryjewski, LS Levin, MC Hudson, KL Bost. "Osteoblasts produce monocyte chemoattractant protein-1 in a murine model of osteomyelitis and infected human bone tissue " Bone. 37: 2003. 504-512.
78. Mukaida, N, SA Ketlunsky, K Matsushima. The cytokine handbook. Amsterdam: Academic Press, 2003.
79. Waage, A, P Brandtzaeg, A Halstensen, P Kierulf, T Espevik. "The complex pattern of cytokines in serum from patients with meningococcal septic shock." J Exp Med. 169: 1989. 333-338.
80. Faure, C, M-T Linossier, L Malaval, M-H Lafage-Proust, S Peyroche, L Vico, A Guignandon. "Mechanical signals modulated vascular endothelial growth factor-A

(VEGF-A) alternative splicing in osteoblastic cells through actin polymerisation." Bone. 42: 2008. 1092-1101.
81. Wels, J, RN Kaplan, S Rafii, D Lyden. "Migratory neighbors and distant invaders: tumor-associated niche cells." Genes Dev. 22: 2008. 559-574.
82. Kaplan, RN, B Psaila, D Lyden. "Bone marrow cells in the 'pre-metastatic niche': within bone and beyond." Cancer Metastasis Rev. 25: 2006. 521-529.
83. Paget, S. "The distribution of secondary growths in cancer of the breast." Cancer Metastasis Rev. 8: 1889. 98-101.
84. Kaushansky, K. "Lineage-specific hematopoietic growth factors." N Engl J Med. 354: 2006. 2034-2045.
85. Giunciuglio, D, T Cai, C Filanti, P Manduca, A Albini. "Effect of osteoblast supernatants on cancer cell migration and invasion." Cancer Lett. 97: 1995. 69-74.
86. Starzec, A, R Vassy, A Martin, M Lecouvey, MD Benedetto, M Crepin, GY Perret. "Antiangiogenic and antitumor activities of peptide inhibiting the vascular endothelial growth factor binding to neuropilin-1." Life Sciences. 79: 2006. 2370-2381.
87. Moonga, BS, OA Adebanjo, H-J Wang, X Li, XB Wu, B Troen, A Inzerillo, E Abe, C Minkin, CL-H Huang, M Zaidi. "Differential effects of interleukin-6 receptor activation on intracellular signaling and bone resorption by isolated rat osteoclasts." J Endocrinol. 173: 2002. 395-405.
88. Niida, S, M Kaku, H Amano, H Yoshida, H Kataoka, S Nishikawa, K Tanne, N Maeda, S-I Nishikawa, H Kodama. "Vascular endothelial growth factor can substitute for macrophage colony-stimulating factor in the support of osteoclastic bone resorption." J Exp Med. 190: 1999. 293-298.
89. Kim, MS, CJ Day, NA Morrison. "MCP-1 is induced by RANKL, promotes human osteoclast fusion and rescues GM-CSF suppression of osteoclast formation." J Biol Chem. 280: 2005. 16163-16169.
90. Lu, Y, Z Cai, G Xiao, ET Keller, A Mizokami, Z Yao, GD Roodman, J Zhang. "Monocyte chemotactic protein-1 mediates prostate cancer-induced bone resorption." Cancer Res. 67: 2007. 3646-3653.
91. Kim, MS, CJ Day, CI Selinger, CL Magno, SRJ Stephen, NA Morrison. "MCP-1-induced human osteoclast-like cells are tartrate-resistant acid phosphatase, NFATc1, and calcitonin receptor-positive but require receptor activator of NFB ligand for bone resorption." J Biol Chem. 281: 2006. 1274-1285.
92. Niida, S, T Kondo, S Hiratsuka, S-I Hayashi, N Amizuka, T Noda, K Ikeda, M Shibuya. "VEGF receptor 1 signaling is essential for osteoclast development and bone marrow formation in colony-stimulating factor-1 deficient mice." Proc Nat Aca Sci. 102: 2005. 14016-14021.
93. Horowitz, MC, JA Lorenzo. Local regulators of bone: IL-1, TNF, Lymphotoxin, Interferon-γ, IL-8, IL-10, IL-4, the LIF/IL-6 Family, and additional cytokines. In: Bilezikian, JP, LG Raisz, GA Rodan, eds. Principles of bone biology. San Diego: Academic Press; 2002:961-978.
94. Takeshita, A, Y Chen, A Watanabe, S Kitano, S Hanazawa. "TGF-beat induces expression of monocyte chemoattractant JE/monocyte chemoattractant protein 1 via transcriptional factor AP-1 induced by protein kinase in osteoblastic cells." J Immunol. 155: 1995. 419-426.

95. Lebrecht, A, C Grimm, T Lantzsch, E Ludwig, L Heflerb, E Ulbrich, H Koelbla. "Monocyte Chemoattractant Protein-1 Serum Levels in Patients with Breast Cancer." Tumor Biol. 25: 2004. 14-17.
96. Hefler, L, C Tempfer, G Heinze, K Mayerhofer, G Breitenecker, S Loeodolter, A Reinthaller, C Kainz. "Monocyte chemoattractant protein-1 serum levels in ovarian cancer patients." Br J Cancer. 81: 1999. 855-859.
97. Zou, Y-R, AH Kottmann, M Kuroda, I Tainwchi, DR Littman. "Function of the chemokine receptor CXCR4 in hematopoeisis and in cerebellar development." Nature. 393: 1998. 595-599.
98. Nagasawa, T, S Hirota, K Tachibana, N Takakura, S Nishikawa, Y Kitamura, N Yoshida, H Kikutani, T Kishimoto. "Defects of B-cell lymphopoiesis and bone marrow myelopoiesis in mice lacking the CXC chemokine PBSF/SDF-1." Nature. 382: 1996. 635-638.
99. Sun, Y-X, A Schneider, Y Jung, J Wang, J Dai, J Wang, K Cook, NI Osman, AJ Koh-Paige, J Shim, KJ Pienta, ET Keller, LK McCauley, RS Taichamn. "Skeletal localization and neutralization of the SDF-1 (CXCL12)/CXCR4 axis blocks prostate cancer metastasis and growth in osseous sites in vivo." J Bone Min Res. 20: 2004. 318-329.
100. Kang, Y, PM Siegel, W Shu, M Drobnjak, SM Kakonen, C Cordon-Cardo, TA Guise, J Massague. "A multigenic program mediating breast cancer metastasis to bone." Cancer Res. 3: 2003. 537-549.
101. Geminder, H, O Sagi-Assif, L Goldberg, T Meshel, G Rechavi, IP Witz, A Ben-Baruch. "A possible role for CXCR4 and its ligand, the CXC chemokine stromal cell-derived factor-1, in the development of bone marrow metastases in neuroblastoma." J Immunol. 167: 2001. 4747-4757.
102. Taichman, RS, C Cooper, ET Keller, KJ Pienta, NS Taichman, LK McCauley. "Use of stromal cell-derived factor-1/CXCR4 pathway in prostate cancer metastases to bone." Cancer Res. 62: 2002. 1832-1837.
103. Liang, Z, T Wu, H Lou, X Yu, RS Taichman, SK Lau, S Nie, J Umbreit, H Shim. "Inhibition of breast cancer metastasis by selective synthetic polypeptide against CXCR4." Cancer Res. 64: 2004. 4302-4308.
104. Lapteva, N, AG Yang, DE Sanders, RW Strube, SY Chen. "CXCR4 knockdown by small interfering RNA abrogates breast tumor growth in vivo." Cancer Gene Ther. 12: 2005. 84-89.
105. Welm, AL, JB Sneddon, C Taylor, DSA Nuyten, MJ van de Vijver, BH Hasegawa, JM Bishop. "The macrophage-stimulating protein pathway promotes metastasis in a mouse model for breast cancer and predicts poor prognosis in humans." Proc Nat Aca Sci USA. 104: 7570-7575.
106. Wang, M-H, D Wang, Y-Q Chem. "Oncogenic and invasive potentials of human macrophage-stimulating protein receptor, the RON receptor tyrosine kinase " Carcinogenesis. 24: 2003. 1291-1300.
107. Kurihara, N, D Bertolini, T Suda, Y Akiyama, GD Roodman. "IL-6 stimulates osteoclast-like multinucleated cell formation in long term human marrow cultures by inducing IL-1 release." J Immunol. 144: 1990. 4226-4230.
108. Gabrilovich, DID, M. M. Vascular endothelial growth factor. In: Thomson, AW, MT Lotze, eds. The cytokine handbook. 4th ed. Amsterdam: Academic Press; 2003:1017-1034.

109. Schick, PK, J Walker, B Profeta, L Denisova, V Bennett. "Synthesis and secretion of von willebrand factor and fibronectin in megakaryocytes at different phases of maturation." Arterioscler Thromb Vasc Biol. 17: 1997. 797-801.
110. Williams, N, I Bertoncello, H Jackson, J Arnold, H Kavnoudias. "The role of interleukin 6 in megakaryocyte formation, megakaryocyte development and platelet production." Ciba Found Symp. 167: 1992. 160-173.
111. Casella, I, T Feccia, C Chelucci, P Samoggia, G Castelli, R Guerriero, I Parolini, E Petrucci, E Pelosi, O Morsilli, M Gabbianelli, U Testa, C Peschle. "Autocrine-paracrine VEGF loops potentiate the maturation of megakaryocyte precursors through Flt1 receptor." Blood. 101: 2002. 1316-1323.
112. Folman, CC, AEGK Von Den Borne, IHJAM Rensink, W Gerritsen, CE Van der Schoot, M De Haas, L Aarden. "Sensitive measurement of thrombopoietin by a monoclonal antibody based sandwich enzyme-linked immunosorbent assay." Thromb Haemost. 78: 1997. 1262-1267.
113. Perry, M, K Redding, W Alexander, J Tobias. "Mice rendered severely deficient in megakaryocytes through targeted gene deletion of the thrombopoitin receptor c-Mpl have a normal skeletal phenotype." Calcif Tissue Int. 81: 2007. 2240231.
114. Pederson, L, B Winding, NT Foged, TC Spelsberg, MJ Oursler. "Identification of breast cancer cell line-derived paracrine factors that stimulate osteoclast activity." Cancer Res. 59: 1999. 5849-5855.
115. Guise, TA, JJ Yin, SD Taylor, Y Kumagai, M Dallas, BF Boyce, Y T., M GR. "Evidence for a causal role of parathyroid hormone-related protein in the pathogenesis of human breast-cancer-mediated osteolysis." J Clin Invest. 98: 1996. 1544-1549.

Part 11: SUPPORTING DATA

Cell Line	Tumorigenic	Metastatic	Type	Species
MDA-231	+	+	Epithelial	Human
MDA-231PY	+	+	Epithelial	Human
MDA-231BO	+	+	Epithelial	Human
MDA-231BR	+	+	Epithelial	Human
MDA-435P	+	+	Epithelial	Human
MDA-435BRMS	+	-	Epithelial	Human
MDA-231BRMS	+	-	Epithelial	Human
MDA-468P	+	-	Epithelial	Human
HBL-100	+	-	Epithelial	Human
MCF-10A	-	-	Epithelial	Human
hTERT-HME1	-	-	Epithelial	Human
HC11	-	-	Epithelial	Mouse
Comma-D1	-	-	Epithelial	Mouse
Primary Mammary Epithelial	-	-	Epithelial	Mouse
Primary Mammary Fibroblast	-	-	Fibroblast / Mesenchymal	Mouse
NIH/3T3 Fibroblast	-	-	Fibroblast / Mesenchymal	Mouse
3T3-L1 Fibroblast	-	-	Fibroblast / Mesenchymal	Mouse
Adipocyte	-	-	Fibroblast / Mesenchymal	Mouse

Table 2.1: Characteristics of cells utilized for experimentation.

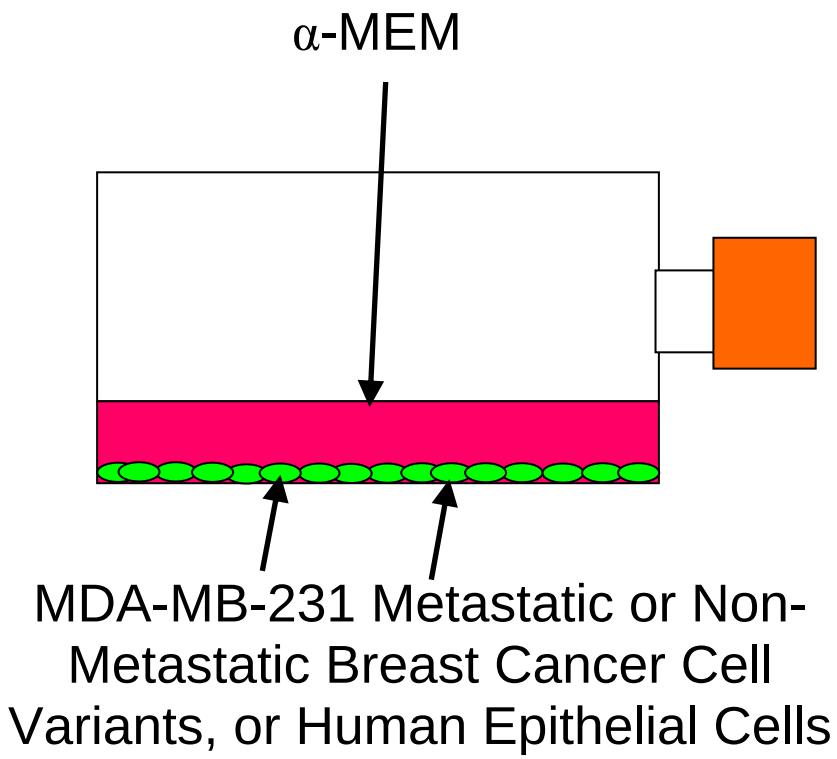

Figure 2.1: Diagram of conditioned medium preparation. Cells of interest were grown to confluence in their respective growth medium. Growth medium was removed, cells are washed, and medium replaced with α-MEM (base medium of MC3T3-E1 osteoblasts). Twenty-four hours later, conditioned medium was collected.

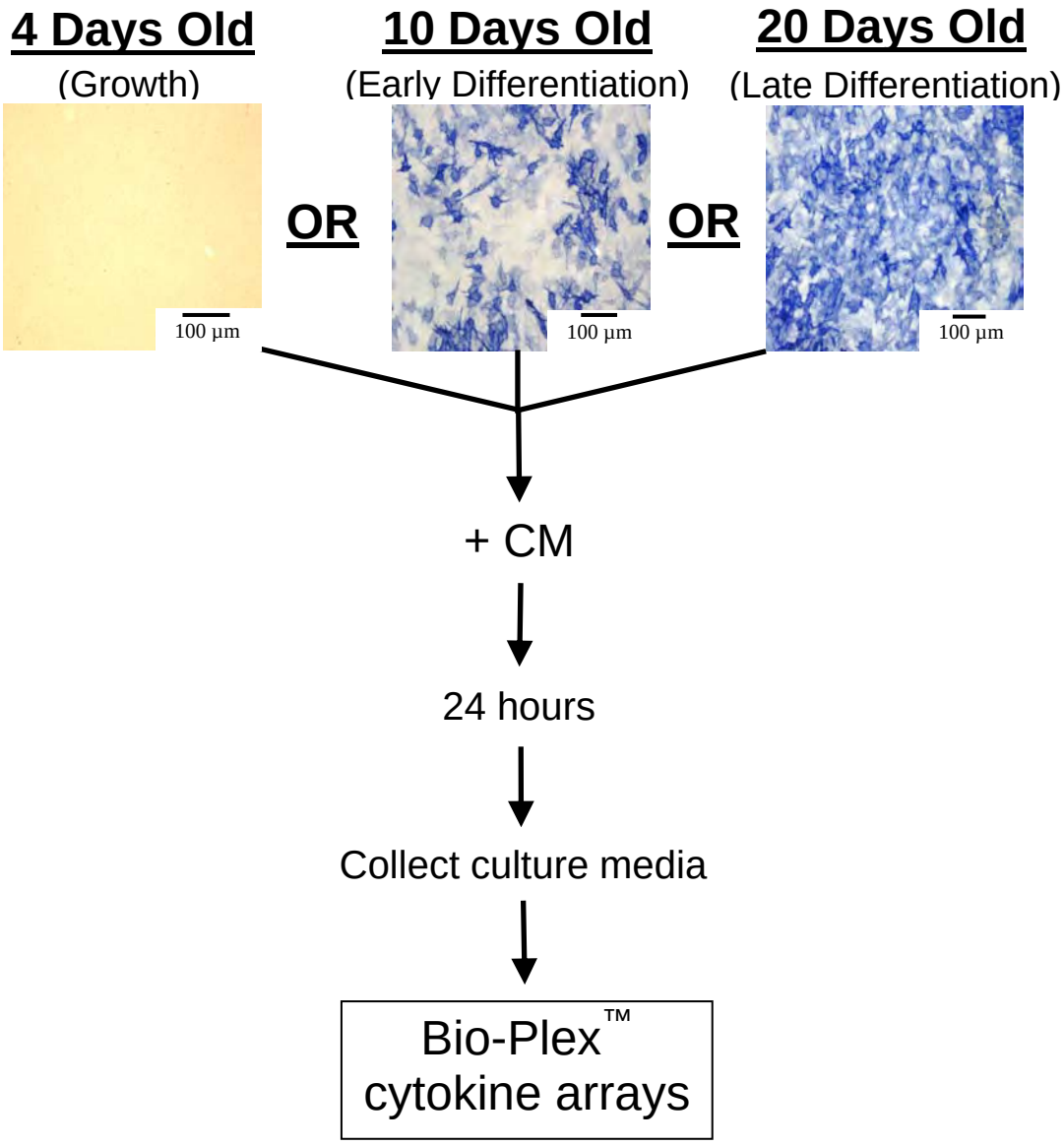

Figure 2.2: MC3T3-E1 cell *in vitro* experimental assay design. Shown are images of osteoblasts stained with alkaline phosphatase.

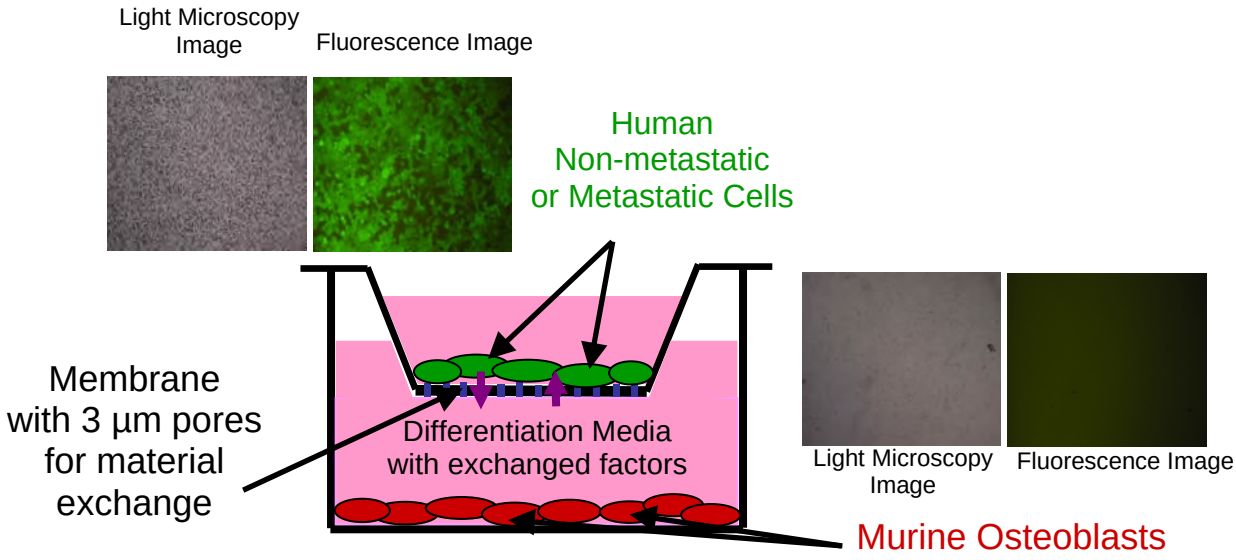

Figure 2.3: The indirect transwell system co-culture experimental design. MC3T3-E1 osteoblasts were grown to either 10 or 20 days in 24 well plates. At day 9 or 19 of osteoblast differentiation, human cells (MDA-231W, MDA-231PY, MDA-231BO, MDA-231BR, MDA-231BRMS, MDA-468P, and hTERT-HME1) were plated in transwell inserts at the following ratios of osteoblast : human cell: "10:1," "1:1," and "1:2." Twenty-four hours later, on day 10 or 20, media were removed from wells and inserts, cells rinsed, and media replaced. Human cell inserts were transferred to wells containing 10 or 20 day old osteoblasts. Three days later, culture media were collected, and assayed for cytokine expression.

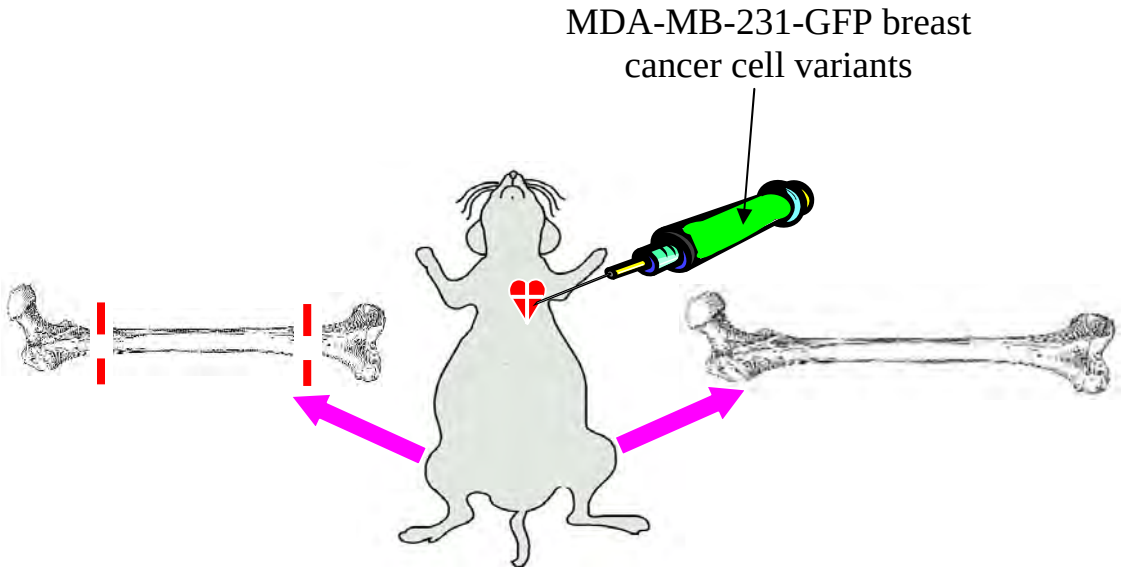

Figure 2.4: The *in vivo* intracardiac inoculation experimental design. Athymic mice were inoculated via intracardiac injection with MDA-MB-231-GFP breast cancer cell variants. Three weeks post-inoculation, some mice were inoculated via tail vein injection with Brefeldin A. Six hours post-Brefeldin A inoculation, all mice were euthanized. Femurs and tibiae were harvested for fluorescence stereo-microscopy, immunohistochemistry, MRI, µCT, and densitometry. Femurs were cut, bone marrow flushed, and femurs and bone marrow independently cultured, and later assayed for cytokine expression. Blood and bone marrow were collected, serum extracted, and assayed for cytokine expression.

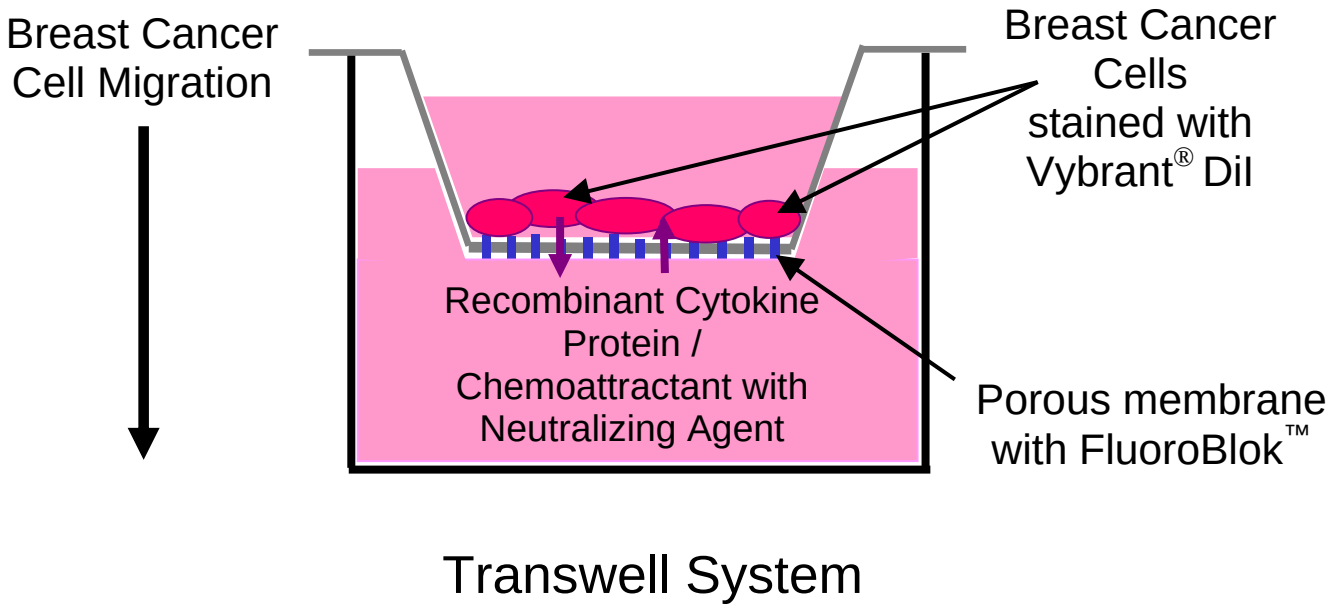

Figure 2.5: An illustration of the inflammatory cytokine bioactivity (chemoattraction) experimental design. Breast cancer cells stained with Vybrant® DiI were seeded in the upper chamber of a transwell system. Recombinant cytokine protein or chemoattractant with neutralizing antibody was added to the bottom chamber. After 24 hours, breast cancer cells that had migrated toward the chemoattractant were counted.

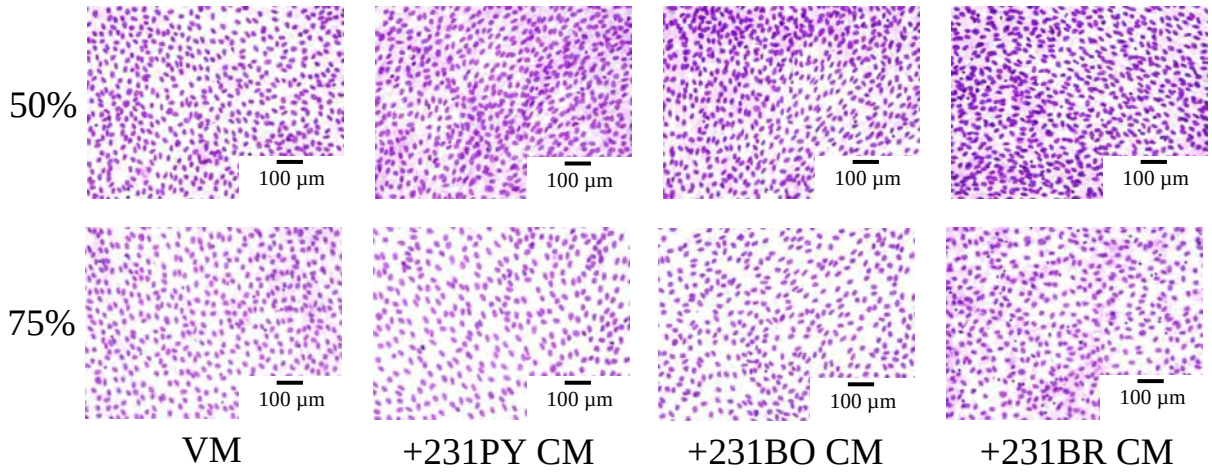

Figure 3.1: MC3T3-E1 cell morphology was not altered by MDA-MB-231 human metastatic breast cancer variant conditioned medium. MC3T3-E1 cells were plated at 1 x 10^5 cells / ml in 35 mm^2 dishes. Twenty-four hours later, growth medium was exchanged for either 50 or 75% MDA-MB-231 human metastatic breast cancer variant conditioned medium. MC3T3-E1 cells were grown an additional 4 days and stained using a LeukoStat™ stain kit to visualize cell morphology. Three biological replicates were carried out per experiment; this experiment was repeated three times. Shown are representative images.

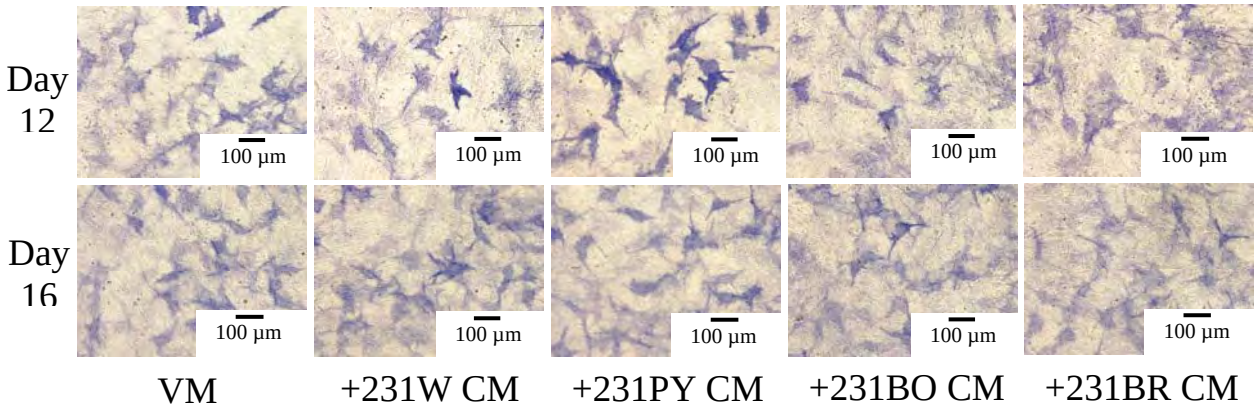

Figure 3.2: Differentiated MC3T3-E1 cells, treated with metastatic breast cancer variant conditioned medium for 24 hours, expressed alkaline phosphatase. MC3T3-E1 cells were grown to 12 or 16 days and treated with MDA-MB-231 human metastatic breast cancer variant conditioned medium. Twenty-four hours later, cells were stained for alkaline phosphatase expression. Three biological replicates were carried out per experiment; this experiment was repeated three times. Shown are representative images.

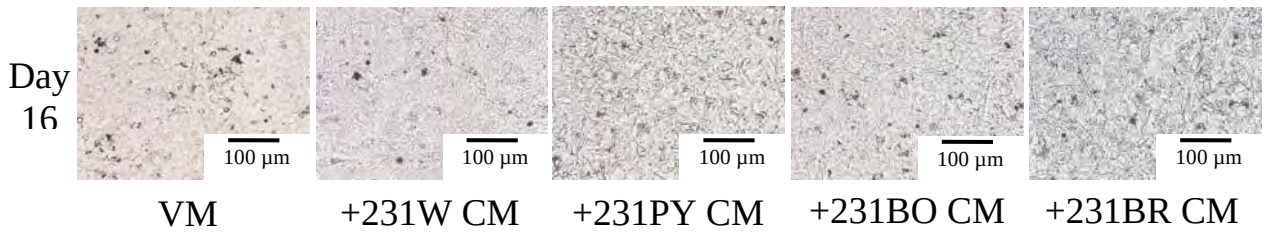

Figure 3.3: Differentiated MC3T3-E1 cells, treated with metastatic breast cancer variant conditioned medium for 24 hours, deposit calcium. MC3T3-E1 cells were grown to 16 days and treated with MDA-MB-231 human metastatic breast cancer variant conditioned medium. Twenty-four hours later, cells were assessed for their ability to deposit calcium via Von Kossa. Three biological replicates were carried out per experiment; this experiment was repeated three times. Shown are representative images.

A) 12 Day old Osteoblasts

	Specific Alkaline Phosphatase Activity (IU/L) of Two Samples		
Conditioned Medium Treatment	IU/L	Mean	Standard Deviation
VM	-	4.8	0
MDA-231W	-	3.4	0
MDA-231PY	3.4, 4.1	3.7	0.48
MDA-231BO	3.4, 4.1	3.7	0.48
MDA-231BR	4.1, 4.8	4.4	0.48

B) 16 Day old Osteoblasts

	Specific Alkaline Phosphatase Activity (IU/L) of Two Samples		
Conditioned Medium Treatment	IU/L	Mean	Standard Deviation
VM	4.8, 7.5	6.1	1.92
MDA-231W	-	5.4	0
MDA-231PY	5.4, 6.1	5.8	0.48
MDA-231BO	5.4, 6.1	5.8	0.48
MDA-231BR	4.1, 6.1	5.1	1.44

Table 3.1: Differentiated MC3T3-E1 cells, treated with metastatic breast cancer variant conditioned medium for 24 hours, expressed alkaline phosphatase enzyme activity. MC3T3-E1 cells were grown to 12 or 16 days and treated with MDA-MB-231 human metastatic breast cancer variant conditioned medium. Forty-eight hours later, culture supernatants were collected and assayed for alkaline phosphatase enzyme activity. Shown are the means and standard deviations of the specific activities of alkaline phosphatase as measured in two samples at 405 nm at 4 minutes.

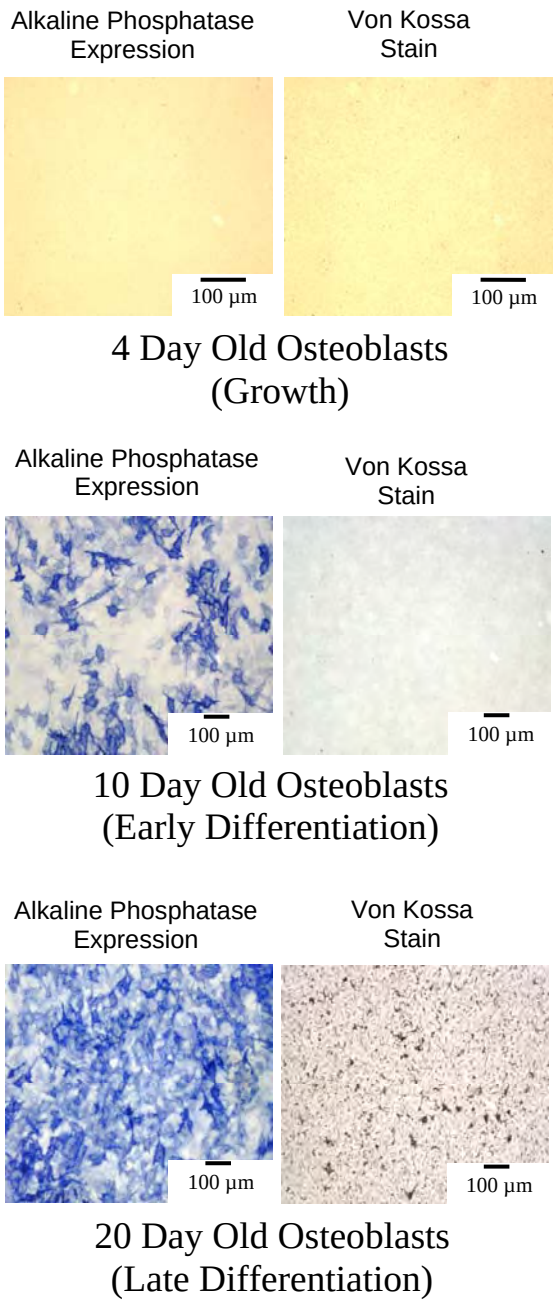

Figure 3.4: MC3T3-E1 cells expressed alkaline phosphatase and deposit calcium. MC3T3-E1 cells were grown to 4, 10, or 20 days and stained for alkaline phosphatase expression and mineralization via Von Kossa. Three biological replicates were carried out per experiment; this experiment was repeated twice. Shown are representative images.

	Cytokine				
Cell Type	**IL-6**	**MCP-1**	**VEGF**	**MIP-2 / IL-8**	**KC / GRO-α**
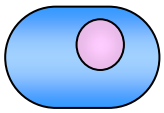 Osteoblast	++	+++	+	+	+

Table 3.2: MC3T3-E1 cells express inflammatory cytokines. MC3T3-E1 cells were grown to ~90% confluency and growth medium exchanged for α-MEM. Twenty-four hours later, the conditioned medium was collected and Bio-Rad Bio-Plex™ Murine Cytokine Assays were conducted to quantitate cytokine expression. Cytokine expression is represented by – (negligible: <0.01 ng/ml), + (little: 0.01 – 0.08 ng/ml), ++ (modest amount: 0.08 – 0.5 ng/ml), and +++ (substantial amount: >0.5 ng/ml). Cytokine concentration was normalized to 1 million cells; variation between batches of conditioned medium was less than 15%. At least two individual batches of conditioned medium were assayed.

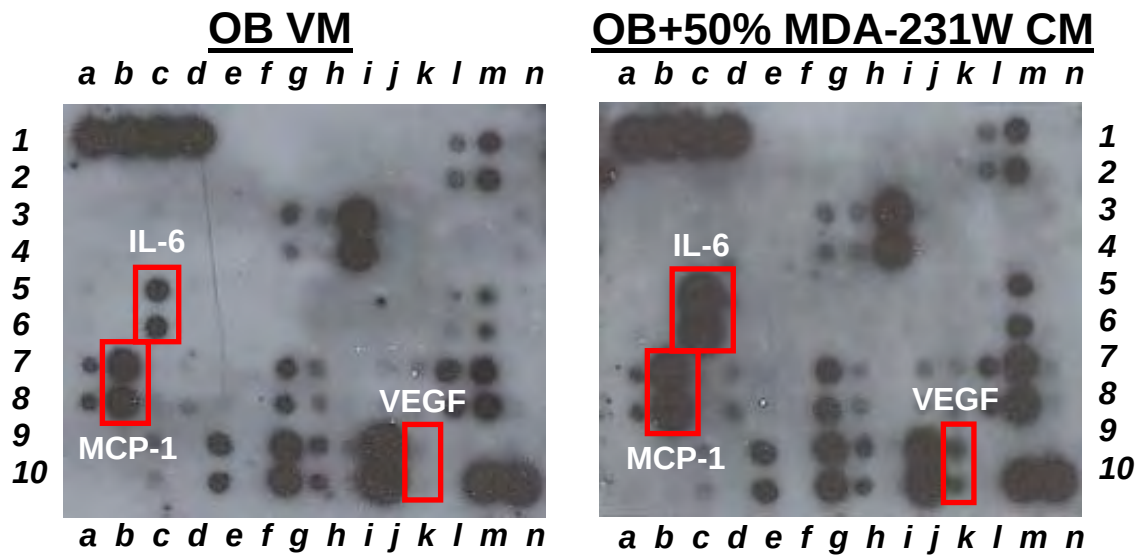

RayBio® Mouse Array System III

	a	b	c	d	e	f	g	h	i	j	k	l	m	n
1	POS	POS	POS	POS	Blank	Axl	BLC	CD30L	CD30T	CD40	CRG-2	CTACK	CXCL16	Eotaxin
2	NEG	NEG	NEG	NEG	Blank	Axl	BLC	CD30L	CD30T	CD40	CRG-2	CTACK	CXCL16	Eotaxin
3,4	Eotaxin-2	Fas Ligand	Fracta-lkine	G-CSF	GM-CSF	IFN-γ	IGFBP-3	IGFBP-5	IGFBP-6	IL-1α	IL-1β	IL-2	IL-3	IL-3 Rb
5,6	IL-4	IL-5	IL-6	IL-9	IL-10	IL-12 p40/70	IL-12 p70	IL-13	IL-17	KC	Leptin R	Leptin	LIX	L-Selectin
7,8	Lympho-tactin	MCP-1	MCP-5	M-CSF	MIG	MIP-1α	MIP-1γ	MIP-2	MIP-3β	MIP-3α	PF-4	P-Selectin	RANTES	SCF
9	SDF-1α	TARC	TCA-3	TECK	TIMP-1	TNFα	sTNF RI	sTNF RII	TPO	VCAM-1	VEGF	Blank	Blank	Blank
10	SDF-1α	TARC	TCA-3	TECK	TIMP-1	TNFα	sTNF RI	sTNF RII	TPO	VCAM-1	VEGF	Blank	POS	POS

Figure 3.5: Osteoblast-derived cytokines were increased in the presence of metastatic breast cancer cell conditioned medium. MC3T3-E1 cells grown to 10 days in MC3T3-E1 differentiation medium were treated with MDA-MB-231W metastatic breast cancer conditioned medium. Twenty-four hours later the culture medium was collected and assayed for cytokine expression. The top panels are cytokine expression as detected by chemiluminescence. The bottom panel is a table of cytokines present on the array. The experiment was repeated three times. Shown is a representative experiment.

Bio-Rad Bio-Plex™ 32 Plex Murine Cytokine Assay (Mouse Group I 23-plex plus Mouse Group II 9-plex)

Cytokine	Cytokine	Cytokine
IL-1α	IL-13	TNF-α
IL-1β	IL-17	IL-15
IL-2	Eotaxin	IL-18
IL-3	G-CSF	FGF basic
IL-4	GM-CSF	LIF
IL-5	IFN-γ	M-CSF
IL-6	KC	MIG
IL-9	MCP-1	MIP-2
IL-10	MIP-1α	PDGF-BB
IL-12 p40	MIP-1β	VEGF
IL-12 p70	RANTES	xxx

Table 3.3: Bio-Rad Bio-Plex™ 32 x-Plex Murine Cytokine Assay. A Bio-Rad Bio-Plex™ 32 x-plex Murine Cytokine Assay was used to quantitate the MC3T3-E1-derived cytokine response to MDA-MB-231 human metastatic breast cancer variant CM. Cytokines identified as having substantial increases in osteoblast-derived cytokine production included IL-6, KC, MCP-1, MIP-2, and VEGF.

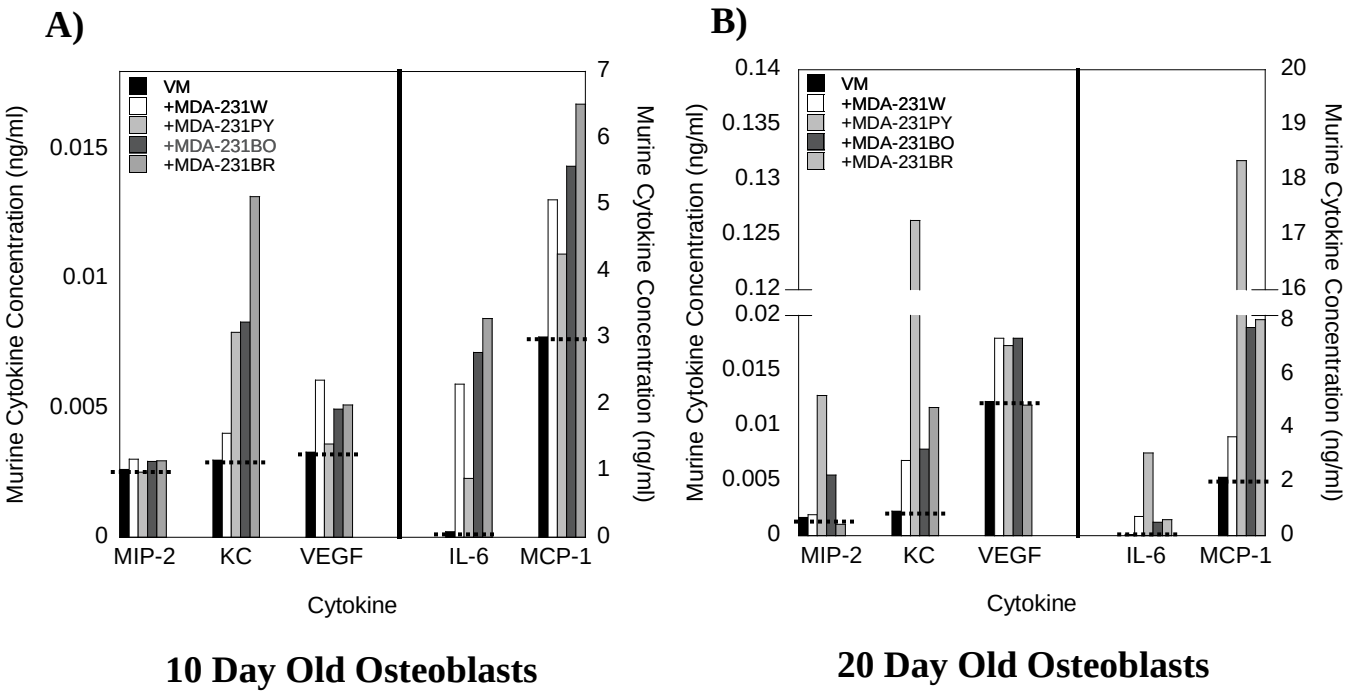

Figure 3.6: Osteoblasts increased inflammatory cytokine production in response to human metastatic breast cancer conditioned medium. MC3T3-E1 cells were grown to either 10 or 20 days and treated with human metastatic breast cancer cell variant CM as described in the Materials and Methods. The culture supernatants were assayed for osteoblast-derived cytokines using a Bio-Rad Bio-Plex™ Murine Cytokine Assay. A) MC3T3-E1 cells grown to 10 days; B) MC3T3-E1 cells grown to 20 days. Supernatants from osteoblasts treated with vehicle medium are represented by the black bar; and in order, MDA-MB-231W CM treatment, white bar; MDA-MB-231PY CM treatment, light grey bar; MDA-MB-231BO CM treatment, dark grey bar; MDA-MB-231BR CM treatment, medium grey bar. The dashed line represents VM cytokine expression. Three biological replicates were cultured per experiment, and the experiment performed twice for a total of six biological replicates. Shown are the results of one representative experiment.

A) 10 Day Old Osteoblasts

	Cytokine				
	Range of Murine Cytokine Expression (ng/ml)				
Osteoblast Treatment	**IL-6**	**MCP-1**	**MIP-2**	**KC**	**VEGF**
VM	0.085	3.01	0.0026	0.0029	0.0033
Human Metastatic Breast Cancer Variant CM	0.89-3.3	4.3-6.5	0.0029-0.003	0.004-0.013	0.0036-0.006

B) 20 Day Old Osteoblasts

	Cytokine				
	Range of Murine Cytokine Expression (ng/ml)				
Osteoblast Treatment	**IL-6**	**MCP-1**	**MIP-2**	**KC**	**VEGF**
VM	0.04	2.2	0.0017	0.0022	0.012
Human Metastatic Breast Cancer Variant CM	0.5-3.1	3.7-18.3	0.001-0.013	0.006-0.13	0.012-0.018

Table 3.4: Osteoblasts increased inflammatory cytokine production in response to human metastatic breast cancer conditioned medium. MC3T3-E1 cells were cultured as described in the legend to Figure 3.6. Shown are the ranges of cytokine production of osteoblasts treated with human metastatic breast cancer cell conditioned media from the representative experiment shown in Figure 3.6A or B. Range of murine cytokine expression of A) 10 or B) 20 day old osteoblasts treated for 24 hours with VM or CM from human metastatic breast cancer variants.

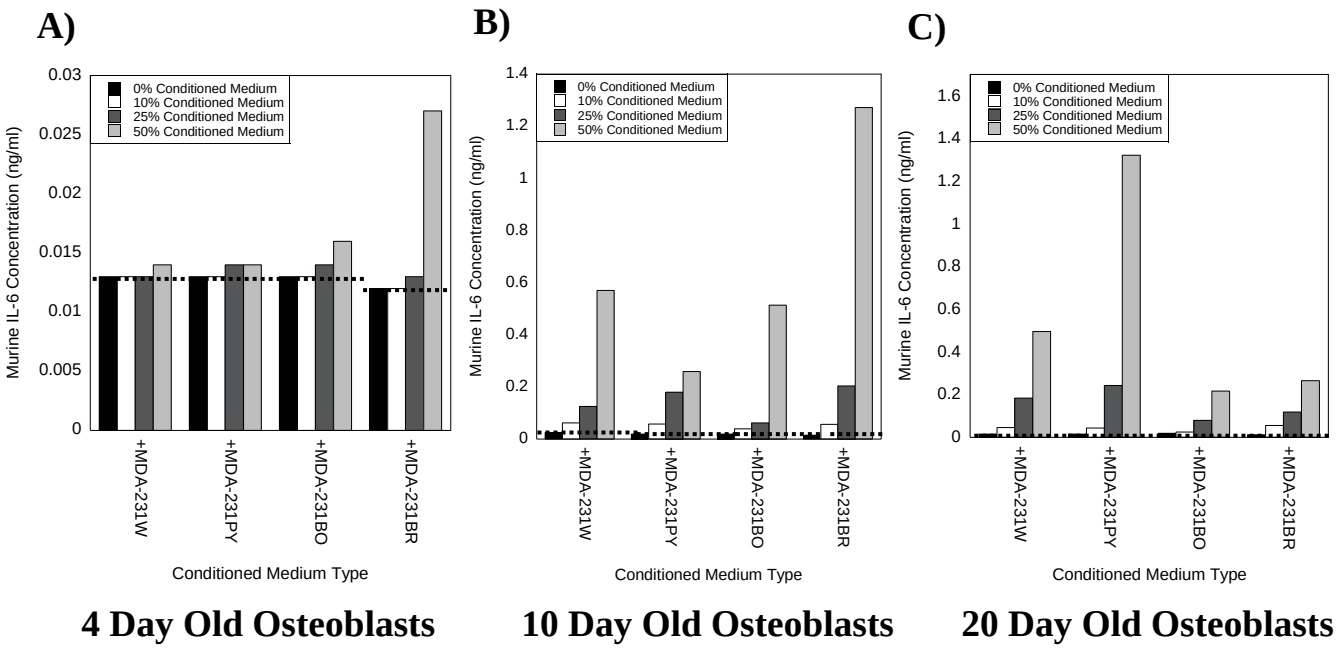

Figure 3.7: Osteoblast-derived IL-6 cytokine response to human metastatic breast cancer conditioned medium was dose-dependent. MC3T3-E1 cells were grown to either 4, 10, or 20 days and treated with VM or 10, 25, or 50% human metastatic breast cancer cell variant conditioned medium as described in the Materials and Methods. The culture supernatant was assayed for osteoblast-derived cytokine production using standard sandwich ELISAs. MC3T3-E1 cells grown to A) 4 days; B) 10 days; C) 20 days. Supernatants from osteoblasts treated with vehicle medium (0% BCCM) are represented by the black bar; and in order, 10% BCCM treatment, white bar; 25% BCCM treatment, dark grey bar; 50% BCCM treatment, light grey bar. The dashed line represents VM cytokine expression. Three biological replicates were cultured per experiment, and the experiment performed twice for a total of six biological replicates. Shown are the results of representative experiments.

A) 4 Day Old Osteoblasts

	Osteoblast Treatment			
	VM	**10% BCCM**	**25% BCCM**	**50% BCCM**
Range of Murine IL-6 Concentration (ng/ml)	0.01-0.02	0.018-0.025	0.022-0.025	0.023-0.031

B) 10 Day Old Osteoblasts

	Osteoblast Treatment			
	VM	**10% BCCM**	**25% BCCM**	**50% BCCM**
Range of Murine IL-6 Concentration (ng/ml)	0.015-0.025	0.04-0.062	0.062-0.2	0.26-1.3

C) 20 Day Old Osteoblasts

	Osteoblast Treatment			
	VM	**10% BCCM**	**25% BCCM**	**50% BCCM**
Range of Murine IL-6 Concentration (ng/ml)	0.012-0.019	0.025-0.056	0.08-0.24	0.22-1.3

Table 3.5: Osteoblasts increased inflammatory cytokine production in a dose-dependent manner in response to human metastatic breast cancer conditioned medium. MC3T3-E1 cells were cultured as described in the legend to Figure 3.7. Shown are the ranges of cytokine production of osteoblasts treated with VM or 10, 25, or 50% human metastatic breast cancer cell variant conditioned media from the representative experiment described in Figure 3.7A-C. Range of murine IL-6 cytokine concentration of A) 4, B) 10, or C) 20 day old osteoblasts treated with VM or 10, 25, or 50% human metastatic breast cancer variant conditioned medium for 24 hours.

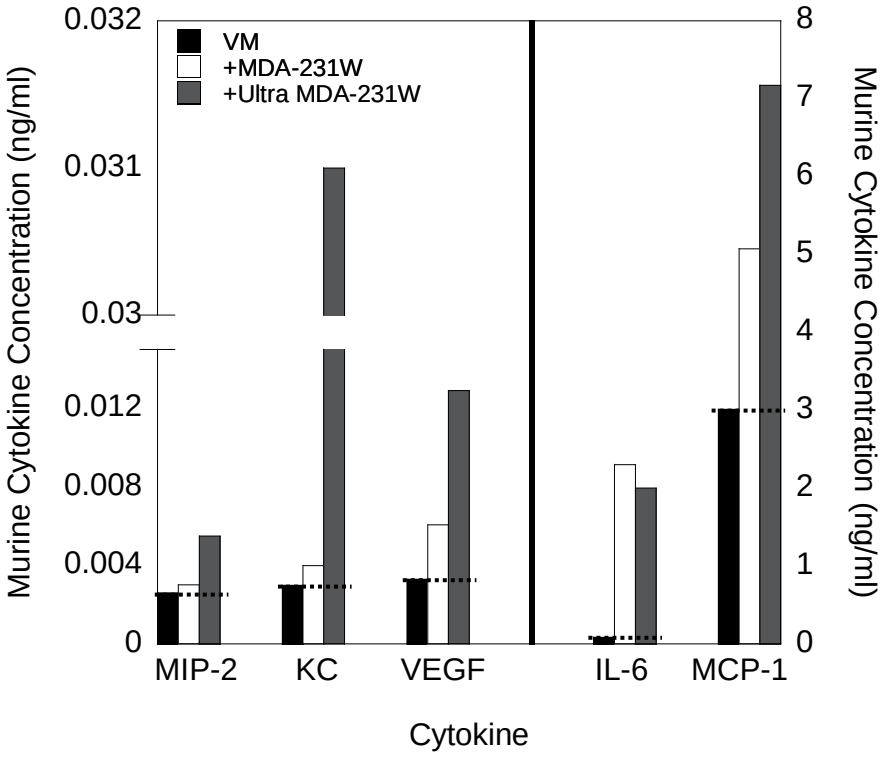

Figure 3.8: Factors causing osteoblasts to increase cytokine production were not removed by ultracentrifugation of human metastatic breast cancer conditioned medium. MC3T3-E1 cells were grown to 10 days and treated with ultracentrifuged human metastatic breast cancer cell CM as described in the Materials and Methods. The culture supernatants were assayed for osteoblast-derived cytokines using a Bio-Rad Bio-Plex™ Murine Cytokine Assay. Supernatants from osteoblasts treated with vehicle medium are represented by the black bar; and in order, MDA-MB-231W breast cancer CM treatment, white bar; ultracentrifuged MDA-MB-231W breast cancer CM treatment, dark grey bar. The dashed line represents VM cytokine expression. Two biological replicates were cultured per experiment, and the experiment performed twice for a total of four biological replicates. Shown are the results of one representative experiment.

	Cytokine				
	Murine Cytokine Expression (ng/ml)				
Osteoblast Treatment	**IL-6**	**MCP-1**	**MIP-2**	**KC**	**VEGF**
VM	0.085	3.01	0.003	0.003	0.003
MDA-231W CM	2.3	5.1	0.003	0.004	0.006
MDA-231W ultracentrifuged CM	2.0	7.18	0.005	0.031	0.013

Table 3.6: Factors causing osteoblasts to increase cytokine production were not removed by ultracentrifugation of human metastatic breast cancer conditioned medium. MC3T3-E1 cells were cultured as described in the legend to Figure 3.8. Shown is the murine cytokine expression of one representative experiment of 10 day old osteoblasts cultured for 24 hours with A) VM, B) MDA-MB-231W, or C) MDA-MB-231W ultracentrifuged human metastatic breast cancer cell conditioned medium.

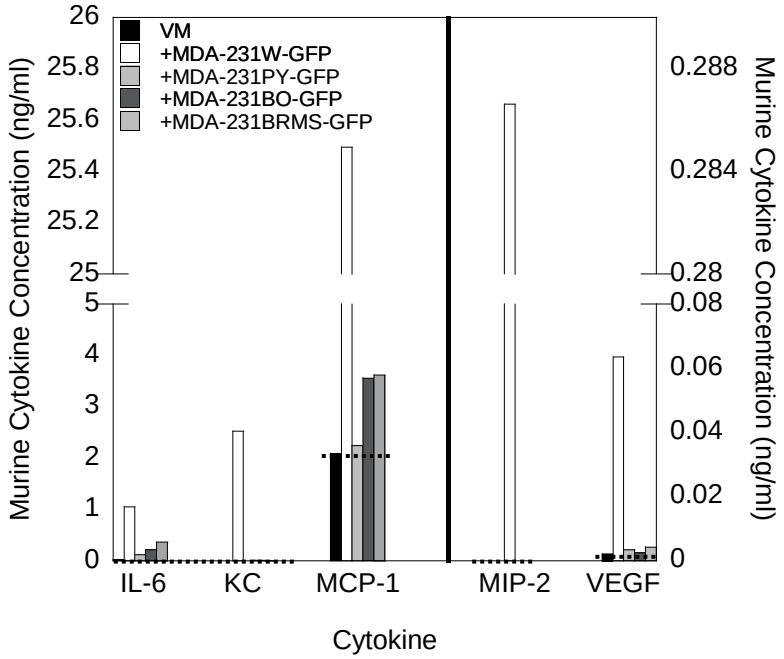

Figure 3.9: Osteoblasts increased inflammatory cytokine production in response to human MDA-231-GFP variant breast cancer conditioned medium. MC3T3-E1 cells were grown to 10 days and treated with CM from human MDA-231-GFP variant breast cancer cell variants as described in the Materials and Methods. The culture supernatants were assayed for osteoblast-derived cytokine production using a Bio-Rad Bio-Plex™ Murine Cytokine Assay. Supernatants from osteoblasts treated with vehicle medium are represented by the black bar; and in order, MDA-MB-231W-GFP BCCM treatment, white bar; MDA-MB-231PY-GFP BCCM treatment, light grey bar; MDA-MB-231BO-GFP BCCM treatment, dark grey bar, MDA-MB-231BRMS-GFP treatment, medium grey bar. The dashed line represents VM cytokine expression. Three biological replicates were cultured per experiment, and the experiment performed twice for a total of six biological replicates. Shown are the results from one representative experiment.

	Cytokine				
	Range of Murine Cytokine Expression (ng/ml)				
Osteoblast Treatment	**IL-6**	**MCP-1**	**MIP-2**	**KC**	**VEGF**
VM	0.021	2.3	0	0	0.002
MDA-231-GFP variant CM	0.08-1.1	2.1-31	0-0.3	0.005-3.0	0.001-0.07

Table 3.7: Osteoblast-derived cytokines were increased in the presence of conditioned medium from MDA-MB-231-GFP variants. MC3T3-E1 cells were cultured as described in the legend to Figure 3.9. Shown is the range of murine cytokine production of osteoblasts treated with MDA-MB-231-GFP variant conditioned media from the representative experiment shown in Figure 3.8. Range of murine cytokine expression of 10 day old osteoblasts cultured for 24 hours with VM or CM from human metastatic breast cancer GFP variants.

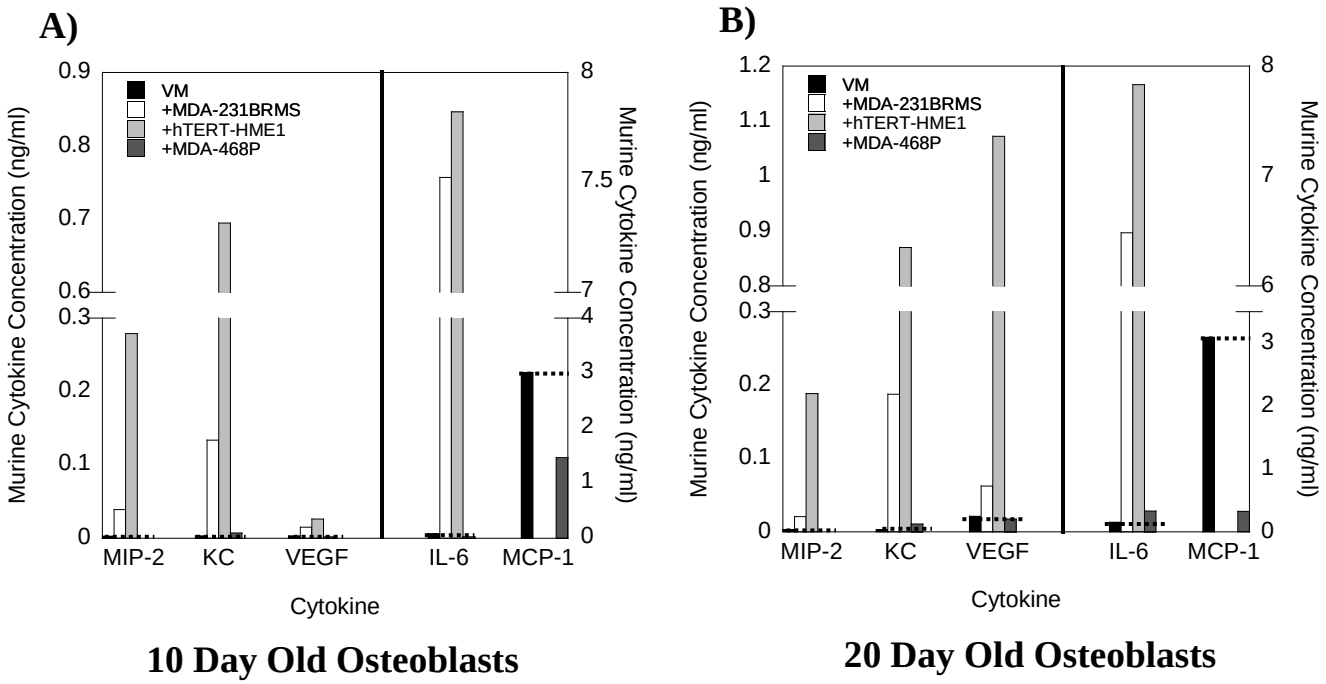

Figure 3.10: Osteoblasts increased inflammatory cytokine production, except for MCP-1, in response to human epithelial cell conditioned medium. MC3T3-E1 cells were grown to either 10 or 20 days and treated with human epithelial cell variant CM as described in the Materials and Methods. The culture supernatants were assayed for osteoblast-derived cytokine production using a Bio-Rad Bio-Plex™ Murine Cytokine Assay. MC3T3-E1 cells grown to A) 10; or B) 20 days. Supernatants from osteoblasts treated with vehicle medium are represented by the black bar; MDA-MB-231BRMS BCCM treatment, white bar; hTERT-HME CM treatment, light grey bar; MDA-MB-468P BCCM treatment, dark grey bar. The dashed line represents VM cytokine expression. Three biological replicates were cultured per experiment, and the experiment performed twice for a total of six biological replicates. Shown are the results of representative experiments.

A) 10 Day Old Osteoblasts

	Cytokine				
	Range of Murine Cytokine Expression (ng/ml)				
Osteoblast Treatment	**IL-6**	**MCP-1**	**MIP-2**	**KC**	**VEGF**
VM	0.085	3	0.0026	0.0029	0.0033
Human Epithelial Cell Variant CM	0.025-7.8	0-1.46	0-0.28	0.007-0.69	0.001-0.026

B) 20 Day Old Osteoblasts

	Cytokine				
	Range of Murine Cytokine Expression (ng/ml)				
Osteoblast Treatment	**IL-6**	**MCP-1**	**MIP-2**	**KC**	**VEGF**
VM	0.15	3.09	0.0028	0.0026	0.021
Human Epithelial Cell Variant CM	0.33-7.8	0-0.32	0-0.18	0.01-0.87	0.017-1.07

Table 3.8: Osteoblasts increased inflammatory cytokine production, except for MCP-1, in response to human epithelial cell variant conditioned medium. MC3T3-E1 cells were cultured as described in the figure legend to Figure 3.10. Shown are the ranges of murine cytokine production of osteoblasts treated with human epithelial cell variant conditioned media from the representative experiments shown in Figure 3.10A or B. Range of murine cytokine expression of A) 10 or B) 20 day old osteoblasts treated with VM or human epithelial cell variant CM for 24 hours.

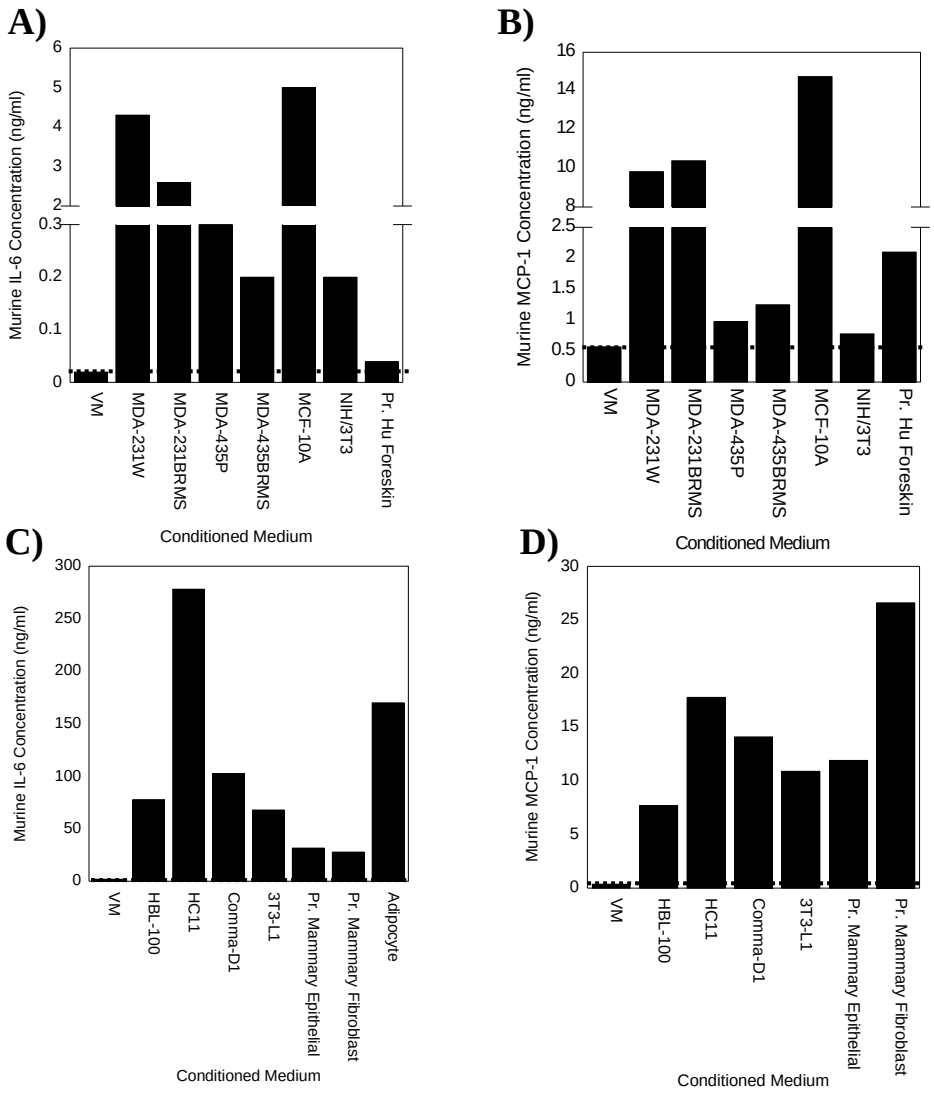

Figure 3.11: Osteoblasts increased inflammatory cytokine production in response to epithelial and mesenchymal variant conditioned medium. MC3T3-E1 cells were grown to 10 days and treated with human epithelial or mesenchymal cell variant CM as described in the Materials and Methods. The culture supernatants were assayed for osteoblast-derived IL-6 or MCP-1 production using standard sandwich ELISAs. A-C) Murine IL-6 expression; B-D) murine MCP-1 expression. Supernatants from osteoblasts treated with vehicle medium are represented by the dashed line. Cell lines (Table 2.1) are indicated on the x-axis of the bar graphs. Three biological replicates were cultured per experiment, and the experiment performed twice for a total of six biological replicates. Shown are representative experiments.

	Cytokine	
	Murine Cytokine Expression (ng/ml)	
Osteoblast Treatment	**IL-6**	**MCP-1**
VM	0.02	0.53
MDA-231W CM	4.3	9.8
MDA-231BRMS CM	2.6	10.4
MDA-435 CM	0.27	0.98
MDA-435BRMS CM	0.24	1.3
MCF-10A CM	5	14.8
NIH/3T3 CM	0.17	0.78
Pr. Hu Foreskin CM	0.04	2.1
VM	1.8	0.4
HBL-100 CM	77.7	17.7
HC11 CM	278.1	17.8
Comma-D1 CM	102.7	14.1
3T3-L1 CM	67.9	10.9
Pr. Mammary Epithelial CM	31.7	11.9
Pr. Mammary Fibroblast CM	27.7	26.6
Adipocyte CM	170	Below the range of detection (0.002 ng/ml)

Table 3.9: Osteoblasts increased inflammatory cytokine production in response to human epithelial and mesenchymal cell variant conditioned medium. MC3T3-E1 cells were cultured as described in the legend to Figure 3.11. Shown are the concentrations of murine IL-6 and MCP-1 in the representative experiment described in Figure 3.11 produced when 10 day old osteoblasts were treated for 24 hours with 1) VM, 2) MDA-231W, 3) MDA-231BRMS, 4) MDA-435, 5) MDA-435BRMS, 6) MCF-10A, 7) NIH/3T3, 8) Pr. Hu Foreskin, 9) HBL-100, 10) HC11, 11) Comma-D1, 12) 3T3-L1, 13) Pr. Mammary Epithelial, 14) Pr. Mammary Fibroblast, or 15) Adipocyte CM (Table 2.1).

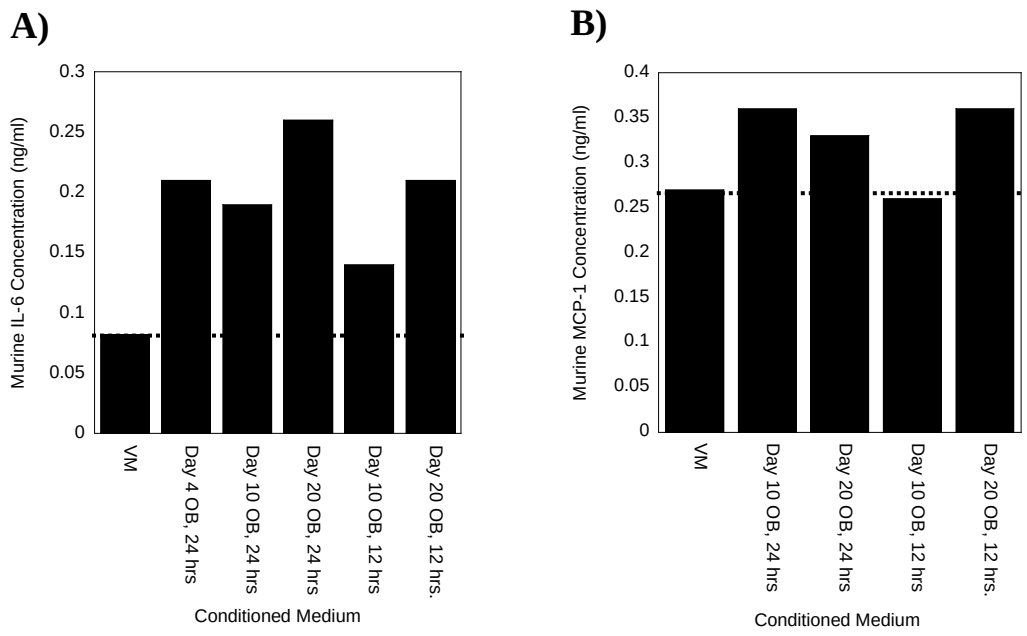

Figure 3.12: Osteoblasts-derived inflammatory cytokine production did not increase with treatment of osteoblast conditioned medium. MC3T3-E1 cells were grown to 10 days and treated with osteoblast CM as described in the Materials and Methods. The culture supernatants were assayed for osteoblast-derived IL-6 or MCP-1 production using standard sandwich ELISAs. A) Murine IL-6 expression; B) murine MCP-1 expression. Supernatants from osteoblasts treated with vehicle medium are represented by the dashed line. Conditioned medium treatment with 1) VM, 2) MC3T3-E1 cells grown to 4 days, conditioned medium collected after 24 hours, 3) MC3T3-E1 cells grown to 10 days, conditioned medium collected after 24 hours, 4) MC3T3-E1 cells grown to 20 days, conditioned medium collected after 24 hours, 5) MC3T3-E1 cells grown to 10 days, conditioned medium collected after 12 hours, or 6) MC3T3-E1 cells grown to 20 days, conditioned medium collected after 12 hours is listed on the x-axis. Three biological replicates were cultured per experiment, and the experiment performed twice for a total of six biological replicates. Shown are representative experiments.

	Cytokine	
	Murine Cytokine Expression (ng/ml)	
Osteoblast Treatment	**IL-6**	**MCP-1**
VM	0.082	0.27
Day 4 OB, 24 hr CM	0.21	Not measured
Day 10 OB, 24 hr CM	0.19	0.36
Day 20 OB, 24 hr CM	0.26	0.33
Day 10 OB, 12 hr CM	0.14	0.26
Day 20 OB, 12 hr CM	0.21	0.36

Table 3.10: Osteoblasts did not increase inflammatory cytokine production in response to osteoblast conditioned medium. MC3T3-E1 cells were cultured as described in the legend to Figure 3.10. Shown are the concentrations of IL-6 and MCP-1 in the representative experiment described in Figure 3.12 produced when 10 day old osteoblasts were treated for 24 hours with 1) VM, 2) MC3T3-E1 cells grown to 4 days, conditioned medium collected after 24 hours, 3) MC3T3-E1 cells grown to 10 days, conditioned medium collected after 24 hours, 4) MC3T3-E1 cells grown to 20 days, conditioned medium collected after 24 hours, 5) MC3T3-E1 cells grown to 10 days, conditioned medium collected after 12 hours, or 6) MC3T3-E1 cells grown to 20 days, conditioned medium collected after 12 hours.

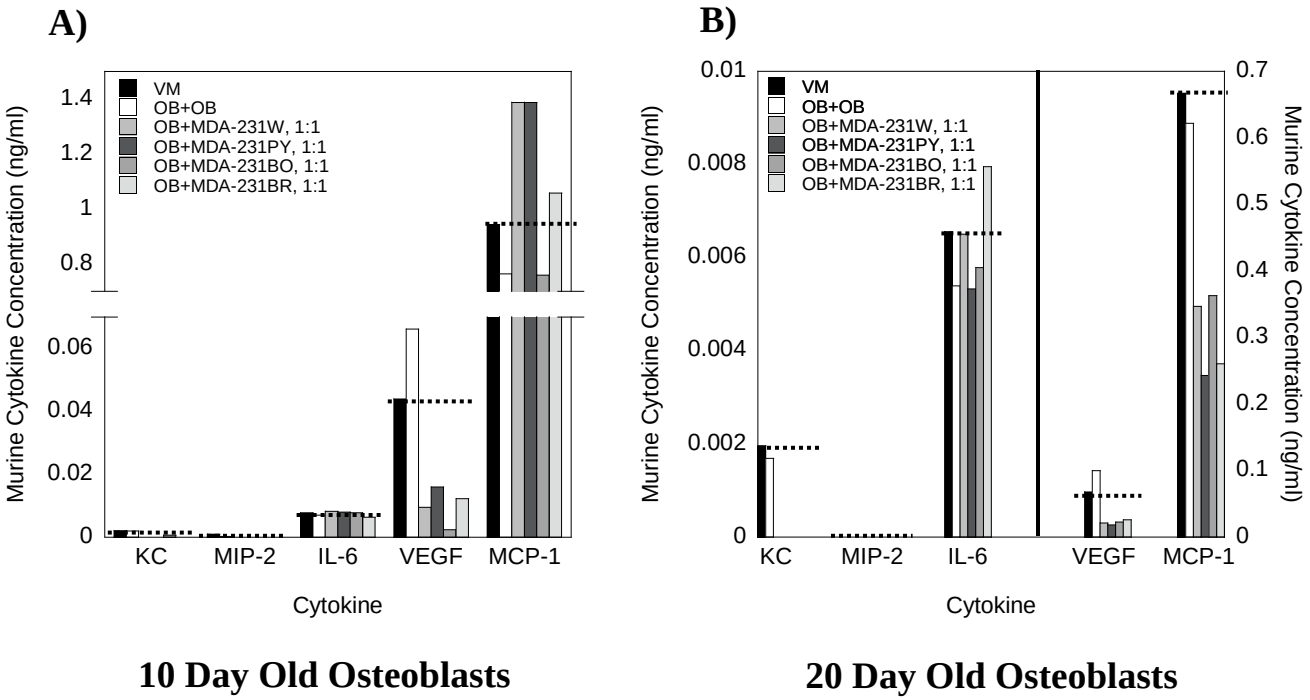

Figure 3.13: Osteoblast-derived cytokines, except for MCP-1, were not increased when MC3T3-E1 cells were co-cultured indirectly in a transwell system with human metastatic breast cancer cell variants. MC3T3-E1 cells were grown to either 10 or 20 days and co-cultured indirectly with MDA-MB-231 human metastatic breast cancer cell variants in a transwell system at a ratio of 1 osteoblast : 1 breast cancer cell. Seventy-two hours later, the resultant culture supernatants were collected and subjected to a Bio-Rad Bio-Plex™ Murine Cytokine Assay to quantitate cytokine expression. Osteoblast-derived cytokine expression of A) MC3T3-E1 cells grown to 10 days; B) MC3T3-E1 cells grown to 20 days. The cytokine concentration of osteoblasts cultured alone is represented by the black bar; osteoblasts co-cultured indirectly with: osteoblasts, white bar; MDA-MB-231W cells, light grey bar; MDA-MB-231PY, dark grey bar; MDA-MB-231BO, medium grey bar; MDA-MB-231BR, very light grey bar. The dashed line represents VM cytokine expression. Shown are representative experiments.

A) 10 Day Old Osteoblasts

	Cytokine				
	Range of Murine Cytokine Expression (ng/ml)				
Osteoblast Treatment	**IL-6**	**MCP-1**	**MIP-2**	**KC**	**VEGF**
VM	0.007	0.94	0.001	0.002	0.04
Osteoblast + osteoblast	0.007	0.76	0.002	0.002	0.06
Osteoblast + MDA-231 breast cancer cell variant	0.006-0.008	0.76-1.4	0	0-0.0006	0.002-0.016

B) 20 Day Old Osteoblasts

	Cytokine				
	Range of Murine Cytokine Expression (ng/ml)				
Osteoblast Treatment	**IL-6**	**MCP-1**	**MIP-2**	**KC**	**VEGF**
VM	0.006	0.67	0	0.001	0.07
Osteoblast + osteoblast	0.005	0.62	0	0.001	0.1
Osteoblast + MDA-231 breast cancer cell variant	0.005-0.008	0.24-0.36	0	0	0.02-0.1

Table 3.11: Osteoblast-derived cytokines, except for MCP-1, were not increased when MC3T3-E1 cells were co-cultured indirectly in a transwell system with human metastatic breast cancer cell variants. MC3T3-E1 cells were co-cultured, indirectly in a transwell system with MDA-MB-231W metastatic breast cancer cell variants as described in the legend to Figure 3.13. Shown are the ranges of murine cytokine production of osteoblasts co-cultured indirectly with human metastatic breast cancer cells from the representative experiment shown in Figure 3.13A or B. Range of murine cytokine production of A) 10 day old, or B) 20 day old MC3T3-E1 cells co-cultured indirectly in a transwell system with MDA-MB-231 human metastatic breast cancer cell variants.

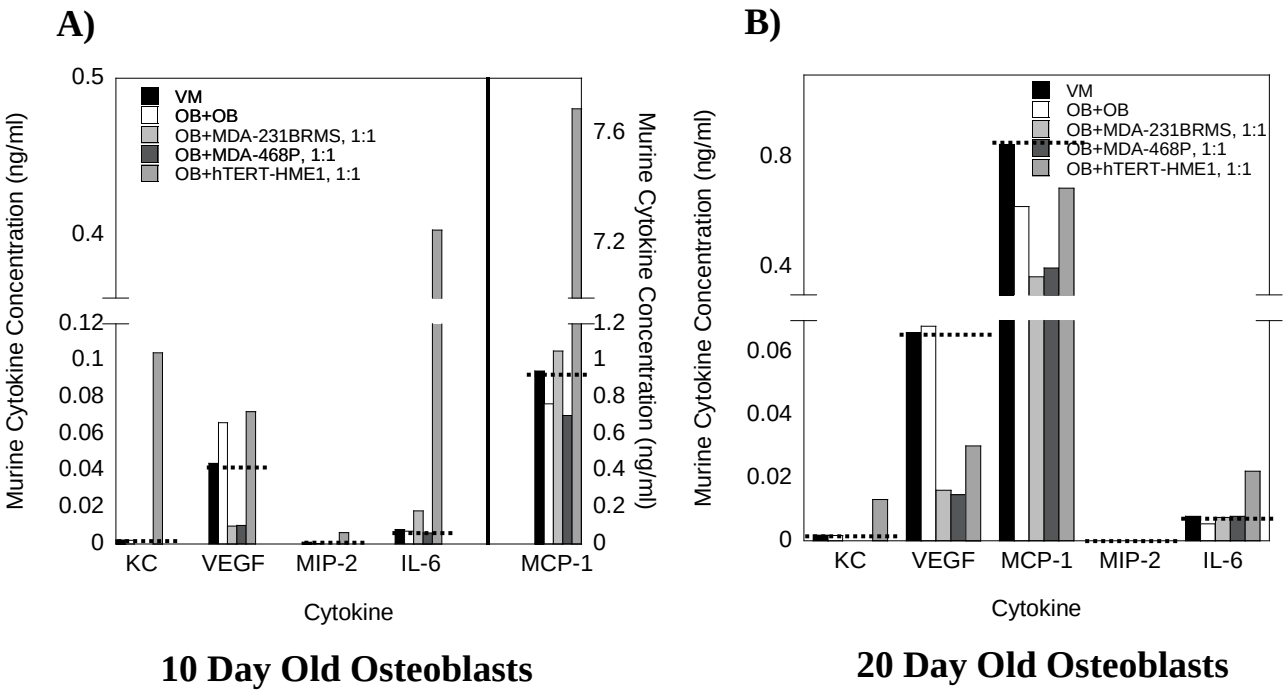

Figure 3.14: Osteoblast-derived cytokines were not increased when MC3T3-E1 cells were indirectly co-cultured in a transwell system with human epithelial cell variants, except for indirect co-culture with hTERT-HME1 cells.

MC3T3-E1 cells were grown to either 10 or 20 days and co-cultured indirectly in a transwell system with human epithelial cell variants (MDA-MB-231BRMS, MDA-MB-468P, or hTERT-HME1) at a ratio of 1 osteoblast : 1 epithelial cell. Seventy-two hours later, the resultant culture supernatants were collected and subjected to a Bio-Rad Bio-Plex™ Murine Cytokine Assay to quantitate cytokine expression. Osteoblast-derived cytokine expression of A) MC3T3-E1 cells grown to 10 days; B) MC3T3-E1 cells grown to 20 days. The cytokine concentration of osteoblasts cultured alone is represented by the black bar; osteoblasts co-cultured indirectly in a transwell system with, in order: osteoblasts, white bar; MDA-MB-231BRMS cells, light grey bar; MDA-MB-468P, dark grey bar; hTERT-HME1, medium grey bar. The dashed line represents VM cytokine expression. Shown are the results of representative experiments.

A) 10 Day Old Osteoblasts

	Cytokine				
	Range of Murine Cytokine Expression (ng/ml)				
Osteoblast Treatment	**IL-6**	**MCP-1**	**MIP-2**	**KC**	**VEGF**
VM	0.007	0.94	0.001	0.002	0.04
Osteoblast + osteoblast	0.006	0.76	0.0003	0.002	0.06
Osteoblast + MDA-231BRMS or MDA-468	0.006	0.7-1	0	0	0.009-0.015
Osteoblast + hTERT-HME1	0.4	7.7	0.006	0.1	0.07

B) 20 Day Old Osteoblasts

	Cytokine				
	Range of Murine Cytokine Expression (ng/ml)				
Osteoblast Treatment	**IL-6**	**MCP-1**	**MIP-2**	**KC**	**VEGF**
VM	0.008	0.85	0	0.002	0.07
Osteoblast + osteoblast	0.005	0.62	0	0.002	0.07
Osteoblast + MDA-231BRMS or MDA-468	0.007-0.008	0.37-0.4	0	0	0.015-0.016
Osteoblast + hTERT-HME1	0.02	0.69	0	0.013	0.03

Table 3.12: Osteoblast-derived cytokines were not increased when MC3T3-E1 cells were indirectly co-cultured in a transwell system with human epithelial cell variants, except for indirect co-culture with hTERT-HME1 cells. MC3T3-E1 cells were co-cultured indirectly in a transwell system with human epithelial cell variants as described in the legend to Figure 3.16. Shown are the ranges of murine cytokine expression of osteoblasts co-cultured indirectly with human metastatic breast cancer cells in a transwell system from the representative experiment shown in Figure 3.14A or B. Range of cytokine production of A) 10 day old, or B) 20 day old MC3T3-E1 cells co-cultured indirectly in a transwell system with human epithelial cell variants.

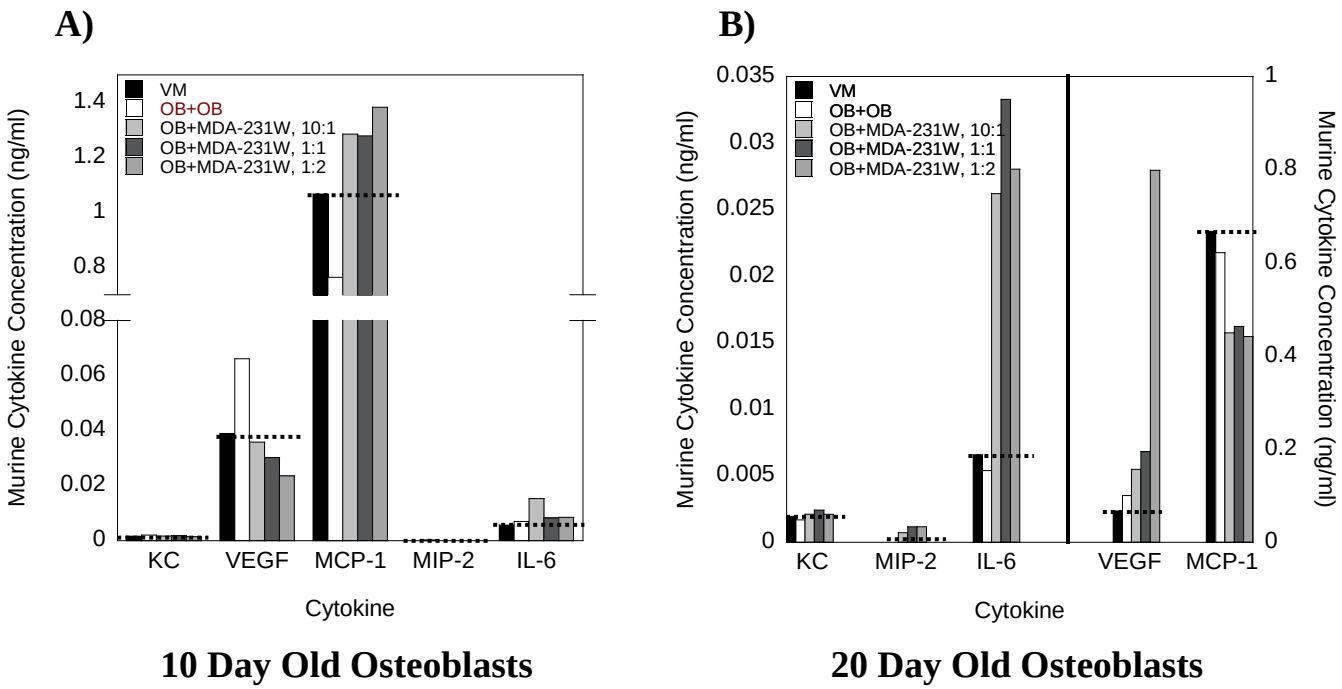

Figure 3.15: Osteoblast-derived cytokine expression, except for VEGF, did not change when MC3T3-E1 cells were co-cultured indirectly in a transwell system with increasing numbers of human metastatic breast cancer cells. MC3T3-E1 cells were grown to either 10 or 20 days and co-cultured indirectly in a transwell system with MDA-MB-231W human metastatic breast cancer cells at osteoblast : breast cancer cell ratios of 10:1, 1:1, or 1:2. Seventy-two hours later, the resultant culture supernatants were collected and subjected to a Bio-Rad Bio-Plex™ Murine Cytokine Assay to quantitate cytokine expression. MC3T3-E1 cells grown to A) 10 days or B) 20 days. The cytokine concentration of cancer cells cultured alone is represented by the black bar; osteoblasts co-cultured indirectly in a transwell system with : osteoblasts: white bar; 10:1 MDA-MB-231W cells, light grey bar; 1:1 MDA-MB-231W cells, dark grey bar; 1:2 MDA-MB-231W cells, medium grey bar. The dashed line represents VM cytokine expression. Shown are the results from representative experiments.

A) 10 Day Old Osteoblasts

	Cytokine				
	Range of Murine Cytokine Expression (ng/ml)				
Osteoblast Treatment	**IL-6**	**MCP-1**	**MIP-2**	**KC**	**VEGF**
VM	0.006	1.1	0	0.001	0.04
Osteoblast + osteoblast	0.007	0.8	0	0.002	0.07
Osteoblast + MDA-231W at numbers of 10:1, 1:1, and 1:2	0.008-0.015	1.3-1.4	0	0.0015-0.0018	0.02-0.04

B) 20 Day Old Osteoblasts

	Cytokine				
	Range of Murine Cytokine Expression (ng/ml)				
Osteoblast Treatment	**IL-6**	**MCP-1**	**MIP-2**	**KC**	**VEGF**
VM	0.006	0.7	0	0.002	0.06
Osteoblast + osteoblast	0.005	0.6	0	0.002	0.1
Osteoblast + MDA-231W at numbers of 10:1, 1:1, and 1:2	0.026-0.03	0.4-0.5	0.0007-0.001	0.002-0.0024	0.16-0.8

Table 3.13: Osteoblast-derived cytokine expression, except for VEGF, did not change when MC3T3-E1 cells were co-cultured indirectly in a transwell system with increasing numbers of human metastatic breast cancer cells. MC3T3-E1 cells were co-cultured indirectly in a transwell system with MDA-MB-231W human metastatic breast cancer cells as described in the legend to Figure 3.15. Shown are the range of murine cytokine expression of MC3T3-E1 cells co-cultured indirectly with MDA-MB-231W human metastatic breast cancer cells at numbers of 10:1, 1:1, or 1:2 from the representative experiment shown in Figure 3.15. Range of murine cytokine production of A) 10 day old, or B) 20 day old MC3T3-E1 cells co-cultured indirectly in a transwell system with human metastatic breast cancer cells.

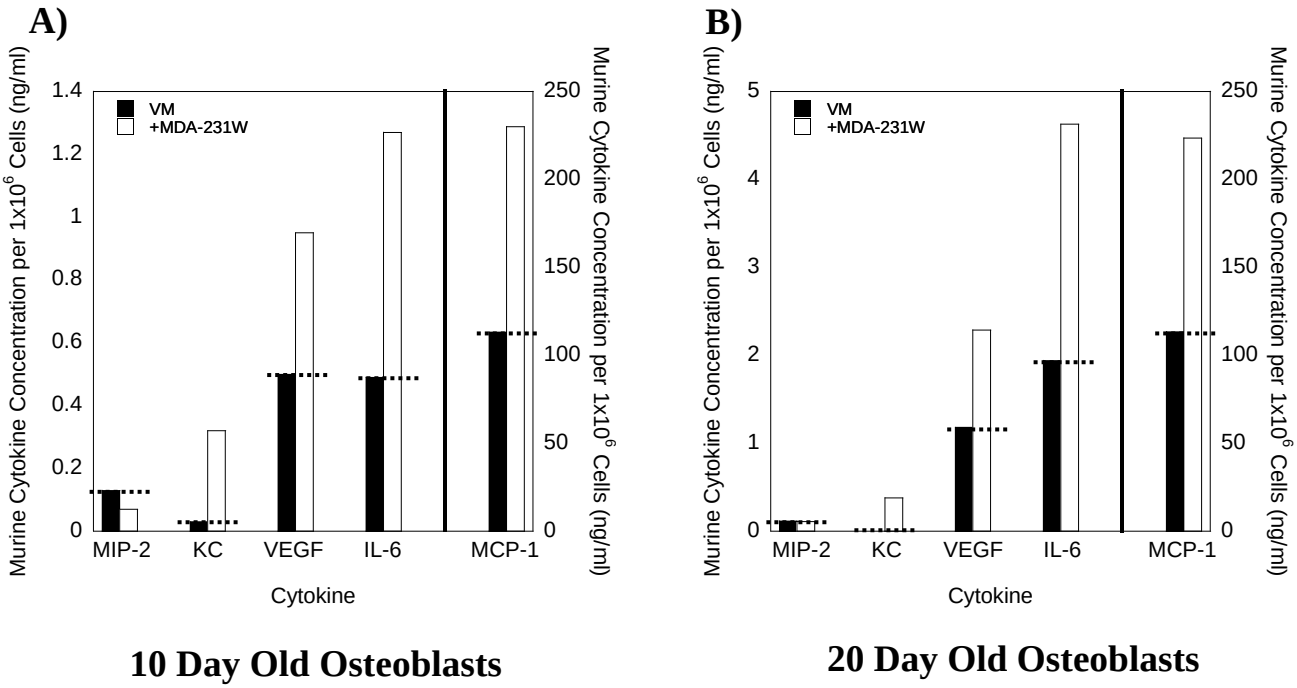

Figure 3.16: Osteoblast-derived cytokines were increased in the presence of human metastatic breast cancer cells. MC3T3-E1 cells were grown to either 10 or 20 days and co-cultured with MDA-MB-231W human metastatic breast cancer cells at a ratio of 10 osteoblasts : 1 breast cancer cell. Forty-eight hours later, the resultant culture supernatants were collected and subjected to a Bio-Rad Bio-Plex™ Murine Cytokine Assay to quantitate cytokine expression. Osteoblast-derived cytokine expression of A) MC3T3-E1 cells grown to 10 days; B) MC3T3-E1 cells grown to 20 days. The cytokine concentration of osteoblasts cultured alone is represented by the black bar; osteoblasts co-cultured for 48 hours with MDA-MB-231W human metastatic breast cancer cells, white bar. The dashed line represents VM cytokine expression. Shown are the results from representative experiments.

A) 10 Day Old Osteoblasts

	Cytokine				
	Murine Cytokine Expression (ng/ml)				
Osteoblast Treatment	**IL-6**	**MCP-1**	**MIP-2**	**KC**	**VEGF**
VM	0.5	113.2	0.1	0.03	0.5
MC3T3-E1 cells + MDA-231W cells	1.3	230.0	0.07	0.03	1.0

B) 20 Day Old Osteoblasts

	Cytokine				
	Murine Cytokine Expression (ng/ml)				
Osteoblast Treatment	**IL-6**	**MCP-1**	**MIP-2**	**KC**	**VEGF**
VM	1.9	113.5	0.1	0	1.2
MC3T3-E1 cells + MDA-231W cells	4.6	223.6	0.1	0.4	2.3

Table 3.14: Osteoblast-derived cytokines were increased in a direct co-culture with human metastatic breast cancer cells. MC3T3-E1 cells were directly co-cultured with MDA-MB-231W human metastatic breast cancer cells as described in the legend to Figure 3.13. Shown is the murine cytokine expression of MC3T3-E1 cells directly co-cultured with MDA-MB-231W human metastatic breast cancer cells from the representative experiment shown in Figure 3.16A or B. Murine cytokine production of A) 10 day old or B) 20 day old osteoblasts co-cultured with human metastatic breast cancer cells.

	Cytokine				
Cell Type	**IL-6**	**MCP-1**	**VEGF**	**MIP-2 / IL-8**	**KC / GRO-α**
Breast Cancer Cell 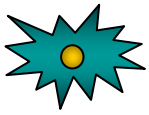	++	-	++	++	++
 Human Epithelial Cell	+	-	++	++	+++
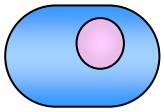 Osteoblast	++	+++	+	+	+

Table 4.1: MC3T3-E1 cells, human metastatic breast cancer, and human epithelial cell variants express inflammatory cytokines, but only MC3T3-E1 cells express large amounts of MCP-1. MC3T3-E1 cells, human metastatic breast cancer cell variants (MDA-231W, MDA-231PY, MDA-231BO, and MDA-231BR), and human epithelial cells (MDA-231BRMS, MDA-468P, hTERT-HME1) were grown to ~90% confluency and growth media exchanged for α-MEM. Twenty-four hours later, the conditioned media was collected and Bio-Rad Bio-Plex™ Murine or Human Cytokine Assays were conducted to quantitate cytokine expression. Cytokine expression is represented by – (negligible: <0.01 ng/ml), + (little: 0.01 – 0.08 ng/ml), ++ (modest amount: 0.08 – 0.5 ng/ml), and +++ (substantial amount: >0.5 ng/ml). Cytokine concentration was normalized to 1 million cells; variation between batches of conditioned medium was less than 15%. At least two individual batches of conditioned medium were assayed per cell variant.

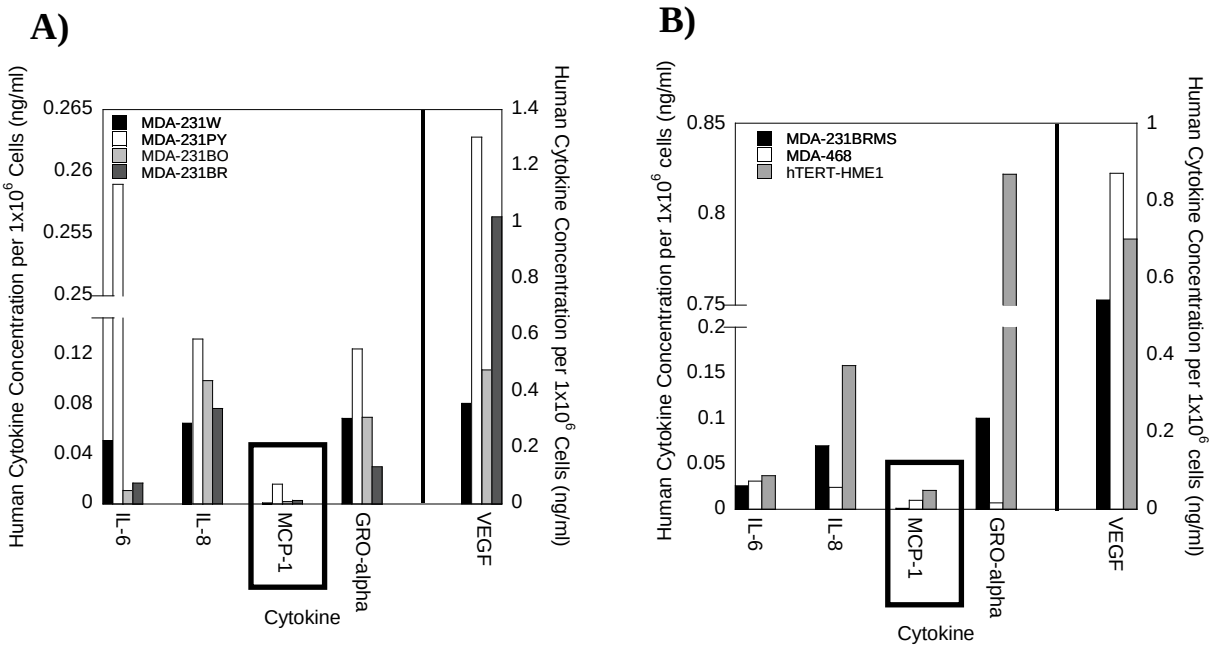

Figure 4.1: Conditioned medium from human metastatic breast cancer and human epithelial cell variants contained inflammatory cytokines. MDA-MB-231 human metastatic breast cancer and human epithelial cell variants were grown to ~90% confluency and growth media exchanged for α-MEM. Twenty-four hours later, the conditioned media was collected and a Bio-Rad Bio-Plex™ Human Cytokine Assay conducted to quantitate human cytokine expression. Cytokine concentration was normalized to 1 million cells; variation between batches of conditioned medium was less than 15%. Cytokine concentration from MDA-231W BCCM is represented by the black bar; MDA-231PY BCCM, white bar; MDA-231BO BCCM, light grey bar; MDA-231BR BCCM, dark grey bar; MDA-231BRMS BCCM, black bar; MDA-468 BCCM, white bar, hTERT-HME1 conditioned medium, medium grey bar. Three individual batches of conditioned medium were assayed per cell variant. Shown are representative experiments.

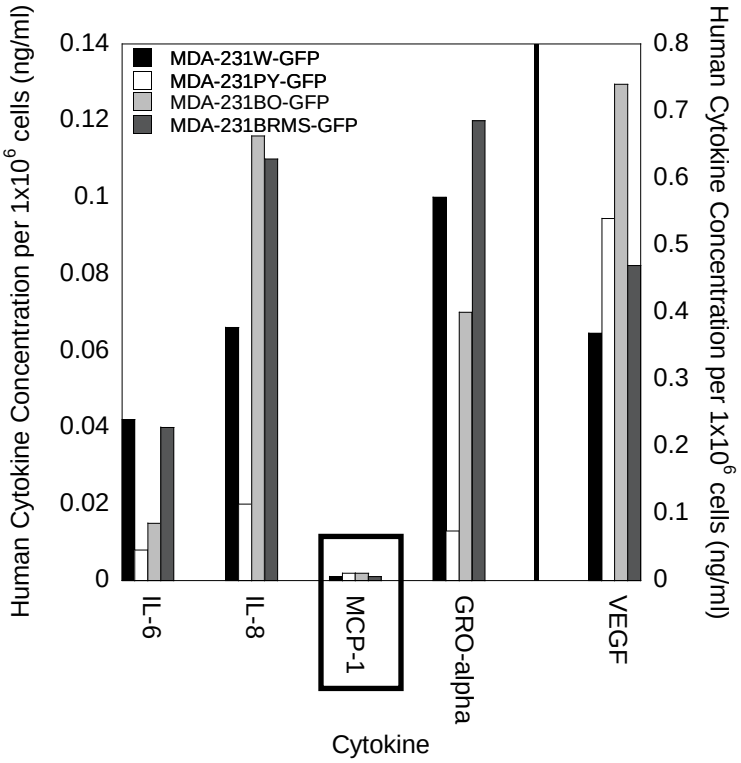

Figure 4.2: Human breast cancer cell-GFP variants express inflammatory cytokines. MDA-MB-231 human breast cancer cell-GFP variants were grown to ~90% confluency and growth media exchanged for α-MEM. Twenty-four hours later, the conditioned media was collected and a Bio-Rad Bio-Plex™ Human Cytokine Assay conducted to quantitate human cytokine expression. Cytokine concentration was normalized to 1 million cells; variation between batches of conditioned medium was less than 15%. Cytokine concentration from MDA-231W-GFP BCCM is represented by the black bar; MDA-231PY-GFP BCCM, white bar; MDA-231BO-GFP BCCM, light grey bar; MDA-231BRMS-GFP BCCM, dark grey bar. Three individual batches of conditioned medium were assayed per MDA-MB-231 breast cancer variant. Shown are representative experiments.

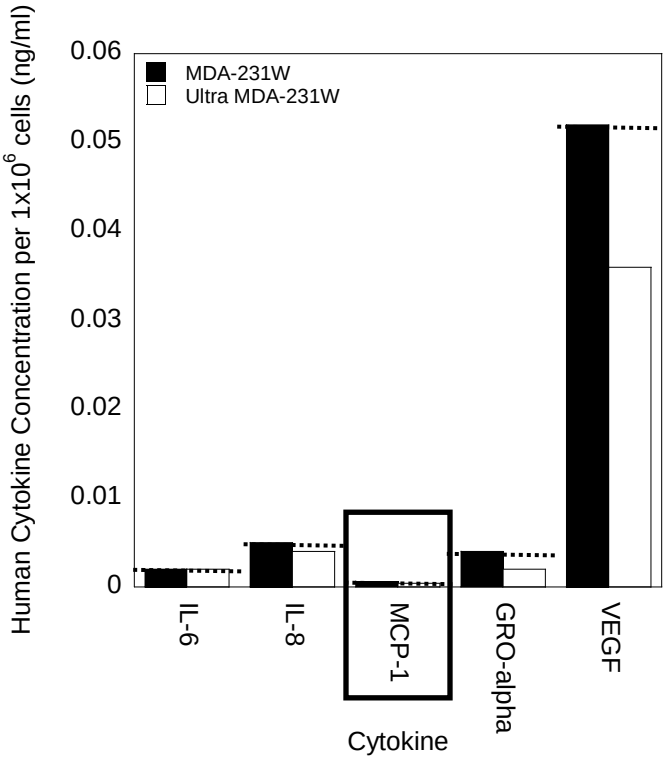

Figure 4.3: Cancer cell-derived cytokines were expressed in the soluble fraction of conditioned medium. MDA-MB-231 human metastatic breast cancer cells were grown to ~90% confluency and growth media exchanged for α-MEM. Twenty-four hours later, the conditioned medium was collected, ultracentrifuged at 100,000 xg, and ultracentrifuged BCCM assayed for cytokine expression via a Bio-Rad Bio-Plex™ Human Cytokine Assay. Cytokine concentration was normalized to 1 million cells; variation between batches of conditioned medium was less than 15%. Cytokine concentration from MDA-231W BCCM is represented by the black bar; ultracentrifuged MDA-231W BCCM, white bar. The dashed line represents BCCM that was not ultracentrifuged. Two individual batches of conditioned medium were assayed. Shown are representative experiments.

	Cytokine				
	Human Cytokine Expression (ng/ml)				
BCCM Type	**IL-6**	**MCP-1**	**IL-8**	**GRO-α**	**VEGF**
MDA-231W CM	0.002	0.0006	0.005	0.004	0.052
MDA-231W ultracentrifuged CM	0.002	0.0004	0.004	0.002	0.036

Table 4.2: Cancer cell-derived cytokines were expressed in the soluble fraction of conditioned medium. MDA-MB-231W metastatic breast cancer cells were cultured as described in the legend to Figure 4.3. Shown are the human cytokine expression of MDA-MB-231W CM and MDA-MB-231W CM that was ultracentrifuged at 100,000 xg. Listed are the cytokine production of MDA-MB-231W BCCM or ultracentrifuged BCCM from human metastatic breast cancer cells cultured alone.

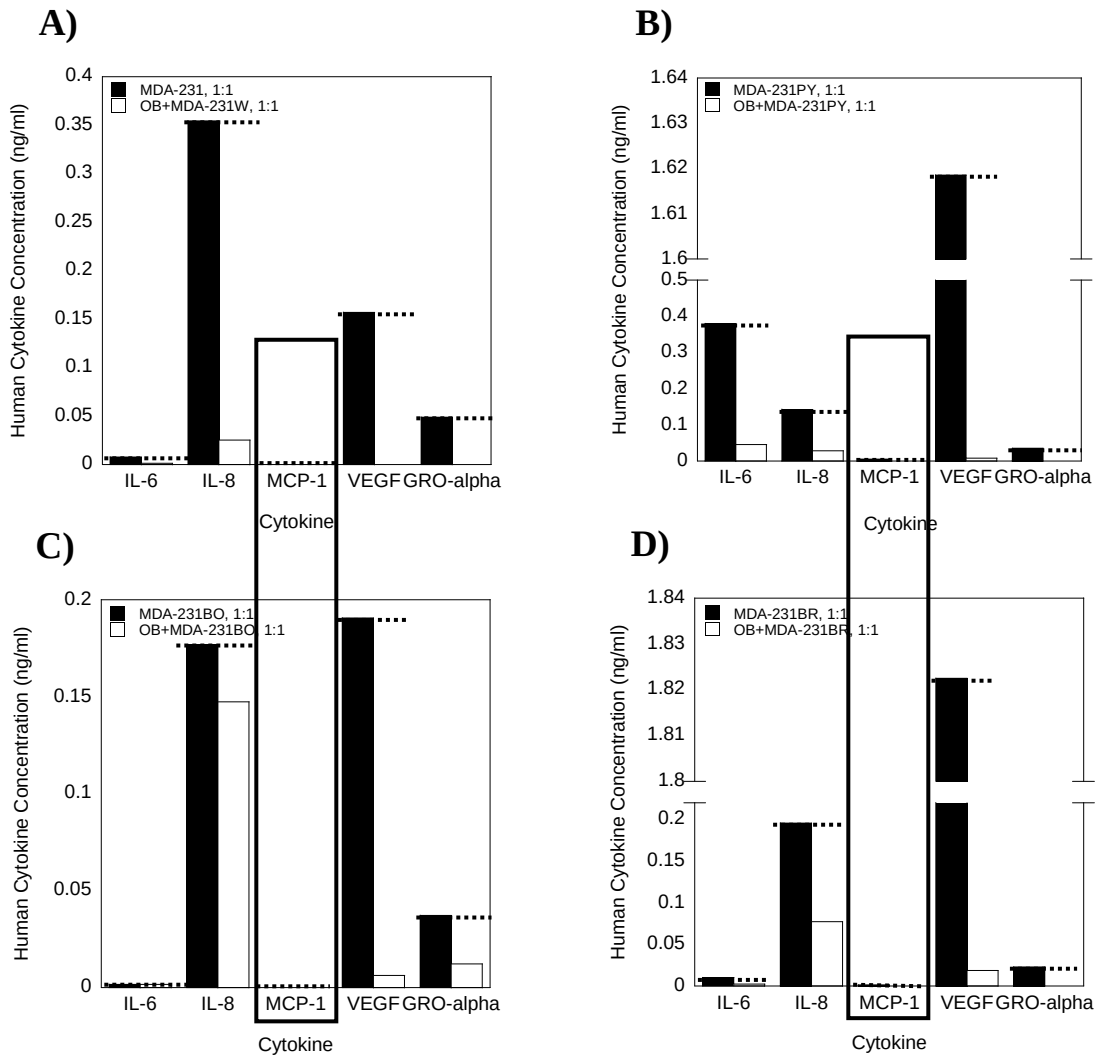

Figure 4.4: Cancer cell-derived cytokines decreased in an indirect transwell system co-culture system with 10 day old murine osteoblasts. MDA-MB-231 human metastatic cell variants were co-cultured indirectly in a transwell system with MC3T3-E1 cells grown to 10 days at a ratio of 1 osteoblast : 1 breast cancer cell. Seventy-two hours later, the resultant culture supernatants were collected and subjected to a Bio-Rad Bio-Plex™ Human Cytokine Assay to quantitate cytokine expression. Cancer cell-derived cytokine expression of MC3T3-E1 cells co-cultured indirectly in a transwell system with A) MDA-MB-231W; B) MDA-MB-231PY; C) MDA-MB-231BO; or D) MDA-MB-231BR human metastatic breast cancer cells. The cytokine concentration of cancer cells cultured alone is represented by the black bar; osteoblasts co-cultured indirectly in a transwell system with cancer cells, white bar. The dashed line represents VM cytokine expression. Shown are the results of representative experiments.

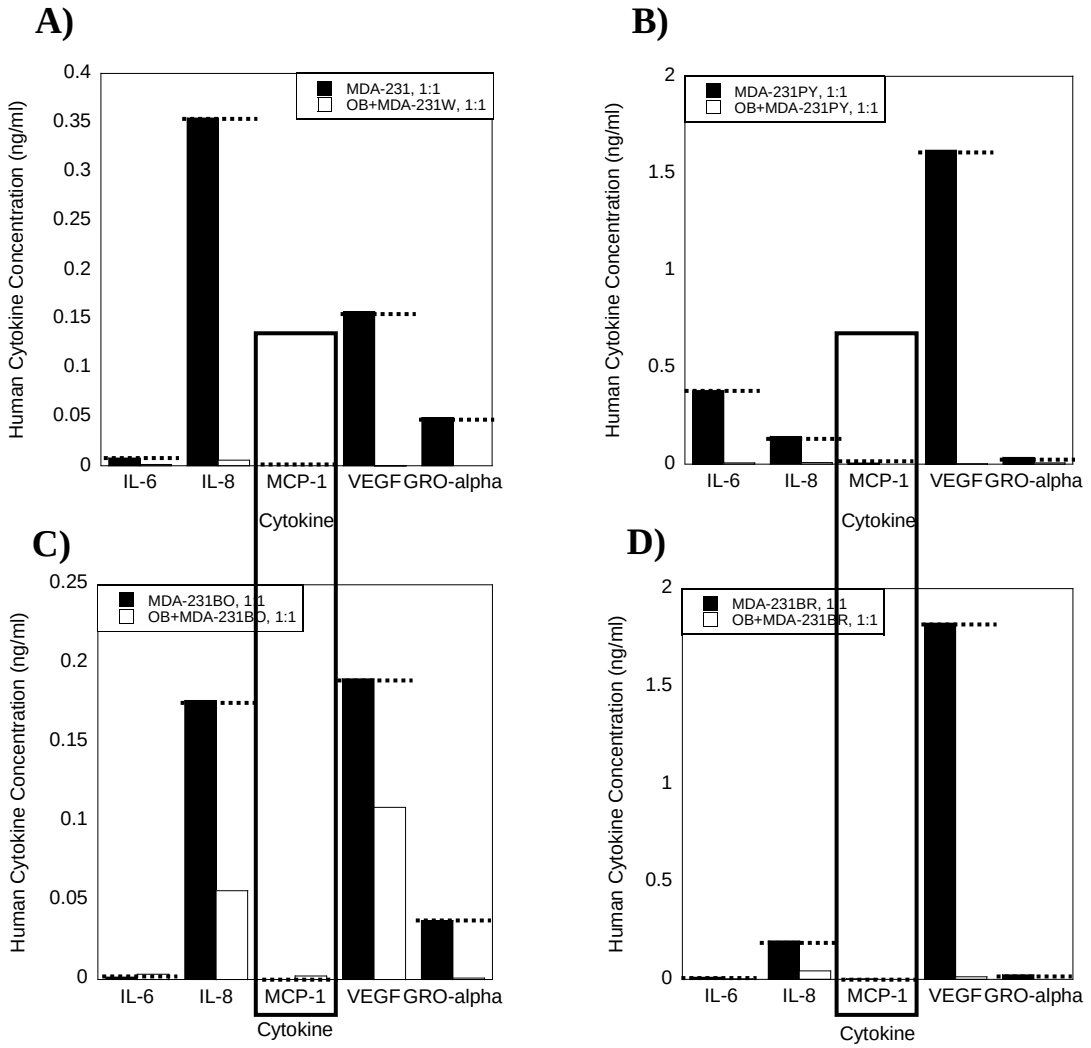

Figure 4.5: Cancer cell-derived cytokines decreased in an indirect transwell system co-culture with 20 day old murine osteoblasts. MDA-MB-231 human metastatic cell variants were co-cultured indirectly in a transwell system with MC3T3-E1 cells grown to 20 days at a ratio of 1 osteoblast : 1 breast cancer cell. Seventy-two hours later, the resultant culture supernatants were collected and subjected to a Bio-Rad Bio-Plex™ Human Cytokine Assay to quantitate cytokine expression. Cancer cell-derived cytokine expression of MC3T3-E1 cells co-cultured indirectly in a transwell system with A) MDA-MB-231W; B) MDA-MB-231PY; C) MDA-MB-231BO; or D) MDA-MB-231BR human metastatic breast cancer cells. The cytokine concentration of cancer cells cultured alone is represented by the black bar; osteoblasts co-cultured indirectly in a transwell system with cancer cells, white bar. The dashed line represents VM cytokine expression. Shown are the results of representative experiments.

A) Breast Cancer Cell Interaction with 10 Day Old Osteoblasts

	Cytokine				
	Range of Human Cytokine Expression (ng/ml)				
Cancer Cell Treatment	**IL-6**	**MCP-1**	**IL-8**	**GRO-α**	**VEGF**
VM	0.001-0.38	0	0.14-0.35	0.02-0.05	0.14-1.8
Cancer cell + cancer cell	0.03	0.02	0.3	0.11	4.1
MDA-231 cell variants + osteoblast	0.001-0.05	0	0.03-0.15	0-0.01	0-0.02

B) Breast Cancer Cell Interaction with 20 Day Old Osteoblasts

	Cytokine				
	Range of Human Cytokine Expression (ng/ml)				
Cancer Cell Treatment	**IL-6**	**MCP-1**	**IL-8**	**GRO-α**	**VEGF**
VM	0.001-0.4	0	0.14-0.35	0.02-0.05	0.16-1.8
Cancer cell + cancer cell	0.03	0.02	0.3	0.11	4.1
MDA-231 cell variants + osteoblast	0.001-0.007	0	0.005-0.06	0-0.007	0-0.11

Table 4.3: Cancer cell-derived cytokines decreased in an indirect transwell co-culture system with murine osteoblasts. MDA-MB-231 human metastatic breast cancer cell variants were co-cultured indirectly in a transwell system with MC3T3-E1 cells as described in the legends to Figures 4.4 and 4.5. Shown are the ranges of human cytokine expression of 10 or 20 day old osteoblasts co-cultured indirectly with human metastatic breast cancer cell variants in the representative experiments in Figures 4.4 and 4.5. Range of cytokine production of human metastatic breast cancer cell variants co-cultured indirectly in a transwell system with A) 10 day old, or B) 20 day old MC3T3-E1 cells.

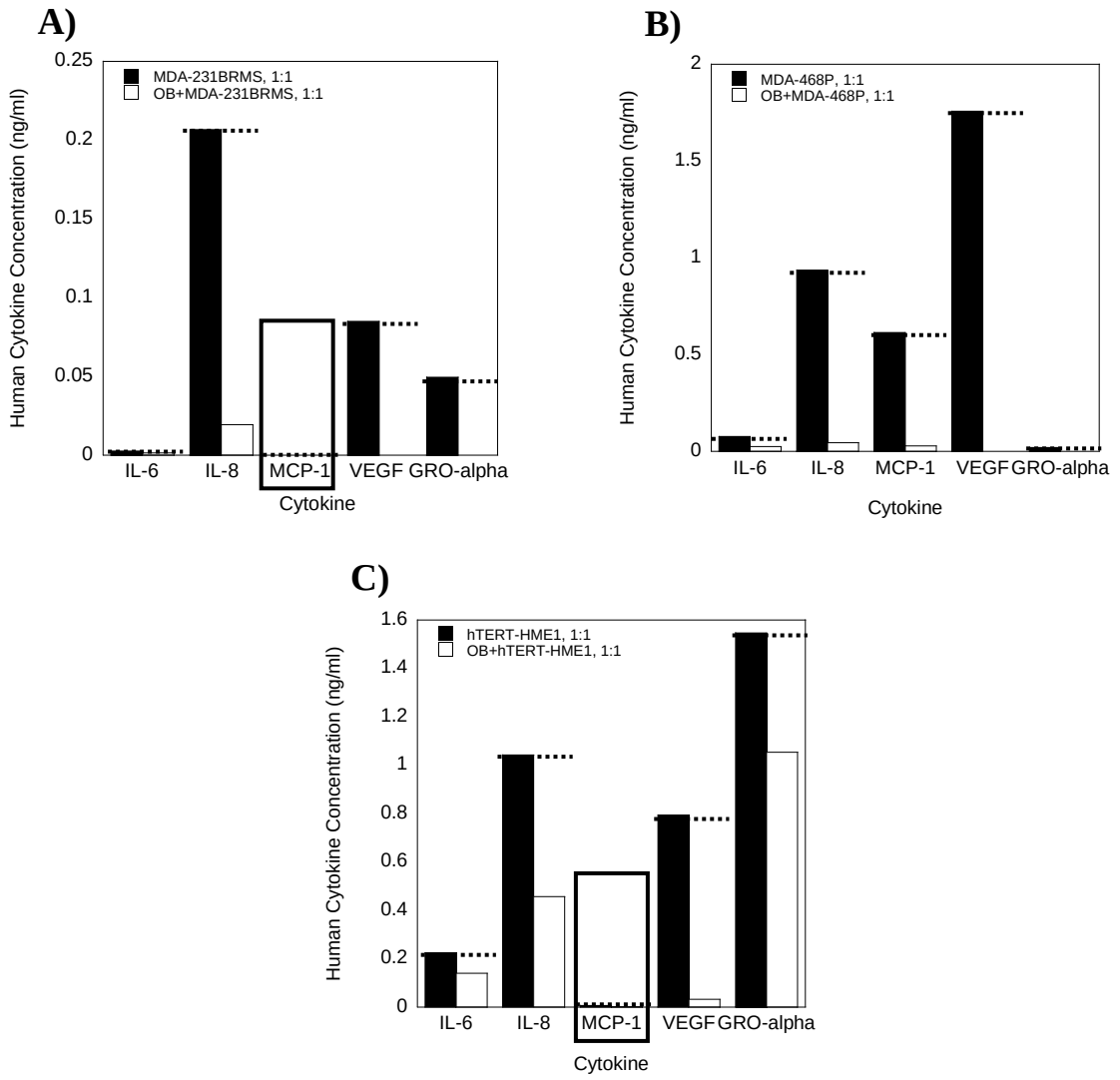

Figure 4.6: Human epithelial cell-derived cytokines decreased in an indirect transwell co-culture system with 10 day old murine osteoblasts. Human epithelial cell variants were co-cultured indirectly in a transwell system with MC3T3-E1 cells grown to 10 days at a ratio of 1 osteoblast : 1 human epithelial cell. Seventy-two hours later, the resultant culture supernatants were collected and subjected to a Bio-Rad Bio-Plex™ Human Cytokine Assay to quantitate cytokine expression. Human epithelial cell-derived cytokine expression of MC3T3-E1 cells co-cultured indirectly in a transwell system with A) MDA-MB-231BRMS; B) MDA-MB-468P; or C) hTERT-HME1 cells. The cytokine concentration of cancer cells cultured alone is represented by the black bar; osteoblasts co-cultured indirectly in a transwell system with human epithelial cell variants, white bar. The dashed line represents VM cytokine expression. Shown are the results of representative experiments.

A) Breast Cancer Cell Interaction with 10 Day Old Osteoblasts

	Cytokine				
	Range of Human Cytokine Expression (ng/ml)				
Osteoblast Treatment	**IL-6**	**MCP-1**	**IL-8**	**GRO-α**	**VEGF**
VM	0.002-0.2	0	0.2-1.0	0.02-1.5	0.09-1.8
Cancer cell + cancer cell	0.03	0.02	0.3	0.11	4.1
MDA-231 cell variants + osteoblast	0.001-0.14	0	0.02-0.46	0-1.1	0-0.03

B) Breast Cancer Cell Interaction with 20 Day Old Osteoblasts

	Cytokine				
	Range of Human Cytokine Expression (ng/ml)				
Osteoblast Treatment	**IL-6**	**MCP-1**	**IL-8**	**GRO-α**	**VEGF**
VM	0.002-0.2	0	0.2-1.0	0.02-1.5	0.9-1.8
Cancer cell + cancer cell	0.03	0.02	0.3	0.11	4.1
MDA-231 cell variants + osteoblast	0.02-0.47	0	0.1-0.9	0-1.7	0-0.08

Table 4.4: Human epithelial cell-derived cytokines decreased in an indirect transwell system co-culture system with murine osteoblasts. Human epithelial cell variants were co-cultured indirectly in a transwell system with MC3T3-E1 cells as described in the legends to Figures 4.6-4.7. Shown are the ranges of human cytokine expression of 10 or 20 day old osteoblasts co-cultured indirectly with the human epithelial cell variants MDA-MB-231BRMS, MDA-MB-468P, and hTERT-HME1 cells in the representative experiments shown in Figures 4.6-4.7. Range of cytokine production of A) 10 day old, or B) 20 day old MC3T3-E1 cells co-cultured indirectly in a transwell system with human epithelial cell variants.

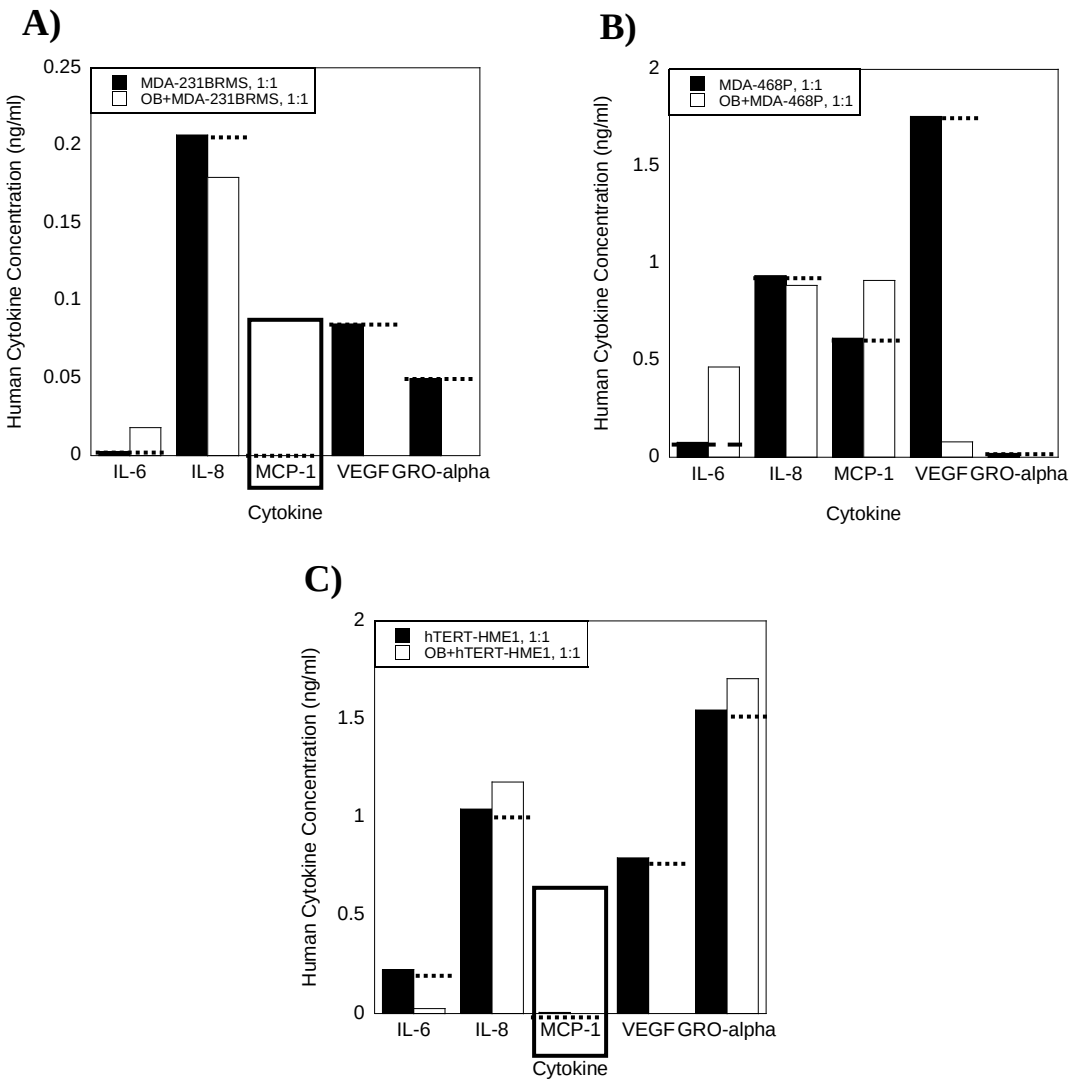

Figure 4.7: Human epithelial cell-derived cytokines decreased in an indirect transwell co-culture system with 20 day old murine osteoblasts. Human epithelial cell variants were co-cultured indirectly in a transwell system with MC3T3-E1 cells grown to 20 days at a ratio of 1 osteoblast : 1 human epithelial cell. Seventy-two hours later, the resultant culture supernatants were collected and subjected to a Bio-Rad Bio-Plex™ Human Cytokine Assay to quantitate cytokine expression. Human epithelial cell-derived cytokine expression of MC3T3-E1 cells co-cultured indirectly in a transwell system with A) MDA-MB-231BRMS; B) MDA-MB-468P; or C) hTERT-HME1 cells. The cytokine concentration of cancer cells cultured alone is represented by the black bar; osteoblasts co-cultured indirectly in a transwell system with human epithelial cells, white bar. The dashed line represents VM cytokine expression. Shown are the results of representative experiments.

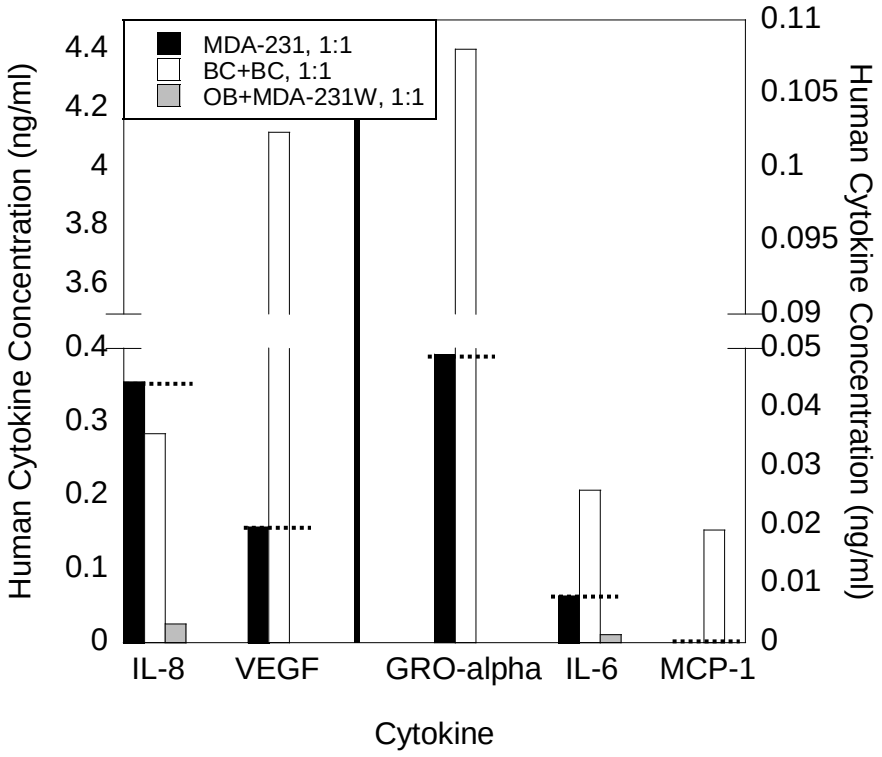

Figure 4.8: Cancer cell-derived cytokines were decreased when breast cancer cells were co-cultured indirectly in a transwell system with breast cancer cells. MDA-MB-231W human metastatic breast cancer cells were co-cultured indirectly in a transwell system with MC3T3-E1 cells grown to 10 days at a ratio of 1 osteoblast : 1 breast cancer cell. MDA-MB-231W human metastatic breast cancer cells were co-cultured indirectly in a transwell system with MDA-MB-231W human metastatic breast cancer cell at a ratio of 1 cancer cell : 1 cancer cell as a control. Seventy-two hours later, the resultant culture supernatants were collected and subjected to a Bio-Rad Bio-Plex™ Human Cytokine Assay to quantitate human cytokine expression. Cancer cell-derived cytokine expression of cancer cells cultured alone is represented by the black bar; cancer cells co-cultured indirectly in a transwell system with cancer cells, white bar, 10 day old MC3T3-E1 cells co-cultured indirectly in a transwell system with MDA-MB-231W human metastatic breast cancer cells, medium grey bar. The dashed line represents VM cytokine expression. Shown are the results from one representative experiment.

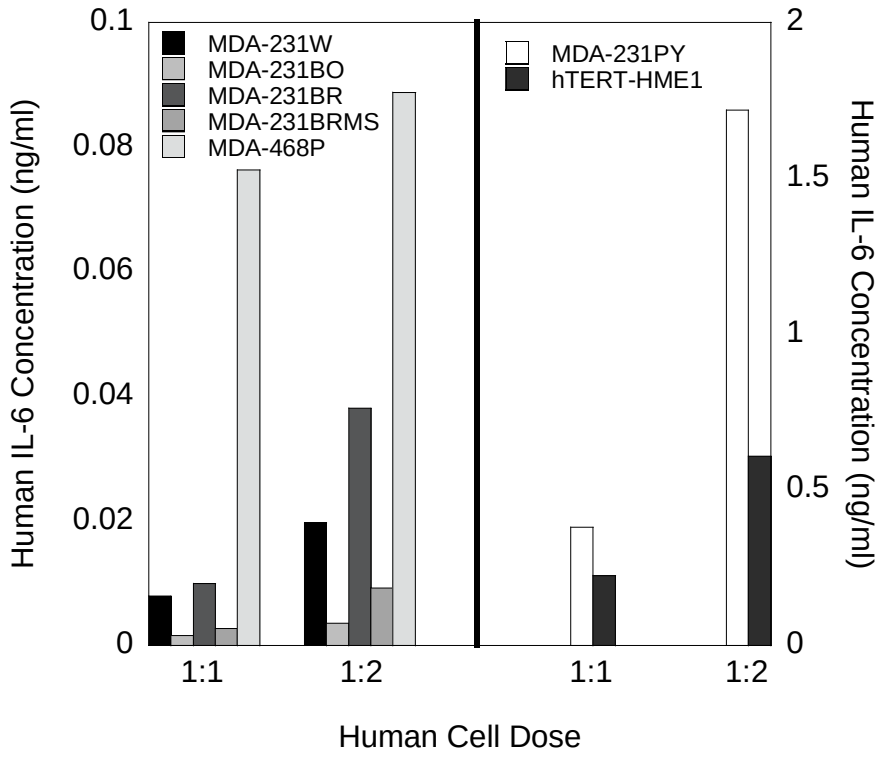

Figure 4.9: Human-derived IL-6 expression was dose-dependent. MDA-MB-231 human metastatic or human epithelial cell variants were cultured alone in a transwell system in two different quantities as described in the Materials and Methods: 1) Dose #1 (representing the indirect transwell co-culture of osteoblast : human cell ratio of 1:1) or 2) Dose #2 (representing the indirect transwell co-culture of osteoblast : human cell ratio of 1:2). Seventy-two hours later, the resultant culture supernatants were collected and subjected to a Bio-Rad Bio-Plex™ Human Cytokine Assay to quantitate cytokine expression. The cytokine concentration of MDA-MB-231W cells cultured alone is represented by the black bar; MDA-MB-231PY: white bar; MDA-MB-231BO: light grey bar; MDA-MB-231BR: dark grey bar; MDA-MB-231BRMS: medium grey bar; MDA-MB-468P: very light grey bar; hTERT-HME1: very dark grey bar. Shown are the results of one representative experiment.

	Human IL-6 Expression (ng/ml)	
	Human Cell Dose	
Type of Human Cell	**1**	**2**
MDA-231W	0.007	0.01
MDA-231PY	0.001	0.003
MDA-231BO	0.001	0.003
MDA-231BR	0.009	0.04
MDA-231BRMS	0.002	0.009
MDA-468P	0.08	0.09
hTERT-HME1	0.2	0.6

Table 4.5: Human IL-6 expression was dose-dependent. Human cells were cultured alone in a transwell system as described in the legend to Figure 4.9. Shown is the human IL-6 expression of the representative experiment shown in Figure 4.9 of human metastatic breast cancer or human epithelial cell variants cultured alone in two different quantities in a transwell system.

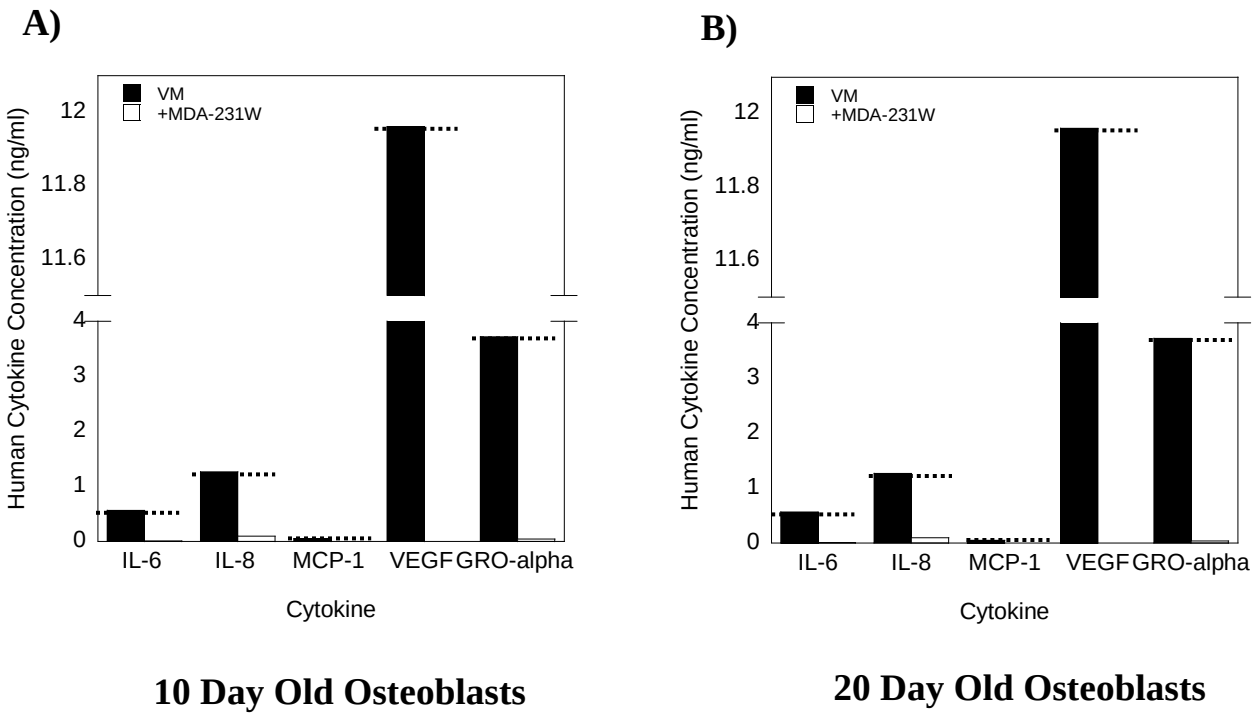

Figure 4.10: Cancer cell-derived cytokines are decreased in the presence of osteoblasts. MDA-MB-231W human metastatic breast cancer cells were co-cultured directly with MC3T3-E1 cells grown to either 10 or 20 days at a ratio of 10 osteoblasts : 1 breast cancer cell. Forty-eight hours later, the resultant culture supernatants were collected and subjected to a Bio-Rad Bio-Plex™ Human Cytokine Assay to quantitate cytokine expression. Cancer cell-derived cytokine expression of A) MC3T3-E1 cells grown to 10 days; B) MC3T3-E1 cells grown to 20 days. The cytokine concentration of breast cancer cells cultured alone is represented by the black bar; MDA-MB-231W human metastatic breast cancer cells co-culture for 48 hours with MC3T3-E1 cells, white bar. The dashed line represents VM cytokine expression. Shown are the results of representative experiments.

A) Breast Cancer Cell Interaction with 10 Day Old Osteoblasts

	Cytokine				
	Human Cytokine Expression (ng/ml)				
Condition	**IL-6**	**IL-8**	**MCP-1**	**VEGF**	**GRO-α**
VM	0.57	1.3	0.05	12.0	3.7
MDA-231W cells + 10 Day Old MC3T3-E1 cells	0.007	0.09	0	0	0.04

B) Breast Cancer Cell Interaction with 20 Day Old Osteoblasts

	Cytokine				
	Human Cytokine Expression (ng/ml)				
Condition	**IL-6**	**IL-8**	**MCP-1**	**VEGF**	**GRO-α**
MDA-231W CM	0.57	1.3	0.05	12.0	3.7
MDA-231W cells + 20 Day Old MC3T3-E1 cells	0.006	0.09	0	0	0.04

Table 4.6: Cancer cell-derived cytokines are decreased in the presence of osteoblasts. MDA-MB-231W human metastatic breast cancer cells were co-cultured directly with MC3T3-E1 cells as described in the legend to Figure 4.10. Shown is the human cytokine expression from the representative experiment shown in Figure 4.10 of MDA-MB-231W human metastatic breast cancer cells co-cultured directly with MC3T3-E1 cells. Listed is the human-derived cytokine production of A) 10 day old or B) 20 day old osteoblasts co-cultured with human metastatic breast cancer cells.

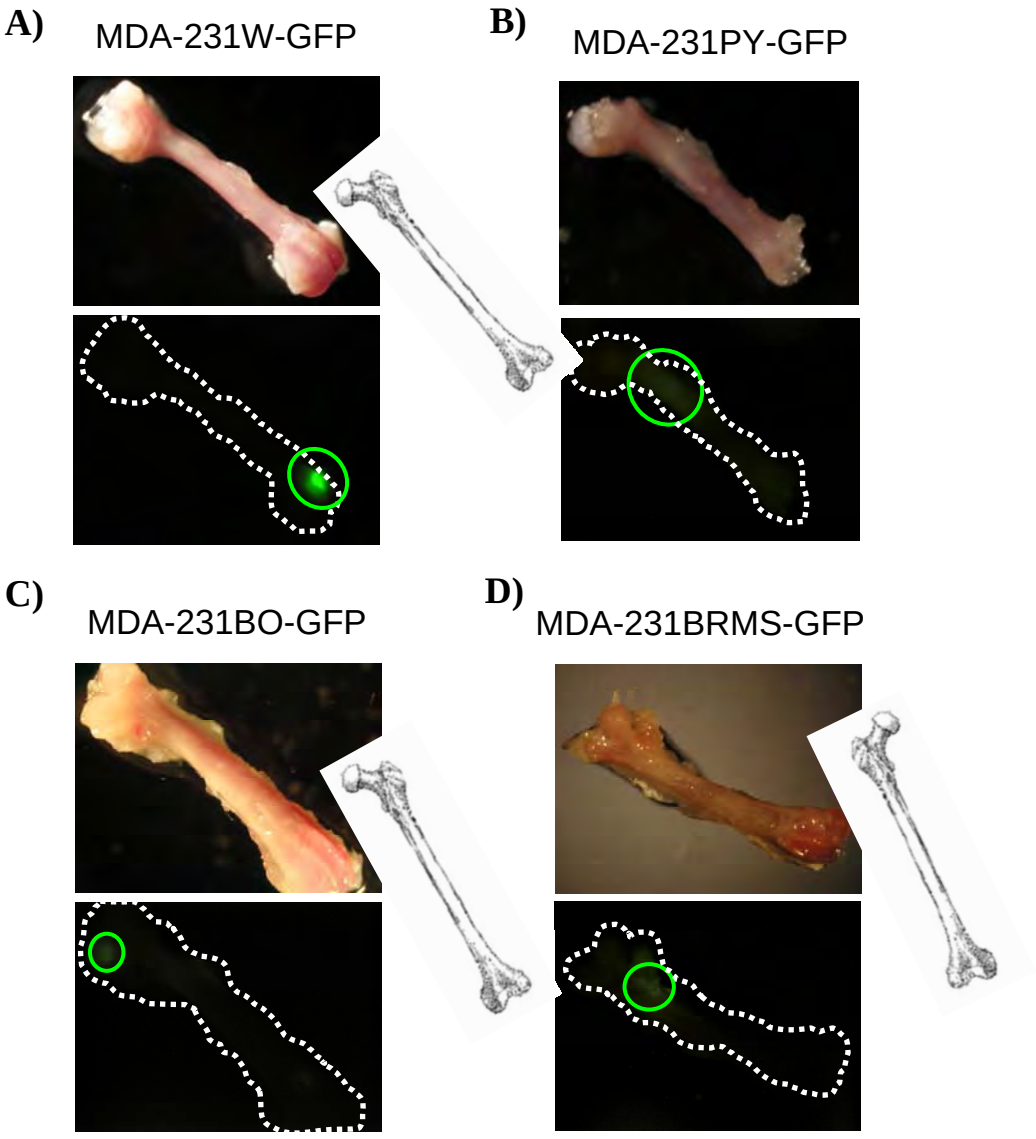

Figure 5.1: Human breast cancer cells trafficked to the femurs of cancer-bearing mice. MDA-MB-231W-GFP, MDA-MB-231PY-GFP, MDA-MB-231BO-GFP, and MDA-MB-231BRMS-GFP human breast cancer cells were inoculated into the left cardiac ventricle of athymic mice as described in the Materials and Methods. Three weeks post-inoculation, the mice were euthanized, femurs harvested, cleaned free of soft tissue and photographed using light and fluorescent stereo-microscopes. Light and fluorescent images of a femur from mice inoculated with A) MDA-MB-231W-GFP; B) MDA-MB-231PY-GFP; C) MDA-MB-231BO-GFP; and D) MDA-MB-231BRMS-GFP human breast cancer cells. Circled are colonies of human breast cancer cells that formed in the ends of long bones of mice. Six mice were inoculated per MDA-MB-231-GFP human breast cancer variant. Shown are representative images.

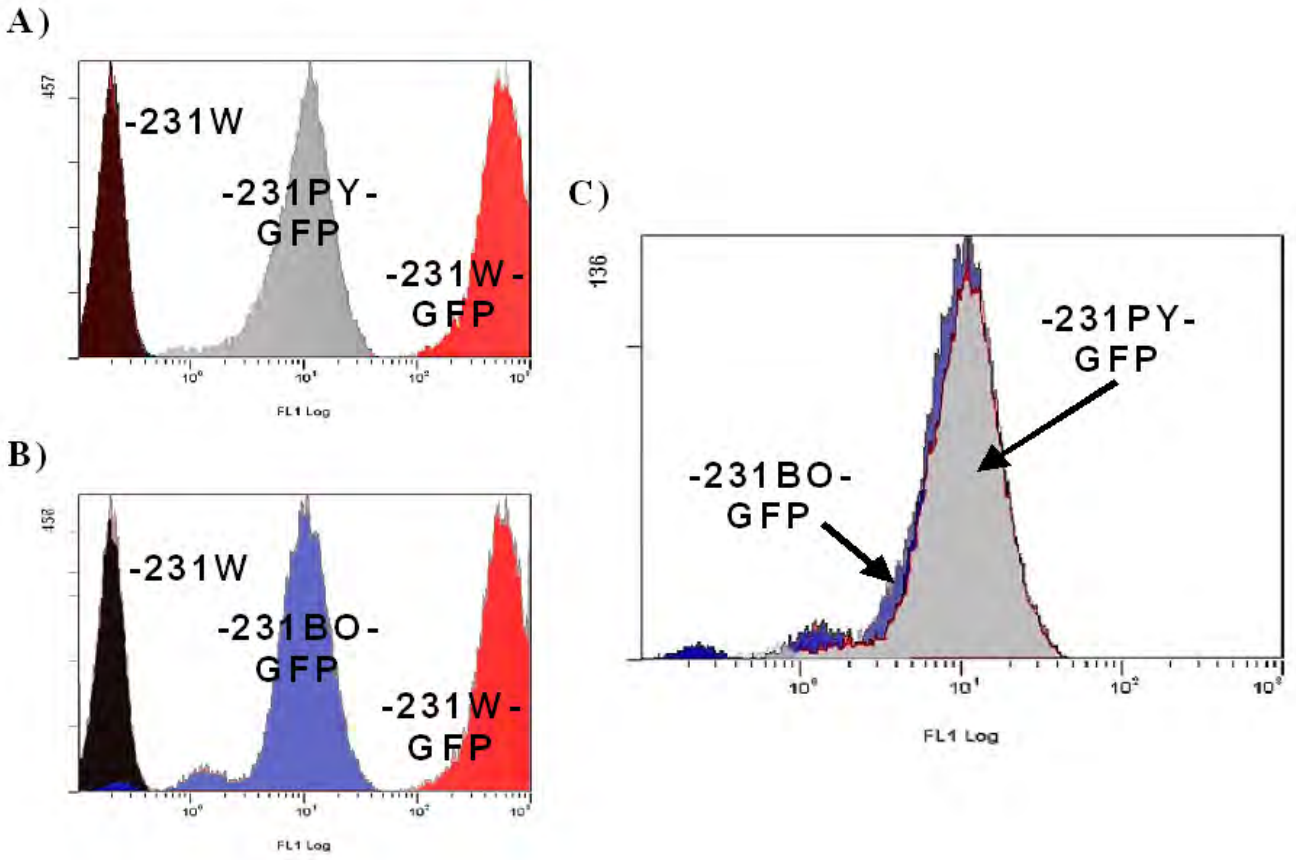

Figure 5.2: MDA-MB-231W-GFP human metastatic breast cancer cells were more fluorescent than MDA-MB-231PY-GFP or MDA-MB-231BO-GFP human metastatic breast cancer cell variants. MDA-MB-231W-GFP, MDA-MB-231PY-GFP, and MDA-MB-231BO-GFP human metastatic breast cancer cells were assayed via flow cytometry for their GFP fluorescence. Flow cytometry peaks of MDA-MB-231W, black peak; MDA-MB-231W-GFP, red peak; MDA-MB-231PY-GFP, grey peak; and MDA-MB-231BO-GFP, blue peak. A) MDA-MB-231PY-GFP compared with MDA-MB-231W and MDA-MB-231W-GFP; B) MDA-MB-231BO-GFP compared with MDA-MB-231W and MDA-MB-231W-GFP; C) MDA-MB-231PY-GFP compared with MDA-MB-231BO-GFP.

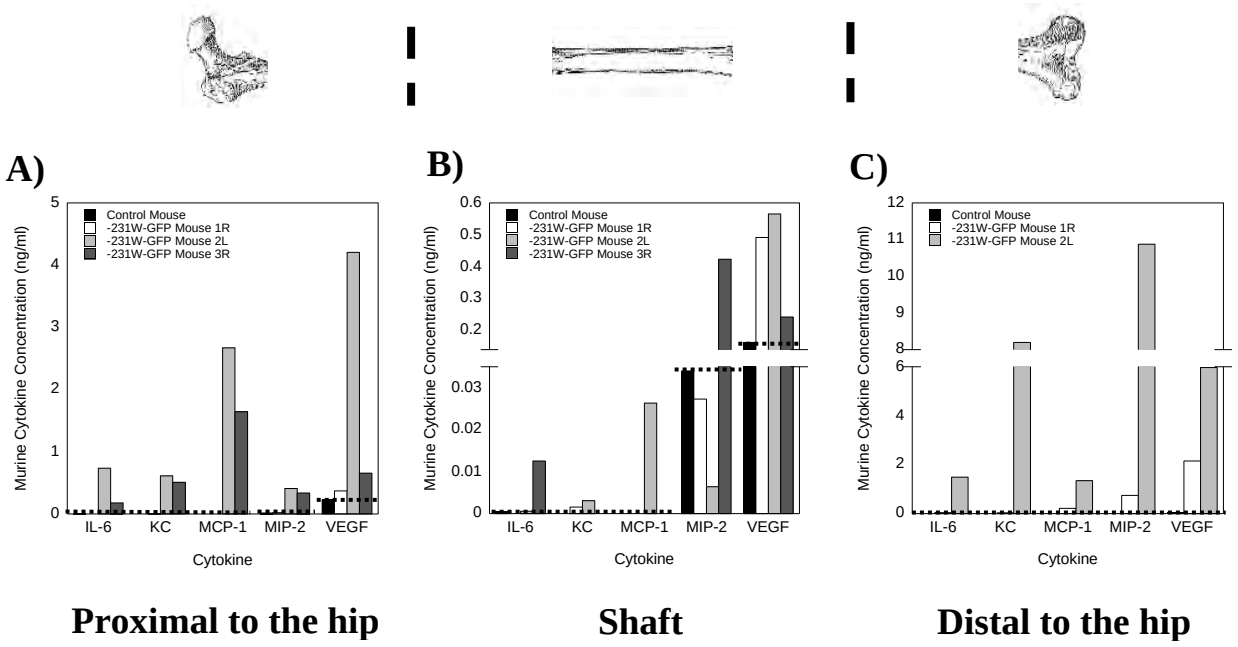

Figure 5.3: Bone-derived cytokine production was increased in MDA-MB-231W-GFP cancer-bearing mice. Bone-derived cytokine production was quantitated in bone regions proximal to the hip, shaft, and distal to the hip as described in the Materials and Methods. Femurs from control and cancer-bearing mice were cut into metaphyses and diaphysis, flushed free of bone marrow, and bone pieces proximal and distal to the hip, and shaft were independently crushed and cultured for 24 hours in α-MEM. The culture supernatants were assayed for cytokine expression using a Bio-Rad Bio-Plex™ Murine Cytokine Assay. Shown is the bone-derived cytokine production for the regions A) proximal to the hip, B) shaft, and C) distal to the hip. The bone-derived cytokine concentrations of the control mouse are represented by the black bar; MDA-MB-231W-GFP cancer-bearing mouse #1, white bar; MDA-MB-231W-GFP cancer-bearing mouse #2, light grey bar; MDA-MB-231W-GFP cancer-bearing mouse #3, dark grey bar. The dashed line represents control mouse cytokine expression. One femur from each of three mice was used, and four mice assayed per MDA-MB-231 breast cancer variant.

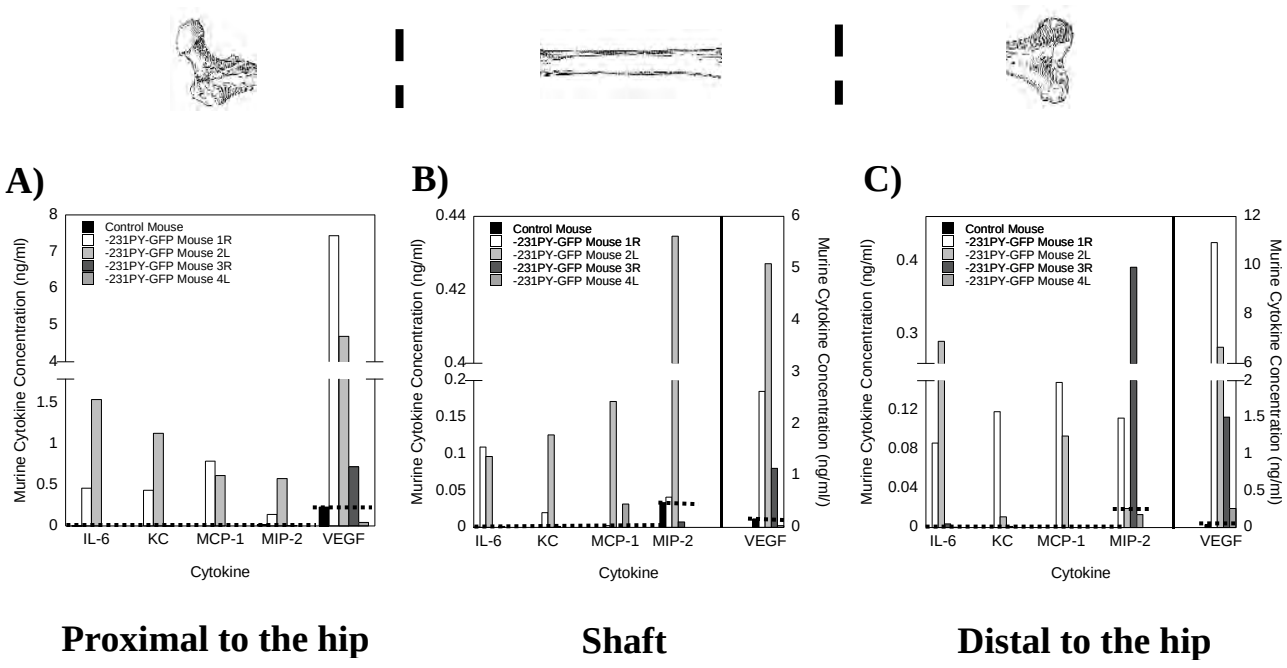

Figure 5.4: Bone-derived cytokine production was increased in MDA-MB-231PY-GFP cancer-bearing mice. Bone-derived cytokine production was quantitated in bone regions proximal to the hip, shaft, and distal to the hip as described in the Materials and Methods and the legend to Figure 5.3. Shown is the bone-derived cytokine production for the regions A) proximal to the hip, B) shaft, and C) distal to the hip. The bone-derived cytokine concentrations of the control mouse are represented by the black bar; MDA-MB-231PY-GFP cancer-bearing mouse #1, white bar; MDA-MB-231PY-GFP cancer-bearing mouse #2, light grey bar; MDA-MB-231PY-GFP cancer-bearing mouse #3, dark grey bar; MDA-MB-231PY-GFP cancer-bearing mouse #4, medium grey bar. The dashed line represents control mouse cytokine expression. One femur from each of three mice was used, and four mice assayed per MDA-MB-231 breast cancer variant.

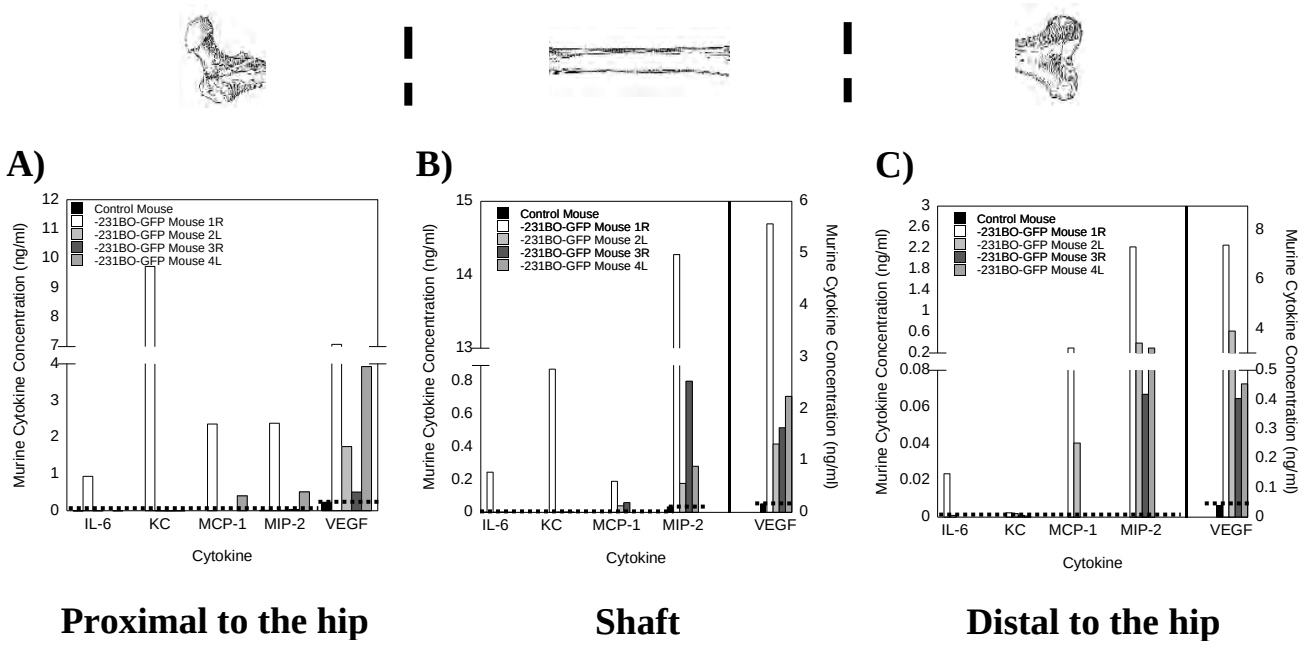

Figure 5.5: Bone-derived cytokine production was increased in MDA-MB-231BO-GFP cancer-bearing mice. Bone-derived cytokine production was quantitated in bone regions proximal to the hip, shaft, and distal to the hip as described in the Materials and Methods and the legend to Figure 5.3. Shown is the bone-derived cytokine production for the regions A) proximal to the hip, B) shaft, and C) distal to the hip. The bone-derived cytokine concentrations of the control mouse are represented by the black bar; MDA-MB-231BO-GFP cancer-bearing mouse #1, white bar; MDA-MB-231BO-GFP cancer-bearing mouse #2, light grey bar; MDA-MB-231BO-GFP cancer-bearing mouse #3, dark grey bar; MDA-MB-231BO-GFP cancer-bearing mouse #4, medium grey bar. The dashed line represents control mouse cytokine expression. One femur from each of three mice was used, and four mice assayed per MDA-MB-231 breast cancer variant.

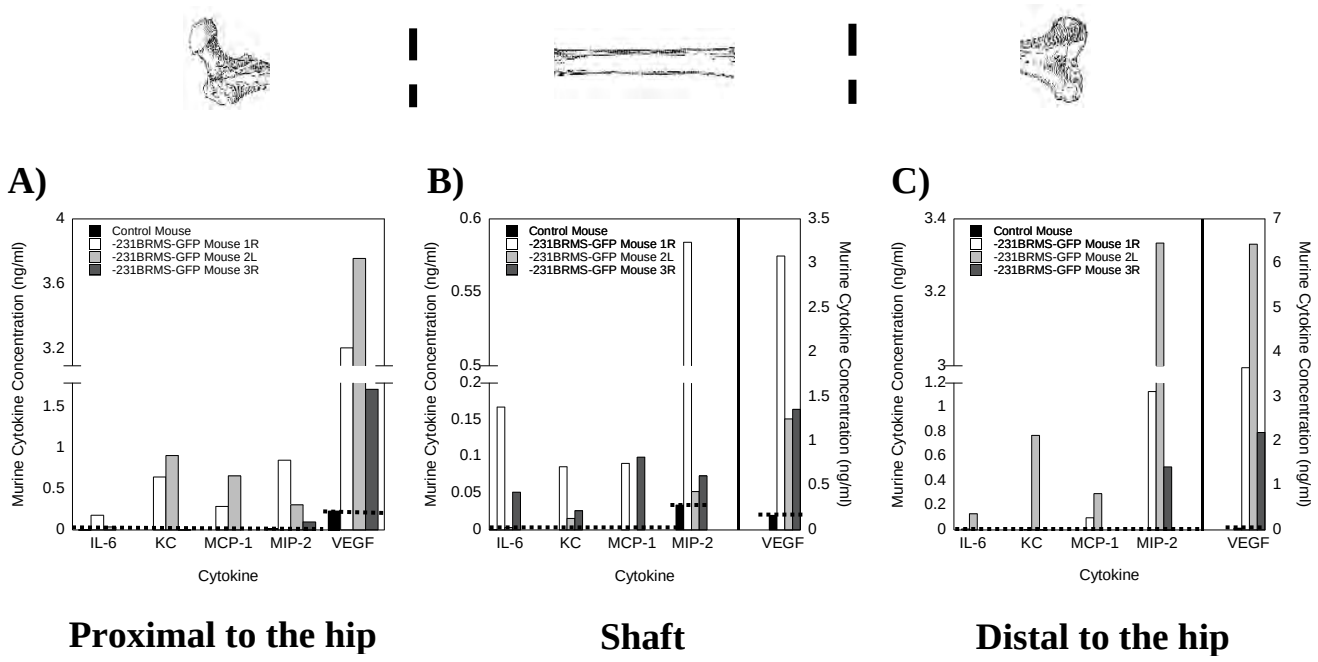

Figure 5.6: Bone-derived cytokine production was increased in MDA-MB-231BRMS-GFP cancer-bearing mice. Bone-derived cytokine production was quantitated in bone regions proximal to the hip, shaft, and distal to the hip as described in the Materials and Methods and in the legend to Figure 5.3. Shown is the bone-derived cytokine production for the regions A) proximal to the hip, B) shaft, and C) distal to the hip. The bone-derived cytokine concentrations of the control mouse are represented by the black bar; MDA-MB-231BRMS-GFP cancer-bearing mouse #1, white bar; MDA-MB-231BRMS-GFP cancer-bearing mouse #2, light grey bar; MDA-MB-231BRMS-GFP cancer-bearing mouse #3, dark grey bar. The dashed line represents control mouse cytokine expression. One femur from each of three mice was used, and four mice assayed per MDA-MB-231 breast cancer variant.

	Cytokine Fold Increase Compared to Non-cancer-bearing mice		
	Region of Murine Femur		
Cancer cell inoculant	**Proximal to the hip**	**Shaft**	**Distal to the hip**
MDA-231W-GFP	0-2.7	0-0.57	0.03-11
MDA-231PY-GFP	0-7.4	0.007-5.1	0-11
MDA-231BO-GFP	0-9.7	0.0002-14	0.0008-7.4
MDA-231BRMS-GFP	0-3.2	0-3	0.001-6.4

Table 5.1: Bone-derived cytokine production was increased in cancer-bearing mice. MDA-MB-231-GFP breast cancer cell variants were inoculated via intracardiac injection into athymic nude mice as described in the legend to Figure 5.3. Shown are the fold increases in bone-derived cytokines of cancer-bearing mice compared to non-cancer-bearing mice in the regions proximal and distal to the hip, and bone shaft.

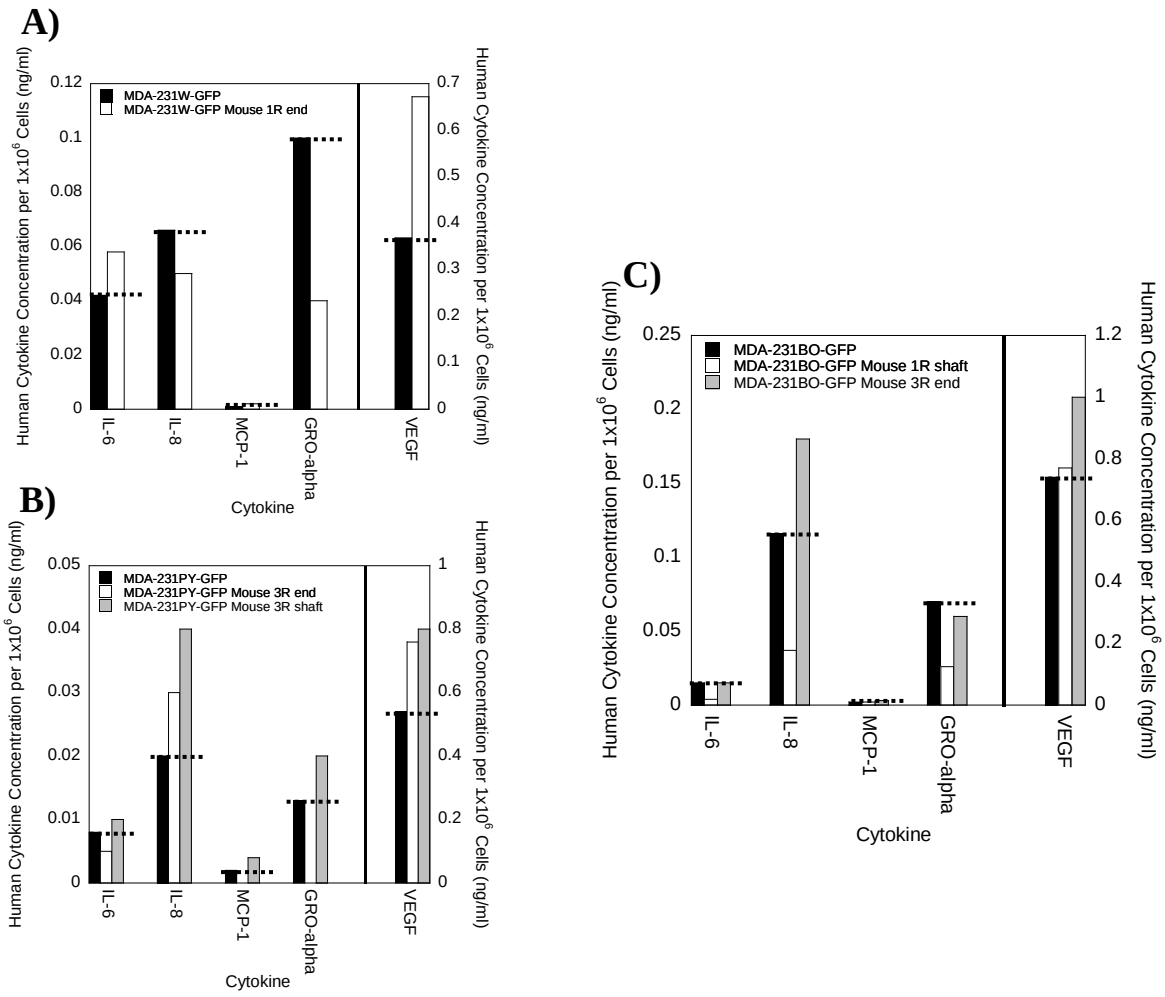

Figure 5.7: The bone microenvironment minimally altered cancer cell-derived cytokine production. Cancer cells were retrieved from the bone marrow of athymic mice three weeks post-inoculation and cultured as listed in the Materials and Methods. Retrieved cell conditioned media were collected and subjected to a Bio-Rad Bio-Plex™ Human Cytokine Assay. Cytokines were normalized to 1 million cells. Retrieved BCCM from mice inoculated with A) MDA-MB-231W-GFP cells, B) MDA-MB-231PY-GFP cells, and C) MDA-MB-231BO-GFP cells. The cancer cell-derived cytokine production of cancer cells not exposed to the bone microenvironment (control) is represented by the black bar; retrieved cancer cells exposed to the bone microenvironment from: mouse #1, white bar; mouse #2, light grey bar. The dashed line represents cytokine concentrations from the conditioned medium of cells pre-inoculation.

A) Fold Increase in Human Cytokines

Cancer cell inoculant	Range of the Fold Increase of Human Cytokines Compared to the BCCM of the Same Cells Pre-inoculation
MDA-231W-GFP	0.15-2
MDA-231PY-GFP	1.25-2
MDA-231BO-GFP	1.5-1.6
MDA-231BRMS-GFP	None retrieved

B) Fold Decrease in Human Cytokines

Cancer cell inoculant	Range of Percent Decrease of Human Cytokines Compared to the BCCM of the Same Cells Pre-inoculation
MDA-231W-GFP	17-60%
MDA-231PY-GFP	37.5-100%
MDA-231BO-GFP	63-73%
MDA-231BRMS-GFP	None retrieved

Table 5.2: The bone microenvironment minimally altered cancer cell-derived cytokine production. MDA-MB-231-GFP breast cancer cell variants were retrieved from cancer-bearing mice as described in the legend to Figure 5.7. Shown are the A) fold increases or B) percent decreases of human cytokines from conditioned medium of cancer cells retrieved from cancer-bearing mice compared to the conditioned medium of the same cells pre-inoculation.

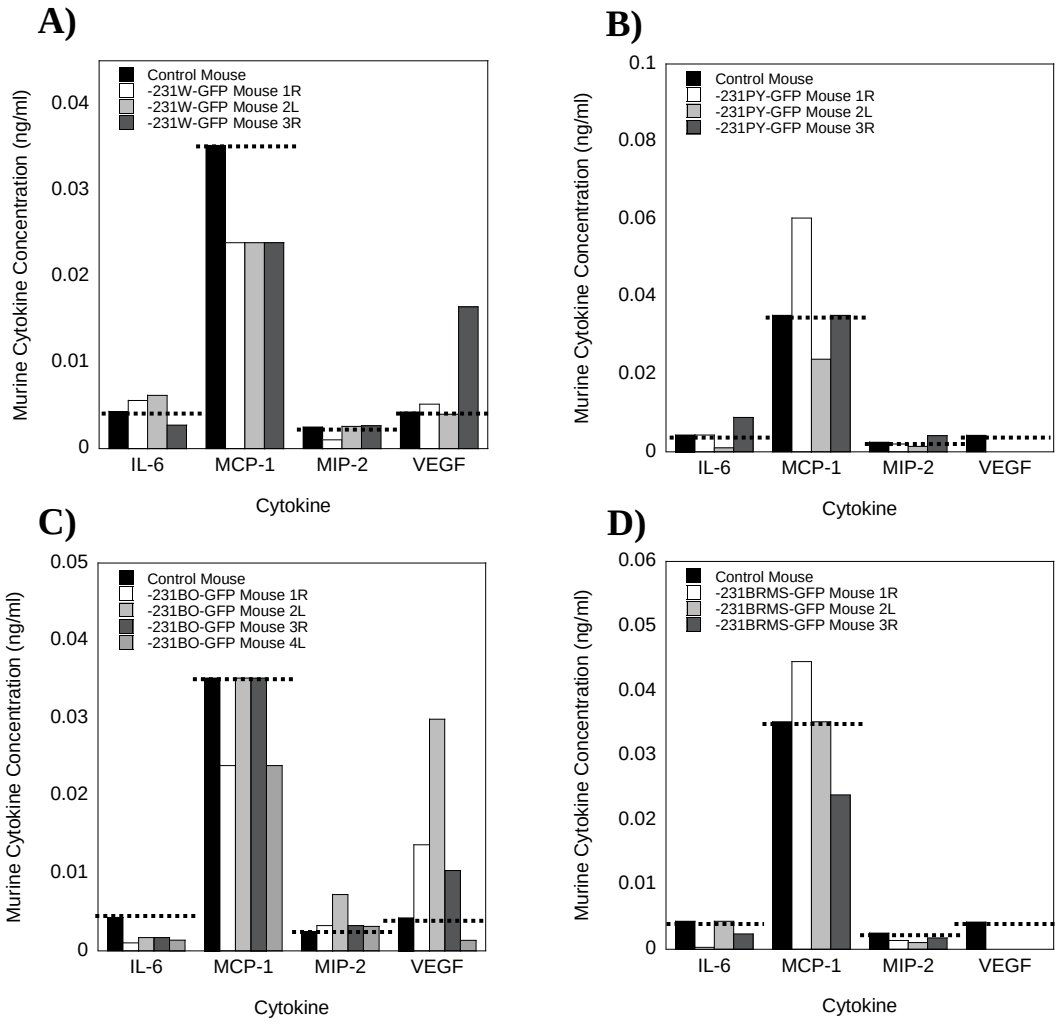

Figure 5.8: Murine-derived cytokine expression was minimally altered in the bone marrow plasma from the bone metaphyses of cancer-bearing mice. Bone marrow plasma was collected from the bone marrow of athymic mice three weeks post-inoculation and processed as listed in the Materials and Methods. Bone marrow plasma was subjected to a Bio-Rad Bio-Plex™ Murine Serum Cytokine Assay. Bone marrow plasma collected from the bone metaphyses of mice inoculated with A) MDA-MB-231W-GFP cells, B) MDA-MB-231PY-GFP cells, C) MDA-MB-231BO-GFP cells, and D) MDA-MB-231BRMS-GFP cells. The murine-derived cytokine production of bone marrow plasma from a control mouse is represented by the black bar; bone marrow plasma of cancer-bearing mouse #1, white bar; mouse #2, light grey bar; mouse#3, dark grey bar; mouse #4, medium grey bar. The dashed line represents control bone marrow plasma cytokine concentrations.

A) Fold Increase in Murine Cytokines

	Fold Increase of Murine Cytokines Compared to Non-cancer-bearing Mice	
Cytokine	**Ends**	**Shaft**
IL-6	0-2	1.2-3
MIP-2	0-3	1.8-16
MCP-1	0-2	No change
KC	None present	None present
VEGF	1.25-7	0-29

B) Percent Decrease in Murine Cytokines

	Percent Decrease of Murine Cytokines Compared to Non-cancer-bearing Mice	
Cytokine	**Ends**	**Shaft**
IL-6	65-95%	33-66%
MIP-2	No change	No decrease
MCP-1	34%	40-92%
KC	None present	None present
VEGF	100%	No decrease

Table 5.3: Murine-derived cytokines were minimally altered in the bone marrow plasma of cancer-bearing mice. The bone marrow plasma of the femoral ends and shaft from mice inoculated with MDA-MB-231-GFP breast cancer cell variants was obtained as described in the legend to Figures 5.8-5.9. Shown are the A) fold increases or B) percent decreases of murine cytokines from the bone marrow plasma of cancer-bearing mice compared to non-cancer-bearing mice.

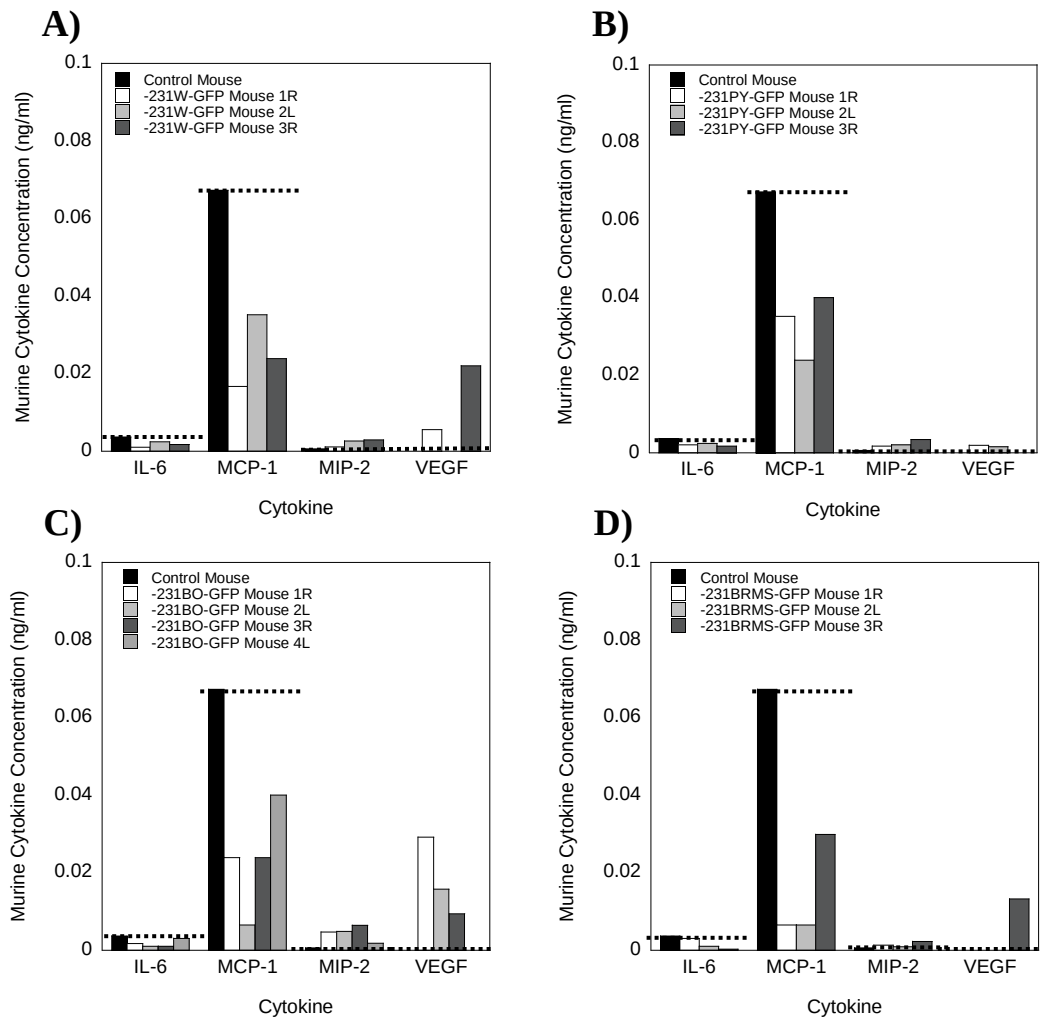

Figure 5.9: Murine-derived cytokines were minimally altered in the bone marrow plasma from the bone diaphyses of cancer-bearing mice. Bone marrow plasma was collected from the bone marrow of athymic mice three weeks post-inoculation and processed as listed in the Materials and Methods. Bone marrow plasma was subjected to a Bio-Rad Bio-Plex™ Murine Serum Cytokine Assay. Bone marrow plasma collected from the bone diaphyses of mice inoculated with A) MDA-MB-231W-GFP cells, B) MDA-MB-231PY-GFP cells, C) MDA-MB-231BO-GFP cells, and D) MDA-MB-231BRMS-GFP cells. The murine-derived cytokine production of bone marrow plasma from a control mouse is represented by the black bar; bone marrow plasma of cancer-bearing mouse #1, white bar; mouse #2, light grey bar; mouse#3, dark grey bar; mouse #4, medium grey bar. The dashed line represents control bone marrow plasma cytokine concentrations.

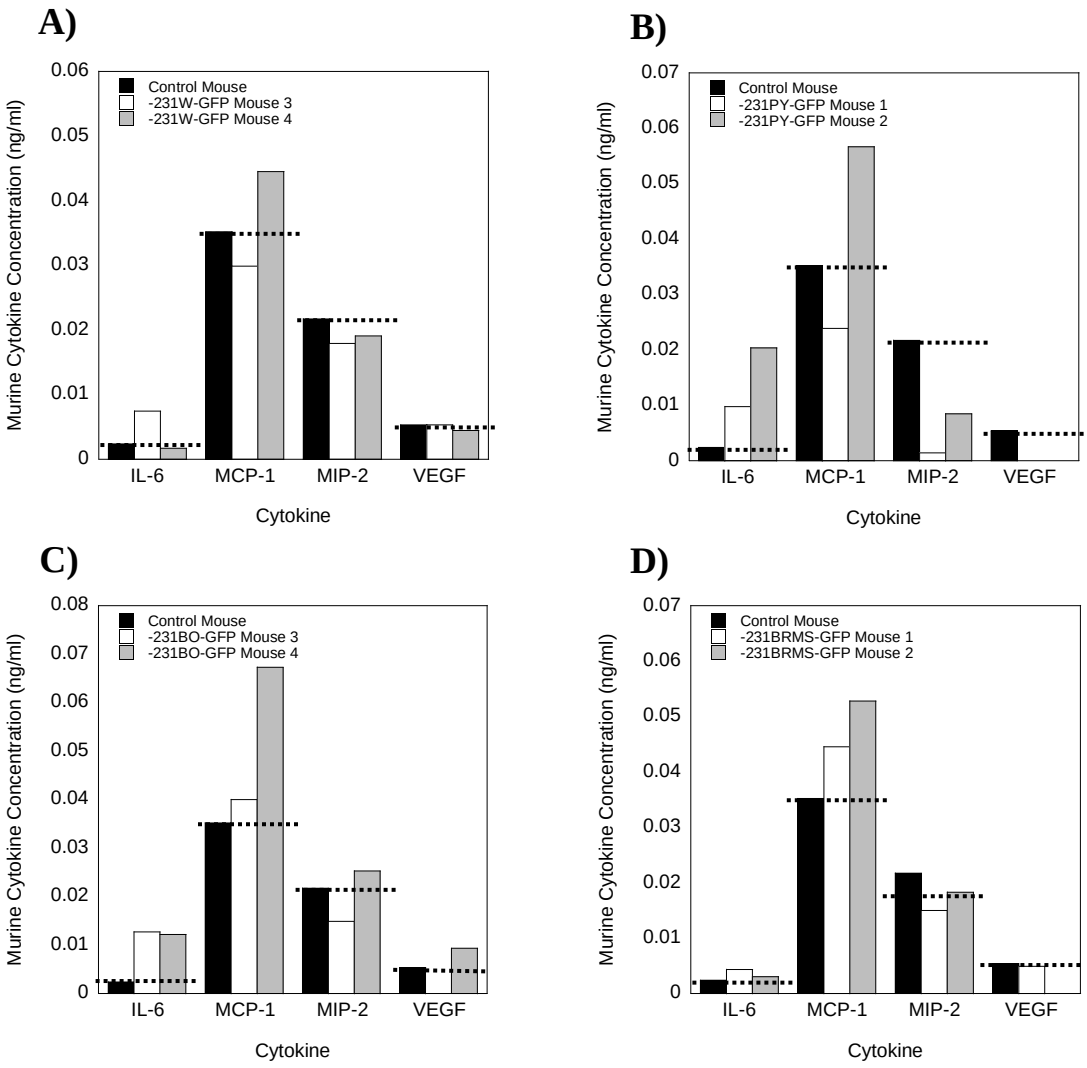

Figure 5.10: Murine-derived cytokines were minimally altered in the blood serum of cancer-bearing mice. Blood serum was collected from athymic mice three weeks post-inoculation and processed as listed in the Materials and Methods. Blood serum was subjected to a Bio-Rad Bio-Plex™ Murine Serum Cytokine Assay. Blood serum collected from mice inoculated with A) MDA-MB-231W-GFP cells, B) MDA-MB-231PY-GFP cells, C) MDA-MB-231BO-GFP cells, and D) MDA-MB-231BRMS-GFP cells. The murine-derived cytokine production of bone marrow plasma from a control mouse is represented by the black bar; bone marrow plasma of cancer-bearing mouse #1, white bar; mouse #2, light grey bar. The dashed line represents control bone marrow plasma cytokine concentrations.

A) Fold Increase in Murine Cytokines

Cytokine	Range of the Fold Increase of Murine Cytokines Compared to Non-cancer-bearing Mice
IL-6	2-10
MIP-2	1.2-1.5
MCP-1	1.3-1.9
KC	None present
VEGF	1.5-1.8

B) Percent Decrease in Murine Cytokines

Cytokine	Range of the Percent Decrease of Murine Cytokines Compared to Non-cancer-bearing Mice
IL-6	No decrease
MIP-2	20-62%
MCP-1	0-12%
KC	None present
VEGF	20-100%

Table 5.4: Murine-derived cytokines were minimally altered in the blood serum of cancer-bearing mice. The blood serum from mice inoculated with MDA-MB-231-GFP breast cancer cell variants was obtained as described in the legend to Figure 5.10. Shown are the A) fold increases or B) percent decreases of murine cytokines from the blood serum of cancer-bearing mice compared to non-cancer-bearing mice.

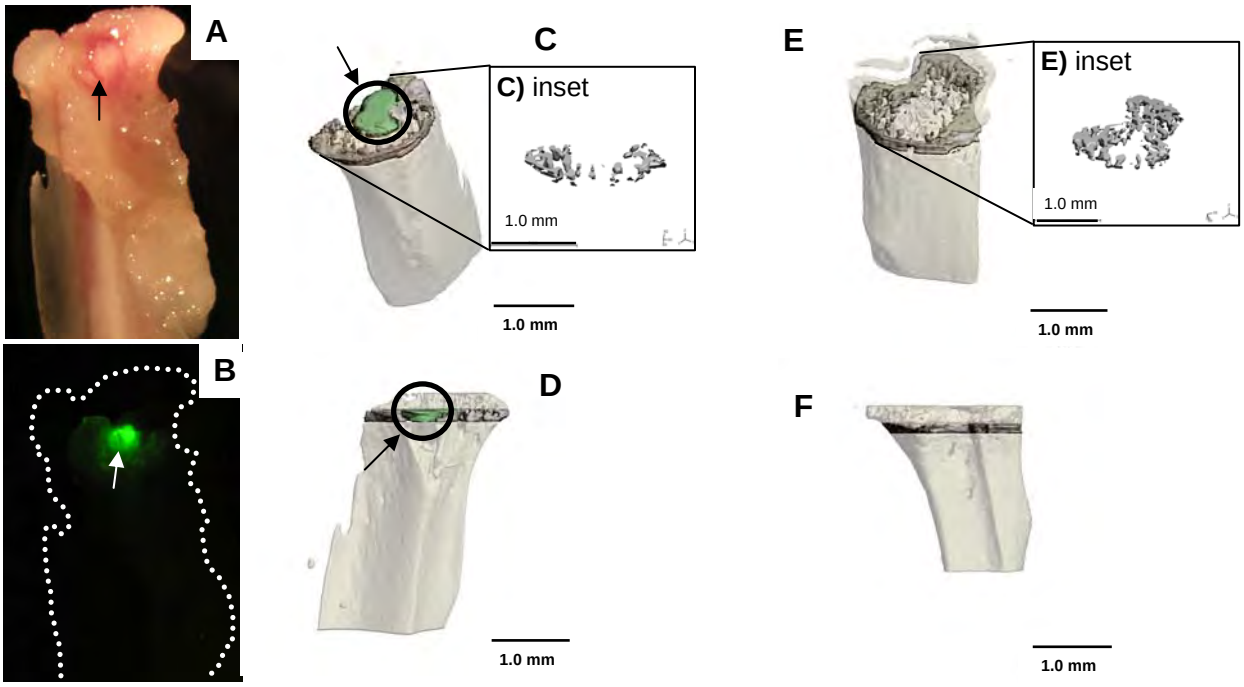

Figure 5.11: Human Metastatic Breast Cancer Cells Colonized Trabecular Bone. Six week old female athymic mice were inoculated in the left cardiac ventricle via intracardic injection with MDA-MB-231-GFP metastatic breast cancer cell variants as described in the Materials and Methods. Control, non-cancer-bearing mice were untreated. Three weeks post-inoculation, mice were euthanized, tibiae and femurs harvested, cleaned free of soft tissue, and photographed using a fluorescent stereomicroscope. A µCT40 Desktop MicroCT Scanner was used to assess bone architecture. A) The light microscopy image of a cancer-bearing tibia, where B) a tumor was detected in the metaphyseal region proximal to the knee by fluorescence stereo-microscopy. C and D) A three dimensional µCT model of the metaphyseal region illustrates that the tumor (arrow) localized in the trabecular bone (dark grey) in an anterior view (C) and posterior view (D). C, (inset) the volume of trabecular bone in the cancer-bearing and control tibia (E, inset). Control tibia with trabecular bone (grey) as seen from an E) anterior and F) posterior view. Scans were performed independently on one control tibia and femur and one cancer-bearing tibia and femur from mice inoculated with each MDA-MB-231-GFP cancer cell variant. Tibiae and femurs were from different mice. Shown are representative images.

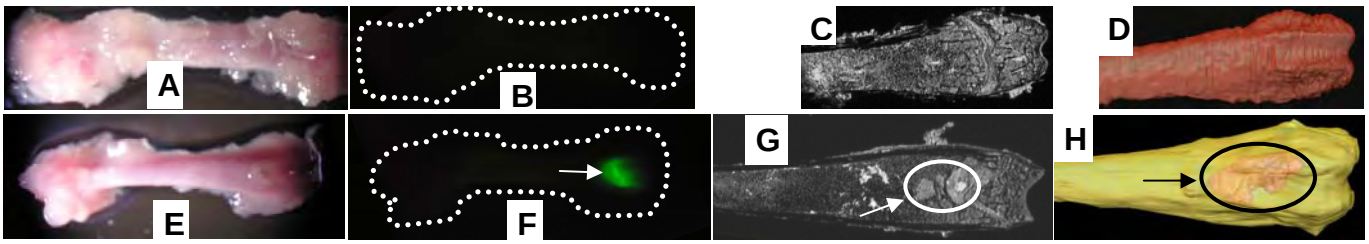

Figure 5.12: Tumor volume was estimated via MRI. Femurs were imaged via MRI to assess for tumor cell presence and volumetric analyses. A, E) Light microscopy image and B, F) corresponding fluorescent microscopy image of representative control (A-D) and MDA-MB-231W-GFP cancer-bearing (E-H) murine femurs. In the cancer-bearing femur, tumor cells were localized in the area distal to the hip (F, arrow). C, G) Corresponding MRI images. In the cancer-bearing femur, the tumor is represented as a large white object in the region distal to the hip (G, arrow). D, H) Corresponding three dimensional models. Control femur (D) is cancer-free, whereas the tumor is illustrated in-situ in the cancer-bearing femur (H). Three control and three MDA-MB-231W-GFP cancer-bearing femurs were scanned. Shown are representative images.

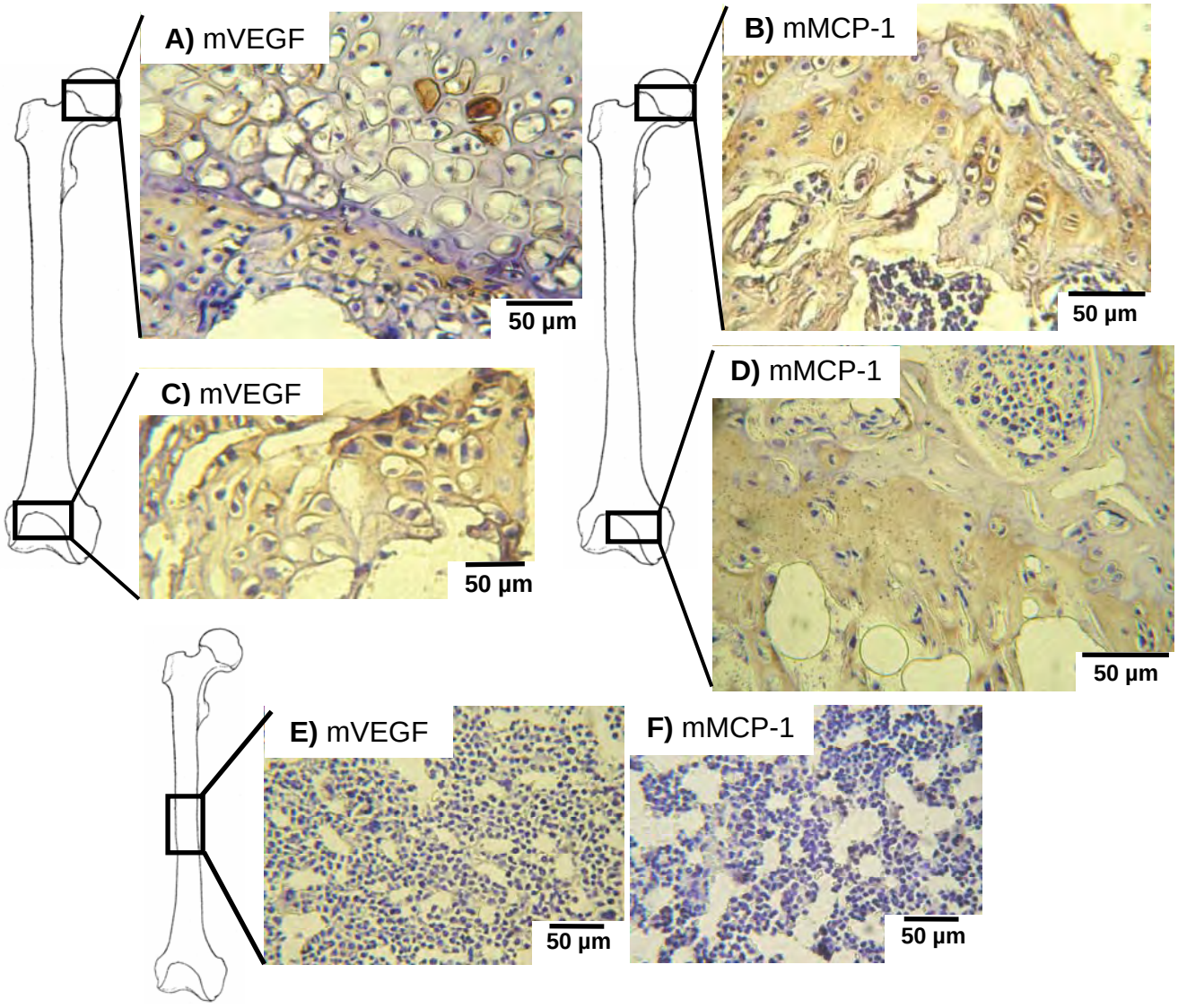

Figure 5.13: Murine MCP-1 and VEGF were localized to the trabecular bone in both non-cancer-bearing and cancer-bearing mice. Femurs harvested from athymic nude mice, inoculated as described in the Materials and Methods, were cryosectioned in 10 µm thick longitudinal sections, and stained for murine VEGF or murine MCP-1 via immunohistochemistry and visualized using a brown DAB chromogen stain. Slides were counterstained using Gill's Hematoxylin. A, C) Murine VEGF and B, D) murine MCP-1 were localized in trabecular bone of the femur in the regions proximal and distal to the hip. Neither murine E) VEGF nor F) MCP-1 were found in the bone marrow. Shown are representative images.

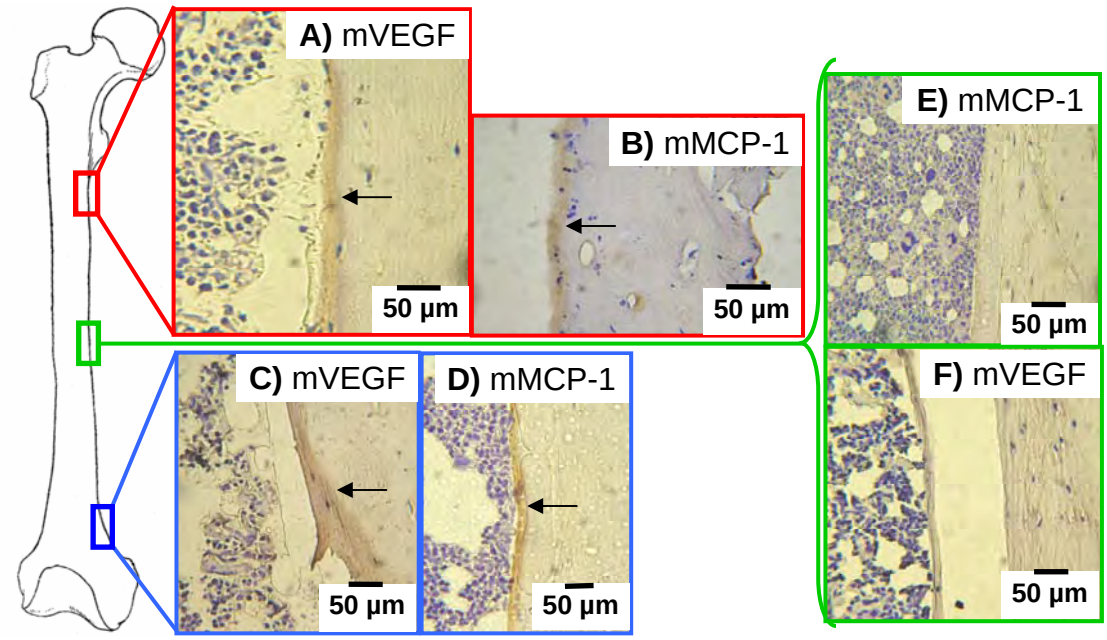

Figure 5.14: Murine MCP-1 and VEGF were localized in the matrix near the trabecular bone, but not in the bone shaft. Femurs harvested from athymic nude mice, were assayed as described in the legend to Figure 5.13. A, C) Murine VEGF (arrows) and B, D) murine MCP-1 (arrows) were localized in cortical bone slightly inferior to the trabecular bone proximal and distal to the hip. Neither E) murine MCP-1 nor F) murine VEGF were localized in cortical bone of the bone shaft. Shown are representative images.

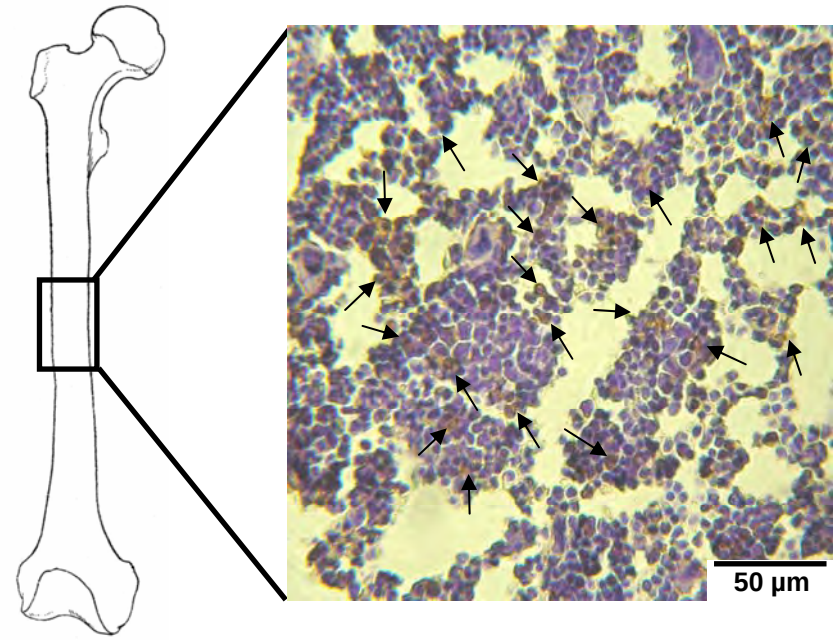

Figure 5.15: Murine IL-6 was located in the bone marrow. Femurs harvested from athymic nude mice, inoculated as described in the Materials and Methods, were cryosectioned in 10 µm thick longitudinal sections, and stained for murine IL-6 via immunohistochemistry and visualized using a brown DAB chromogen stain. Murine IL-6 was localized throughout the bone marrow, as indicated by the arrows, but was not present in the trabecular or cortical bone. Slides were counterstained using Gill's Hematoxylin. Shown is a representative image.

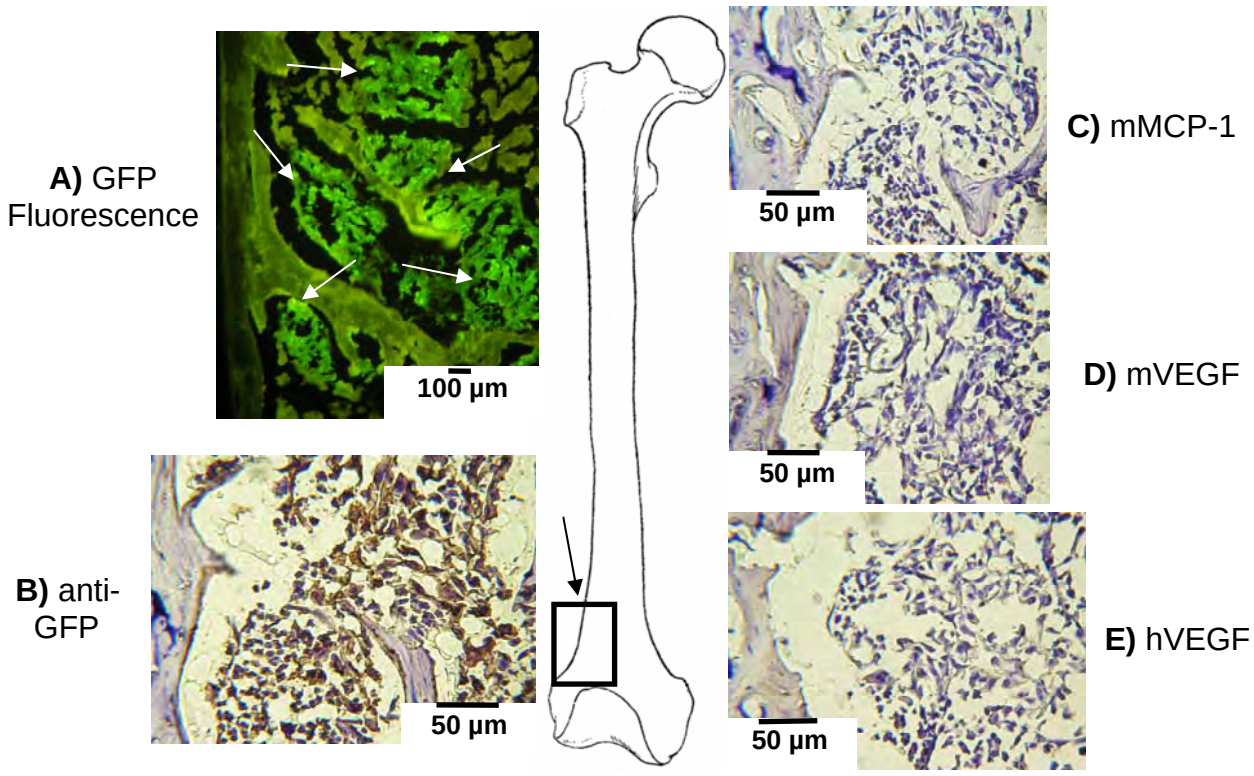

Figure 5.16: Cytokine expression was not detected directly adjacent to the tumor. Femur sections from athymic mice were prepared as described in the Materials and Methods. Sections were photographed and stained via immunohistochemistry for murine MCP-1, murine VEGF, human VEGF, or anti-GFP IgG. MDA-MB-231W-GFP cells were detected in trabecular bone of the region distal to the hip (box, arrow) A) The fluorescent microscope image of tumor cells (arrows) present in the trabecular bone distal to the hip. B) Corresponding anti-GFP IgG image. Neither C) murine MCP-1, D) murine VEGF, nor E) human VEGF were detected within ~150 µm distance from the tumor. At least three independent sections were stained per bone, and two bones examined per inoculated MDA-MB-231-GFP variant or non-cancer-bearing mice. Shown are representative images.

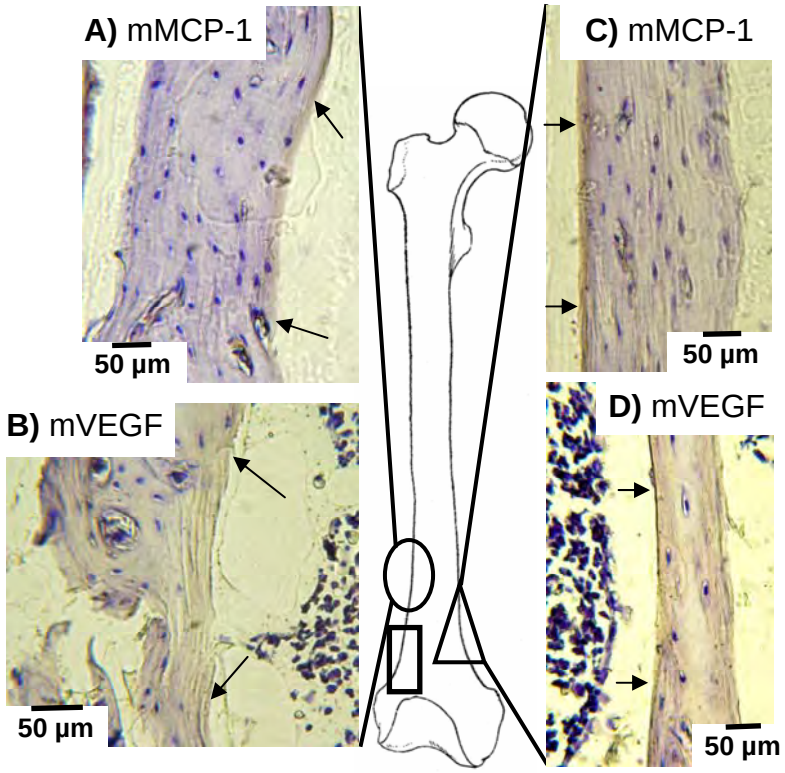

Figure 5.17: Murine MCP-1 and VEGF were present in a gradient that increased away from the tumor. Femur sections from athymic mice were prepared as described in the Materials and Methods. Sections were photographed and stained via immunohistochemistry for murine MCP-1, murine VEGF, or human VEGF. A) Murine MCP-1 (arrows) and B) murine VEGF (arrows) were detected in the cortical bone superior to the tumor (circle) and present in a gradient extending away from the tumor. C) Murine MCP-1 (arrows) and D) murine VEGF (arrows) were detected in the cortical bone (triangle) of the side opposite the tumor. In this example, the tumor was located in the trabecular bone distal to the hip (rectangle). At least three independent sections were stained per bone, and two bones examined per inoculated MDA-MB-231-GFP variant or non-cancer-bearing mice. Shown are representative experiments.

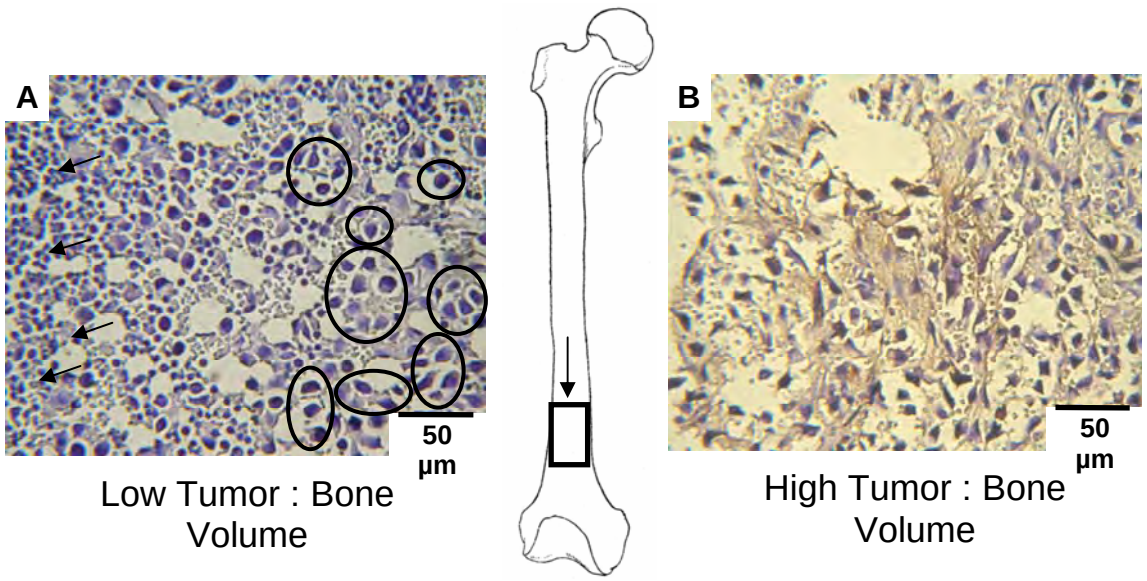

Figure 5.18: Human VEGF expression increased with increased tumor size. Femur sections from athymic mice were prepared as described in the Materials and Methods. Sections were photographed and stained via immunohistochemistry for human VEGF expression. A) Human VEGF expression was not detected in the femur from a mouse allowed to progress three weeks post-inoculation. Large human tumor cells (right, circles) were present with small murine bone marrow cells (left, arrows). B) Human VEGF expression increased with tumor volume. At least three independent sections were stained per bone, and two bones examined per inoculated MDA-MB-231-GFP variant or non-cancer-bearing mice. Shown are representative experiments.

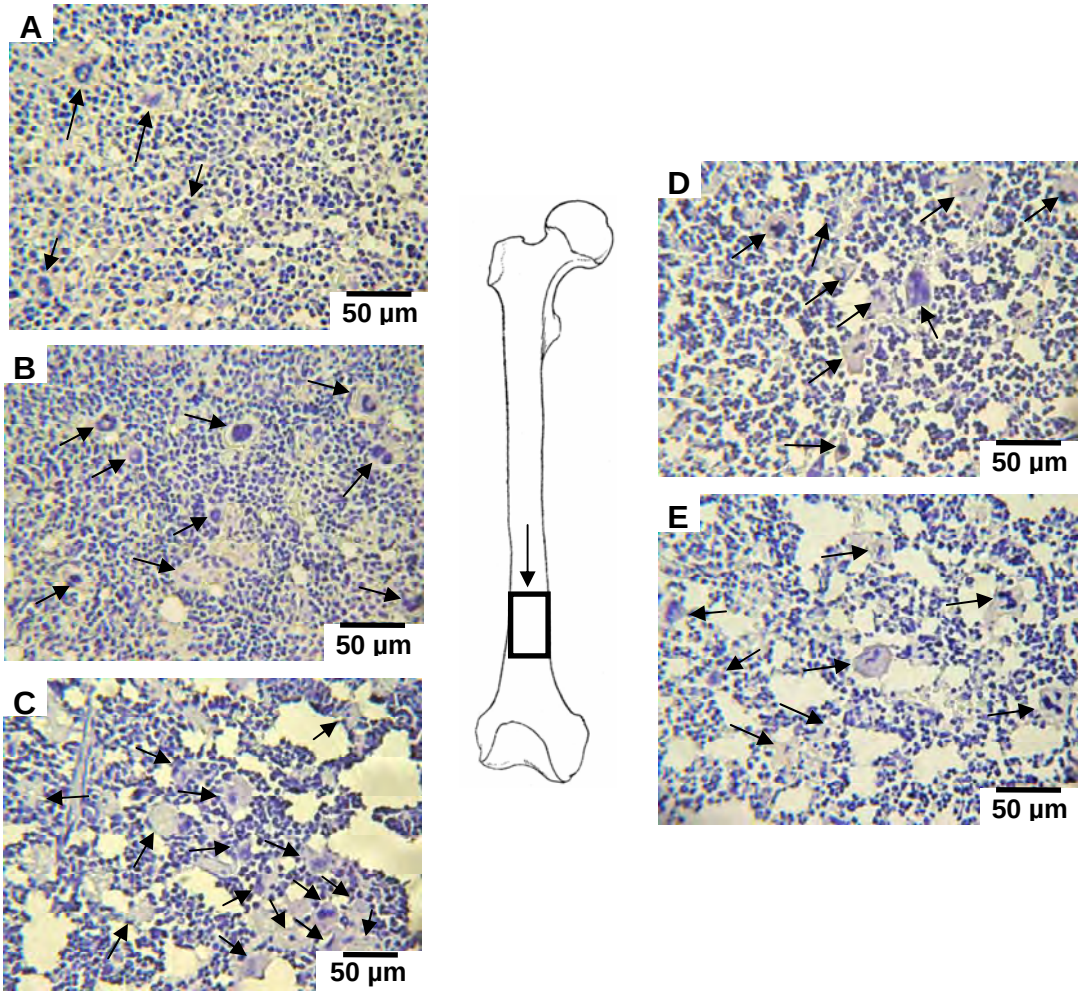

Figure 5.19: Megakaryocyte numbers increased in cancer-bearing femur sections. Murine femur sections were prepared as described in the Materials and Methods. A) Bone marrow from the femur of a non-cancer-bearing mouse. Three megakaryocytes are identified by arrows in the field of view. Bone marrow from the femur of a mouse three weeks post-injection inoculated with a B) MDA-MB-231W-GFP; C) MDA-MB-231PY-GFP; D) MDA-MB-231BO-GFP; E) MDA-MB-231BRMS-GFP breast cancer cell variants. No tumors were detected by fluorescence stereo-microscopy or immunohistochemistry. B) Nine; C) sixteen; D) nine; and E) eight megakaryocytes are identified in the field of view by arrows. At least three independent sections were stained per bone, and two bones examined per inoculated MDA-MB-231-GFP variant or non-cancer-bearing mice. Shown are representative experiments.

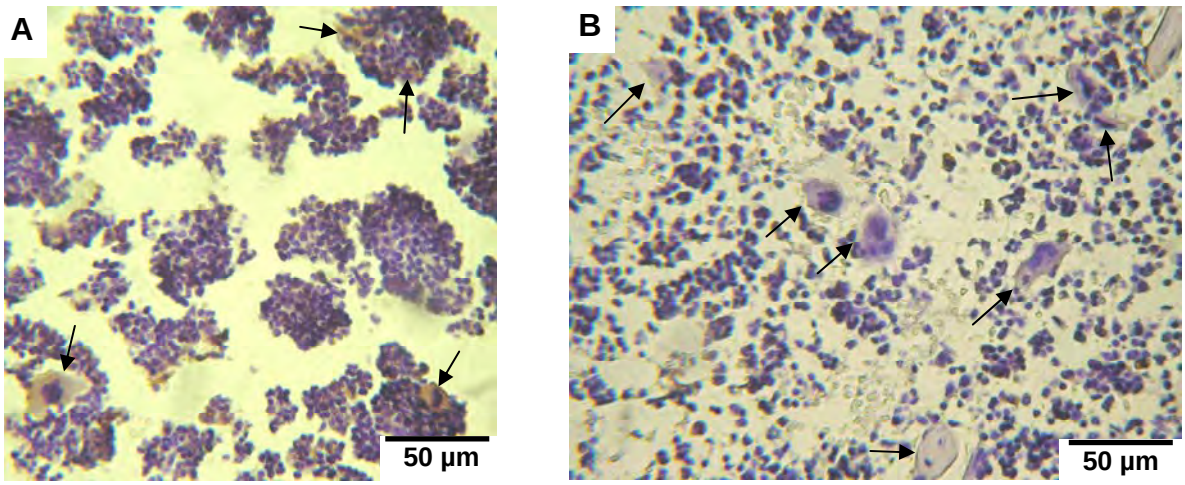

Figure 5.20: Femur sections from non-cancer-bearing mice stained positive for the CD41 antigen. Femurs harvested from athymic nude mice, inoculated as described in the Materials and Methods, were cryosectioned in 10 µm thick longitudinal sections, and stained for anti-CD41 via immunohistochemistry and visualized using a brown DAB chromogen stain. Slides were counterstained using Gill's Hematoxylin. A) Bone marrow from the femur of a non-cancer-bearing mouse. CD41 positive staining megakaryocytes were detected by immunohistochemistry for anti-CD41, and are indicated by arrows. B) Bone marrow from the femur of a cancer-bearing mouse. Megakaryocytes did not stain for the CD41 antigen, and are indicated by arrows. At least three independent sections were stained per bone, and two bones examined per inoculated MDA-MB-231-GFP variant or non-cancer-bearing mice. Shown are representative experiments.

Femurs from Mice Injected with Brefeldin A

Femurs from Mice NOT Injected with Brefeldin A

Figure 5.21: Brefeldin A altered the color of murine femurs. Brefeldin A was inoculated via tail vein injection into control or cancer-bearing mice three weeks post-cancer cell inoculation as described in the materials and methods. Six hours post-Brefeldin A injection, mice were euthanized, femurs harvested, cleaned free of soft tissue, and photographed. Right: femurs from mice inoculated with Brefeldin A; left: femurs from mice not injected with Brefeldin A.

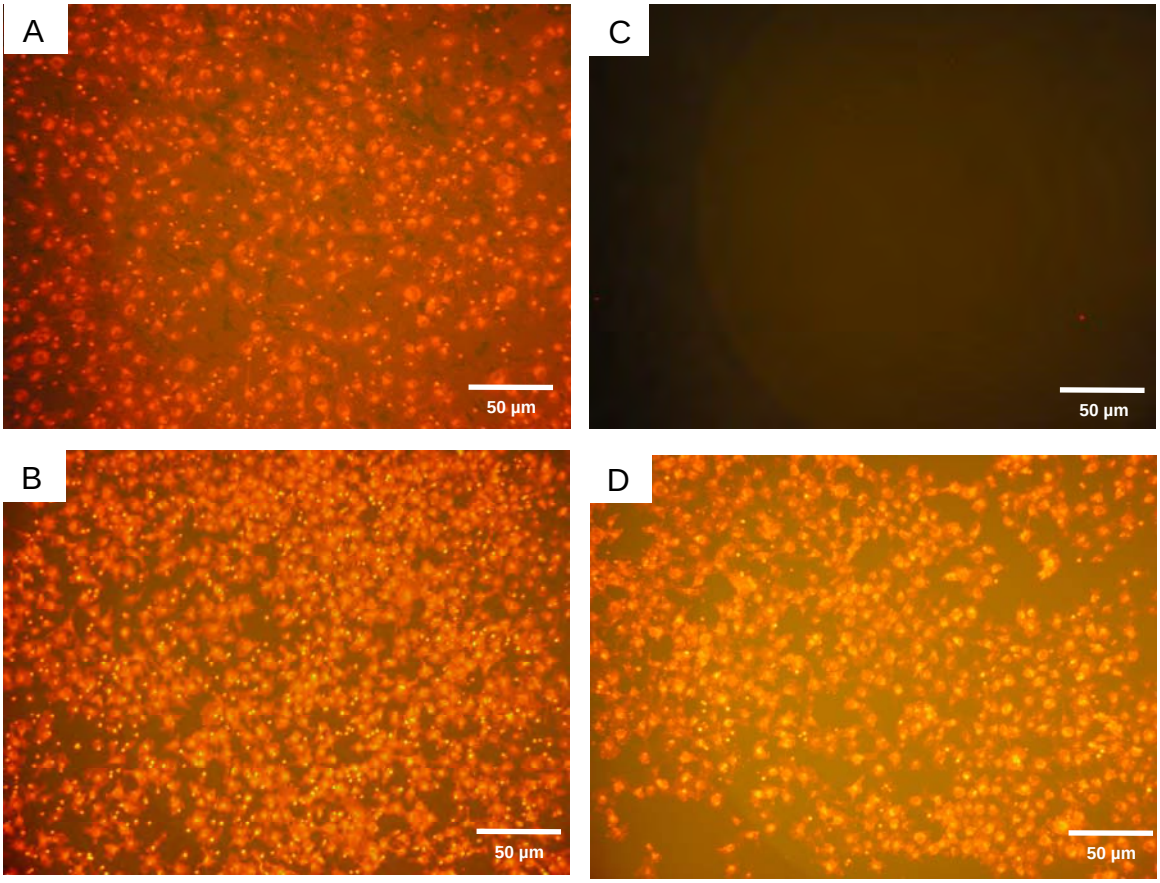

Figure 6.1: Osteoblast conditioned medium was a chemoattractant for MDA-MB-231W human metastatic breast cancer cells. MDA-MB-231W human metastatic breast cancer cells stained with Vybrant DiI were seeded in the upper chamber of a transwell plate system with treatments as described in the Materials and Methods. Twenty-four hours later, transwell membranes were removed from culture inserts and migrated MDA-MB-231W human metastatic breast cancer cells counted. MDA-MB-231W human metastatic breast cancer cell migration when the cancer cells were subjected to conditioned medium collected from MC3T3-E1 cells grown to A) 10 or B) 20 days; C) 25 ng/ml recombinant human IL-6 protein plus 100 ng/ml recombinant human VEGF protein; or D) conditioned medium collected from MC3T3-E1 cells grown to 10 days plus 5 ng/ml anti-IL-6, anti-KC, and anti-VEGF mouse neutralizing antibody. Each treatment was conducted at least twice. Shown are representative experiments.

Chemoattractant	Average Number of MDA-MB-231W Human Metastatic Breast Cancer Cells Per Field of View that Migrated Toward the Chemoattractant	Standard Deviation
Conditioned medium from osteoblasts grown to 10 days	860	131.2
Conditioned medium from osteoblasts grown to 20 days	980	138.6
Human IL-6 plus VEGF recombinant protein	0	0
Conditioned medium from osteoblasts grown to 10 days incubated with anti-murine IL-6, KC, and VEGF	970	189.0
Conditioned medium from osteoblasts grown to 10 days incubated with anti-TGF-$\beta_{1,2,3}$	950	268.6

Table 6.1: Osteoblast conditioned medium was a chemoattractant for MDA-MB-231W human metastatic breast cancer cells. MC3T3-E1 cells were cultured as described in the legend to Figure 3.17. Shown are the average number and standard deviation of human metastatic breast cancer cells per field of view that were chemoattracted to 1) the conditioned medium of osteoblasts that were grown to 10 or 20 days, 2) human IL-6 plus VEGF recombinant protein, 3) the conditioned medium of osteoblasts that were grown to 10 days incubated with anti-murine IL-6, KC, and VEGF, and 4) the conditioned medium of osteoblasts that were grown to 10 days incubated with anti-TGF-$\beta_{1,2,3}$. Three random fields of view were counted per membrane insert, and the counts averaged for the number of MDA-MB-231W human metastatic breast cancer cells that migrated toward the chemoattractant.

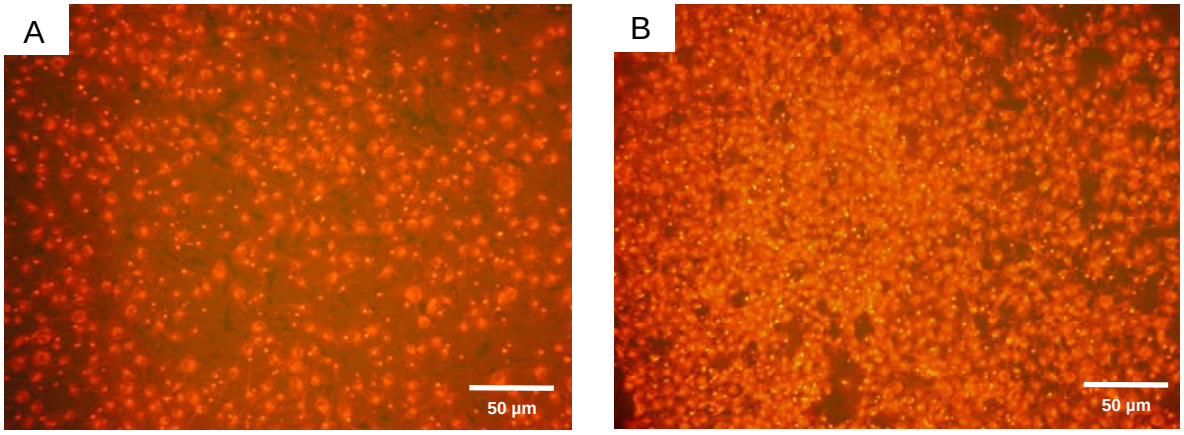

Figure 6.2: A neutralizing antibody to TGF-$\beta_{1,2,3}$ did not alter MDA-MB-231W human metastatic breast cancer cell migration. MDA-MB-231W human metastatic breast cancer cells stained with Vybrant DiI were seeded in the upper chamber of a transwell plate system with treatments as described in the Materials and Methods. Twenty-four hours later, transwell membranes were removed from culture inserts and migrated MDA-MB-231W human metastatic breast cancer cells counted. MDA-MB-231W human metastatic breast cancer cell migration when the cancer cells were subjected to A) conditioned medium that was collected from MC3T3-E1 cells grown to 10 days; and B) conditioned medium that was collected from MC3T3-E1 cells grown to 10 days incubated with 5 µg/ml anti-TGF-$\beta_{1,2,3}$. Each treatment was conducted at least twice. Shown are representative experiments.

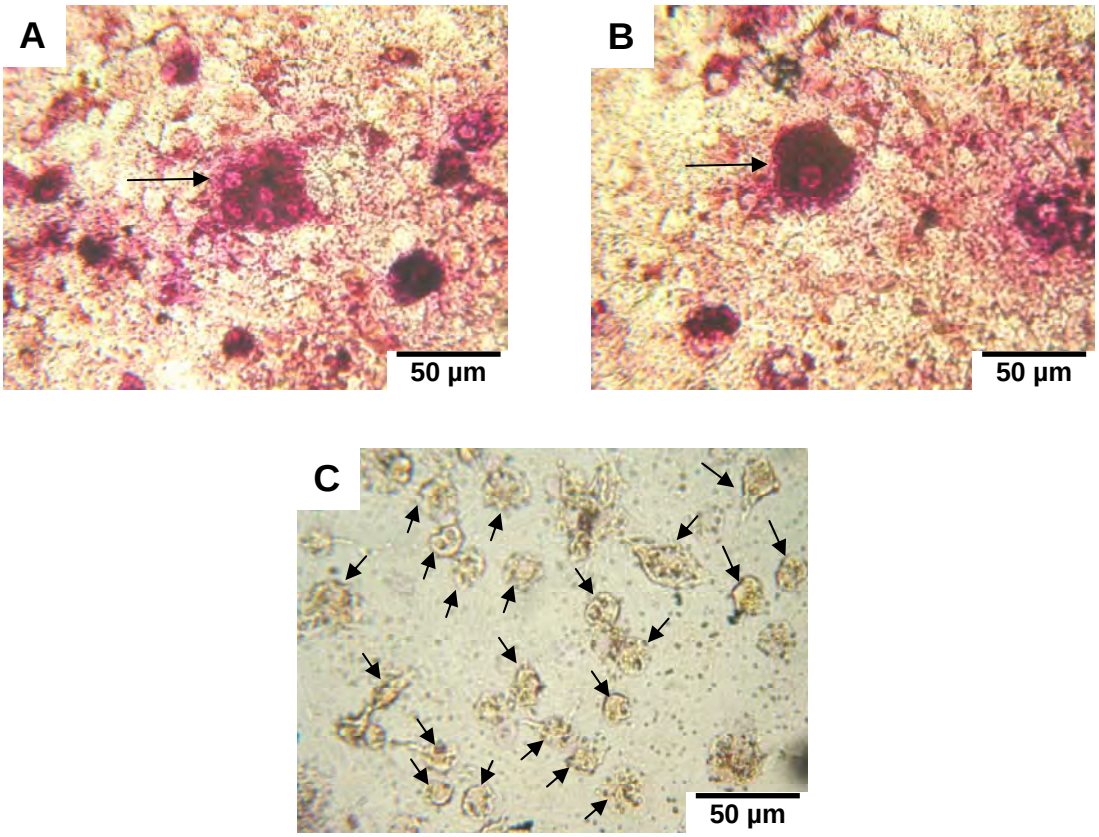

Figure 6.3: Supernatants from osteoblasts cultured with breast cancer cells or their conditioned medium elicited the formation of TRAP positive osteoclasts. Bone marrow monocytes were plated and treated as described in the Materials and Methods. Fourteen days later, osteoclast formation was determined via TRAP stain. A) Multi-nucleated, TRAP positive osteoclast indicated by arrow; B) mono-nucleated, TRAP positive cell indicated by arrow; C) TRAP negative cells indicated by arrows. Three biological replicates were carried out per condition. Shown are representative images.

	Range of TRAP Positive Cell Formation	
Bone Marrow Monocyte Treatment	**TRAP Positive Mono-nucleate**	**TRAP Positive Multi-nucleate**
Growth medium alone	0	0
Positive control (+100 ng/ml M-CSF, +50 ng/ml RANK-L)	7	0
Day 10 OBCM	12-49	0
Day 20 OBCM	0-139	0
MDA-231W BCCM	11-919	0-2
Culture supernatant of 10 day old osteoblasts + MDA-231W CM	78-275	0-4
Culture supernatant of 20 day old osteoblasts + MDA-231W CM	0-364	0
Culture supernatant of 10 day old osteoblasts + MDA-231W cells	0-458	0-2
Culture supernatant of 20 day old osteoblasts + MDA-231W cells	94-377	1-3
+1 ng/ml murine IL-6	0-476	0
+10 ng/ml murine IL-6	0	0
+100 ng/ml murine IL-6	0	0

Table 6.2: Supernatants from osteoblasts cultured with breast cancer cells or their conditioned medium elicited the formation of TRAP positive osteoclasts. Bone marrow monocytes were plated and treated as described in the Materials and Methods. Fourteen days later, osteoclast formation was determined via TRAP stain. Three biological replicates were carried out per condition. Shown are the ranges of TRAP positive cell formation.

	Specific Alkaline Phosphatase Activity (IU/L)	
Condition	Mean	Range
0.4 μm pore MDA-231GFP	3.9	3.4-4.8
0.4 μm pore MDA-231W	3.9	2.0-4.8
3 μm pore MDA-231GFP	3.2	0-7.5
3 μm pore MDA-231W	1.6	0.7-2.0

Table 6.3: Osteoblasts produced alkaline phosphatase when co-cultured indirectly in a transwell system with human metastatic breast cancer cells. MC3T3-E1 cells were grown to 11 days and co-cultured indirectly in a transwell system with MDA-MB-231W or GFP human metastatic breast cancer cells at the manufacturer recommended 1.89×10^4 cells / 33 mm^2 for a 24 well insert. Four days later, the resultant culture supernatants were collected and assayed for alkaline phosphatase enzyme activity. Three biological replicates were carried out per condition. Shown are the means and ranges of specific activity of alkaline phosphatase as measured at 405 nm at 4 minutes.

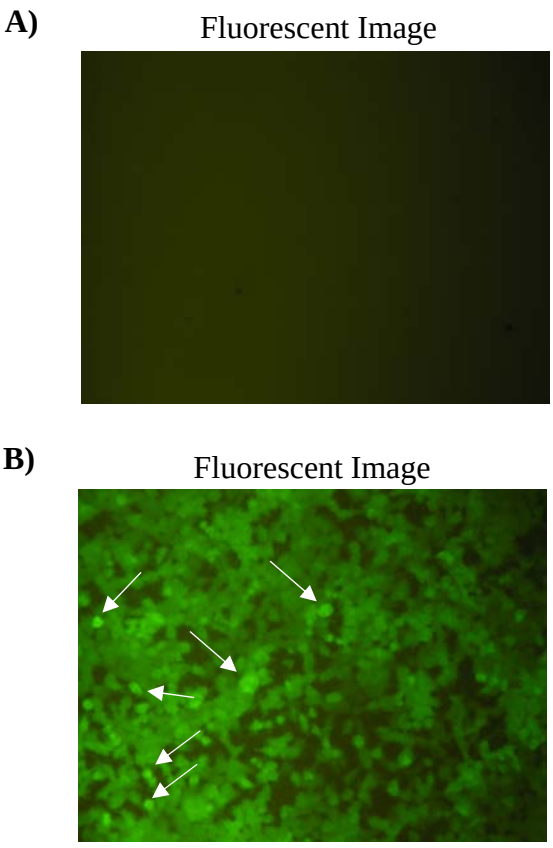

Figure 6.4: Human metastatic breast cancer cells did not migrate to a MC3T3-E1 cell layer after 4 days of indirect co-culture in a transwell system. MC3T3-E1 cells were grown to 11 days and co-cultured indirectly in a transwell system with MDA-MB-231GFP human metastatic breast cancer cells at the manufacturer recommended 1.89×10^4 cells / 33 mm^2 for a 24 well insert. Four days later, the cells were photographed to assess for cancer cell migration. Fluorescent image of A) MC3T3-E1 cells plated on the bottom of a 24 well plate; B) MDA-MB-231GFP human metastatic breast cancer cells in a transwell plate insert with 3 μm pores. These images were taken on an inverted fluorescent microscope (i.e. looking from the bottom up through the plate and insert). GFP-modified breast cancer cells that have migrated through the pores are indicated by arrows in B. Three biological replicates were carried out per condition. Shown are representative images.

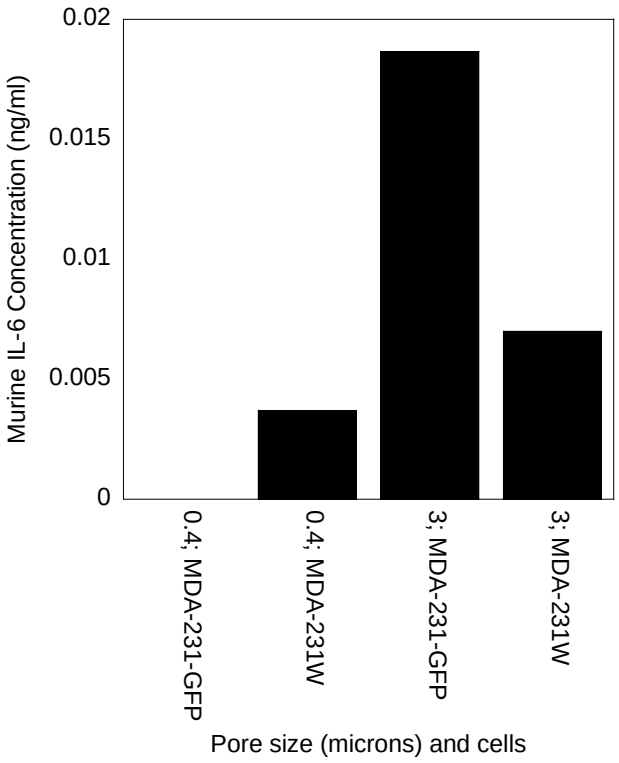

Figure 6.5: Osteoblasts produced IL-6 when co-cultured indirectly in a transwell system with human metastatic breast cancer cells. MC3T3-E1 cells were grown to 11 days and indirectly co-cultured in a transwell system with MDA-MB-231W or GFP human metastatic breast cancer cells at manufacturer recommended 1.89 x 10^4 cells / 33 mm^2 for a 24 well insert. Four days later, the resultant culture supernatants were collected and assayed for IL-6 expression via standard sandwich murine ELISAs. Three biological replicates were carried out per condition. Shown is a representative experiment.

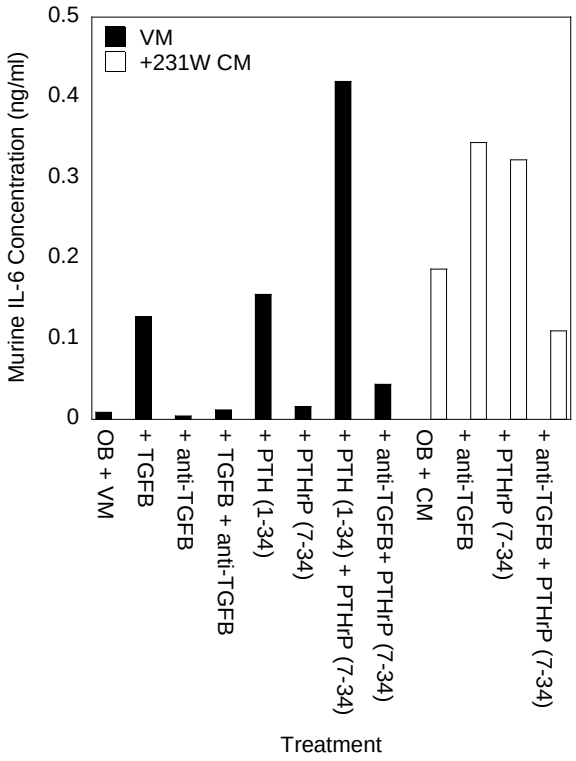

Figure 6.6: Neither PTHrP nor anti-TGF-β effectively block the osteoblast-derived inflammatory stress response elicited by human metastatic breast cancer cells. MC3T3-E1 cells plated at 1 x 10^5 cells/ml in 35 mm dishes were cultured for 16 days with 2% Serum Replacement 3 (Sigma). MC3T3-E1 cells were treated with: 1) VM, 2) CM, 3) 2 ng/ml TGF-β_1, 4) 5 μg/ml anti-TGF-$\beta_{1,2,3}$ ± CM, 5) 2 ng/ml TGF-β_1 + 5 μg/ml anti-TGF-$\beta_{1,2,3}$, 6) 5 x 10^{-9} M PTH (1-34) protein, 7) 5 x 10^{-7} M PTHrP (7-34) (antagonist) ± CM, 8) 5 x 10^{-9} M PTH (1-34) protein + 5 x 10^{-7} M PTHrP (7-34) (antagonist), or 9) 5 μg/ml anti-TGF-$\beta_{1,2,3}$ + 5 x 10^{-7} M PTHrP (7-34) (antagonist) ± CM. When anti-TGF-$\beta_{1,2,3}$ antibody or TGF-β_1 recombinant protein were used, they were incubated with MC3T3-E1 differentiation medium at 37˚C for one hour prior to the addition to cells. PTH (1-34) or PTHrP (7-34) were added to cells for one hour at 37˚C prior to addition of differentiation medium. Resultant culture supernatants were obtained after 24 hours of incubation and assayed via ELISAs for the presence of murine IL-6. Osteoblast vehicle medium treatment is represented by the black bar; MDA-MB-231W conditioned medium treatment, white bar. Three biological replicates were carried out per condition. Shown is a representative experiment.

Cytokine	Receptor Present on Cancer Cells	Maintenance Factor for Cancer Cells	Osteoclasto-genesis
IL-6 (IL-6R)	[7, 196, 198]	[196]	[7, 200]
IL-8/MIP-2 (CXCR1/2)	[7, 197, 198]	[57]	[7, 61]
GRO-α/KC (CXCR1/2)	[197, 198]	unknown (binds to the same receptor as IL-8/MIP-2	unknown (binds to the same receptor as IL-8/MIP-2
VEGF (VEGFR1/Flt VEGFR2/KDR VEGFR3/NRP1)	[142, 147, 199, 201]	[147, 201-203]	[204, 205]
MCP-1 (CCR2)	[7, 197, 198]	unknown	[206]

Table 9.1: Roles of osteoblast-derived cytokines in bone metastatic breast cancer.

References are given in brackets ([]).

Cytokine	Metaphyses without Bone Marrow	Diaphyses without Bone Marrow	Metaphyses Plus Bone Marrow	Bone Marrow from Metaphyses
MIP-2	+++	+	+++	0
MCP-1	+++	+	+++	0
KC	+++	0	+++	0

+++ = strongly expressed cytokine, + = faintly expressed cytokine, 0 = no cytokine detected.

Table 9.2: Inflammatory cytokines detected in cultures from murine femurs.
Murine femurs from non-cancer-bearing athymic mice were harvested and fractionated into metaphyses, diaphyses, or bone flushed free of bone marrow. The isolated metasphyseal or diaphyseal bone pieces were crushed and cultured. Marrow was also cultured. Media were collected and tested after 24 hours. Expression levels indicate relative cytokine expression as opposed to quantity.

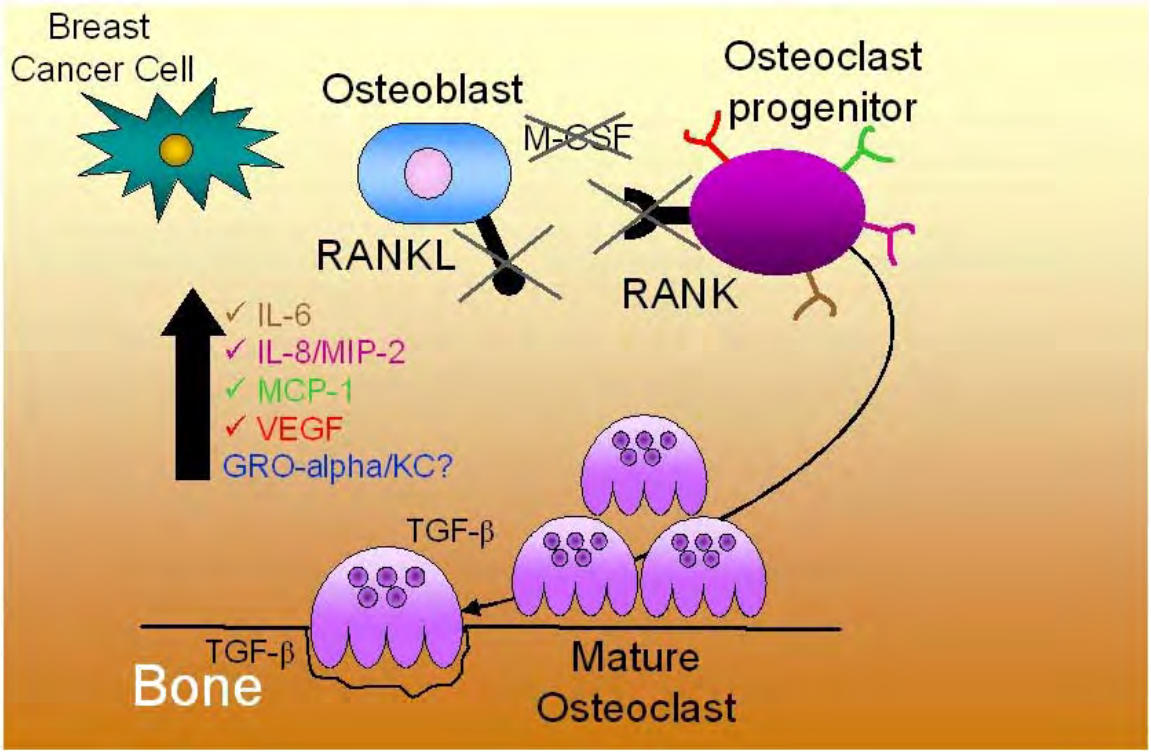

Figure 9.1: Proposed model of cytokine involvement in bone metastatic breast cancer. Osteoblast-derived IL-6, KC, MCP-1, MIP-2, and VEGF are produced during normal bone remodeling in the metaphyseal region of long bones. Metastatic breast cancer cells are attracted to the bone microenvironment through a yet unidentified chemoattractant. Breast cancer cell arrival in the bone induces osteoblasts to increase their production of inflammatory cytokines, leading to increased osteoclastogenesis and bone resorption independent of the RANK-RANKL pathway (crosses). Additional breast cancer maintenance factors, such as TGF-β, are released from bone, further facilitating breast cancer cell colonization and survival.

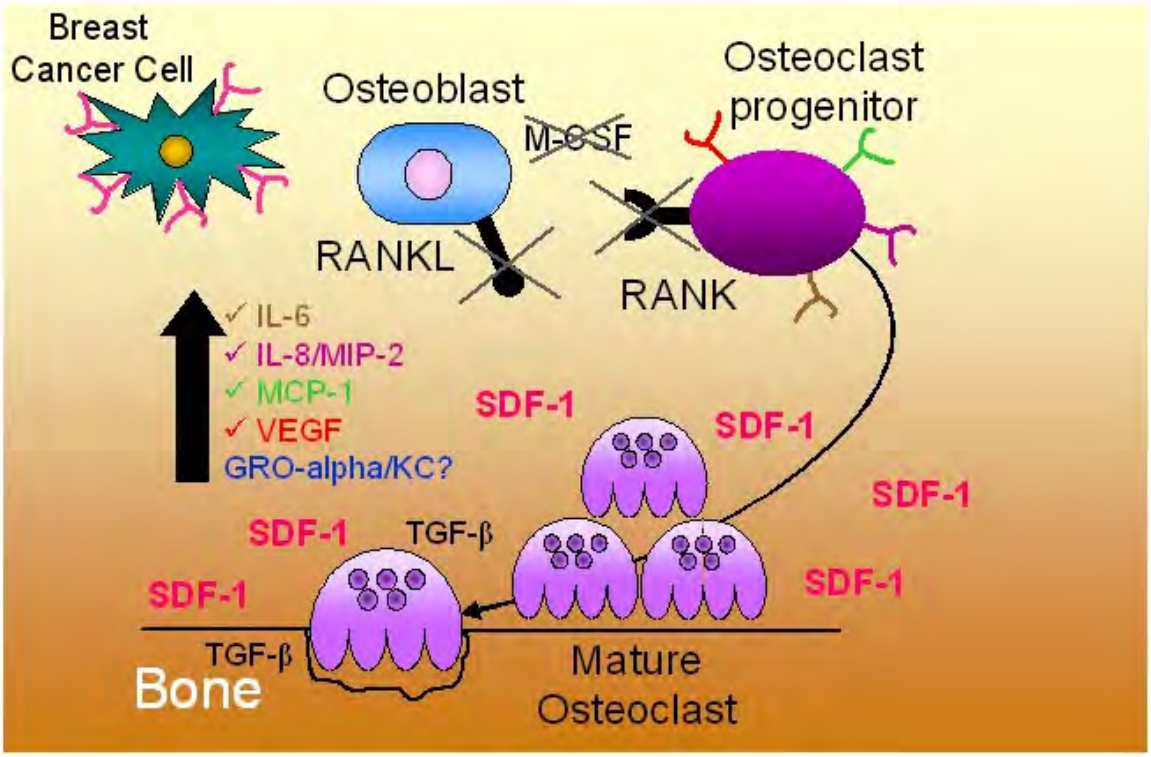

Figure 9.2: Proposed model of breast cancer metastases to the bone. Osteoblast-derived IL-6, KC, MCP-1, MIP-2, and VEGF are produced during normal bone remodeling. Metastatic breast cancer cells that bear the CXCR4 receptor are attracted to SDF-1 present in the bone microenvironment. Breast cancer cell arrival in the bone induces osteoblasts to increase their production of inflammatory cytokines, leading to increased osteoclastogenesis and bone resorption, independent of the RANK-RANKL pathway (crosses). Additional breast cancer maintenance factors, such as TGF-β, are released from bone, further facilitating breast cancer cell colonization and survival.

Part 12: APPENDICES

1) Publication: Phadke, PA, Mercer, RR, Harms JF, Jia, Y, Kappes, JC, Frost, AR, Jewell, JL, **Bussard, KM,** Nelson, S, Moore, C, Gay, CV, Mastro, AM, Welch, DR. "Kinetics of Metastatic Breast Cancer Cell Trafficking in Bone." Clinical Cancer Research. 12: (5) 1431. 2006.

2) Publication: Kinder, M, Chislock, EM, **Bussard, KM**, Shuman, LA, Mastro, AM. Metastatic Breast Cancer Induces an Osteoblast Inflammatory Response. Experimental Cell Research. 314: (1), 173. 2008.

3) Publication: **Bussard, KM**, Gay, CV, Mastro, AM. The Microenvironment in Metastasis: What is Special About Bone? Cancer Metastasis Reviews. 27: (1), 41. 2008.

4) Abstract: **Bussard, KM,** Shuman, LS, Mercer, RR, Phadke, PA, Nelson, SM, Jewell, JL, Chislock, EM, Kinder, M, Welch, DR, Gay, CV, Mastro, AM. "The Interaction of Metastatic Breast Cancer Cells with Osteoblasts." Presented at the CrossOver 2005 Meeting sponsored by The Huck Institutes of The Life Sciences and The Materials Research Institute, The Pennsylvania State University, October 13-14, 2005.

5) Abstract: **Bussard, KM,** Phadke, PA, Mercer, RR, Harms JF, Jia, Y, Kappes, JC, Frost, AR, Jewell, JL, Nelson, S, Moore, C, Gay, CV, Mastro, AM, Welch, DR. "Kinetics of Metastatic Breast Cancer Cell Trafficking in Bone." Presented at the American Association for Cancer Research Annual Meeting's Tumor Biology Minisymposium, April 1-5, 2006.

6) Abstract: **Bussard, KM,** Chislock, EM, Kinder, M, Gay, CV, Mastro, AM. "A Classic Set of Osteoblast-Derived Inflammatory Cytokines is Produced in Response to Bone Metastatic Breast Cancer." The 11 th International Congress of the Metastasis Research Society, Tokushima, Japan, September 3-6, 2006.

7) Abstract: **Bussard, KM**, Mastro, AM. "Osteoblast-derived Inflammatory Cytokines are Produced in Response to Human Metastatic Breast Cancer Cells." The 100th Annual American Association for Cancer Research Annual Meeting, Los Angeles, CA, April 14-18, 2007. Proceedings of the 97th Annual Meeting for American Association for Cancer Research, Volume 48.

8) Abstract: **Bussard, KM**, Mastro, AM. "Osteoblasts Naturally Produce Cytokines that Influence the Tumor Microenvironment in Bone Metastatic Breast Cancer." Skeletal Complications of Malignancy V, The Paget Foundation. October 25-27, 2007.

9) Abstract: **Bussard, KM**, Mastro, AM. "Osteoblast-Derived Cytokines are Major Mediators in Facilitating Bone Metastatic Breast Cancer." Presented at the American Association for Cancer Research Annual Meeting's Tumor Biology Minisymposium, April 12-16, 2008.

10) Abstract: **Bussard, KM**, Mastro, AM. "The Role of Osteoblast-Derived Cytokines in Bone Metastatic Breast Cancer." Era of Hope Meeting, Baltimore, MD, June 25-28, 2008.

11) K Bussard, Curriculum Vitae.

Kinetics of Metastatic Breast Cancer Cell Trafficking in Bone

Pushkar A. Phadke,[1] Robyn R. Mercer,[6] John F. Harms,[1] Yujiang Jia,[2] Andra R. Frost,[1,3,5] Jennifer L. Jewell,[6] Karen M. Bussard,[6] Shakira Nelson,[6] Cynthia Moore,[1] John C. Kappes,[2] Carol V. Gay,[6] Andrea M. Mastro,[5,6] and Danny R. Welch[1,3,4,5]

Abstract

Purpose: *In vivo* studies have focused on the latter stages of the bone metastatic process (osteolysis), whereas little is known about earlier events, e.g., arrival, localization, and initial colonization. Defining these initial steps may potentially identify the critical points susceptible to therapeutic intervention.

Experimental Design: MDA-MB-435 human breast cancer cells engineered with green fluorescent protein were injected into the cardiac left ventricle of athymic mice. Femurs were analyzed by fluorescence microscopy, immunohistochemistry, real-time PCR, flow cytometry, and histomorphometry at times ranging from 1 hour to 6 weeks.

Results: Single cells were found in distal metaphyses at 1 hour postinjection and remained as single cells up to 72 hours. Diaphyseal arrest occurred rarely and few cells remained there after 24 hours. At 1 week, numerous foci (2-10 cells) were observed, mostly adjacent to osteoblast-like cells. By 2 weeks, fewer but larger foci ($\geq$50 cells) were seen. Most bones had a single large mass at 4 weeks (originating from a colony or coalescing foci) which extended into the diaphysis by 4 to 6 weeks. Little change ($<$20%) in osteoblast or osteoclast numbers was observed at 2 weeks, but at 4 to 6 weeks, osteoblasts were dramatically reduced (8% of control), whereas osteoclasts were reduced modestly (to $\sim$60% of control).

Conclusions: Early arrest in metaphysis and minimal retention in diaphysis highlight the importance of the local milieu in determining metastatic potential. These results extend the Seed and Soil hypothesis by demonstrating both intertissue and intratissue differences governing metastatic location. Ours is the first *in vivo* evidence that tumor cells influence not only osteoclasts, as widely believed, but also eliminate functional osteoblasts, thereby restructuring the bone microenvironment to favor osteolysis. The data may also explain why patients receiving bisphosphonates fail to heal bone despite inhibiting resorption, implying that concurrent strategies that restore osteoblast function are needed to effectively treat osteolytic bone metastases.

Authors' Affiliations: Departments of [1]Pathology and [2]Medicine-Hematology/Oncology, [3]Comprehensive Cancer Center, [4]Center for Metabolic Bone Disease, [5]National Foundation for Cancer Research, Center for Metastasis Research, University of Alabama at Birmingham, Birmingham, Alabama, and [6]Department of Biochemistry and Molecular Biology, Pennsylvania State University, University Park, Pennsylvania

Received 8/19/05; revised 11/1/05; accepted 12/15/05.

Grant support: U.S. Army Medical Research and Materiel Command (DAMD-17-02-1-0541, DAMD-17-03-01-0584, and DAMD 17-02-1-0358) and the University of Alabama at Birmingham Breast Specialized Programs of Research Excellence (P50-CA89019). Additional support was provided by CA87728, the National Foundation for Cancer Research, Center for Metastasis Research, and the Pennsylvania Department of Health Breast Cancer Program.

The costs of publication of this article were defrayed in part by the payment of page charges. This article must therefore be hereby marked *advertisement* in accordance with 18 U.S.C. Section 1734 solely to indicate this fact.

Note: P.A. Phadke and R.R. Mercer contributed equally to this work.

This work was submitted in partial fulfillment of the requirements for the University of Alabama at Birmingham Graduate Program in Molecular and Cellular Pathology (P.A. Phadke) and Penn State Graduate Program in Biochemistry and Molecular Biology (R.R. Mercer).

Requests for reprints: Danny R. Welch, Department of Pathology, University of Alabama at Birmingham, Volker Hall G-019A, 1670 University Boulevard, Birmingham, AL 35294-0019. Phone: 205-934-2961; Fax: 205-975-1126; E-mail: DanWelch@uab.edu.

doi:10.1158/1078-0432.CCR-05-1806

Breast cancer has a remarkable predilection to colonize bone, with an incidence between 70% and 85% in patients (1–3). At the time of death, metastatic bone disease accounts for the bulk of tumor burden (4). For women with bone metastases, the complications—severe, often intractable pain, pathologic fractures, and hypercalcemia—are catastrophic. Despite its obvious clinical importance, very little is understood about the fundamental mechanisms responsible for breast cancer metastasis to bone. Research progress has been hampered by the dearth of, and technical difficulties inherent in, the current models.

Most models of metastasis poorly recapitulate the pathogenesis of breast cancer. The ideal model would involve dissemination from an orthotopic site (i.e., mammary fat pad), colonization, and osteolysis. None of the currently available human breast xenograft models spread to bone following orthotopic implantation and only one murine model metastasizes to bone from the mammary fat pad (5). Furthermore, most human cell lines do not metastasize to bone in mice regardless of route of injection. The most commonly used model of breast cancer metastasis to bone involves injection of tumor cells into the arterial circulation via the left ventricle of the heart (4, 6–8). This route of injection minimizes first-pass filtration through pulmonary capillaries, thereby allowing more cells to reach the bone.

Current methods to detect bone metastases are insufficiently sensitive (e.g., radiography) or are impractical for adequately statistically powered experiments because of costs or labor-intensiveness. Radiography can detect osteolytic lesions only after more than half of the calcified bone matrix has been degraded (9). Microcomputerized tomography is not widely available, but is likewise of insufficient resolution to recognize single tumor cells. Serial sectioning (which would be required to locate rare single cells) is cost-prohibitive, except for small studies. As a result, experiments have been limited to late events of metastatic bone disease, such as osteolysis. Therefore, antecedent events (i.e., arrival, lodging, intraosseous trafficking, and colonization) have not been studied except by inference.

To overcome some of the technical limitations, more sensitive methods using reporter molecules, such as luciferase (10) or β-galactosidase (LacZ) have recently been described (11–13). Luciferase, although it allows for *in situ* detection of tumor cells in the bone, does not allow for microscopic localization of the cells. Because luminescence depends on a fully viable cell, use of luciferase is limited *ex vivo*. β-Galactosidase is excellent for studies at the histologic level but cannot be used for studies involving intact bone unless the lesions are macroscopic. Diffusion or distribution of substrate into bone is also a complication.

Fluorescent molecules, like enhanced green fluorescent protein (GFP), have also been employed with some success in the early detection of bone metastasis (14–16). We recently used the GFP-tagged MDA-MB-435 metastatic human breast cancer cell line to reveal formation of osteolytic bone lesions following intracardiac injection in athymic mice (15). Like luciferase, GFP can be used to detect lesions *in situ*, even though the limits of detection are restrictive (~0.5-1 mm). During experiments designed for other purposes, we detected single tumor cells in bone within minutes postinjection. Because to the best of our knowledge, no one had ever systematically studied the earliest tumor cell-bone interactions (except by serendipitous histologic sections), we decided to use the power of GFP to begin addressing the early events associated with breast tumor cells that have already disseminated to bone.

It has long been recognized that, once cells arrive in the bone, they alter homeostasis. Turnover of the skeleton is dynamic and continuous throughout embryonic development and adulthood. Calcified bone matrix turns over completely, on average, every decade (17, 18). Calcified matrix remodeling involves an interplay between osteoblasts (bone forming cells) and osteoclasts (bone resorbing cells). Altering the balance of activities results either in excessive bone deposition (osteopetrosis) or bone loss (osteoporosis). Although larger individual bone lesions contain regions that are both osteopetrotic and osteoporotic, most breast cancer bone metastases are not osteolytic. The current paradigm suggests that tumor cells influence osteoclast activity (4, 19). Using the GFP model of breast cancer metastasis to bone, we sought to identify key tumor cell–bone cell interactions (and the timing of those interactions) that occur during the pathogenesis of bone metastasis.

Materials and Methods

Cell lines and culture. Metastatic human breast carcinoma cell line, MDA-MB-435 (MDA-435), a generous gift from Dr. Janet Price (University of Texas M.D. Anderson Cancer Center, Houston, TX), was stably transfected with pEGFP-N1 (BD Biosciences Clontech, Palo Alto, CA) by electroporation (Bio-Rad Model GenePulser, Hercules, CA; 220 V, 960 μ Fd, $\infty\Omega$) or transduced with a HIV type 1-based, lentiviral vector system constitutively expressing enhanced GFP (20, 21). For the lentivirus, the GFP coding sequence was inserted into the vector 5′ of the internal ribosome entry site and puromycin sequences, each of which were under control of the early cytomegalovirus promoter. Infectious stock were prepared by transfection of 293T cells and used at a multiplicity of infection of ~10.

The origin of MDA-MB-435 has been questioned because the cells express melanoma-associated genes in cDNA microarray experiments. However, the patient was reported only to have a breast carcinoma. Because MDA-MB-435 cells express milk proteins (22), it is most simple to conclude that the cells are poorly differentiated breast carcinoma.

Parental cells were cultured in a mixture (1:1 vol/vol) of DMEM and Ham's F12 media (DMEM/F12; Invitrogen, Carlsbad, CA) supplemented with 2 mmol/L L-glutamine, 1 mmol/L sodium pyruvate, 0.02 mmol/L nonessential amino acids, 5% fetal bovine serum (Atlanta Biologicals, Norcross, GA), without antibiotics or antimycotics (cDME/F12). All cultures were confirmed to be negative for *Mycoplasma* spp. infection using a PCR-based test (TaKaRa, Shiga, Japan).

GFP-expressing cells were grown in cDME/F12 plus G418 (Geneticin, 500 μg/mL, Invitrogen) or puromycin (500 μg/mL, Fisher Scientific, Hampton, NH). The brightest 15% (lentiviral) or 25% (pEGFP) fluorescing cells were sorted using either Coulter EPICS V cell sorter (Beckman-Coulter, Fullerton, CA) or a BD FACSaria cell sorter (BD Biosciences Immunocytometry Systems, San Jose, CA).

Intracardiac injections. Cells at 80% to 90% confluency were detached using a mixture of 0.5 mmol/L EDTA and 0.05% trypsin in Ca^{+2}-, Mg^{+2}-, and $NaHCO_3$-free HBSS. Viable cells were counted using a hemacytometer and resuspended at a final concentration of 1.5×10^6 cells/mL in ice-cold HBSS. Cells were not used unless viability was >95%, but was usually >98%. Female athymic mice ages between 4 and 6 weeks (Harlan Sprague-Dawley, Indianapolis, IN) were anesthetized by i.m. administration of a mixture of ketamine-HCl (129 mg/kg), and xylazine (4 mg/kg). Cells (3×10^5 in 0.2 mL) were injected into the left ventricle of the heart between the third and fourth or between the fourth and fifth intracostal space. The presence of bright red, as opposed to burgundy, colored blood prior to and at the end of each inoculation confirmed injection of the entire volume into the arterial system. Mice were necropsied at 1, 2, 4, 8, 24, 48, and 72 hours and 1, 2, 4, and 6 weeks postinoculation following anesthesia with ketamine/xylazine and euthanasia by cervical dislocation. At least two independent experiments were done with 5 to 12 mice per experimental group. Not all time points were collected for every experiment.

Although widespread skeletal metastases develop after intracardiac injection (15, 23), the experiments reported here focused exclusively on the femur, a common site for metastasis that is easily accessible. The femurs were removed and examined by low magnification (×2-10) fluorescence stereomicroscopy and histologic and histomorphometric analyses (24, 25). Some femurs were divided into proximal and distal metaphyses plus cortical shaft (diaphysis) from which the marrow was collected and cells examined by flow cytometry or quantitative real-time PCR. Corroborating experiments were done with the contralateral femur to assure that there was no bias for sidedness.

Mice were maintained under the guidelines of the NIH, the University of Alabama at Birmingham, and the Pennsylvania State University. All protocols were approved and monitored by the appropriate Institutional Animal Care and Use Committees.

Fluorescence microscopy. To visualize metastases derived from the GFP-tagged cell lines, whole femurs (dissected free of soft tissue using a no. 11 scalpel blade with gauze used to grip and remove tissue remnants) were placed into Petri dishes containing ice-cold Ca^{+2}- and Mg^{+2}-free Dulbecco's PBS and examined by fluorescence microscopy using a Leica MZFLIII dissecting microscope with ×0.5 objective and

GFP fluorescence filters ($\lambda_{excitation}$ = 480 ± 20 nm; $\lambda_{emission}$, 510 nm barrier; Leica, Deerfield, IL). Photomicrographs were collected using a MagnaFire digital camera (Optronics, Goleta, CA), and ImagePro Plus 5.1 software (Media Cybernetics, Silver Spring, MD).

Bone fixation and storage. Intact, dissected femurs from individual mice were placed in 25 mL glass scintillation vials and fixed in freshly prepared 4% paraformaldehyde in Ca^{+2}- and Mg^{+2}-free Dulbecco's PBS or in periodate-lysine-paraformaldehyde solution (26) at 4°C for 24 to 48 hours. GFP fluorescence was difficult to maintain in fixed tissues and bone sections; however, we were able to overcome this limitation by maintaining the samples at 4°C (27). Bones destined for histologic sectioning were subsequently removed and decalcified in 0.5 mol/L EDTA in Ca^{+2}- and Mg^{+2}-free Dulbecco's PBS.

Bone histomorphometry. Bones were dehydrated in increasing concentrations of ethanol and embedded in a mixture of 80:20 methyl methacrylate and dibutylphthalate. Serial coronal sections (5 μm) were obtained using a Leica 2265 microtome. The distal ends of femurs (spongiosa) were analyzed. Sections were first stained with Sanderson's rapid bone stain for 2 minutes. Once tumor cells were identified, subsequent sections were stained with Goldner's trichrome and tartrate-resistant acid phosphatase (TRAP). Histomorphometry was done at the University of Alabama at Birmingham Center for Metabolic Bone Disease Histomorphometry and Molecular Analysis Core Facility by the method of Parfitt et al. (24, 25) using Bioquant image analysis software (R&M Biometrics, Nashville, TN).

Immunohistochemistry. Paraffin-embedded samples were sectioned (5 μm, coronal or sagittal), deparaffinized, and rehydrated before antigen retrieval by microwaving for ~8 minutes at full power (700 W) in a 10 mmol/L citrate buffer (pH 6). Samples were boiled for 5 minutes in the microwave oven. Endogenous peroxidase activity was blocked by treatment with 3% hydrogen peroxide for 5 minutes. Sections were blocked with 1% goat serum for 1 hour. Slides were incubated with primary rabbit polyclonal anti-GFP IgG (1:250; Molecular Probes, Eugene, OR) for 1 hour, followed by secondary biotinylated anti-rabbit antibody (TITRE; Level 2 Ultra Streptavidin Detection System, Signet Labs, Dedham, MA). Detection was achieved using Biogenex liquid DAB kit (Biogenex, San Ramon, CA) and slides were counterstained using hematoxylin. GFP-positive tumor samples served as positive controls. Negative controls were done by omitting the primary antibody.

Some femurs were fixed in a solution of 2% paraformaldehyde containing 0.075 mol/L lysine and 0.01 mol/L sodium periodate (pH 7.4), 4°C for 24 hours in an attempt to maintain alkaline phosphatase activity (26). Although the alkaline phosphatase activity was not well preserved, fluorescence was maintained; fluorescent MDA-435^{GFP} cells could be observed in femurs taken throughout the time course. Following decalcification as described above, the bones were embedded in paraffin. Paraffin-embedded bones were sectioned lengthwise into 10 μm sections and several sections throughout the bone were analyzed. The sections were deparaffinized, rehydrated, and stained for apoptotic cells with a modified terminal nucleotidyl transferase–mediated nick end labeling (TUNEL) procedure using Cy-5 rather than FITC-labeled dUTP (28). Bone sections were first scanned at ×20 magnification using a fluorescence confocal microscope. Areas in which GFP-positive cells were detected were further analyzed at ×40 magnification with both fluorescence and phase microscopy. Fluorescent images were captured at two wavelengths $\lambda_{excitation}$ = 480 ± 20 nm ($\lambda_{emission}$, 520 nm for GFP) and $\lambda_{excitation}$ = 647 nm ($\lambda_{emission}$, 670 nm for Cy-5). A comparison of the numbers of breast cancer cells detected by fluorescence microscopy versus use of anti-GFP gave essentially the same trends (data not shown).

TRAP-positive cells were determined in the femurs of mice at various times following inoculation with metastatic breast cancer cells. Two to eight sections from two to four bones per time period were stained for the presence of TRAP by immunohistochemistry (Sigma-Aldrich, St. Louis, MO). After staining, the sections were viewed with a fluorescent light microscope at ×20 magnification. Three images (1,349 pixels/500 μm) from the distal end and three images from the proximal end were collected and converted into JPEG format. The number of TRAP-positive cells was counted in each image. The Image J program (NIH) was used to calculate the bone area in each field.

Some decalcified femurs were cryosectioned and stained for alkaline phosphatase activity (Sigma-Aldrich). The sections were examined with a light microscope, the images digitally collected, and analyzed for the amount of alkaline phosphatase stain per area of bone at the growth plate and in the trabecular region. The data were calculated as ratio of the mm^2 of the alkaline phosphatase stain to mm^2 of bone.

Flow cytometric and DNA analysis. Femurs were removed from five to six mice at each time and cut into the distal and proximal metaphyses and the diaphysis. Bone marrow was flushed from these regions with a 1 mL tuberculin syringe fitted with a 26-gauge needle. The marrow in the center of the diaphysis was collected separately from the endosteal marrow close to the cortical bone as previously described (29). For flow cytometry, the RBC were lysed with ACK solution (15 mmol/L NH_4Cl, 1 mmol/L $KHCO_3$, 0.1 mmol/L Na_2 EDTA) and the remaining cells were fixed with 2% paraformaldehyde. Samples were stored at 4°C until they were analyzed by flow cytometry (Coulter XL-MCL) using standardized fluorescent beads (10 μm; Sphero AccuCount Rainbow Fluorescent particles, Spherotech, Libertyville, IL) to estimate the total number of cancer cells present. Standard curves were also generated by adding known numbers of MDA-MB-435 cells to mouse bone marrow cells. The samples of the mixtures of cells were prepared in the same way as the experimental samples. A background value of 200 cells was determined from the data obtained from the control animals in which no GFP-positive cells were present.

For DNA analysis, marrow was centrifuged and frozen in Ca^{+2}- and Mg^{+2}-free Dulbecco's PBS. At a later time, DNA was prepared from the samples with a DNeasy kit (Qiagen, Valencia, CA). The DNA was subjected to quantitative real-time PCR (Nucleic Acid Facility, Penn State, University Park, PA) using primers to detect the *HERVK* gene (human endogenous retrovirus, group K), a gene found in the human but not in the mouse genome (30). To establish a standard curve, MDA-435^{GFP} cells were counted, diluted, and added to preparations of mouse bone marrow cells. DNA was isolated from these samples and treated as the experimental samples for PCR. Although one cell could be detected in the standard curve samples, a more conservative cutoff of 150 cells was used due to practical considerations, i.e., cell extract volumes and variations in the amount of mouse DNA present in each sample.

Statistics. Each series of injections involved between 5 and 15 mice per experimental group or time. Femurs were apportioned for various subsequent analyses. Comparisons between groups were done by one-way ANOVA with Student-Neumann-Kuels or Tukey's post-tests. Statistical significance was defined as a probability $P \leq 0.05$.

Results

Kinetics of MDA-435^{GFP} tumor cells trafficking in the bone. Numerous solitary fluorescent cells could be visualized in the intact bone (i.e., the bone is not cut, but has been stripped of surrounding muscle) 1 hour following intracardiac injection using fluorescence microscopy (Fig. 1A1). The majority (>90%) of cells were found in the metaphyseal regions, not in the diaphysis, by fluorescence. Routine identification of single tumor cells using H&E stain, although possible, proved difficult. Even with evidence that tumor cells were present in the bone (i.e., by fluorescence), we could not always unambiguously identify single tumor cells in histologic sections stained by H&E.

To facilitate detection of solitary tumor cells by histology and to determine their positions within the trabeculae, cellular

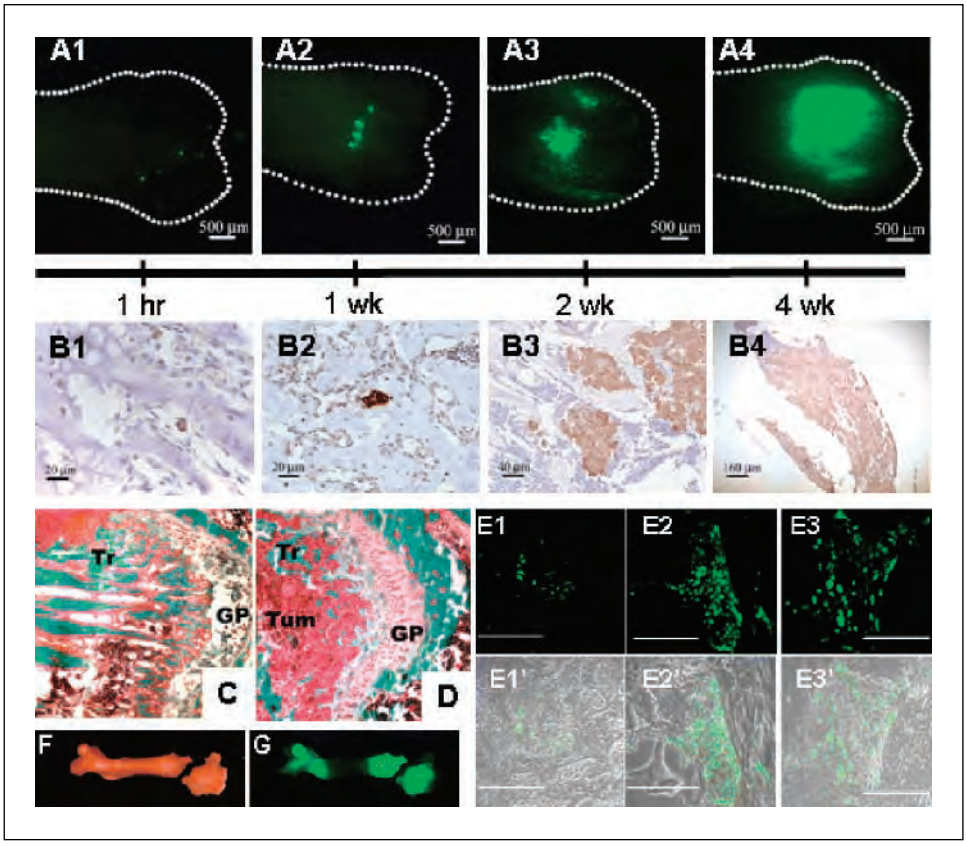

Fig. 1. The kinetics of MDA-435^{GFP} metastatic growth in the femur following intracardiac injection. Whole femurs were dissected and fluorescent foci were visualized in the intact bones using a fluorescent stereomicroscope. *A,* fluorescent foci were observed, mainly in the distal end of femurs, as shown at 1 hour (*A1*), 1 week (*A2*), 2 weeks (*A3*), and 4 weeks (*A4*). *B,* MDA-435^{GFP} cells were detected by anti-GFP immunohistochemistry (*brown staining cells*) in femurs at 1 hour (*B1*, single cell), 1 week (*B2*, clusters of two to three cells), 2 weeks (*B3*), and 4 weeks (*B4*). With time, the number of fluorescent foci decreased as the size increased. Independent tumor deposits often coalesced. *C* and *D,* representative images of distal ends of femur stained with Goldner's trichrome stain (*C,* normal bone; *D,* 4 weeks). The amount of trabecular bone (*Tr*, stained teal) is significantly lower in bone containing tumor cells, reflective of osteolytic degradation. Tumor cells (*Tum*) infiltrating the metaphyseal area near epiphyseal growth plate (*GP*) are labeled for reference. *E,* fluorescent tumor cell foci in trabecular bone in paraffin-embedded sections at 2 weeks (*E1*), 4 weeks (*E2*), and 6 weeks (*E3*) postinjection. Magnification line indicates 100 μm. E1′, E2′, and E3′ are composites of fluorescent and phase images. Representative bright field (*F*) and fluorescent (*G*) images of a mouse femur at 4 weeks show two large metastatic foci, one at each end. The distal end shows an iatrogenic fracture, presumably due to weakness caused by tumor cell – induced osteolysis.

location was estimated in two dimensions using fluorescence. Then, serial histologic sections were cut from the regions exhibiting fluorescence. Although this manipulation increased the odds of finding sections containing single cells, it was not always possible to detect cells in every 5 to 10 μm section stained using anti-GFP antisera. Nonetheless, as implied by the fluorescence data, most tumor cells were located in the primary spongiosa of the metaphysis of the distal femur (Fig. 1B and E). Although fluorescent cells were not frequently detected in the femoral head at 1 hour postinjection, some GFP-positive cells were detected by immunohistochemistry (data not shown). There was no evidence of unusual inflammation or immune cell infiltration at the sites of tumor cell arrest or colonization.

In a third, parallel approach, we detected cells without visualization constraints or sampling errors associated with sectioning, instead quantifying tumor cells in various marrow compartments using flow cytometry or real-time PCR. Separation of the marrow from metaphyses and diaphysis followed by flow cytometry or real-time PCR to detect MDA-435^{GFP} cells revealed a slightly different pattern of tumor cell distribution within the bone at the early times, but an entirely consistent pattern of distribution at the later times (Fig. 2). These methods were limited because precise separation of the diaphysis from the metaphysis was not consistent. Therefore, cancer cells at the interface between bone regions could not be localized with certainty. Histologic sections confirmed precise localization (Fig. 1). As a whole, the various methods to assess localization were largely confirmatory. In addition, we also determined that cancer cells in the diaphysis were mostly located next to the endosteal bone rather than in the marrow in the center of the shaft. By 4 to 6 weeks, >95% of tumor cells were found in the endosteal marrow (Fig. 5).

Of the 3×10^5 cells injected per mouse, a small fraction were detectable in the femurs (Table 1), as expected, because cells are distributed throughout the body following injection into the arterial circulation. Flow cytometry and real-time PCR were used to quantify the number of cells present. Cells were flushed from the marrow space in the metaphyseal and diaphyseal regions and examined by flow cytometry to detect GFP-tagged cells (Fig. 2). In addition, DNA isolated from the bone marrow was analyzed for the presence of human DNA by real-time PCR using a human-specific primer/probe set (Fig. 2). Regardless of the method, seeding of the femurs with breast cancer cells was rare (44 ± 6 cells; 0.01% per femur; Table 1). As a result, the absolute numbers were highly variable between mice and between techniques. Thus, the total number of single cells identified was not sufficient to perform statistical analyses with adequate power. Nonetheless, we did observe several consistent changes. First, solitary cells in the diaphysis were seldom detected beyond 24 hours in any of the mice, until metaphyseal lesions had apparently extended into the diaphyses at later times (Figs. 1G and 2). Second, the number of fluorescent foci (i.e., cell masses) detected by fluorescent stereomicroscopy decreased progressively beginning from 1 to 72 hours. This result is consistent with the clearance of disseminated tumor cells from other organs (31, 32). Third, single cells persisted in the femur for up to 72 hours. In general, evidence of cell division prior to 72 hours postinoculation was infrequent.

Whereas initial proliferation of arrested cells was delayed, distinct metastatic foci (5 ± 1) were easily detected by fluorescence microscopy of the intact bone (Fig. 1A2) as well as immunohistochemistry in the femur at 1 week (Fig. 1B2) and fluorescence microscopy of bone sections (Fig. 1E). Most of the foci were small and consisted of <10 cells (i.e., only three to four cell divisions). Although most metastatic lesions were localized at the distal end, a fraction of the bones had fluorescent foci growing at the proximal ends as well.

By 2 weeks, larger but fewer foci (2.8 ± 0.5) were detected at the distal end (Fig. 1A3 and B3). The foci were comprised of clusters of ~50 cells. These progressively increased in size and decreased in number to an average of one metastatic focus at 4 weeks, presumably by coalescence (Fig. 1A4, B4, and G). By 6 weeks, tumor cells directly extended into the diaphysis, and in some cases, the whole medullary canal was occupied by tumor. Histomorphometry of the lesions revealed loss of most trabecular bone by 4 to 6 weeks (compare Fig. 1D and Fig. 1C).

Tumor cell modification of the bone microenvironment. Histomorphometric analysis further showed specific modification of the microenvironment when tumor cells were present (Fig. 3). We had previously shown that MDA-435^{GFP} cells form radiographically detectable osteolytic lesions within 4 to 6 weeks following intracardiac injection (15). That finding was corroborated by histomorphometry showing that calcified bone volume decreased as tumor volume increased

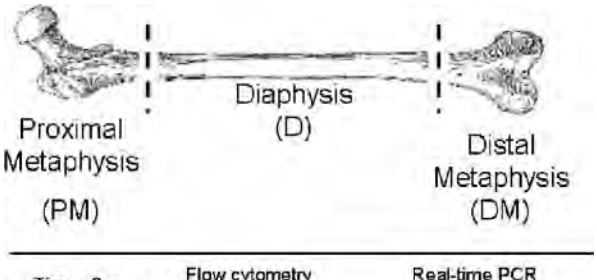

Time after injection	Flow cytometry			Real-time PCR		
	PM	D	DM	PM	D	DM
1 hr	1/5	2/5	0/5	4/5	3/5	2/5
4hr	2/5	2/5	0/5	4/5	4/5	3/5
24 hr	0/5	0/5	0/5	0/4	4/4	0/4
72 hr	2/5	1/5	2/5	2/5	4/5	1/5
1 wk	1/5	1/5	0/5	3/5	5/5	4/5
4 wk	2/5	2/5	3/5	4/5	5/5	5/5
6wk	0/3	1/3	2/3	2/3	3/3	3/3

Femoral ends were separated from the shaft with scissors. The proximal (PM) and distal (DM) metaphyses and the diaphysis (D) were flushed with ice-cold saline. Cells were collected and prepared for flow cytometry or DNA isolation and subsequent analysis by real-time PCR using HERVK, a human-specific gene. In practice, the limit of detection of MDA-435^{GFP} cells by flow cytometry was ~200 cells; by PCR it was ~150 cells. Shown are the numbers of animals in which the cancer cells were detected at various times and the bone areas in which they were found. The denominator is the number of bones examined at each time. Please note: the data presented are incidence only. The calculated number of cells is presented in Table 1 for each time.

Fig. 2. Detection of MDA-435^{GFP} metastatic cells by flow cytometry or real-time quantitative PCR in the metaphyseal and diaphyseal ends of the femur at various times following intracardiac inoculation.

Table 1. Retention of MDA-435^{GFP} cells in the femur following intracardiac injection

Time postinjection	Number of MDA-435^{GFP} cells in the femur
	Geometric mean (±1 SD)
1 h	41 (16-104)
4 h	54 (5-529)
24 h	40 (7-270)
72 h	44 (11-180)
1 wk	41 (20-82)
4 wk	11,271 (2,893-43,915)

NOTE: Marrow containing tumor cells was isolated from femurs as described in Materials and Methods. The number of MDA-435^{GFP} cells was determined by real-time quantitative PCR using probes for the human gene, HERVK. Shown are log-transformed data for four to five mice per group and only mice containing MDA-MB-435^{GFP} cells were included in the analysis.

(Fig. 3A). A decrease of 97% in the ratio of osteoid surface to bone surface at the 4-week point to osteoblast loss or loss-of-function as a major contributor to the decrease in calcified bone volume. This finding is consistent with previous work showing that MDA-MB-435 and MDA-MB-231 cells induce osteoblast apoptosis (33) and retard osteoblast differentiation (34) *in vitro*.

Importantly, osteoblast number per trabecular bone surface area in the metastatic lesions decreased with time (Fig. 3B). Bones from uninjected, age-matched mice served as negative controls. By 2 weeks, the number of osteoblasts decreased by ~20% in tumor-bearing mice. By 4 weeks, however, the decrease was more dramatic (~92% decrease; Fig. 3B). The decrease in osteoblast number was accompanied by an increase in the number of apoptotic osteoblasts observed by TUNEL (Figs. 3D and G, and 4A). Apoptotic osteoblasts were found at both proximal and distal ends of the femur, but little change in the number of apoptotic osteoblasts was observed in the diaphysis until tumor cells were routinely observed in that portion of the bone (Fig. 4A). This finding suggested that osteoblast apoptosis was occurring mostly when tumor cells were present. Supporting this hypothesis, TUNEL-positive osteoblasts were found almost exclusively in the presence (≤50 μm) of GFP-positive breast cancer cells (Figs. 3G and 4B). Previous (33) and current experiments (data not shown) have shown almost no tumor cell apoptosis when adjacent to osteoblasts. Bone sections stained for alkaline phosphatase, a marker for osteoblasts, showed a dramatic decrease as tumor burden increased (Fig. 3H-J). The ratio of the area occupied by alkaline phosphatase-positive cells per area of trabecular bone in the femurs of cancer-bearing mice was significantly lower compared with healthy mice (2.0 ± 0.6 versus 9.6 ± 1.7, respectively; $P \leq 0.0001$). In contrast, alkaline phosphatase activity in chondrocytes located in the growth plate was not significantly different (control, 25.9 ± 4.7; tumor bearing, 24.1 ± 5.0).

The number of osteoclasts remained unchanged at 2 weeks, but unexpectedly, a consistent decrease (~35-40% or to 60%

of control) in osteoclast number was observed at later times (Fig. 3C). This difference was evident by both quantitative histomorphometric analysis (Fig. 3C) and TRAP staining (Fig. 3E and F). The absolute number of both cell populations decreased so that the ratio of osteoblasts to osteoclasts decreased from an average of 40 to only 4 by 4 weeks.

Discussion

Bone is the most common site for metastases from breast carcinomas and their sequela account for approximately two-thirds of the costs associated with treating women with the disease (4, 36). As with most metastases, symptoms occur relatively late in disease progression. Whereas prevention of metastases altogether is ideal, restriction of progression to an asymptomatic state would improve clinical management of breast cancer. Likewise, repair of already existing lesions would benefit patients whose disease progression has been halted. As a result, understanding the antecedent steps for bone metastasis and osteolysis should provide insights for developing therapeutic interventions.

The results presented here are, to the best of our knowledge, the first to describe the behavior of breast cancer cells at the earliest times after they have arrived in the femur. Although the femur may not represent the behavior of tumor cells in all bones, it is a common site of secondary colonization both in patients with breast cancer and in experimental models. Therefore, we considered it an appropriate site for studying the process.

Single tumor cells were detected in the femur 1 hour after introduction into the arterial circulation (Fig. 5B). It is noteworthy that, even at this early time, tumor cells arrested primarily in the metaphyses rather than diaphyses. Although it is possible that differential expression of adhesion molecules may be found in metaphyseal versus diaphyseal bone

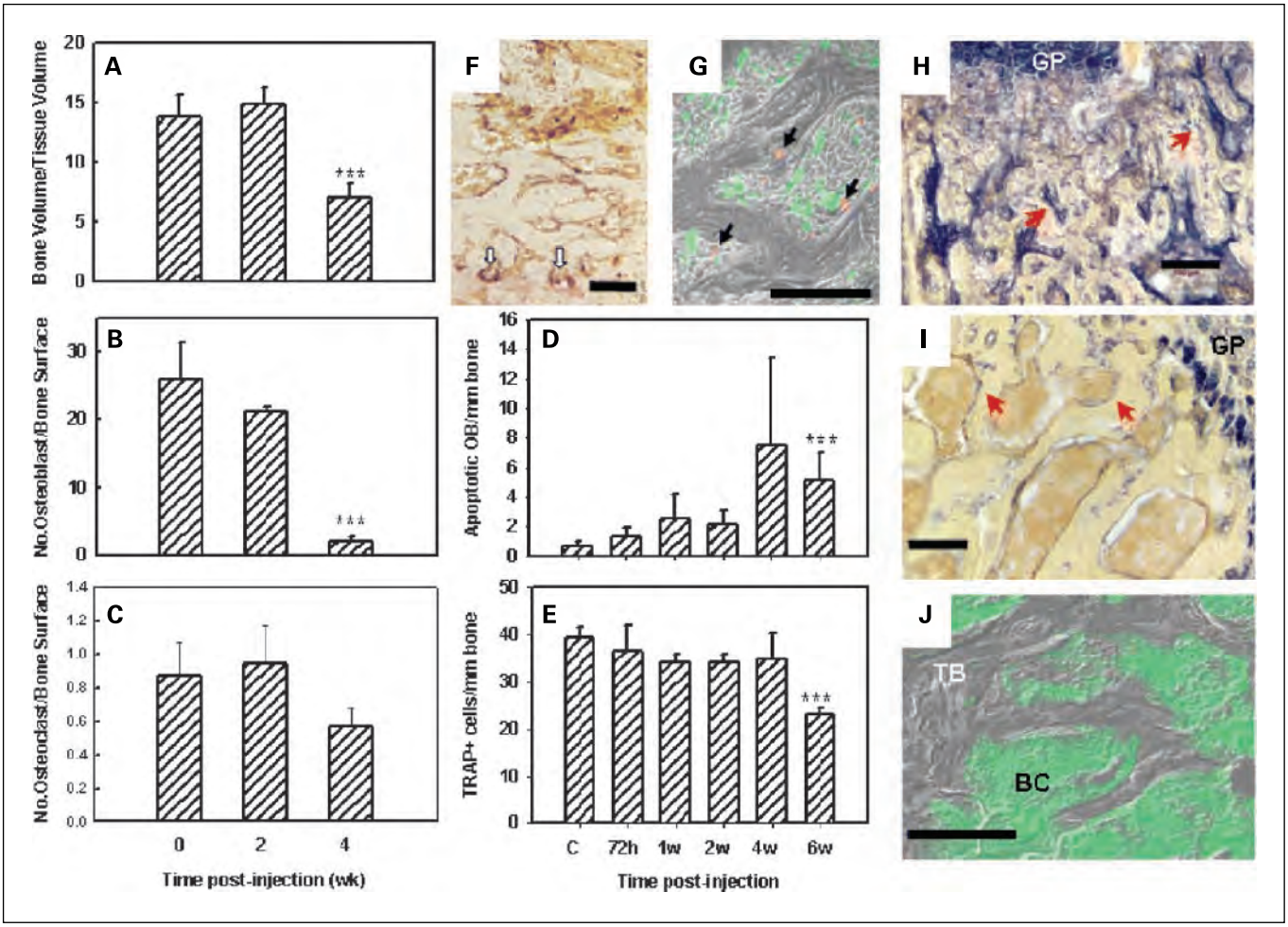

Fig. 3. MDA-435^{GFP} breast cancer cells diminished osteoblast and osteoclast numbers in colonized bone as evaluated by quantitative bone histomorphometry, immunohistochemistry, and fluorescent microscopy. *A-C,* histomorphometric analyses (*A,* bone volume to tissue volume; *B,* number of osteoblast per bone surface; *C,* number of osteoclast per bone surface). *D,* the number of apoptotic osteoblast (TUNEL-positive) per linear bone surface at times following inoculation of tumor cells. *E,* the number of osteoclasts (staining for TRAP) per linear bone surface at times following inoculation of tumor cells. *A-E,* significantly different ($P \leq 0.05$) from normal bone. *F,* representative image of osteoclast staining for TRAP (*red stain with white arrows*) taken from a section of femur 2 weeks after tumor cell inoculation. *G,* merged photomicrograph of MDA-435^{GFP} tumor cells (*green*) surrounding apoptotic osteoblast (*red*, TUNEL using Cy-5 probe) taken from a femur 6 weeks following inoculation. *H, I, J,* cryosections from a femur taken 4 weeks after tumor inoculation. *H,I,* stained for alkaline phosphatase activity (*blue staining by red arrows*) indicative of osteoblast; *J,* merged fluorescent and phase images showing trabecular bone (*TB*) surrounded by MDA-435^{GFP} cells (*BC*). Alkaline phosphatase activity was greatly diminished in the trabecular bone of tumor-bearing femurs but was still present in the growth plate (*GP*). Bars, 100 μm.

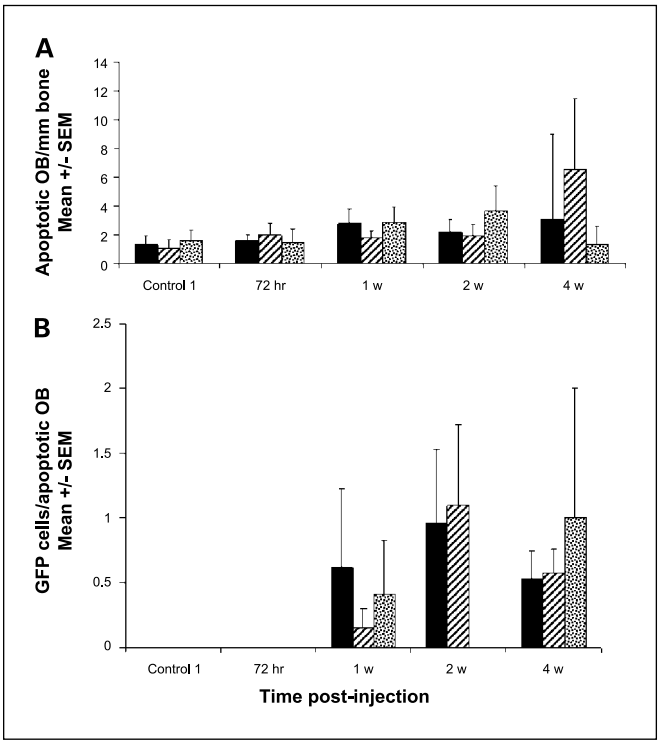

Fig. 4. The presence of metastatic breast cancer cells in close proximity to apoptotic osteoblasts increased with time following inoculation of MDA-435^{GFP}. *A,* apoptotic osteoblasts, detected by TUNEL, were counted in proximal and distal ends of paraffin sections of femur at times following tumor cell inoculation. *B,* number of MDA-435^{GFP} cells within a 50 μm radius of each apoptotic osteoblast. Averages from three femurs per time period. Proximal femur (*hatched columns*), distal femur (*stippled columns*), average over femur (*solid columns*). Apoptotic osteoblasts in the diaphyses were extremely rare.

vasculature (reviewed in ref. 37), anatomic and physiologic mechanisms are also likely to be important factors. Approximately 90% of the blood flow goes to the metaphyseal regions whereas a smaller fraction is found in the diaphyses (reviewed in ref. 38). Additionally, blood flow in the diaphysis is still largely vessel-based, whereas in the metaphyses, it is more sinusoidal. In the sinusoids, the rate of blood flow is <10% of that found in capillaries or other vessels (reviewed in ref. 37). Because of the sluggish blood flow, weaker adhesion molecules would not be subject to negative selection as when cells experience stronger sheer forces. However, arrest is not the only variable involved. The relatively rare cells initially seeding the diaphysis fail to remain there for prolonged periods. It is also possible that cancer cells follow a gradient of growth factors or cytokines. We have preliminary evidence[7] that several cytokines are found at much greater concentrations in the metaphysis compared with the diaphysis. The limitations of the present study cannot discriminate between loss of tumor cells to immune killing, apoptosis, sheer forces, etc., versus migration of tumor cells from the diaphysis to the metaphysis.

The earliest arriving tumor cells were mostly located in close proximity to osteoblasts and the bone-lining cells (Fig. 1B). In general, although the animal-to-animal variability was considerable, the majority of cells tended to be in the endosteal marrow, rather than in central marrow (Fig. 5G), suggesting that traversal from the sinusoids to trabecular space occurs relatively rapidly. This pattern is similar to that reported for hematopoietic precursors in bone marrow (29). Regardless of intra-osseous location, the trend was for tumor

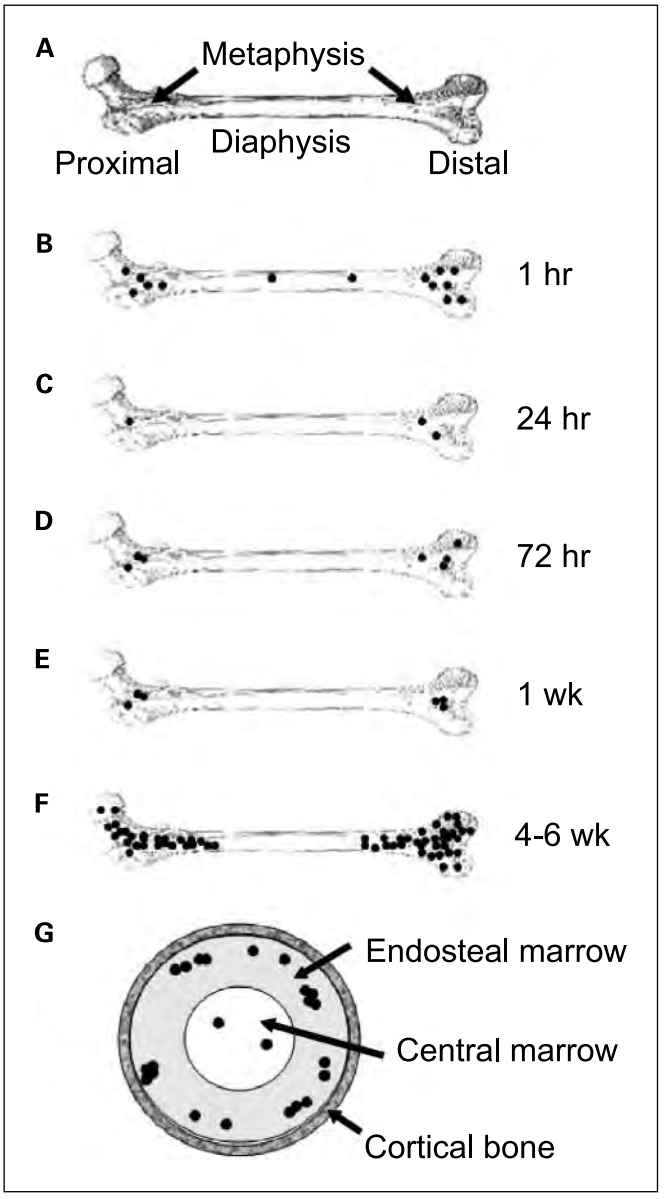

Fig. 5. Schematic diagram depicting colonization of the femur by MDA-435^{GFP} cells. A normal femur is diagramed and labeled for reference (*A*). Single cells (●) arrive in the bone marrow within 1 hour after intracardiac injection (*B*), with a distribution proportionate to the relative blood flow to regions of the bone. Most cells arresting in the bone are cleared within 24 hours (*C*). Of those remaining, the vast majority are still single cells but all are located in the metaphyses. A fraction of the surviving cells begin to proliferate by 72 hours (*D*) with little change in the number of foci, or size of tumor cell clusters, at 1 week postinoculation (*E*). The lesions progressively grow in size so that by 4 to 6 weeks, the mass of the metastases is large and the number of independently seeded cells are indiscernible because the foci have coalesced. Despite not seeding and remaining in the diaphyses, metastases extends into the bone shaft as the lesions grow (*F*). Flushing of bone marrow in established metastases as depicted in Fig. 2, revealed that most of the tumor cells are found in endosteal marrow (~90%) or in the central marrow (~10%), but never in the cortical bone of the diaphysis, as depicted in a cross-sectional view (*G*).

[7] A.M. Mastro, K.M. Bussard, and L. Shuman, unpublished observations.

cell numbers to decline during the first 72 hours after arrival (Fig. 5C and D).

It was somewhat surprising to find that most tumor cells had not begun to proliferate within 72 hours because proliferation typically begins much sooner (i.e., <48 hours) in lungs and orthotopic sites.[8] The period of quiescence or dormancy could be relevant because recent clinical studies have shown that 20% to 100% of women with breast cancer have evidence of disseminated tumor cells in the skeleton (35, 39, 40). Disseminated occult tumor cells within bone are thought to be in a sanctuary from which tertiary metastases could form and are thought to be responsible for late (sometimes months or years) recurrences. Based on abundant evidence from multiple experimental models, the fraction of disseminated cells progressing to overt metastasis is small. However, the presence of disseminated cells predicts poor prognosis in many tumor types, emphasizing that their presence at non-orthotopic sites should not be ignored (39, 40).

What triggers the conversion from dormant to proliferative cells remains unknown and is the subject of intense current investigation. The data presented here do not clarify the mechanistic issue, except to note that there is a substantial delay (72 hours) before the breast carcinoma cells begin to divide. Perhaps, during that time, tumor cells are altering the microenvironment. At our limits of detection, we could not tell whether there was balanced division (i.e., one of two of the progeny died or were eliminated) or whether tumor cells were adapting to the bone microenvironment prior to initiating growth. Upon arriving at a secondary site, tumor cells may remain dormant, undergo a limited number of cell divisions, or continue proliferating to form an overt mass. Presumably, the decisions are based on the response to signal(s) from the local microenvironment. There are self-evident cues that the tissue environment controls the development of bone metastasis based on the patterns of metastasis observed—e.g., metaphyseal > diaphyseal; distal > proximal; endosteal marrow > central marrow. The findings support and extend Stephen Paget's Seed and Soil hypothesis, by which he explains the predilection of breast carcinomas to colonize bone over other tissues (41). In short, Paget posited that tumor cells (seeds) were best suited for growth only in certain tissues (soils). The data presented here indicate that the soil may differ even within individual bones. Indeed the patterns of clinical bone metastases show marked preference for proximal and trabecular bone compared with distal or cortical bone (4). Surprisingly, the metastases arising from injection of MDA-435^{GFP} cells showed the opposite pattern—a slight, but consistent, penchant for distal, compared with proximal, femur. The pattern was consistent regardless of the method used to detect tumor cells. Hence, trivial experimental variables cannot explain why, in this model, metastases develops in the distal femur with greater frequency. One possibility invokes anatomic differences between mice and humans. Mice have extremely different gaits and mechanical pressures on their joints. Because tumor cells are generally predisposed to colonize injured tissues, biomechanical stresses on the knees in mice could, in part, explain the difference in arrest and colonization patterns between the species.

Notwithstanding preferential arrest/adhesion and growth in the metaphyses, metastatic breast carcinoma cells could still survive and grow in the diaphyses when the metastatic lesions are large enough. This growth pattern may suggest that tumor cells renovate the bone microenvironment sufficiently to reduce (or eliminate?) negative signals or that they can induce the production of positive factors from local, nontumor cells. Whether neoplastic cells have surpassed a threshold number, or whether some negative influence on tumor cells has been overcome, the incapacity to colonize diaphyses is not absolute.

It is widely accepted that metastatic breast carcinoma cells manipulate the bone microenvironment to induce osteolysis. In particular, tumor cell activation of osteoclasts via the "vicious cycle" of secretion of PTHrP or RANK ligand has been implicated in bone resorption (4, 19, 42). However, we previously hypothesized that the balance of bone deposition and resorption could be altered as well by reducing osteoblast number or differentiation and/or activity (33). *In vitro* coculture of metastatic human breast carcinoma cells or their conditioned medium with human osteoblasts resulted in apoptosis of the osteoblasts (33). The *in vivo* data presented here extend the previous findings by demonstrating that osteoblasts in the regions colonized by MDA-435^{GFP} are also eliminated.

It is possible that changes in the ratio of osteoblasts to osteoclasts in tumor-infiltrated bone tilts the balance in favor of increasing osteoclastic activity, thereby promoting osteolysis. The dramatic decrease in osteoblasts observed by 4 weeks prompted closer examination of osteoblast apoptosis at multiple times using TUNEL. The number of apoptotic osteoblasts progressively increased until later times, perhaps due to the already decreased number of osteoblasts. Interestingly, at earlier times (<4 weeks) at least one tumor cell was in direct contact (≤50 μm) with each TUNEL-positive osteoblast (Figs. 3E and 4B). Although this finding does not prove that tumor cells directly induce apoptosis, the data are consistent with this hypothesis. We also found with *in vitro* studies that breast cancer cell–conditioned medium prevented osteoblasts from differentiating as evidenced by lack of production of alkaline phosphatase, osteocalcin, and bone siaoloprotein (34). In this current study, the lack of alkaline phosphatase activity (Fig. 3H and I) may be due, in part, to failure of preosteoblasts to differentiate as well as apoptosis of mature osteoblasts. In either case, the outcome is the same, lack of functional osteoblasts.

Ours is the first *in vivo* evidence that tumor cells influence not only osteoclasts, as widely believed and showed, but also osteoblasts. The findings may explain, in part, the failure of bisphosphonate-treated patients to repair osteolytic bone lesions (43)—i.e., if there are no osteoblasts to reconstitute the bone, the lesions will remain.

It was surprising that osteoclast numbers were dramatically reduced in late-stage bone metastasis. Perhaps it should not have been because Orr, Mundy, and colleagues previously described that tumor cells themselves (i.e., in the absence of osteoclasts) could resorb bone (44, 45). The published data, although somewhat controversial, and the evidence presented here leave open the possibility that further progression of osteoclast-initiated osteolysis is possible. Furthermore, previous publications have shown significantly diminished osteoblast and osteoclast numbers in late stage breast carcinoma

[8] Unpublished observations.

metastasis to bone (46–48). Based on heterogeneity among tumors for multiple variables, molecular mechanisms of bone metastasis may vary while yielding the same end point, osteolysis.

A potential criticism of the reported work is that the findings are based on a single cell line. Given the heterogeneity of tumors and the redundant mechanisms from which each can choose to accomplish a given task, we are careful not to overgeneralize. Nonetheless, most key observations reported here have been replicated in the MDA-MB-231 breast carcinoma model of bone metastasis. MDA-MB-231 cells form osteolytic lesions with similar distribution as those found in MDA-MB-435. With expansion of bone lesions, osteoblast numbers decrease in MDA-MB-231 as well.[9] Assuming that the essential elements of osteolytic metastasis are observed in multiple breast carcinoma models, the findings reported here have significant implications with regard to control of bone metastasis in the clinic.

Foremost, the osteoblast is key. Whereas tumor cells could initiate growth prior to osteolysis, one of the earliest observed changes is the elimination of bone-forming cells. Even if bone resorption is controlled exogenously (i.e., by treatment with bisphosphamates), repair of defects is not possible. Because the structural integrity of the skeleton is critical to survival and quality of life, comprehensive treatment needs to restore bone matrix as well as limit osteolysis. By studying the trafficking of tumor cells within the bone and the effect of their presence on normal bone physiology, insights regarding how to improve control of bone metastasis will be forthcoming. Since the submission of this article, a report (49) describing a role for Dickkopf-1 in a Wnt-mediated pathway in prostate cancer cell osteoblastic lesions was published. Whether breast cancer–mediated osteolysis via impairment of osteoblast function is regulated by Dickkopf-1 or other components of the Wnt signaling pathway remains to be determined.

[9] P.A. Phadke and D.R. Welch, unpublished observations.

Acknowledgments

We are indebted to the superb technical assistance from Virginia R. Gilman as well as Patti Lott at the University of Alabama at Birmingham, Center for Metabolic Bone Disease Histomorphometry Core Facility, the University of Alabama at Birmingham Breast Specialized Programs of Research Excellence Tissue Core Facility, Deborah Grove and the Penn State Nucleic Acid Core Facility, and the Penn State Electron Microscopy and Histology Core Facility. We appreciate the critical reading of the manuscript and helpful suggestions from Dr. Tom Clemens.

References

1. Body JJ. Metastatic bone disease: clinical and therapeutic aspects. Bone 1992;13:S57–62.
2. Coleman RE. Skeletal complications of malignancy. Cancer 1997;80:1588–94.
3. Coleman RE, Rubens RD. The clinical course of bone metastases from breast cancer. Br J Cancer 1987;55:61–6.
4. Mundy GR. Metastasis: metastasis to bone: causes, consequences and therapeutic opportunities. Nat Rev Cancer 2002;2:584–93.
5. Lelekakis M, Moseley JM, Martin TJ, et al. A novel orthotopic model of breast cancer metastasis to bone. Clin Exp Metastasis 1999;17:163–70.
6. Chirgwin JM, Guise TA. Molecular mechanisms of tumor-bone interactions in osteolytic metastases. Crit Rev Eukaryot Gene Expr 2000;12:159–78.
7. Guise TA. Parathyroid hormone-related protein and bone metastases. Cancer 1997;80:1572–80.
8. Yoneda T, Sasaki A, Mundy GR. Osteolytic bone metastasis in breast cancer. Breast Cancer Res Treat 1994;32:73–84.
9. Averbuch SD. New bisphosphonates in the treatment of bone metastases. Cancer 1993;72:3443–52.
10. Wetterwald A, van der Pluijm G, Que I, et al. Optical imaging of cancer metastasis to bone marrow—a mouse model of minimal residual disease. Am J Pathol 2002;160:1143–53.
11. Holleran JL, Miller CJ, Culp LA. Tracking micrometastasis to multiple organs with *lacZ*-tagged CWR22R prostate carcinoma cells. J Histochem Cytochem 2000;48:643–51.
12. Amhlaoibh RN, Hoegh-Andersen P, Brünner N, et al. Measurement of tumor load and distribution in a model of cancer-induced osteolysis: a necessary precaution when testing novel anti-resorptive therapies. Clin Exp Metastasis 2004;21:65–74.
13. Sung V, Cattell DA, Bueno JM, et al. Human breast cancer cell metastasis to long bone and soft organs of nude mice: a quantitative assay. Clin Exp Metastasis 1997;15:173–83.
14. Murphy BO, Joshi S, Kessinger A, Reed E, Sharp JG. A murine model of bone marrow micrometastasis in breast cancer. Clin Exp Metastasis 2002;19:561–9.
15. Harms JF, Welch DR. MDA-MB-435 human breast carcinoma metastasis to bone. Clin Exp Metastasis 2003;20:327–34.
16. Yang M, Baranov E, Jiang P, et al. Whole-body optical imaging of green fluorescent protein-expressing tumors and metastases. Proc Natl Acad Sci U S A 2000;97:1206–11.
17. Manolagas SC. Birth and death of bone cells: basic regulatory mechanisms and implications for the pathogenesis and treatment of osteoporosis. Endocr Rev 2000;21:115–37.
18. Parfitt AM. Osteonal and hemi-osteonal remodeling: the spatial and temporal framework for signal traffic in adult human bone. J Cell Biochem 1994;55:273–86.
19. Roodman GD. Mechanisms of disease: mechanisms of bone metastasis. N Engl J Med 2004;350:1655–64.
20. Van Tine BA, Kappes JC, Banerjee NS, et al. Clonal selection for transcriptionally active viral oncogenes during progression to cancer. J Virol 2004;78:11172–86.
21. Chen W, Wu X, Levasseur DN, et al. Lentiviral vector transduction of hematopoietic stem cells that mediate long-term reconstitution of lethally irradiated mice. Stem Cells 2000;18:352–9.
22. Sellappan S, Grijalva R, Zhou XY, et al. Lineage infidelity of MDA-MB-435 cells: expression of melanocyte proteins in a breast cancer cell line. Cancer Res 2004;64:3479–85.
23. Harms JF, Welch DR, Samant RS, et al. A small molecule antagonist of the α-v, β-3 integrin suppresses MDA-MB-435 skeletal metastasis. Clin Exp Metastasis 2004;21:119–28.
24. Parfitt AM. Bone histomorphometry: proposed system for standardization of nomenclature, symbols, and units. Calcif Tissue Int 1988;42:284–6.
25. Parfitt AM, Drezner MK, Glorieux FH, et al. Bone histomorphometry: standardization of nomenclature, symbols, and units. Report of the ASBMR Histomorphometry Nomenclature Committee. J Bone Miner Res 1987;2:595–610.
26. Miao D, Scutt A. Histochemical localization of alkaline phosphatase activity in decalcified bone and cartilage. J Histochem Cytochem 2002;50:333–40.
27. Harms JF, Budgeon LR, Christensen ND, Welch DR. Maintaining green fluorescent protein tissue fluorescence through bone decalcification and long-term storage. Biotechniques 2002;33:1197–200.
28. Jewell J, Mastro AM. Using terminal deoxynucleotidy transferase (TDT) enzyme to detect TUNEL-positive, GFP-expressing apoptotic cells. Appl Cell Notes 2002;3:13–4.
29. Mason TM, Lord BI, Hendry JH. The development of spatial distributions of CFU-S and *in vitro* CFC in femora of mice of different ages. Br J Haematol 1989;73:455–61.
30. Mager DL, Medstrand P. Retroviral repeat sequences. In: Anonymous encyclopedia of the human genome. London: Macmillan Publishers Ltd., Nature Publishing Group; 2003. p. 1–7.
31. Goldberg SF, Harms JF, Quon K, Welch DR. Metastasis-suppressed C8161 melanoma cells arrest in lung but fail to proliferate. Clin Exp Metastasis 1999;17:601–7.
32. Fidler IJ. Metastasis: quantitative analysis of distribution and fate of tumor emboli labeled with ^{125}I-5-iodo-2′-deoxyuridine. J Natl Cancer Inst 1970;45:773–82.
33. Mastro AM, Gay CV, Welch DR, et al. Breast cancer cells induce osteoblast apoptosis: a possible contributor to bone degradation. J Cell Biochem 2004;91:265–76.
34. Mercer RR, Miyasaka C, Mastro AM. Metastatic breast cancer cells suppress osteoblast adhesion and differentiation. Clin Exp Metastasis 2004;21:427–35.
35. Masuda TA, Kataoka A, Ohno S, et al. Detection of occult cancer cells in peripheral blood and bone marrow by quantitative RT-PCR assay for cytokeratin-7 in breast cancer patients. Int J Oncol 2005;26:721–30.
36. Lipton A. Management of bone metastases in breast cancer. Curr Treat Options Oncol 2005;6:161–71.
37. Welch DR, Harms JF, Mastro AM, Gay CV. Breast cancer metastasis to bone: evolving models and research challenges. J Musculoskelet Neuronal Interact 2003;3:30–8.
38. Gross TS, Clemens TL. Vascular control of bone remodeling. In: Anonymous advances in organ biology. JAI Press Inc.; 1998. p. 138–60.
39. Pantel K, Woelfle U. Micrometastasis in breast cancer and other solid tumors. J Biol Regul Homeost Agent 2004;18:120–5.
40. Pantel K, Brakenhoff RH. Dissecting the metastatic cascade. Nat Rev Cancer 2004;4:448–56.
41. Paget S. The distribution of secondary growths in cancer of the breast. Lancet 1889;1:571–3.
42. Lynch CC, Hikosaka A, Acuff HB, et al. MMP-7

promotes prostate cancer-induced osteolysis via the solubilization of RANKL. Cancer Cell 2005;7: 485–96.

43. Lipton A, Theriault RL, Hortobagyi GN, et al. Pamidronate prevents skeletal complications and is effective palliative treatment in women with breast carcinoma and osteolytic bone metastases—long term follow-up of two randomized, placebo-controlled trials. Cancer 2000;88:1082–90.

44. Eilon G, Mundy GR. Direct resorption of bone by human breast cancer cells *in vitro*. Nature 1978;276: 726–8.

45. Sanchez-Sweatman OH, Orr FW, Singh G. Human metastatic prostate PC3 cell lines degrade bone using matrix metalloproteinases. Invasion Metastasis 1998; 18:297–305.

46. Stewart AF, Vignery A, Silverglate A, et al. Quantitative bone histomorphometry in humoral hypercalcemia of malignancy: uncoupling of bone cell activity. J Clin Endocrinol Metab 1982;55:219–27.

47. Sanchez Y, Bachant J, Wang H, et al. Control of the DNA damage checkpoint by Chk1 and Rad53 protein kinases through distinct mechanisms. Science 1999; 286:1166–71.

48. Mundy CR, Altman AJ, Gondek MD, Bandelin JG. Direct resorption of bone by human monocytes. Science 1977;196:1109–11.

49. Hall CL, Bafico A, Dai J, Aaronson SA, Keller ET. Prostate cancer cells promote osteoblastic bone metastases through Wnts. Cancer Res 2005;65:7554–60.

EXPERIMENTAL CELL RESEARCH 314 (2008) 173–183

available at www.sciencedirect.com

ScienceDirect

www.elsevier.com/locate/yexcr

Research Article

Metastatic breast cancer induces an osteoblast inflammatory response

Michelle Kinder[1], *Elizabeth Chislock*[1], *Karen M. Bussard*, *Laurie Shuman*, *Andrea M. Mastro*[*]

Department of Biochemistry and Molecular Biology, The Pennsylvania State University, 431 S. Frear Building, University Park, PA 16802, USA

ARTICLE INFORMATION

Article Chronology:
Received 6 June 2007
Revised version received
13 September 2007
Accepted 18 September 2007
Available online 4 October 2007

Keywords:
Breast cancer
IL-6
IL-8
Inflammation
Metastasis
MCP-1
Osteoblasts

ABSTRACT

Breast cancer preferentially metastasizes to the skeleton, a hospitable environment that attracts and allows breast cancer cells to thrive. Growth factors released as bone is degraded support tumor cell growth, and establish a cycle favoring continued bone degradation. While the osteoclasts are the direct effectors of bone degradation, we found that osteoblasts also contribute to bone loss. Osteoblasts are more than intermediaries between tumor cells and osteoclasts. We have presented evidence that osteoblasts contribute through loss of function induced by metastatic breast cancer cells. Metastatic breast cancer cells suppress osteoblast differentiation, alter morphology, and increase apoptosis. In this study we show that osteoblasts undergo an inflammatory stress response in the presence of human metastatic breast cancer cells. When conditioned medium from cancer cells was added to human osteoblasts, the osteoblasts were induced to express increased levels of IL-6, IL-8, and MCP-1; cytokines known to attract, differentiate, and activate osteoclasts. Similar findings were seen with murine osteoblasts and primary murine calvarial osteoblasts. Osteoblasts are co-opted into creating a microenvironment that exacerbates bone loss and are prevented from producing matrix proteins for mineralization. This is the first study implicating osteoblast produced IL-6, IL-8 (human; MIP-2 and KC mouse), and MCP-1 as key mediators in the osteoblast response to metastatic breast cancer cells.

Introduction

Breast cancer is the second deadliest form of cancer for women in the United States, largely due to its tendency to metastasize. Once metastasis occurs, the relative 5-year survival rate drops precipitously from over 90% to less than 10% depending on the site of the metastasis. For breast cancer, the skeleton is the preferred site of metastasis. Nearly 50% of primary and about 70% of secondary metastases target bone [1–3]. Within the skeletal system, breast cancer cells most frequently colonize the ends of long bones, ribs, and vertebrae; these areas contain rich microvasculature closely juxtaposed to metabolically active trabecular bone surfaces [2].

The metaphyseal area at the ends of long bones contains a complex network of bone cells, hematopoietic cells, and stromal cells. The entry of breast cancer cells into the marrow cavity disturbs the status quo, in particular, the interaction between osteoblasts and osteoclasts. In the adult skeleton,

* *Corresponding author*. Fax: +1 814 863 7024.
E-mail address: a36@psu.edu (A.M. Mastro).
[1] Submitted in partial fulfillment of the honors thesis requirement of the Schreyer Honors College.

0014-4827/$ – see front matter © 2007 Elsevier Inc. All rights reserved.
doi:10.1016/j.yexcr.2007.09.021

these two cell types are responsible for the slow and continuous turnover of bone [4]. When metastatic breast cancer cells invade the bone microenvironment, the balance is upset in favor of net bone loss. Indeed, breast cancer metastasis usually results in osteolytic lesions due to activated osteoclasts that degrade bone matrix. The bone loss can cause severe pain, pathologic fractures, spinal cord and nerve compression, hypercalcemia, and bone marrow suppression [2]). In addition, growth factors released from the matrix promote cancer cell proliferation and contribute to what has been described as "the vicious cycle"[5]. In particular, transforming growth factor-beta (TGF-β) and insulin growth factor-1 (IGF-1), which are released from the matrix during bone degradation, stimulate the production of parathyroid hormone-related protein (PTHrP) that fosters cancer cell growth [5–8].

Furthermore, growth factors released from the matrix, substances secreted by the cancer cells and osteoblasts contribute to the metastatic microenvironment. Some osteoblast factors, such as receptor activator of nuclear factor kappa B ligand (RANKL) and osteoprotogerin (OPG), are part of the normal osteoblast-osteoclast signaling cross talk. Others, such as interleukin-6 (IL-6), IL-8, and monocyte chemoattractant protein-1 (MCP-1), may indicate an osteoblast inflammatory response. It has been known for a long time that chronic inflammation, which occurs as part of the cancer cell's interaction with the stromal environment, supports cancer progression and metastasis [9]. Fibroblasts, endothelial cells, cells of the blood and lymph vasculature, as well as transient cells of the innate and adaptive immune systems all affect cancer cell growth and metastasis. Under ordinary conditions, communication within the stromal network is carried out by cytokines, chemokines, and other peptides. A disruption of homeostasis by trauma, microorganisms, foreign materials, or cancer cells results in drastic changes in the levels and types of cytokines expressed [10]. The stromal environment in metaphyseal bone is no exception. Any circumstance that changes the balance between osteoblasts and osteoclasts may lead to bone loss. For example, osteomyelitis brought about by *M. tuberculosis* or *S. aureus* is associated with uncontrolled inflammation and especially high levels of IL-8, RANTES, and MCP-1 [11]. Titanium transplant-induced bone loss has been traced to an osteoblast stress response with high levels of IL-8, MCP-1, and IL-6 [12]. These cytokines have been shown to attract and activate osteoclasts as well as cells of the immune system, thus perpetuating bone loss [13].

While it is likely that tumor-infiltrating lymphocytes, neutrophils, and macrophages are a potent source of inflammatory molecules, we present evidence in this paper that metastatic breast cancer cells can directly induce osteoblasts to express increased levels of inflammatory stress response molecules, specifically IL-6, IL-8 (macrophage inflammatory protein-2 [MIP-2], KC), and MCP-1. Moreover, the osteoblast response was mediated by soluble factors and occurred independently of direct cancer cell–osteoblast contact. Their ultimate target is the osteoclast.

Current therapies are directed at blocking osteoclast activity. Bisphosphonates such as clodronate, ibandronate, pamidronate, and zoledronic acid are the current standard of care for most metastases to bone. These synthetic analogues of inorganic pyrophosphates inhibit osteoclast activity and slow lesion formation. Although they reduce skeletal-related events, they are not curative. They do not lead to restoration of the bone and do not eliminate the cancer cells [14]. The osteoblasts appear to be functionally paralyzed [15].

We have previously reported that osteoblasts exposed to metastatic breast cancer cells or their conditioned media show an increase in apoptosis, suppression of production of bone matrix proteins, and a change in morphology [16–18]. The results of this study indicate that the osteoblasts also switch into an inflammatory mode in the presence of the breast cancer cells. These osteoblast-produced inflammatory cytokines, different from those made by the cancer cells, can target osteoclast precursors that are effectors of osteolysis. Therefore, osteoblasts contribute to the osteolytic phenotype due to loss of bone deposition functions as well as to increased production of osteoclast activating cytokines.

Materials and methods

Cell lines

Osteoblasts

hFOB 1.19 cells are human fetal osteoblasts that have been immortalized with a temperature-sensitive SV40 large T antigen. At a permissive temperature of 34 °C, they proliferate; incubation at 39 °C show their growth and fosters osteoblast differentiation [19]. These cells, a gift from Dr. Thomas Spelsberg, were cultured at 34 °C, 5% CO_2 in hFOB growth medium, which consists of Dulbecco's Modified Eagle's Medium (DMEM):Ham's F-12 (1:1) (Sigma, St. Louis, MO), 10% fetal bovine serum (FBS) (Sigma), and penicillin 100 U/ml/streptomycin 100 μg/ml (Sigma). For experiments, hFOB 1.19 osteoblasts at 85–90% confluency were cultured at 39 °C, for 2–3 days in a hFOB differentiation medium, [DMEM:Ham's F-12 1:1, 10% charcoal-stripped FBS, penicillin 100 U/ml/streptomycin 100 μg/ml, 10^{-8} M Vitamin D_3 (Biomol, Plymouth Meeting, PA), 10^{-8} M Vitamin K (menadione) (Sigma), and 50 μg/ml Vitamin C (ascorbic acid) (Sigma)]. As indicated for various experiments, hFOB 1.19 cells were plated at approximately 4×10^3 cells/cm^2 in T-25 flasks, 35 mm, or 6-well culture plates.

MC3T3-E1 cells, a murine pre-osteoblast line capable of differentiation and mineralization in culture [20], were a gift from Dr. Norman Karin, University of Delaware. MC3T3-E1 cells were maintained in an MC3T3-E1 growth medium of alpha Minimum Essential Medium (αMEM) (Mediatech, Herdon, VA), 10% neonatal FBS (Cansera, Roxdale, Ontario), and penicillin 100 U/ml/streptomycin 100 μg/ml. For experiments as indicated, MC3T3-E1 cells were plated at 10^4 cells/cm^2 in MC3T3-E1 differentiation medium (αMEM, 10% FBS, penicillin 100 U/ml/streptomycin 100 μg/ml, 50 μg/ml ascorbic acid, and 10 mM β-glycerophosphate (Sigma)).

Breast cancer cells

MDA-MB-231 cells, a human metastatic breast cancer line derived from a pleural effusion [21], were a gift from Dr. Danny Welch, University of Alabama, Birmingham. The cells were maintained in a breast cancer growth medium of DMEM, 5% FBS, and penicillin 100 U/ml/streptomycin 100 μg/ml.

Primary osteoblasts from neonatal mouse calvariae

Osteoblasts were isolated from neonatal mouse calvariae and cultured as described [22]. Animal use was approved by the IACUC of the Pennsylvania State University. Briefly, 2 to 5 calvariae were dissected from 2 day, C57bl/6, mouse pups. The calvariae were rinsed with PBS, cut into pieces, and incubated with 4ml of digestion solution [0.64 mg/ml Collagenase type IA (Sigma) and 0.05% trypsin in PBS] at 37° for 20 min with shaking immediately before incubation and again after 10 min. After the 20-min incubation, the solution containing the cells was collected and 700 μl of FBS was added. The calvariae pieces were washed with 2 ml of DMEM and the wash added to the digestion solution containing cells, and centrifuged (300×*g*, 4 min). The cell pellet was resuspended in calvariae growth medium (DMEM, 10% FBS, penicillin 100 U/ml/streptomycin 100 μg/ml, 100 μg/ml ascorbic acid) and plated in a 6-well plate, 2 ml cell suspension per well (pool 1). This procedure was repeated three more times (pools 2–4). The following day, culture media were replaced with fresh growth medium and cells were monitored until ~85% confluency was reached. The cells were trypsinized [0.25% trypsin/2.21 mM EDTA in Hanks' Balanced Salt Solution (CellGro, Mediatech, Herndon, VA)]. Pools 1 and 2 were combined and pools 3 and 4 were combined. Cells were plated at a cell density of 1 to 2×10^4 cells/cm^2 in calvariae growth medium. The next day the culture media was removed and calvariae differentiation medium (DMEM, 10% FBS, penicillin 100 U/ml/streptomycin 100 μg/ml, 100 μg/ml ascorbic acid, 40 ng/ml dexamethasone) was added to the cells and changed twice a week until the desired osteoblast age was reached. Combined pools 3 and 4, 14 days from addition of differentiation medium, were used in experiments described in this study.

Conditioned media preparation

MDA-MB-231 breast cancer cells were grown to 90% confluency. Breast cancer growth medium was removed and the cultures rinsed once with PBS. DMEM:Ham's F12 (for use with hFOB 1.19 cells) or αMEM (for use with MC3T3-E1 cells) was added to the cancer cells (20 ml in a T-150 flask, ~1.3×10^5 cells/cm^2). Cultures were incubated for 24 h. Breast cancer cell conditioned medium (BCCM) was collected, centrifuged (300×*g*, 10 min) to remove cellular debris, and stored at −20 °C. hFOB 1.19 cell conditioned medium was prepared similarly. hFOB 1.19 cells (80% confluent) were rinsed one time with PBS before serum-free DMEM:Ham's F-12 1:1 and penicillin 100 U/ml/streptomycin 100 μg/ml were added, collected after 24 h of incubation, centrifuged to remove debris, and stored at −20 °C.

Conditioned media treatments of osteoblasts

Vehicle media (VM) consisted of differentiation media appropriate for each of the cell lines used. A 2× differentiation medium was formulated for each of the osteoblast cell lines. For hFOB 1.19, medium consisted of DMEM: Ham's F12, 20% FBS, 2×10^{-8} M 1,25 dihydroxyvitamin D_3, 2×10^{-8} M vitamin K, 100 μg/mL ascorbic acid, 200 IU/ml penicillin, and 200 μg/ml streptomycin. For MC3T3-E1, the medium consisted of αMEM, 20% neonatal FBS, 100 μg/ml ascorbic acid, 20 mM β-glycerophosphate, 200 IU/ml penicillin, and 200 μg/ml streptomycin. Conditioned media (CM) was comprised of one half volume BCCM and one half volume 2× osteoblast differentiation medium appropriate for the osteoblast line used in the experiment. This scheme ensured that concentrations of serum and differentiation factors were identical for VM and CM.

Peptides and cytokines

TGF-β and anti-TGF-β neutralizing antibody were purchased from R&D Systems, (Minneapolis, MN) and used at concentrations indicated. The antibody was incubated with VM or CM for 1 h at 37 °C prior to culturing with the osteoblasts. Parathyroid hormone (PTH) (1–34) was obtained from Sigma, St. Louis, MO.

Cytokine analyses

Cytokines in the culture medium were detected using RayBio® Mouse Cytokine Antibody Array III System for MC3T3-E1 and RayBio® Human Array System I for hFOB 1.19 cells (Norcross, GA). Cytokine protein levels were quantitated using sandwich ELISAs following the protocols recommended by R&D Systems. Intra-assay variation was typically less than 15%. Select cytokines were quantitated with Bio-Plex™ Mouse and Human Cytokine Assay System (Bio-Rad, Hercules, California).

Statistical analyses

Statistical analyses were carried out using SAS, For Windows (SAS Version 9.1, SAS Institute, Cary, NC). Main effects were evaluated using one-way analysis of variance (ANOVA). Data were used for analyses of all variables. Statistical significance was defined as a probability $P<0.05$ in all analyses. *N* values for individual experiments are provided in the figure legends.

Results

The production of IL-6, IL-8, and MCP-1 by hFOB 1.19 cells was increased in the presence of breast cancer conditioned medium and was dose-dependent

When hFOB 1.19 were approximately 90% confluent, they were rinsed with PBS and treated with either VM or CM. Twenty-four hours later, the culture media were collected and screened with a RayBio® Human Cytokine Array. Among the 62 cytokines in the screen, IL-6, IL-8, and MCP-1 levels were readily detected (Fig. 1A). In this array, no cytokines were detected in the BCCM alone (Fig. 1B). Medium from VM-treated osteoblasts also had no detectable levels of cytokines in this array (data not shown).

In order to quantitate detected cytokine levels, standard ELISAs were carried out. The BCCM was assayed for the presence of human IL-6, IL-8, and MCP-1. In this assay, 73 pg/ml IL-6, 449 pg/ml IL-8, and <2 pg/ml MCP-1 were detected. These basal levels of cytokines were subtracted in the data that follow. At a later time, we assayed BCCM with a multiplex assay (Bio-Rad Bio-Plex™) and found 50 pg/ml IL-6, 51 pg/ml IL-8 and 1.6 pg/ml MCP-1.

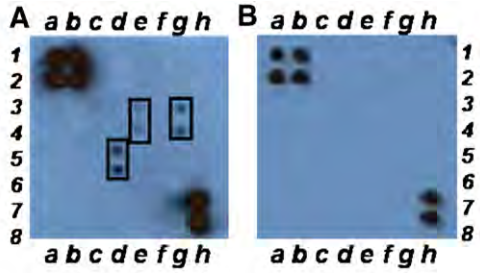

RayBio® Human Array System I

	a	b	c	d	e	f	g	h
1,2	Pos	Pos	Neg	Neg	G-CSF	GM-CSF	GRO	GRO-α
3,4	IL-1α	IL-2	IL-3	IL-5	IL-6	IL-7	IL-8	IL-10
5,6	IL-13	IL-15	IFN-γ	MCP-1	MCP-2	MCP-3	MIG	RANTES
7,8	TGF-β1	TNF-α	TNF-β	Blank	Blank	Blank	Blank	Pos

Fig. 1 – hFOB 1.19 secreted cytokines detected by a cytokine array. hFOB 1.19 cells were grown in growth medium at 34 °C until they reached approximately 80–90% confluency. Growth medium was removed, cells rinsed with PBS, and subsequently treated with VM or CM for 24 h at 34 °C. The resultant culture supernatant was collected, centrifuged to remove debris, and analyzed with a RayBio® Human Cytokine Protein Array System I. (A) Array results of culture supernatants of hFOB cells treated with CM. From left to right: positive control (a,b,1,2), MCP-1 (d5,6), IL-6 (e3,4), IL-8 (g3,4), positive control (h7,8). (B) Array results of MDA-MB-231 BCCM alone. Positive controls (a,b,1,2 and h7,8). No cytokines were detected.

To define the osteoblast cytokine response to BCCM and determine whether the stage of osteoblast differentiation was important for this response, hFOB 1.19 were treated with CM for 24 h after various days of culture. hFOB 1.19 were grown to confluency at 34 °C and on day 6 transferred to 39 °C to allow for differentiation. At days 3, 5, and 7 after transfer, the cells were treated with either VM or CM. Twenty-four hours later, the culture medium was collected and assayed by ELISA for human IL-6, IL-8, and MCP-1. On days 4 and 6, the hFOB 1.19 cells treated with VM contained undetectable levels of IL-6, while the osteoblasts treated with CM contained 0.11 ng/ml and 0.26 ng/ml IL-6 respectively (Fig. 2A). However, the differences were more pronounced as the osteoblasts differentiated. For example, a 24-h exposure of 8 day-differentiated osteoblasts to CM led to a 5- to 10-fold increase in IL-6 (~10 ng/ml) (Fig. 2A). At this time the cytokine levels of IL-6 from cells treated with VM increased to about 1 ng/ml.

A similar pattern was found with IL-8 (Fig. 2B). Cytokine concentrations in osteoblasts treated with VM were low (0.02 ng/ml) during the early differentiation stage; however, the concentration of IL-8 increased to 0.26 ng/ml by day 8. Treatment with CM increased osteoblast production of IL-8 by nearly five times (1.26 ng/ml) when compared to treatment with VM at the same time (0.26 ng/ml).

Osteoblast production of MCP-1 displayed a different pattern of expression than IL-8 and IL-6. MCP-1 increased in cells treated both with VM and CM. However, the concentrations of MCP-1 were higher in cultures of osteoblasts treated with CM than with VM (Fig. 2C). This increase in MCP-1 was

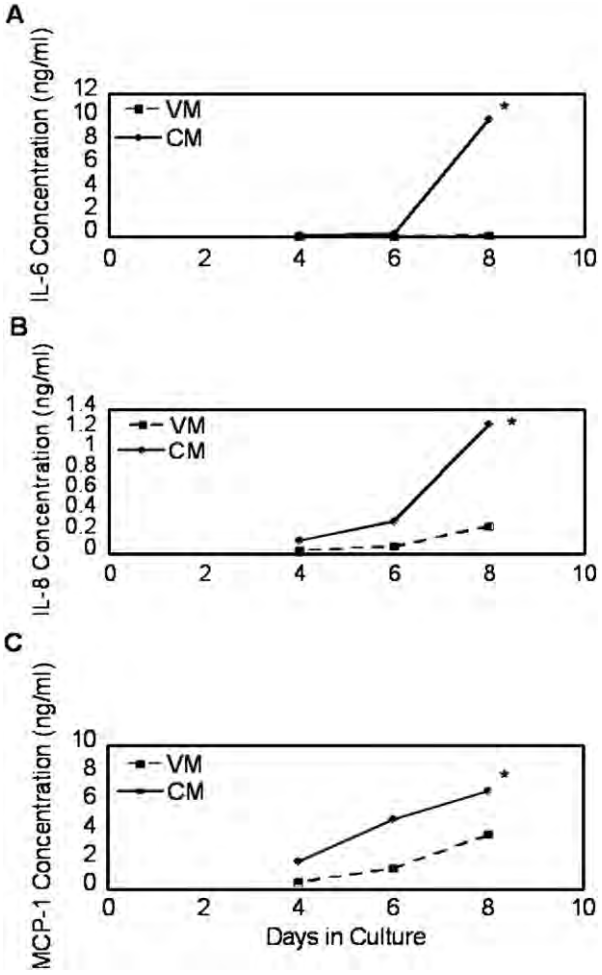

Fig. 2 – Increase in secretion of IL-6 by hFOB 1.19 at various stages of differentiation in the presence of breast cancer conditioned medium. hFOB 1.19 were grown at 34 °C until confluency (day 6) when they were changed to differentiation conditions as indicated in the methods section. Twenty-four hours prior to the indicated day, osteoblasts were treated with either VM or CM. The resultant culture supernatants were collected and assayed by ELISA. (A) IL-6; (B) IL-8; (C) MCP-1. The concentration of IL-6 in the BCCM alone was approximately 73 pg/ml, IL-8 was 449 pg/ml and MCP-1 was undetectable (<2 pg/ml). These baseline cytokine levels were subtracted from values obtained after hFOB treatment with CM. Experiment was performed twice for days 4 and 6 and eight times for day 8 with similar results. Shown is a representative experiment. By paired t-test, *P=0.004 for IL-6, and 0.001 for IL-8 in a total of 5 separate experiments. *P=0.022 for MCP-1 in a total of 4 separate experiments (P value calculations included data not shown).

maintained throughout all stages of osteoblast differentiation (day 4 osteoblasts treated with VM=0.47 ng/ml MCP-1, CM=1.92 ng/ml MCP-1; day 8 osteoblasts treated with VM=3.77 ng/ml MCP-1, CM=6.84 ng/ml MCP-1).

The dose response of CM-treated osteoblast cytokine expression was determined by treating hFOB 1.19 with 50%, 25%, and 12.5% BCCM. After 24 h, the resultant culture supernatants were collected and assayed by ELISA for IL-6, IL-8, and MCP-1. Osteoblast production of IL-6, IL-8, and MCP-1 increased as the percentage of BCCM was increased (Fig. 3).

To determine if the altered cytokine production was specific to breast cancer conditioned medium, osteoblast cultures were treated with osteoblast CM. There were no significant changes in osteoblast production of IL-6, IL-8, or MCP-1 compared to treatment with VM (data not shown).

Direct co-culture of hFOB 1.19 and MDA-MB-231 breast cancer cells

A direct co-culture model was tested to determine if the changes similar to treatment with CM occurred with cell contact. MDA-MB-231 cells were added to a differentiating (day 8 at 39 °C) monolayer of hFOB 1.19 at a ratio of 1:10, MDA-MB-231 to hFOB cells. MDA-MB-231 and hFOB 1.19 cells were cultured separately as controls. After 24 h, the culture supernatants were collected and assayed for IL-6 and IL-8 by ELISA. The supernatant from the osteoblast-cancer cell co-culture contained nearly 40 ng/ml of IL-6 and 10 ng/ml of IL-8, while the hFOB 1.19 cells alone expressed ~6 ng/ml IL-6 and ~3.5 ng/ml IL-8 (Fig. 4). Breast cancer cells cultured alone expressed

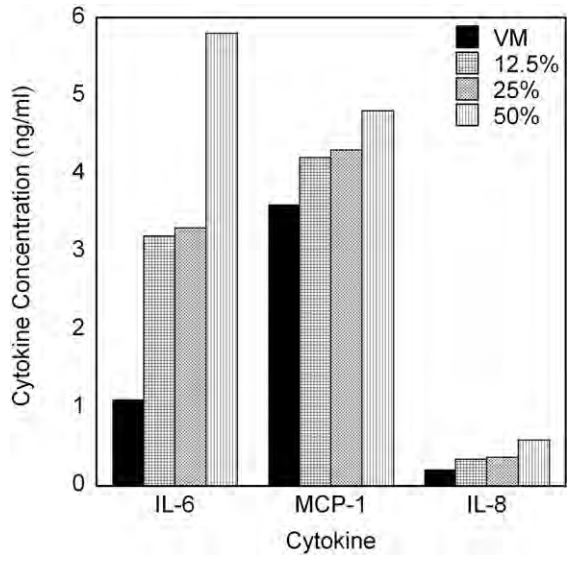

Fig. 3 – The hFOB 1.19 increase in cytokine secretion by breast cancer conditioned medium was dose dependent. hFOB 1.19 cells were plated and grown at 34 °C until confluency when they were changed to differentiation conditions as indicated in the methods section. On day 7, osteoblasts were treated for 24 h with VM or CM at either 50%, 25%, or 12.5% BCCM. The resultant culture supernatants were collected and cytokine levels determined by ELISA.

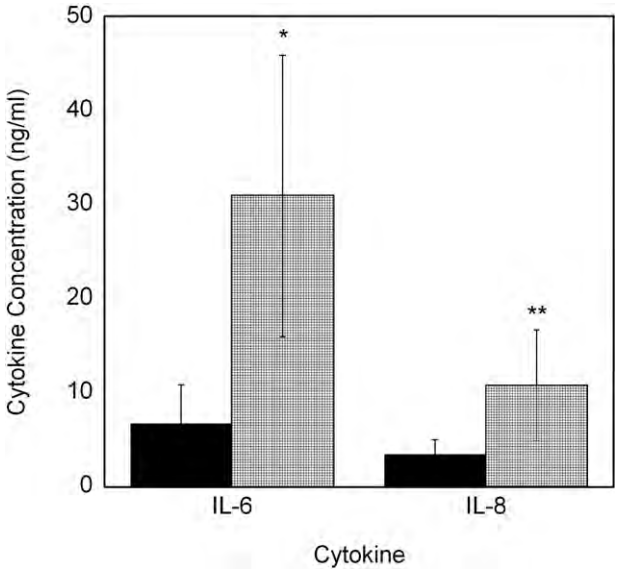

Fig. 4 – Increase in cytokine production by hFOB 1.19 co-cultured directly with MDA-MB-231 Cells. hFOB 1.19 were plated and grown at 34 °C until day 6 when the confluent cultures were moved to 39 °C. On day 7, cells were counted, and MDA-MB-231 metastatic breast cancer cells were added to the existing hFOB osteoblast cultures at a ratio of 1:10 (breast cancer cells: osteoblasts). MDA-MB-231 cells were also plated alone. Cultures were then incubated at 37 °C for 24 h. The resultant culture supernatants were collected and assayed by ELISA for IL-6 and IL-8. Medium from MDA-MB-231 cells cultured alone had undetectable levels of IL-6 and IL-8. Solid bars, hFOB 1.19 cells; checked bars, MDA-MB-231 cells co-cultured with hFOB cells at a 1:10 ratio. $N \geq 2$, $^{*}P < 0.005$; $^{**}P < 0.05$.

<200 pg/ml of IL-6 or IL-8. Therefore, there was a 6-fold increase in IL-6 and a 3-fold increase in IL-8 production under co-culture conditions. While we believe that the cytokines were produced by the osteoblasts, it is possible, in a co-culture situation, the osteoblasts may have stimulated the breast cancer cells to increase cytokine production.

MC3T3-E1 osteoblasts increased cytokine production in the presence of MDA-MB-231 conditioned medium

Due to the temperature-sensitive nature of the hFOB 1.19 cells and the complications of using two human cells lines, we also tested a murine osteoblast line, MC3T3-E1. In initial experiments, the cells were cultured for 25 days in MC3T3-E1 osteoblast differentiation medium before being treated with VM or CM for 24 h. The resultant culture supernatants were collected and assayed with a RayBio® Mouse Cytokine Array III system. There were visible increases in IL-6 and MCP-1 as well as LIX (CXCL 5), macrophage inflammatory protein-1 γ (MIP-1γ), and RANTES (Fig. 5). Similar increases were observed when the MC3T3-E1 cells were treated with CM after 12 days of culture, a time when the osteoblasts were in the early matrix-forming stage (data not shown). These assays were followed by murine ELISAs to confirm and quantify

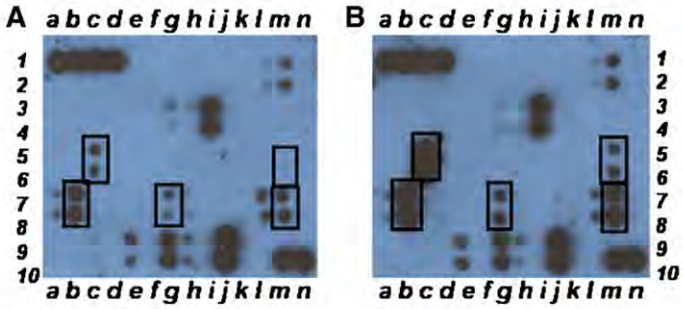

RayBio® Mouse Array System III

	a	b	c	d	e	f	g	h	i	j	k	l	m	n
1	POS	POS	POS	POS	Blank	Axl	BLC	CD30L	CD30T	CD40	CRG-2	CTACK	CXCL16	Eotaxin
2	NEG	NEG	NEG	NEG	Blank	Axl	BLC	CD30L	CD30T	CD40	CRG-2	CTACK	CXCL16	Eotaxin
3,4	Eotaxin-2	Fas Ligand	Fracta-lkine	G-CSF	GM-CSF	IFN-γ	IGFBP-3	IGFBP-5	IGFBP-6	IL-1α	IL-1β	IL-2	IL-3	IL-3 Rb
5,6	IL-4	IL-5	IL-6	IL-9	IL-10	IL-12 p40/70	IL-12 p70	IL-13	IL-17	KC	Leptin R	Leptin	LIX	L-Selectin
7,8	Lympho-tactin	MCP-1	MCP-5	M-CSF	MIG	MIP-1α	MIP-1γ	MIP-2	MIP-3β	MIP-3α	PF-4	P-Selectin	RANTES	SCF
9	SDF-1α	TARC	TCA-3	TECK	TIMP-1	TNFα	sTNF RI	sTNF RII	TPO	VCAM-1	VEGF	Blank	Blank	Blank
10	SDF-1α	TARC	TCA-3	TECK	TIMP-1	TNFα	sTNF RI	sTNF RII	TPO	VCAM-1	VEGF	Blank	POS	POS

Fig. 5 – Conditioned medium from breast cancer cells induced osteoblast cytokine production by MC3T3-E1 cells. After 12 or 25 days in culture, MC3T3-E1 osteoblasts were treated with either VM or CM. Twenty-four hours later, the resultant culture supernatants were collected and a RayBio® Mouse Cytokine Antibody Array III was used to detect changes in osteoblast cytokine production. Shown are the results from 25 days; 12-day results were similar. (A) Murine osteoblast VM cytokine production. (B) Murine osteoblast cytokine production after 24 h treatment with CM. From left to right: MCP-1 (b7,8), IL-6 (c5,6), MIP-1γ (g7,8), LIX (m5,6), and RANTES (m7,8). Osteoblast secretion of cytokines was both induced (LIX) and increased (MCP-1, IL-6, MIP-1γ, and RANTES) when treated for 24 h with CM.

MCP-1 and IL-6 expression. The increases in murine IL-6 were substantial (Fig. 6). For example, osteoblasts treated with VM for 6 h contained 0.72 ng/ml IL-6, whereas treatment for 6 h with CM yielded 4.32 ng/ml. The increases in murine MCP-1, however, were less dramatic (~4 ng/ml compared with ~7 ng/ml, data not shown). Since mice do not express IL-8, we assayed for the murine cytokine MIP-2, thought to function similarly to IL-8 [13]. MIP-2 was detected at low concentrations (~8 pg/ml) but increased with exposure to CM (~100 pg/ml, data not shown). Thus, exposure to BCCM elicited a similar cytokine response in both human and murine osteoblast lines. Additionally, an increased IL-6 response was demonstrated in primary mouse osteoblasts isolated from neonatal calvaria (Fig. 7). Due to the consistent dramatic increase in murine IL-6 production by the treated osteoblasts, IL-6 was designated as the signature cytokine for the inflammatory response.

To determine the response time to BCCM, MC3T3-E1 cells were cultured for 12 days and treated with VM or CM for 2, 4, or 6 h. The resultant culture supernatants were assayed for murine IL-6. As little as 2 h of exposure to the CM elicited a 2-fold increase in murine IL-6 secretion by the osteoblasts (VM treatment, 0.84 ng/ml IL-6; CM treatment, 1.8 ng/ml IL-6). After 6 h, the increase was nearly 5-fold (VM treatment, 0.72 ng/ml IL-6; CM treatment, 4.32 ng/ml IL-6) (Fig. 6).

Parathyroid hormone-related peptide, transforming growth factor-beta, and IL-1beta are candidate factors for mediating the expression of osteoblast cytokines

PTHrP, interleukin-1beta (IL-1β), and TGF-β are reported to be present in breast cancer conditioned media and have been reported to induce at least one cytokine of interest (IL-6, IL-8, or MCP-1) [23,24]. Therefore, they were considered as possible factors secreted by MDA-MB-231 cells that may promote osteoblast cytokine expression.

IL-1 β was not detected therefore, it was eliminated from further consideration. PTHrP was present at 46 pg/ml, approximately 2×10^{-12}M (Andrea Manni, Penn State Hershey). A similar value was reported by Guise et al. [24]. This concentration was too low to bring about an increase in IL-6 expression by the osteoblasts (data not shown). However, TGF-β was found to be present at between 1 and 5 ng/ml depending on the batch of conditioned medium (also see Mercer et al. [17]). These concentrations are sufficient to stimulate IL-6 production by the osteoblasts (see Fig. 8). We tested the

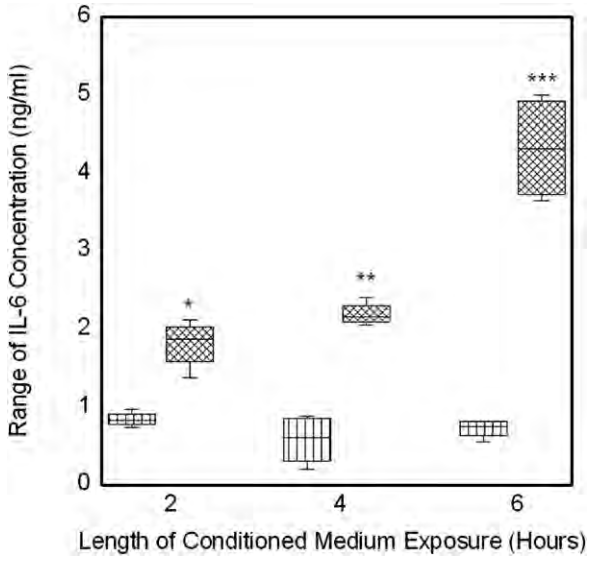

Fig. 6 – Conditioned medium from breast cancer cells rapidly induced osteoblast IL-6 production. After 12 days in culture, MC3T3-E1 osteoblasts were treated with VM or CM for 2, 4, or 6 h. The resultant culture supernatant was collected and murine IL-6 levels measured by ELISA. Shown is the range of IL-6 concentrations vs. hours of exposure to CM treatment in a box plot. Black bar, vehicle medium; checked bar, conditioned medium. N = 2 per condition. *P < 0.005 (2 h); **P < 0.0005 (4 h); ***P < 0.001 (6 h).

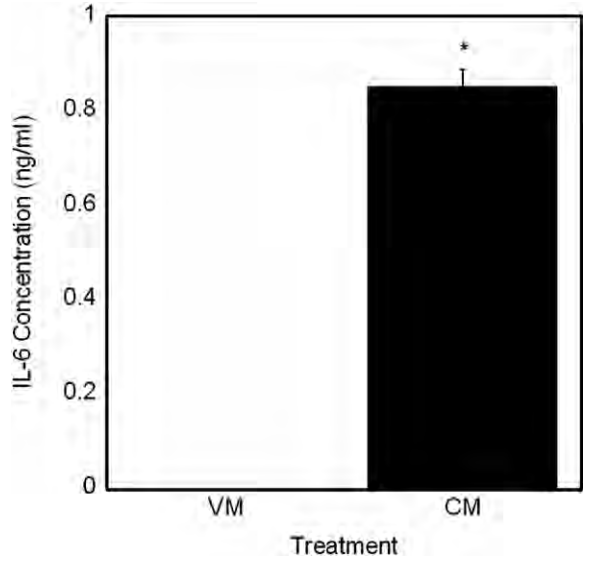

Fig. 7 – Primary murine calvarial osteoblasts secreted IL-6 in response to breast cancer conditioned medium. Primary osteoblasts were isolated from the calvariae of neonatal C57bl/6 mice as described in the methods section. The cells were cultured in calvariae differentiation medium for 14 days before the medium was changed to 50% VM or CM. After 24 h, culture media were collected and murine IL-6 was quantitated by ELISA. Shown are the means ± standard deviation. N = 3 per condition; *P < 0.001.

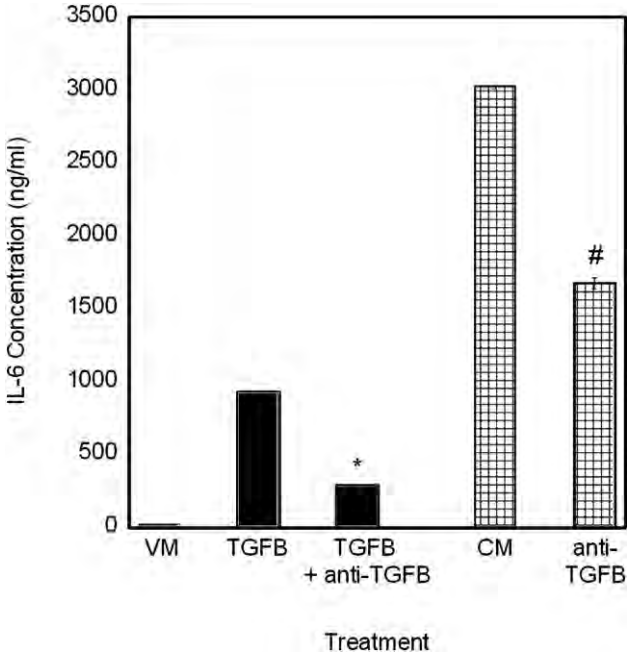

Fig. 8 – TGF-β is partially responsible for the expression of IL-6 by MC3T3-E1. MC3T3-E1 cells were cultured for 15 days. Conditioned medium from MDA-MB-231 cells, containing 1.4 ng/ml TGFβ, later determined by ELISA, was added to the cells at 50% or incubated for 1 h at 37° with 10 μg/ml neutralizing antibody to TGF-$\beta_{1,2,3}$ before addition. Other cultures were incubated with 2.5 ng/ml TGF-β or TGF-β that had been pre-incubated with 10 μg/ml antibody to TGF-$\beta_{1,2,3}$. One set of cultures was incubated with vehicle medium only. After 4 h incubation, the culture media were collected and assayed for IL-6. Black bar, vehicle medium; checked bar, conditioned medium. Shown are the means ± standard deviation of a representative experiment. This experiment was conducted three times in duplicate with similar results (N = 6 per condition); *P < 0.0003; #P < 0.0004.

combination of a suboptimal concentration of 0.5 ng/ml TGF-β with 5×10^{-12} M PTHrP and did not find a synergistic production of IL-6 (data not shown). Therefore, we focused on TGF-β in the breast cancer cell conditioned medium.

We determined the effect of adding a TGF-β neutralizing antibody to the breast cancer cell conditioned medium. Addition of conditioned medium to MC3T3-E1 increased their production of IL-6 nearly 200-fold compared to addition of regular differentiation medium (VM) (Fig. 8). Treatment of the conditioned medium with an excess (10 μg/ml) of neutralizing antibody to TGF-$\beta_{1,2,3}$ reduced osteoblast IL-6 expression by 45% compared with untreated conditioned medium. Addition of TGFβ (2.5 ng/ml) to the osteoblasts increased IL-6 production by approximately 50-fold. This value was reduced by 70% following incubation of the TGFβ antibody with the TGFβ before addition to the cells. We later determined that the conditioned medium contained approximately 1.4 ng/ml TGFβ. Thus, the antibody was far in excess of that required to neutralize 90% of the antigen. A similar result was seen when we used an inhibitor (Tocris, Ly364947) of the TGFβ receptor (data not shown).

Discussion

We found that osteoblasts responded to conditioned medium from MDA-MB-231 human metastatic breast cancer cells with enhanced cytokine expression. Specifically, the osteoblasts increased production of IL-6, MCP-1, and IL-8 (human), three cytokines characterized as osteoblast inflammatory stress proteins. These molecules may help to provide a favorable tumor cell environment as well as initiate osteoclastogenesis. This finding supports the idea that breast cancer metastases create a unique niche in the bone microenvironment by co-opting the normal cells of the bone to favor tumor growth and development. While other cells types are undoubtedly involved in the metastatic and tumorigenic process, here we demonstrate a direct effect of metastatic breast cancer cells on osteoblasts.

Breast cancer metastasis to bone is predominantly an osteolytic disease whereby osteoclasts, not cancer cells, are the cause of bone degradation. According to the "vicious cycle" paradigm [5], cancer cell-secreted PTHrP activates osteoblasts to express RANKL which binds to receptor activator of nuclear factor kappa B (RANK) on osteoclasts leading to their activation and subsequent bone loss. Osteoclast resorption of the bone matrix releases TGF-β that acts on the tumors cells to stimulate more PTHrP. However, osteoclasts are not solely responsible for sustained bone loss. Administration of bisphosphonates to inhibit osteoclast activity does not result in resolution of bone lesions [15]. Lesion formation is slowed but lesions do not heal. Clearly the impact of metastatic breast cancer cells on osteoblasts cannot be ignored.

In a closer examination of the fate of the osteoblasts, it was found that in the presence of MDA-MB-231 breast cancer cells or their conditioned media, cultured osteoblasts exhibited an increase in apoptosis, a change in morphology, and suppression in differentiation and mineralization as evidenced by a lack of expression of alkaline phosphatase, bone sialoprotein, and osteocalcin [16,18]. This increase in osteoblast apoptosis and decrease in alkaline phosphatase expression was also detected *in vivo* in a mouse model [25]. In addition to these phenotypic effects, the current study demonstrates that osteoblasts exhibit an increase in inflammatory cytokines in the presence of metastatic breast cancer cells. A cytokine array revealed that three cytokines in particular, IL-6, IL-8, and MCP-1, increased dramatically when hFOB 1.19 human osteoblasts were treated with CM. IL-6 and IL-8 were also elevated when hFOB 1.19 cells were co-cultured. MC3T3-E1 murine osteoblasts displayed a similar increase in murine IL-6 and MCP-1 when exposed to metastatic breast cancer cell conditioned media. As further evidence, we have also seen an increase in MIP-2 and KC (murine homologues to human IL-8 [13]) both *in vitro* and *ex vivo* (unpublished data). Exposure of primary murine osteoblasts to MDA-MB-231 breast cancer conditioned medium also elicited an increase in murine IL-6. These same cytokines are expressed in high levels by osteoblasts in debris-mediated osteolysis [26], which occurs when particles from prosthetic devices cause a chronic state of inflammation in the bone microenvironment [12]. Additionally, osteoblasts exposed to *M. tuberculosis* or *S. aureus* both *in vitro* and *in vivo* undergo an inflammatory stress response and produce IL-6, IL-8, and MCP-1 [10,27,28]. The infection of bone by these two microbes elicits the chronic inflammatory response and bone damage observed in trauma-induced osteomyelitis. Thus, the present study indicates that breast cancer cells evoke a similar stress response from osteoblasts.

IL-6 is a pleiotropic cytokine that influences many biological events including bone remodeling. In particular, IL-6 plays a role in the formation and activation of osteoclasts both *in vitro* and *in vivo* [29,30]. IL-6 has been implicated in the pathogenesis of bone resorption associated with Paget's disease [31], Gorham-Stout (disappearing bone disease) syndrome [32], and multiple myeloma [33]. Of interest to this study, IL-6 has been shown to induce production of PTHrP in human osteoblastic cells [34]. Soluble PTHrP, which is also derived from tumor cells [35], can stimulate the production of additional osteoblast-derived IL-6 through a feedback loop and facilitate osteoclastogenesis by decreasing the production of OPG and increasing osteoblast expression of RANKL. The bone resorption that subsequently follows releases stored TGF-β from the bone matrix that can in turn enhance breast cancer cell production of PTHrP [35].

In addition to playing a role in osteoclastogenesis and bone resorption, IL-6 has other functions that may contribute to cancer progression. Although the involvement of IL-6 in regulating the growth and apoptosis of breast cancer cells is unclear, IL-6 is known to be a growth factor for myeloma cells [36] and acts as an anti-apoptotic factor for human esophageal carcinoma and multiple myeloma cells [37,38]. In addition, IL-6 downregulates the expression of CXCL10, a chemokine with anti-malignant properties, by MDA-MB-231 cells [39]. IL-6 has also been reported to enhance the migration of T47D breast cancer cells *in vitro* [40]. Furthermore, the importance of IL-6 in cancer progression was demonstrated by a study in which IL-6 signaling in MDA-MB-231 breast cancer cells was blocked. This inhibition resulted in significantly decreased tumor engraftment, size, and metastasis in a nude mouse model [41]. Finally, IL-6 levels in breast cancer patients have been correlated with clinical stage [42,43] and rate of recurrence [44]. In particular, high IL-6 serum levels in patients with advanced or recurrent breast cancer were found to be an unfavorable prognosis indicator [45–47].

Besides acting on cells in the tumor/bone microenvironment, IL-6 has also been found to increase osteoblast production of another cytokine identified in our study: MCP-1. A monomeric polypeptide member of the CC chemokine superfamily [48], MCP-1 is a principle cytokine involved in inflammation and bone remodeling. MCP-1 is known to recruit cells involved in inflammation [13], osteoclast precursors [13], and angiogenesis [49]. These three processes are clearly involved in breast cancer tumorigenesis and lesion formation in the bone. MCP-1 is also normally produced by osteoblasts [50], but also is increased in metastatic cell lines [51].

MCP-1 has been found to be particularly important in cancer cell migration and metastasis. In a study that utilized the metastatic PC3, LNCaP, and bone metastatic LNCaP C4-2B prostate cancer cells, it was found that MCP-1 increased proliferation and invasion [52]. Interestingly, the G-protein-coupled receptor CCR2, the receptor for MCP-1, was found to be present on all the prostate cancer cell lines examined [52]. In addition, prostate cancer cells were found to produce high

levels of MCP-1 compared to primary prostate epithelial cells [53]. In that same study, MCP-1 was shown to mediate prostate cancer tumor-induced osteoclastogenesis and bone resorption [53]. In breast and ovarian cancer patients, MCP-1 serum levels have been correlated with advanced tumor stage [54,55]. In addition, the expression of MCP-1 in squamous cell carcinoma of the esophagus was equated with venous invasion and metastasis [56]. Furthermore, it has been shown that MCP-1 acts as a chemoattractant for myeloma cells [57]. Thus, it is evident that MCP-1 is a key mediator involved in inflammation and cancer cell progression.

IL-8 is a CXC inflammatory cytokine produced by many cell types including osteoblasts [50,58]. IL-8 was first identified as a neutrophil chemoattractant and is now known to attract monocytes and osteoclast precursors as well as promote angiogenesis [13,59]. In the bone, IL-8 has been shown to directly inhibit alkaline phosphatase expression [60] as well as decrease normal bone resorption and increase the motility of osteoclasts to new resorption sites [61]. Interestingly, human osteoclasts have also been shown to secrete high levels of IL-8, indicating the molecule's importance in normal bone remodeling [62].

Along with IL-6 and MCP-1, IL-8 has also been found to be important in cancer cell progression. IL-8 is secreted by many tumor cell lines that are metastatic and osteolytic [63]. In addition, IL-8 appears to play a role in cell motility, invasion, and metastatic potential in human tumors [64–66]. Concerning this present study, increased bone metastatic potential of human breast cancer cells has been associated with the cancer cell's ability to express IL-8. In several studies done by Bendre et al. [58,63,67], metastatic breast cancer cell-derived IL-8 was found to directly stimulate osteoclastogenesis via RANKL dependent and independent mechanisms. In particular, it was proposed that IL-8 plays an important role in the "vicious cycle" of breast cancer cell metastasis to the bone. Breast cancer cell-derived IL-8 increased RANKL expression on osteoblasts, which in turn, facilitated osteoclast formation. In addition, soluble IL-8 directly promoted osteoclastogenesis, leading to bone resorption. Stored TGF-β is then released from the bone matrix that continues to drive the "vicious cycle," amplifying osteolysis and supporting breast cancer bone metastases [58]. IL-8 has also been implicated in the clinical outcome of patients with breast cancer. In a study involving 69 women with operable or advanced breast cancer, elevated serum IL-8 levels were found to be directly associated with the clinical stage of breast cancer and were found to be indicative of a poor prognosis [42,68].

Do these cytokines feedback directly onto the tumor cells? It seems unlikely since the MDA-MB-231 cells do not have receptors for these cytokines. Specifically, as reported in the literature, MDA-MB-231 cells do not express the CXCR1 receptor for IL-8, [63] but do express low levels of CXCR2 mRNA [69]. Nonetheless, neutralizing antibody to IL-8 did not affect the growth of the MDA-MB-231 cells [70]. MDA-MB-231 cells do not express receptors for IL-6 [71,72]. This finding is consistent with their lack of response to IL-6 [73]. There is one report of low expression for the mRNA for the receptor for MCP-1, but none for the protein itself [74]. These reports taken together indicate that the cancer cells would not be expected to respond to these cytokines.

Our hypothesis is that osteoblasts produce these cytokines in response to the cancer cells, and that these cytokines then go on to activate osteoclasts. It is well documented in the literature that IL-6, IL-8, and MCP-1 have osteoclast stimulating properties [67,75–77].

In summary, we have shown that osteoblasts display an inflammatory response when exposed to breast cancer cell conditioned medium. The inflammatory cytokines, IL-6, MCP-1, and IL-8 can target osteoclast precursors and osteoclasts to bring about bone matrix destruction. Thus, osteoblasts contribute to the osteolytic phenotype, both through suppression of bone deposition and production of cytokines that recruit and activate osteoclasts.

Acknowledgments

This work was supported by the U.S. Army Medical and Material Research Command Breast Cancer Program (DAMD 17-02-1-0358 and W81XWH-06-1-0432 to AMM, W81XWH-06-1-0363 to KMB); National Foundation for Cancer Research, Center for Metastasis Research; The Susan G. Komen Breast Cancer Foundation, BCTR104406; The American Institute of Cancer Research, #06A027-REV2; Sigma Xi, Undergraduate Research Grants; President's Fund, and Schreyer Honors College research awards to M.K. and E.C. The authors would like to thank Richard Ball of the Immunomodulation Core, Penn State GCRC (work supported by NIH M01RR10732) for technical advice regarding ELISAs and Donna Sosnoski for editorial assistance.

REFERENCES

[1] E.F. Solomayer, I.J. Diel, G.C. Meyberg, C. Gollan, G. Bastert, Metastatic breast cancer: clinical course, prognosis and therapy related to the first site of metastasis, Breast Cancer Res. Treat. 59 (2000) 271–278.
[2] R.D. Rubens, G.R. Mundy, Cancer and the skeleton, Martin Dunitz, London, 2000.
[3] R.D. Rubens, Bone metastases—the clinical problem, Eur. J. Cancer 34 (1998) 210–213.
[4] G.R. Mundy, D. Chen, B.O. Oyajobi, Bone Remodeling, in: M.J. Favus (Ed.), Primer on the Metabolic Bone Diseases and Disorders of Mineral Metabolism, American Society for Bone and Mineral Research, Washington D.C., 2003, Number of 567 pp.
[5] W. Kozlow, T. Guise, Breast cancer metastasis to bone: mechanisms of osteolysis and implications for therapy, J. Mammary Gland Biol. Neoplasia 10 (2005) 169–180.
[6] T.A. Guise, J.M. Chirgwin, Transforming growth factor-beta in osteolytic breast cancer bone metastases, Clin. Orthop. Relat. Res. 4155 (2003) 532–538.
[7] G.D. Roodman, Biology of osteoclast activation in cancer, J. Clin. Oncol. 19 (2001) 3562–3571.
[8] M. Bendre, D. Gaddy-Kurten, T. Foote-Mon, N.S. Akel, R.A. Skinner, R.W. Nicholas, L.J. Suva, Expression of interleukin 8 and not parathyroid hormone-related protein by human breast cancer cells correlates with bone metastasis in vivo, Cancer Res. 62 (2002) 5571–5579.
[9] K. de Visser, L. Coussens, The inflammatory tumor microenvironment and its impact on cancer development, Contrib. Microbiol. 13 (2006) 118–137.

[10] I. Marriott, Osteoblast responses to bacterial pathogens: a previously unappreciated role for bone-forming cells in host defense and disease progression, Immunol. Res. 30 (2004) 291–308.
[11] K.M. Wright, J.S. Friedland, Regulation of chemokine gene expression and secretion in *Staphylococcus aureus*-infected osteoblasts, Microbes Infect. 6 (2004) 844–852.
[12] E. Fritz, T. Glant, C. Vermes, J. Jacobs, K. Roebuck, Titanium particles induce the immediate early stress responsive chemokines IL-8 and MCP-1 in osteoblasts, J. Orthop. Res. 20 (2002) 490–498.
[13] K.A. Fitzgerald, L.A.J. O'Neill, A.J.H. Gearing, R.E. Callard, The Cytokine Facts Book, Academic Press, New York, 2001.
[14] M. Clemons, G. Dranitsaris, D. Cole, M.C. Gainford, Too much, too little, too late to start again? Assessing the efficacy of bisphosphonates in patients with bone metastases from breast cancer, Oncologist 11 (2006) 227–233.
[15] A. Lipton, Bisphosphonates and breast carcinoma: present and future, Cancer 88 (2000) 3033–3037.
[16] A.M. Mastro, C.V. Gay, D.R. Welch, H.J. Donahue, J. Jewell, R. Mercer, D. DiGirolamo, E.M. Chislock, K. Guttridge, Breast cancer cells induce osteoblast apoptosis: a possible contributor to bone degradation, J. Cell. Biochem. 91 (2004) 265–276.
[17] R. Mercer, C. Miyasaka, A.M. Mastro, Metastatic breast cancer cells suppress osteoblast adhesion and differentiation, Clin. Exp. Metastasis 21 (2004) 427–435.
[18] R.M. Mercer, A.M. Mastro, Cytokines secreted by bone-metastatic breast cancer cells alter the expression pattern of f-actin and reduce focal adhesion plaques in osteoblasts through PI 3K, Exp. Cell Res. 310 (2005) 270–281.
[19] S.A. Harris, R.J. Enger, B.L. Riggs, T.C. Spelsberg, Development and characterization of a conditionally immortalized human fetal osteoblastic cell line, J. Bone Miner. Res. 10 (1995) 178–186.
[20] H. Sudo, H.A. Kodama, Y. Amagai, S. Yamamoto, S. Kasai, In vitro differentiation and calcification in a new clonal osteogenic cell line derived from newborn mouse calvaria, J. Cell Biol. 96 (1983) 191–198.
[21] R. Cailleau, M. Olive, Q.V. Cruciger, Long-term human breast carcinoma cell lines of metastatic origin: preliminary characterization, In Vitro 14 (1978) 911–915.
[22] A. Bakker, J. Klein-Nulend, in: M.P. Helfrich, S.H. Ralston (Ed.), Bone Research Protocols, Humana Press, Totowa, New Jersey, 2003, pp. 19–28.
[23] L. Pederson, B. Winding, N.T. Foged, T.C. Spelsberg, M.J. Oursler, Identification of breast cancer cell line-derived paracrine factors that stimulate osteoclast activity, Cancer Res. 59 (1999) 5849–5855.
[24] T.A. Guise, J.J. Yin, S.D. Taylor, Y. Kumagai, M. Dallas, B.F. Boyce, Y.T., M.G.R., Evidence for a causal role of parathyroid hormone-related protein in the pathogenesis of human breast-cancer-mediated osteolysis, J. Clin. Invest. 98 (1996) 1544–1549.
[25] P.A. Phadke, R.R. Mercer, J.F. Harms, Y. Jia, A.R. Frost, J.L. Jewell, K.M. Bussard, S. Nelson, C. Moore, J.C. Kappes, C.V. Gay, A.M. Mastro, D.R. Welch, Kinetics of metastatic breast cancer cell trafficking in bone, Clin. Cancer Res. 12 (2006) 1431–1440.
[26] E. Fritz, J. Jacobs, T. Glant, K. Roebuck, Chemokine IL-8 induction by particulate wear debris in osteoblasts is mediated by NF-kappaB, J. Orthop. Res. 23 (2005) 1249–1257.
[27] K. Wright, J. Friedland, Complex patterns of regulation of chemokine secretion by Th2-cytokines, dexamethasone, PGE2 in tuberculous osteomyelitis, J. Clin. Immunol. 23 (2003) 184–193.
[28] K.L. Bost, J.L. Bento, C.C. Petty, L.W. Schrum, M.C. Hudson, I. Marriott, Monocyte chemoattractant protein-1 expression by osteoblasts following infection with *Staphylococcus aureus* or Salmonella, J. Interferon Cytokine Res. 21 (2001) 297–304.
[29] N. Kurihara, D. Bertolini, T. Suda, Y. Akiyama, G.D. Roodman, IL-6 stimulates osteoclast-like multinucleated cell formation in long term human marrow cultures by inducing IL-1 release, J. Immunol. 144 (1990) 4226–4230.
[30] K. Black, I.R. Garrett, G.R. Mundy, Chinese hamster ovarian cells transfected with the murine interleukin-6 gene cause hypercalcemia as well as cachexia, leukocytosis and thrombocytosis in tumor-bearing nude mice, Endocrinology 128 (1991) 2657–2659.
[31] G.D. Roodman, N. Kurihara, Y. Ohsaki, A. Kukita, D. Hosking, A. Demulder, J.F. Smith, F.R. Singer, Interleukin 6. A potential autocrine/paracrine factor in Paget's disease of bone, J. Clin. Invest. 89 (1992) 46–52.
[32] R.D. Devlin, H.G. Bone III, G.D. Roodman, Stimulation of osteoclast-like multinucleated cell (MNC) formation in long-term human bone marrow culture by the serum of patients with Gorham-Stout or disappearing bone disease, J. Bone Miner. Res. 9 (1994) S140.
[33] B. Klein, J. Wijdenes, X.-G. Zhang, M. Jourdan, J.-M. Boiron, J. Brochier, J. Liautard, M. Merlin, C. Clement, B. Morel-Fournier, Z.-Y. Lu, P. Mannoni, J. Sany, R. Bataille, Murine anti-interleukin-6 monoclonal antibody therapy for a patient with plasma cell leukemia, Blood 78 (1991) 1198–1204.
[34] C. Guillen, A.R. de Gortazar, P. Esbrit, The interleukin-6/soluble interleukin-6 receptor system induces parathyroid hormone-related protein in human osteoblastic cells, Calcif. Tissue Int. 75 (2004) 153–159.
[35] G. Mundy, Metastasis to bone: causes, consequences and therapeutic opportunities, Nat. Rev., Cancer 2 (2002) 584–593.
[36] N. Nishimoto, T. Kishimoto, Interleukin 6: from bench to bedside, Nat. Clin. Pract. Rheumatol. 2 (2006) 691.
[37] C.M. Leu, F.H. Wong, C. Chang, S.F. Huang, C.P. Hu, Interleukin-6 acts as an antiapoptotic factor in human esophageal carcinoma cells through the activation of both STAT3 and mitogen-activated protein kinase pathways, Oncogene 22 (2003) 7809–7818.
[38] K. Brocke-Heidrich, A.K. Kretzschmar, G. Pfeifer, C. Henze, D. Loffler, D. Koczan, H.J. Thiesen, R. Burger, M. Gramatzki, F. Horn, Interleukin-6-dependent gene expression profiles in multiple myeloma INA-6 cells reveal a Bcl-2 family-independent survival pathway closely associated with Stat3 activation, Blood 103 (2004) 242–251.
[39] L. Goldberg-Bittman, E. Neumark, O. Sagi-Assif, E. Azenshtein, T. Meshel, I.P. Witz, A. Ben-Baruch, The expression of the chemokine receptor CXCR3 and its ligand, CXCL10, in human breast adenocarcinoma cell lines, Immunol. Lett. 92 (2004) 171–178.
[40] A. Badache, N.E. Hynes, Interleukin 6 inhibits proliferation and, in cooperation with an epidermal growth factor receptor autocrine loop, increases migration of T47D breast cancer cells, Cancer Res. 61 (2001) 383–391.
[41] K.S. Selander, L. Li, L. Watson, M. Merrell, H. Dahmen, P.C. Heinrich, G. Muller-Newen, K.W. Harris, Inhibition of gp130 signaling in breast cancer blocks constitutive activation of Stat3 and inhibits in vivo malignancy, Cancer Res. 64 (2004) 6924–6933.
[42] L. Kozlowski, I. Zakrzewska, P. Tokajuk, M.Z. Wojtukiewicz, Concentration of interleukin-6 (IL-6), interleukin-8 (IL-8), and interleukin-10 (IL-10) in blood serum of breast cancer patients, Rocz. Akad. Med. Bailymst. 48 (2003) 82–84.
[43] I. Benoy, R. Salgado, C. Colpaert, R. Weytjens, P.B. Vermeulen, L.Y. Dirix, Serum interleukin 6, plasma VEGF, serum VEGF, and VEGF platelet load in breast cancer patients, Clin. Breast Cancer 2 (2002).
[44] L. Mettler, A. Salmassi, M. Heyer, A. Schmutzier, R. Schollmeyer, W. Jonat, Perioperative levels of interleukin-1beta and interleukin-6 in women with breast cancer, Clin. Exp. Obstet. Gynecol. 31 (2004) 20–22.

[45] G.J. Zhang, I. Adachi, Serum interleukin-6 levels correlate to tumour progression and prognosis in metastatic breast carcinoma, Anticancer Res. 19 (1999) 1427–1432.
[46] H.U. Bozcuk, G.M. Samur, M. Yildiz, T. Ozben, M. Ozdogan, M. Artac, H. Altunbas, I. Akan, B. Savas, Tumour necrosis factor-alpha, interleukin-6, and fasting serum insulin correlate with clinical outcome in metastatic breast cancer patients treated with chemotherapy, Cytokine 27 (2004) 58–65.
[47] R. Salgado, S. Junius, I. Benoy, P. Van Dam, P.B. Vermeulen, E. Van Marck, P. Huget, L.Y. Dirix, Circulating interleukin-6 predicts survival in patients with metastatic breast cancer, Int. J. Cancer 103 (2003) 642–646.
[48] D.T. Graves, Y. Jiang, A.J. Valente, The expression of monocyte chemoattractant protein-1 and other chemokines by osteoblasts, Front. Biosci. 4 (1999) D571–D580.
[49] V. Goede, L. Brogelli, M. Ziche, H.G. Augustin, Induction of inflammatory angiogenesis by monocyte chemoattractant protein-1, Int. J. Cancer 82 (1999) 765–770.
[50] M.C. Horowitz, J.A. Lorenzo, Principles of Bone Biology, Academic Press, San Diego, 2002.
[51] E. Neumark, M.A. Cohn, E. Lukanidin, I.P. Witz, A. Ben-Baruch, Possible co-regulation of genes associated with enhanced progression of mammary adenocarcinomas, Immunol. Lett. 82 (2002) 111–121.
[52] Y. Lu, Z. Cai, D. Galson, G. Xiao, Y. Liu, D. George, M. Melhem, Z. Yao, J. Zhang, Monocyte chemotactic protein-1 (MCP-1) acts as a paracrine and autocrine factor for prostate cancer growth and invasion. Prostate 66 (2006) 1311–1318.
[53] Y. Lu, Z. Cai, G. Xiao, E.T. Keller, A. Mizokami, Z. Yao, G.D. Roodman, J. Zhang, Monocyte chemotactic protein-1 mediates prostate cancer-induced bone resorption, Cancer Res. 67 (2007) 3646–3653.
[54] A. Lebrecht, L. Hefler, C. Tempfer, H. Koelbl, Interleukin-4, interferon-gamma, and monocyte chemoattractant protein-1, Gynecol. Oncol. 83 (2001) 170–171.
[55] L. Hefler, C. Tempfer, G. Heinze, K. Mayerhofer, G. Breitenecker, S. Leodolter, A. Reinthaller, C. Kainz, Monocyte chemoattractant protein-1 serum levels in ovarian cancer patients, Br. J. Cancer 81 (1999) 855–859.
[56] N. Koide, A. Nishio, T. Sato, A. Sugiyama, S. Miyagawa, Significance of macrophage chemoattractant protein-1 expression and macrophage infiltration in squamous cell carcinoma of the esophagus, Am. J. Gastroenterol. 99 (2004) 1667–1674.
[57] K. Johrer, K. Janke, J. Krugmann, M. Fiegl, R. Greil, Transendothelial migration of myeloma cells is increased by tumor necrosis factor (TNF)-alpha via TNF receptor 2 and autocrine upregulation of MCP-1, Clin. Cancer Res. 10 (2004) 1901–1910.
[58] M. Bendre, D. Gaddy, R.W. Nicholas, L.J. Suva, Breast cancer metastasis to bone: it is not all about PTHrP, Clin. Orthop. Relat. Res. 415S (2003) S39–S45.
[59] N. Mukaida, S.A. Ketlunsky, K. Matsushima, The Cytokine Handbook, Academic Press, Amsterdam, 2003.
[60] L.R. Chaudhary, L.V. Avioli, Dexamethasone regulates IL-1 beta and TNF-alpha-induced interleukin-8 production in human bone marrow stromal and osteoblast-like cells, Calcif. Tissue Int. 55 (1994) 16–20.
[61] K. Fuller, J.M. Owens, T.J. Chambers, Macrophage inflammatory protein-1 alpha and IL-8 stimulate the motility but suppress the resorption of isolated rat osteoclasts, J. Immunol. 154 (1995) 6065–6072.
[62] L. Rothe, P. Collin-Osdoby, Y. Chen, T. Sunyer, L. Chaudhary, A. Tsay, S. Goldring, L. Avioli, P. Osdoby, Human osteoclasts and osteoclast-like cells synthesize and release high basal and inflammatory stimulated levels of the potent chemokine interleukin-8, Endocrinology 139 (1998) 4353–4363.
[63] M.S. Bendre, A.G. Margulies, B. Walser, N.S. Akel, S. Bhattacharrya, R.A. Skinner, F. Swain, V. Ramani, K.S. Mohammad, L.L. Wessner, A. Martinez, T.A. Guise, J.M. Chirgwin, D. Gaddy, L.J. Suva, Tumor-derived interleukin-8 stimulates osteolysis independent of the receptor activator of nuclear factor-kappaB ligand pathway, Cancer Res. 65 (2005) 11001–11009.
[64] D. Arenberg, S. Kunkel, P. Polverini, M. Glass, M.D. Burdick, R.M. Strieter, Inhibition of interleukin-8 reduces tumorigenesis of human non-small cell lung cancer in SCID mice, J. Clin. Invest. 97 (1996) 2792–2802.
[65] S. Kim, H. Uehara, T. Karashima, M. Mccarty, N. Shih, I.J. Fidler, Expression of interleukin 8 correlates with angiogenesis, tumorigenicity, and metastasis of human prostate cancer cells implanted orthotopically in nude mice, Neoplasia 3 (2001) 33–42.
[66] R. Singh, M. Varney, IL-8 expression in malignant melanoma: implications in growth and metastases, Histol. Histopathol. 15 (2000) 843–849.
[67] M. Bendre, D.C. Montague, T. Peery, N.S. Akel, D. Gaddy, L.J. Suva, Interleukin-8 stimulation of osteoclastogenesis and bone resorption is a mechanism for the increased osteolysis of metastatic bone disease, Bone 33 (2003) 28–37.
[68] I. Benoy, R. Salgado, P. Van Dam, K. Geboers, E. Van Marck, S. Scharpe, P.B. Vermeulen, L.Y. Dirix, Increased serum interleukin-8 in patients with early and metastatic breast cancer correlates with early dissemination and survival, Clin. Cancer Res. 10 (2004) 7157–7162.
[69] A. Muller, B. Homey, H. Soto, N. Ge, D. Catron, M. Buchanan, T. McClanahan, E. Murphy, W. Yuan, S. Wagner, J. Barrera, A. Mohar, E. Verastegui, A. Zlotnik, Involvement of chemokine receptors in breast cancer metastasis, Nature 410 (2001) 50–56.
[70] M.S. Bendre, A.G. Margulies, B. Walser, N.S. Akel, S. Bhattacharrya, R.A. Skinner, F. Swain, V. Ramani, K.S. Mohammad, L.L. Wessner, A. Martinez, T.A. Guise, J.M. Chirgwin, D. Gaddy, L.J. Suva, Tumor-derived interleukin-8 stimulates osteolysis independent of the receptor activator of nuclear factor-kB ligand pathway, Cancer Res. 65 (2005) 11001–11009.
[71] A.M. Douglas, G.A. Goss, R.L. Sutherland, D.J. Hilton, M.C. Berndt, N.A. Nicola, C.G. Begley, Expression and function of members of the cytokine receptor superfamily on breast cancer cells, Oncogene 14 (1997) 661–669.
[72] J.J. Chiu, M.K. Sgagias, K.H. Cowan, Interleukin 6 acts as a paracrine growth factor in human mammary carcinoma cell lines, Clin. Cancer Res. 2 (1996) 215–221.
[73] D.N. Danforth Jr., M.K. Sgagias, Interleukin-1 alpha and interleukin-6 act additively to inhibit growth of MCF-7 breast cancer cells in vitro, Cancer Res. 53 (1993) 1538–1545.
[74] J.S. Nam, M.J. Kang, A.M. Suchar, T. Shimamura, E.A. Kohn, A.M. Michalowska, V.C. Jordan, S. Hirohashi, L.M. Wakefield, Chemokine (C-C motif) ligand 2 mediates the prometastatic effect of dysadherin in human breast cancer cells, Cancer Res. 66 (2006) 7176–7184.
[75] B. Singh, J.A. Berry, L.E. Vincent, A. Lucci, Involvement of IL-8 in COX-2-mediated bone metastases from breast cancer, J. Surg. Res. 134 (2006) 44–51.
[76] G. Roodman, S. Choi, MIP-1 alpha and myeloma bone disease, Cancer Treat. Res. 118 (2004) 83–100.
[77] S. Kwan Tat, M. Padrines, S. Theoleyre, D. Heymann, Y. Fortun, IL-6, RANKL, TNF-alpha/IL-1: interrelations in bone resorption pathophysiology, Cytokine Growth Factor Rev. 15 (2004) 49–60.

Cancer Metastasis Rev (2008) 27:41–55
DOI 10.1007/s10555-007-9109-4

The bone microenvironment in metastasis; what is special about bone?

Karen M. Bussard · Carol V. Gay · Andrea M. Mastro

Published online: 11 December 2007

Abstract The skeleton is a common destination for many cancer metastases including breast and prostate cancer. There are many characteristics of bone that make it an ideal environment for cancer cell migration and colonization. Metaphyseal bone, found at the ends of long bone, in ribs, and in vertebrae, is comprised of trabecular bone interspersed with marrow and rich vasculature. The specialized microvasculature is adapted for the easy passage of cells in and out of the bone marrow. Moreover, the metasphyseal regions of bone are constantly undergoing remodeling, a process that releases growth factors from the matrix. Bone turnover also involves the production of numerous cytokines and chemokines that provide a means of communication between osteoblasts and osteoclasts, but co-incidentally can also attract and support metastatic cells. Once in the marrow, cancer cells can interact directly and indirectly with osteoblasts and osteclasts, as well as hematopoietic and stromal cells. Cancer cells secrete factors that affect the network of cells in the bone microenvironment as well as interact with other cytokines. Additionally, transient cells of the immune system may join the local mileau to ultimately support cancer cell growth. However, most metastasized cells that enter the bone marrow are transient; a few may remain in a dormant state for many years. Advances in understanding the bone cell-tumor cell interactions are key to controlling, if not preventing metastasis to bone.

Keywords Bone metastasis · Osteoblasts · Osteoclasts · Cytokines · Chemokines

K. M. Bussard · C. V. Gay · A. M. Mastro (✉)
Department of Biochemistry and Molecular Biology,
The Pennsylvania State University,
University Park, PA 16802, USA
e-mail: a36@psu.edu

C. V. Gay
e-mail: cvg1@psu.edu

K. M. Bussard
Department of Veterinary and Biomedical Sciences:
The Pathobiology Graduate Program,
The Pennsylvania State University,
University Park, PA 16802, USA
e-mail: kmb337@psu.edu

1 Tumor cell metastasis

The skeleton is a favored site of metastasis for a number of common tumors. Bone metastases are by far more prevalent than primary tumors of the bone. Based on post-mortem examination, approximately 70% of patients who die from breast or prostate cancer have bone metastases [1]. The incidences from thyroid, kidney, and lung cancer also are high (about 40%). In contrast, it has been noted that bone metastases from cancers of the gastrointestinal tract are uncommon. In many cases, cancer cell metastases are diagnosed in patients before diagnosis of the primary disease. A better understanding of the specificity and the pathogenesis of metastasis will allow for better therapeutic treatments and quality of life for patients.

The metastasis of a primary tumor to distant organs requires a series of coordinated steps. Proliferation of the primary tumor is supported by tumor autocrine factors or local growth factors, such as vascular endothelial growth factor (VEGF), tumor growth factor-beta (TGF-β), and interleukin-6 (IL-6). For a tumor to reach a clinically detectable size, localized neovascularization or angiogenesis must occur. The development of new blood vessels provide an endless supply of nutrients as well as a route for tumor cell migration to secondary sites. Subsequently, local

invasion takes place, which is accomplished by the destruction of the extracellular matrix, including the basement membrane and connective tissue. The process of invasion through a basement membrane is a hallmark characteristic of a metastatic cell. Additionally, tumor cells experience increased motility and reduced adherence allowing them to migrate into lymph or blood vessels. Intravasation into blood vessels at the primary site may occur as a result of excess force or response to a soluble chemotactic factor gradient. After circulating through the vasculature, tumor cells may adhere to vessel endothelium of the target organ and extravasate into the tissue. This movement is facilitated by cancer cell secretion of matrix metalloproteinases (MMPs) and cathepsin-K that destroy surrounding tissue. Finally, tumor cells thrive at the secondary site, a defining characteristic of metastatic tumor cells, only if there is an appropriate environment of paracrine or autocrine factors that aid in growth and vascularization [2–4]. The distribution pattern of cancer cells to the bone is believed to be due to the venous flow from breast and prostate towards the vena cava and into the vertebral venous plexus [5]. Once in the circulation, entry of the cancer cells into the venous circulation of the bone marrow may be facilitated by the slow blood flow and particular anatomy of the venous sinusoids. Nonetheless these steps alone do not explain survival and growth of the cancer cells in the bone.

2 Bone structure

In order to understand the bone-tumor microenvironment, one must consider bone structure and function. Bone is a specialized type of connective tissue, which provides structural support, protective functions, and plays a major role in the regulation of calcium levels in the body [6]. Type I collagen accounts for 95% of the organic bone matrix [7]. The remaining 5% includes proteoglycans and a variety of other non-collagenous proteins [6]. This largely collagenous matrix is hardened through the mineralization process, in which hydroxyapatite ($3Ca[PO_4]_2[OH]_2$) crystals are deposited in the organic matrix [8]. Mineralization increases bone resistance to compression [9], and also contains numerous growth factors, including TGF-β, which are released upon bone resorption [10].

The bones of the body are classified as long bones (e.g. the tibia, femur, and humerus) and flat bones (e.g. the skull, ileum, and mandible). Both types contain cortical and trabecular bone, albeit in different concentrations. Cortical bone, the compact, dense outer protective layer of bone, is made up of tightly packed collagen fibrils [6]. This form of bone is vital for supporting the weight load of the body. On the other hand, trabecular bone, also known as cancellous bone, has a loosely organized, porous matrix and is located in the interior of bone, near the ends. Trabecular bone is metabolically active. All bone matrix undergoes remodeling, but trabecular bone has a greater turnover rate than cortical bone [6].

Long bones are divided into the diaphysis, metaphysis, and epiphysis in a growing individual [11] (Fig. 1). The long bone ends, or epiphyses, are located above the growth plate, where bone elongation occurs. The diaphysis, which is the long, narrow shaft of the bone, is primarily composed of cortical bone. The metaphysis, located near the ends of bones just below the growth plate, is predominantly composed of trabecular bone and is surrounded by hematopoietic marrow, fatty marrow, and blood vessels [11].

3 Cells in the bone microenvironment

Bone is a dynamic structure that undergoes constant remodeling in order to respond to mechanical strain and maintain calcium homeostasis. Bone resorption and deposition occur in a tightly regulated fashion that is orchestrated by three cell types: osteoblasts, osteocytes, and osteoclasts. Osteoblasts are derived from mesenchymal stem cells located in the bone marrow stroma. They synthesize osteoid (i.e. new bone matrix), comprised primarily of collagen and non-collagenous proteins, and also aid in mineralization of the bone matrix. Upon stimulation by bone morphogenetic proteins and local growth factors, the mesenchymal stem cells proliferate and form pre-osteoblasts, which subsequently differentiate into mature osteoblasts [12]. After synthesizing new bone

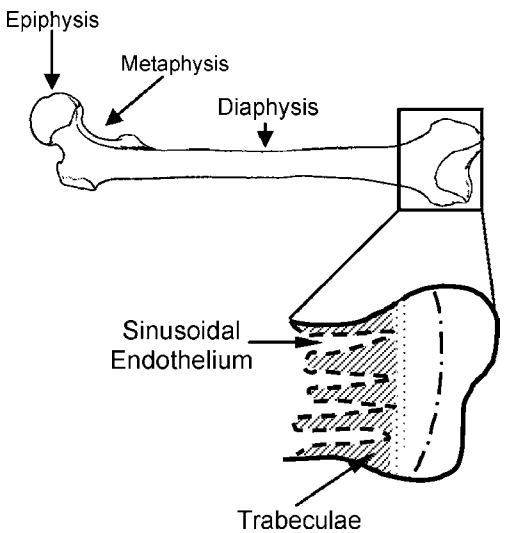

Fig. 1 Diagram of a long bone indicating the major regions and the major structures within the metaphysis, i.e. trabecular bone and the sinusoidal endothelium

matrix, the osteoblast either undergoes apoptosis or becomes embedded in the bone as an osteocyte [13]. These cells have long processes that allow them to remain in contact with other osteocytes and with osteoblasts that line the bone surface. The processes connect the entire matrix through a series of canaliculi [14, 15].

Osteoclasts, responsible for bone resorption, are derived from monocytes in the bone marrow [16]. Monocytes are activated to form osteoclasts through osteoblasts. Osteoblasts express the receptor-activator for NF-κB ligand (RANK-L) on their external surfaces; RANK-L binds to the receptor RANK found on the surface of monocytes. In the presence of macrophage colony stimulating factor (M-CSF), RANK-L promotes cellular fusion of several monocytes to form a multinucleated osteoclast [16]. Activated osteoclasts bind to the bone matrix through $\alpha_v\beta_3$, $\alpha_v\beta_5$, $\alpha_2\beta_1$ integrins located on the membrane surface and also secrete acid and lysosomal enzymes which degrade bone [13, 16].

Other cell types located within the bone microenvironment may also contribute to the bone metastatic niche. These cells can generally be grouped into two categories: stromal and transient. Mesenchymal stem cells in the bone marrow give rise to stromal cells which can differentiate into adipocytes, fibroblasts, chrondrocytes, or osteoblasts. Stromal cells have been found to support the differentiation, proliferation, and survival of both hematopoetic and cancer cells. In particular, it has been found that stromal cells express vascular cell adhesion molecule (VCAM-1). Michigami and colleagues discovered that the presence of VCAM-1 on stromal cells increased the production of bone-resorbing cytokines by myeloma cells. Neutralizing antibody to VCAM-1 or to $\alpha_4\beta_1$ integrin reduced osteolysis [17]. The adipocyte has been found to secrete tumor necrosis factor-alpha (TNF-α), IL-6, and leptin, which stimulate bone resorption and inhibit osteoblast proliferation [18, 19]. Factors secreted by adipocytes have also been implicated in breast cancer proliferation, invasiveness, survival, and angiogenesis [19]. Another type of mesenchymal cell, the fibroblast, has been shown to affect breast cancer cell invasion and contribute to metastatic bone disease. Fibroblast-secreted syndecan-1 was found to increase breast cancer cell proliferation *in vivo* [20]. In addition, fibroblasts secrete inactive MMP-2, which can be activated by breast cancer cells to subsequently increase their invasiveness and migration [21]. Fibroblasts have also been found to stimulate osteoclasts, and thus bone resorption, in a RANK-L dependent manner [22].

Vascular endothelial cells contribute to the formation of a favorable cancer cell microenvironment. New blood vessels, which arise from endothelial cells, are essential for the survival of cancer cells. Investigators have shown that the bone marrow, which has a high microvessel density, is associated with increased bone-tumor metastasis and survival of tumor cells [23]. It has also been found that many tumor-cell secreted factors stimulate endothelial cell proliferation, differentiation, and angiogenesis [23], thus producing a feedback loop that facilitates tumor cell survival in a secondary location.

Transient cells also contribute to the metastatic bone microenvironment. These cells include erythrocytes, T cells, and platelets, all derived from hematopoietic stem cells. In one study it was shown that platelets were directed by MDA-MB-231, a metastatic breast cancer cell line, to secrete LPA (Lysophosphatidic acid ([1-acyl-sn-glycero-3-phosphate]), a phospholipid with diverse biological activities [24]. Overexpression of this molecule and its receptor has been shown to increase tumor growth and metastasis [25]. Platelets may also adhere to cancer cells in the blood stream, allowing them to evade natural killer immune cell surveillance [26]. In addition, platelets may aid in cancer cell attachment to vascular endothelial cell walls [26]. T lymphocytes have been found to express RANKL, also known as TRANCE, and aid in osteoclast formation and activation [16, 27]. Peripheral T cells also secrete TNF-α, which is involved in osteoclastogenesis, inhibits osteoblast cell differentiation, and is a pro-apoptotic factor for osteoblasts [27, 28]. Besides enhancing osteoclastic bone resorption, T cells may be affected by bone metastatic cancer cells as well. As bone resorption is enhanced, TGF-β is released from the bone. This factor can inhibit both T cell proliferation and activity, and natural killer cell function [29]. Thus the immune response is suppressed and tumor cells may escape surveillance. In addition, tumor cell-secreted parathyroid hormone related peptide (PTHrP) and IL-8 may activate T cells, thus enhancing bone resorption and suppressing T cell function [29]. Plasma cells, or antibody-producing B cells, upregulate the receptor CXCR4 upon completion of differentiation [27]. Breast cancer cells, as well as stromal cells, express the ligand to this receptor CXCL12 [Stromal-derived factor-1 (SDF-1)] [27]. This ligand-receptor interaction may facilitate cancer cell migration into and within the bone microenvironment.

Tumor-associated macrophages (TAMs) are an important component of the inflammatory response in tissues [30]. These cells are derived from monocytes and are recruited by monocyte chemotactic peptide (MCP) chemokines [30]. Although activated TAMs kill many cancerous cells through secretion of IL-2, interferon, and IL-12, they also secrete a variety of potent angiogenic and lymphangiogenic growth factors, cytokines, and proteases [31, 32], all of which are involved in the promotion of tumor cell growth and survival. TAMs, as well as tumor cells, produce IL-10 which suppresses the anti-tumor response of cytotoxic T cells [33]. TAMs also induce the expression of VCAM-1 on mesothelial cells, which can aid in tumor cell invasion [34].

4 Bone remodeling

Mineralized bone has an abundance of growth factors, calcium ions, cell adhesion molecules, cytokines, and chemokines that, when released into the microenvironment during bone remodeling, make the skeleton an attractive site for metastatic cancer cells. This observation was first described in 1889 by Stephen Paget, who recognized the nonrandom movement of cancer cells within the body that was unexplained by blood flow. Paget stated "When a plant goes to seed, its seeds are carried in all directions; but they can only grow if they fall on congenial soil" [35]. This 'seed and soil' hypothesis helps to explain the preferential metastasis of certain types of cancers to the bone microenvironment, which provides a fertile soil where cancer cells can grow. Osteoclasts further contribute to this environment by acting as plows to break up the 'soil' and release its 'nutrients' for cancer cell growth and maintenance. Studies have shown that there is a close relationship between bone resorption and tumor cell growth [36].

The relative activities of osteoblasts and osteoclasts are normally tightly coupled in order to maintain a balance between bone formation and degradation. Bone remodeling is regulated both by systemic hormones and locally produced cytokines [37]. Cells in the bone marrow, especially stromal and immune cells, produce cytokines and growth factors that influence the activities of osteoblasts and osteoclasts [38]. However, this balance between bone synthesis and resorption is disturbed in several pathological conditions, including osteoporosis, rheumatoid arthritis, and skeletal metastases, resulting in osteoclast activity in excess of bone deposition by osteoblasts with net bone loss [38].

Osteoclasts likely prime the bone microenvironment for tumor cell growth through bone resorption. Although there is no definitive evidence linking increased bone resorption to increased tumor cell mass, a variety of studies have been carried out with bisphosphonates to investigate this relationship. Bisphosphonates are inorganic pyrophosphates with powerful inhibitory effects on bone resorption. One of their main targets is the osteoclast. Powles et al. showed that the administration of a bisphosphonate, clodronate, was associated with both decreased bone metastasis and death rate in patients with breast cancer [39]. Risedronate was found to reduce tumor burden in addition to osteolytic bone lesions in a nude mouse model [40]. Furthermore, nude mice treated with neutralizing antibodies to PTHrP (key factor involved in the 'vicious cycle' of bone metastasis), also experienced a decrease in tumor burden compared to controls [41, 42]. Even though inhibitors to bone resorption seem to reduce tumor burden in bone, the same does not hold true for soft tissues [39]. In the study carried out by Powles et al., the idea that inhibitors of osteolysis slowed tumor growth in soft tissue was refuted [39]. In addition, there are pre-clinical data suggesting that bisphosphonates have no effect on tumor burden in soft tissues if the drugs are administered after the metastases are already formed [3]. Taken together, these studies illustrate the importance of osteoclasts and the uniqueness of the bone microenvironment for tumor cell growth.

In patients with bone metastatic cancer, usually one of two types of lesions predominate: osteolytic or osteoblastic, although mixed lesions may occur especially early on [36]. During osteolytic metastases, typical for breast cancer metastases, osteoclastogenesis and osteoclast activation results from direct and indirect actions by metastatic cancer cells. Increased bone resorption results. Mastro and colleagues additionally found that bone metastatic breast cancer cells suppress osteoblast function, which includes decreased matrix deposition, decreased proliferation, altered adhesion, and loss of osteoblast differentiation [43–45]. These phenomanae together favor a microenvironment of increased bone turnover with decreased bone deposition similar to that seen in osteoporosis.

On the other hand, cancers such as prostate cancer tend to be predominantly osteoblastic in nature. Excess bone deposition occurs but not necessarily in an ordered fashion. While little is known about the exact mechanisms, endothelin-1 has been implicated in osteoblastic breast cancer metastases [46, 47]. Endothelin-1 has been found to stimulate the formation of new bone through osteoblast proliferation [48], and serum endothelin-1 levels were found to be increased in patients with osteoblastic prostate cancer metastases [49]. In addition to endothelin-1, platelet derived growth factor-BB (PDGF-BB) may also be a mediator for osteoblastic metastases. In a study done by Yi et al., increased expression of PDGF-BB by human metastatic breast cancer cells was correlated with increased bone formation [50]. The exact mechanism has yet to be determined. Regardless of the lesion type, these observations underscore the importance of crosstalk between cancer cells and the bone microenvironment which facilitates bone metastases.

Clinically, patients with breast cancer and other osteolytic metastases but also with osteoblastic prostate bone metastases are treated with bisphosphonate drugs that block osteoclast activity. However, therapies utilizing bisphosphonates, such as ibandronate (Boniva™), are not curative [51]. Lesion progression is slowed, but the pre-existing lesions do not heal [52–55]. Severe bone pain, fractures, hypercalcemia, and spinal cord compression may still occur [3, 10, 56, 57]. The inability of bone to regenerate following bisphosphonate treatment supports the *in vitro* finding that breast cancer cells alter osteoblast function in addition to stimulating osteoclast activity.

Not all bones of the skeleton are equally favored for metastases. The spinal vertebrate, ribs, and the ends of long

bones are preferred destinations of metastases. In general, well vascularized areas and areas of the skeleton containing red marrow are the sites of metastatic colonization. In osteoblastic metastases, bone deposition is usually made on trabecular bone surfaces without prior removal of old bone, but it may also be at sites of prior resorption. In myeloma, a malignancy of B cells, the plasma cells accumulate in the bone marrow and lead to osteolysis. Activation of osteoclasts and bone resorption far exceed bone deposition in this disease. Whether the lesions are overall lytic or blastic, the outcome is bone pain, pathological fracture, nerve compression syndromes and hypercalcemia [58].

5 The metaphyseal region of the bone has unique properties that distinguish it from the diaphysis

Scintigrams of humans with advanced disease clearly indicate that highly vascularized metaphyseal bone is a preferred site for secondary metastasis [1]. A trafficking study with a nude mouse model of metastatic breast cancer revealed that within 2 h of an inoculation of a bolus of metastatic breast cancer cells into the left ventricle of the heart, cancer cells were detected throughout the femur. However, by 24 h they had been cleared from the shaft (diaphysis) but remained at the metaphysis where they grew into large tumor masses [59]. The unique properties of the bone metaphysis make it an attractive site for metastatic cancer cells.

6 Metaphyseal bone: structure and vascularity

Metaphyseal bone is a highly vascularized structure found near the ends of long bone, in ribs and in vertebrate. It is composed of a network of thin bone spicules, sometimes referred to as “spongy bone.” In long bones, these spicules appear as mineralized fingers interspersed with red marrow and are in close proximity to the blood supply. The marrow contains hematopoietic, mesenchymal, and stromal cells. The vascular supply is sinusoidal in nature rather than a bed of capillaries. Lining the trabecular bone surfaces are osteoblasts and bone lining cells which share many properties [60]. Bone lining cells are believed to differentiate into osteoblasts when necessary for bone remodeling. The osteoblasts, as well as the marrow cells, provide an environment rich in growth factors, cytokines and chemotactic factors. These factors, and the vascular structure of the trabecular bone, are crucial for metastatic cancer cell colonization and growth.

The interactions of metastatic breast cancer cells with the vasculature has recently been well documented by Glinsky [61] and is only briefly summarized here. Metastatic foci are often seen where the sinusoid microvasculature is abundant [62]. This phenomenon is likely related to the unique anatomic, hemodynamic, and epithelial properties of the metaphyseal vascular bed. For one, the vasculature does not end in capillaries of small diameter as in most tissues. Instead it consists of voluminous sinusoids with lumens many times the diameter of cancer cells [63]. The sinusoids are within a few microns of the trabecular bone [64]. This unique structure leads to a sluggish flow of blood compared to that seen in the capillary networks of most other tissues [63]. For example, Mazo et al. found the blood flow in venous sinusoids of mouse calvaria to be 30 fold lower than the arterial rate. In another animal model, blood flow rates in canine long bone were assessed with microspheres [65]. It was found that metaphyseal and marrow cavity flow rates in sinusoids were 7–14 ml/min/g tissue, much slower than more rapidly metastasizing tissue such as the post-prandial intestine [66]. Thus cells entering the sinusoids are more “in a lake than in a stream.” In addition, sinusoids are specialized to allow easy movement of hematopoietic cells in and out of the marrow. The walls of the sinusoids are trilaminar and their structure helps explain why tumor cells can easily enter and leave [63]. Stromal endothelial cells line the sinusoidal lumen. These cells do not have tight junctions but may overlap or interdigitate. They rest on a basement membrane, the middle layer, which is irregular and discontinuous. The third layer, facing the bone marrow, is composed of adventitial cells, a type of phagocytic cell, which also do not form a tight layer. Thus the nature of the sinusoidal walls allows for easy two-way movement of hematopoietic and lymphoid cells. This structure is used advantageously by cancer cells [67].

Nevertheless, cellular entry into the sinusoids and migration into the marrow are not sufficient to insure colonization by the cancer cells. In a mouse study, it was observed that many more cancer cells entered the marrow cavity of the femur than remained to colonize it [59]. Presumably, many metastatic cancer cells in the blood can circulate through the bone, but few remain. Cancer cells, similar to leukocytes, migrate through the vasculature using a process of attachment-detachment through cell-adhesion molecules. The endothelial cells of the bone sinusoids constitutively and simultaneously express an array of tethering and adhesive proteins including P-selectin, E-selectin, intercellular adhesion molecule (ICAM-1) and VCAM-1. The vasculature of other tissues only express these molecules when stimulated by inflammatory cytokines [63]. Moreover, vasculature in one part of the bone may be different than other parts. Indeed Makuch et al. [68] found expression of P-selectin, E-selectin, ICAM and VCAM by vascular endothelial cells isolated from trabecular bone and from diaphyseal bone. However the endothelial cells from the trabecular bone but not diaphy-

seal bone showed a significantly increased expression in E-selectin when exposed to conditioned medium from immature osteoblasts. These data can be interpreted to suggest that osteoblasts of immature, metabolically active bone enhance E-selectin expression by nearby endothelial cells. This increase in cell attachment molecules would in turn enhance cancer cell extravasation into the bone marrow. Furthermore as discussed further on, inflammatory cytokines produced by osteoblasts in the presence of breast cancer cells may cause an even greater increase in cancer cell migration. In complementary approaches, others found that prostate cancer cells showed increased adherence to bone marrow microvasculature endothelium than from endothelium of other anatomical sites [69, 70]. Similar findings were reported for breast cancer [71, 72].

7 Adhesion molecules of the vascular endothelium

There has been an ongoing discussion of the roles of adhesion vs. entrapment in the movement of cancer cells into organs. The "leaky" vasculature suggests that entrapment is not the limiting event in bone metastasis. To the contrary, adhesion of metastatic cancer cells to the endothelium appears to play a specific and critical role. Evidence for the role of adhesion molecules has been found, both with prostate and breast cancer cells, which may explain their predilection to the bone [61]. For tumor cells to reach the bone marrow there must be a selective adhesion of the circulatory tumor cells to the endothelium of the bone marrow sinusoids. Therefore the adhesion molecules of the endothelium are of utmost importance.

The movement of cancer cells across the endothelium in the bone marrow has been likened to the movement of leukocytes across the endothelium. While the general patterns are likely the same, the actual molecules involved may differ [73–75]. The reported roles of various adhesion molecules may relate to the particular system, i.e. primary or secondary tumors and the specific organ. For example, selectin-mediated binding of colon cancer cells has been demonstrated to be important for their adhesion to the hepatic microvasculature [76]. This association may not hold for other metastatic tumors [61]. Makuch et al. [68] reported that active osteoblasts influenced E-selectin (but not P or S-selectin) expression on metaphyseal endothelium. The expression of E-selectin depended both on the stage of differentiation of the osteoblasts and the source of the microvasculature endothelium within the bone marrow. Galactin-3 is another molecule that participates in tumor cell, bone microvasculature associations. Galactin-3 and its ligand Thomsen–Friedenreich (TF) antigen are found both on many cancer cells and on microvasculature endothelium. Their interaction appears to be important for the primary arrest of the tumor cells [71, 77]. Another well studied molecule is CD44, the principle cell surface receptor for hyaluronic acid (HA). It is frequently over-expressed on malignant cells. In model systems, its expression correlates with the rate and strength of cancer cell interaction with bone marrow endothelium. CD44 expression on the surface of bone marrow endothelial cells likely acts to bind HA. Cancer cells and bone marrow endothelial cells both appear to express CD44 and HA, and the interaction of the two leads to tethering of the cancer cells to the bone marrow. In addition, there are associated data to suggest that activation of CD44 by HA or by osteopontin is important in downstream signaling through CD44 in bone.

8 Adhesion molecules within the bone marrow cavity

Coordinated bone remodeling involves extensive cell–cell and cell–matrix interactions among osteoblasts, osteoclasts, and bone marrow resident stromal and hematopoietic cells. The sinusoidal endothelium of the bone marrow is a two-way gate, allowing movement in both directions of newly formed and recirculating lymphocytes, hematopoietic stem cells as well as neoplastic cells. The trafficking patterns are organized by adhesion molecules on the circulating cells as well as on the bone marrow reticulocytes. VCAM-1, a member of the immunoglobulin family of cell adhesion molecules, was shown by a radiolabeling technique to be constitutively expressed by bone marrow reticular cells as well as the entire endothelium of the bone marrow sinusoids [78]. Its counter receptor, VLA-4 ($\alpha_4\beta_1$), and ICAM-1, which belongs to a similar family and binds $\alpha_2\beta_1$ integrins, are found on many cancer cells. Thus adhesion molecules which serve normal bone metabolism can be used to the advantage of metastatic tumor cells.

Another integrin member, $\alpha_v\beta_3$ is associated both with breast cancer [79] and osteoblast function [80, 81]. Interestingly, it is over-expressed in metastatic breast cancer cells once they enter the bone [82]. It is the predominant integrin on osteoclasts and appears to be important for syncytia formation and attaching to the bone matrix [83]. Peptomimetic inhibitors of $\alpha_v\beta_3$ were found to significantly reduce metastatic cancer formation when injected prior to tumor cells in a mouse model. However, there was less of an effect when administered after tumor inoculation [84]. The expression of adhesion molecules by osteoclasts has been fairly well determined [85]. Three integrins, $\alpha_v\beta_3$, $\alpha_2\beta_1$, and $\alpha_v\beta_1$, and CD44 are present on osteoclasts.

The survival of cancer cells in the bone depends on their interactions with other cells. Interactions may be physical, with cell adhesion molecules, or through secreted molecules, such cytokines, chemokines, and other growth factors. Adhesion to various cells in the metastatic site

controls anti-apoptotic and proliferative signals (see [84]). Thus the bone marrow displays numerous adhesion molecules that offer opportunities for interactions between cancer cells and normal cells. Some of these interactions do not occur until the cancer cells are in the bone marrow environment after they express new adhesion molecules.

9 Bone remodeling and inflammation

Rodan [86] in an overview of skeletal development and function, points out the similarities between bone remodeling and inflammation. Many of the same cytokines produced by the immune cells as part of an inflammatory response are also produced by osteoblasts. Some of these, IL-1, IL-11, IL-6, PGE and PTHrP, are also osteoclastogenic. Furthermore, both osteoblasts and osteoclasts express toll-like-receptors [87] and respond to trauma, bacterial infection, and metastases with the production of these same molecules [88–90]. In particular, a set of inflammatory stress molecules (IL-6, IL-8, MCP-1, COX-2) appears in normal bone remodeling as well as under these pathogenic conditions [88]. These factors are made by osteoblasts but can also be produced by macrophages. They attract and activate osteoclasts. Osteoclasts degrade bone matrix, leading to the release of many growth factors. This combination of factors creates a very hospitable environment for cancer cells.

10 Cytokines and chemokines

Once established in the bone microenvironment, a 'vicious cycle' is created among metastatic tumor cells, osteoblasts, and osteoclasts that facilitates increased bone turnover and metastatic cell survival. Guise et al. developed a model of breast cancer metastasis to the bone, based on breast cancer cell overproduction of PTHrP [3, 91] that activates osteoblasts to produce RANK-L. Osteoblast-secreted RANK-L binds the RANK receptor on osteoclasts, inducing osteoclast differentiation and bone matrix degradation. In turn, TGF-β, released from the bone matrix, stimulates the cancer cells to produce more PTHrP [43], thus establishing a positive feedback loop. There is additional evidence that breast cancer-derived IL-8 acts prior to PTHrP to stimulate osteoclastogenesis via both RANK-L dependent and independent mechanisms [92–94]. As a result of constituitive osteoclast activation and an inability of osteoblasts to lay down bone matrix, sustained bone degradation occurs [45, 54]. This feedback establishes a vicious cycle, resulting in continued activation of osteoclasts and breast cancer cells. Ultimately, osteolytic lesions are formed at sites of metastases [10, 57].

It should be noted that the presence of PTHrP is not sufficient for cancer cell metastases to the bone. In a study in which 526 patients with operable breast cancer were examined, it was found that those with PTHrP-positive primary tumors had improved survival and were less likely to develop bone metastases [95]. In those patients with bone metastases, PTHrP presence was found not to be significantly associated with tumor size, vascular invasion, or tumor grade [95]. Thus, it is likely that bone metastases are influenced by other factors in the bone microenvironment besides PTHrP.

In addition to the PTHrP, Bendre et al. found an important role for IL-8. IL-8, the human homolog to murine MIP-2, belongs to the family of CXC chemokines and is naturally constitutively produced by osteoblasts [93, 96, 97]. IL-8 is overexpressed in a bone-homing derivative of MDA-MB-231 human metastatic breast cancer cells suggesting an important role in bone metastasis [94]. IL-8 can stimulate osteoclastogenesis by increasing RANK-L or stimulate the formation of osteoclasts in the absence of RANK-L [92]. It is believed that IL-8 is involved in the early stages of breast cancer metastasis by initiating the bone resorption process [93]. IL-8 also has been shown to increase angiogenesis and suppress osteoblast activity [98, 99]. In addition, IL-8 increases cell motility, invasion, and metastatic potential in breast cancer [93]. If overexpressed in breast cancer cells, IL-8 will lead to increased bone metastasis and osteolytic activity [94]. IL-8 stimulates osteoclast activity independently of RANK-L [92]. Bendre et al. suggested that the vicious cycle with PTHrP is first initiated by breast cancer cells secreting IL-8, thereby stimulating bone resorption by osteoclasts. The release of TGF-β from the bone matrix then stimulates cancer cells to produce more PTHrP, thus continuing the vicious cycle [93].

COX-2 and PGE_2 also have been found to contribute to osteoclast activitation and facilitate the creation of a microenvironment favorable for cancer cell metastasis. COX-2 levels and activity correlate with cancer cell metastasis both *in vitro* and *in vivo* [100–102]. COX-2 expression also has been implicated in the growth, invasion, apoptosis, and angiogenesis of breast cancer [103–105]. COX-2 expression in patients with cancer has shown to be a negative prognostic factor [106]. Singh et al. recently conducted a study investigating the involvement of COX-2 in breast cancer metastases to the bone [107]. Interestingly, overexpression of COX-2 correlated with increased production of IL-8 [108], which has also been linked to increased metastatic occurrence [94]. Singh et al. found that COX-2 induced both the formation of PGE_2 and IL-8 specifically in bone metastatic breast cancer cells. Since PGE_2 and IL-8 are mediators of osteoclast activation [109] (through direct or indirect mechanisms of stimulation of RANKL [92]), a system in which there is overexpression of

COX-2 would favor osteolytic cancer metastases. In addition, Hiraga et al. discovered that bone-derived TGF-β stimulated COX-2 expression, thus enhancing bone metastases in breast cancer [110]. TGF-β, released from the bone during bone resorption, stimulates COX-2 expression and subsequently PGE_2 expression in breast cancer cells. PGE_2 upregulates RANKL expression on osteoblasts, leading to osteoclast activation and increased bone turnover [110]. Finally, Hall et al. investigated the involvement of Wnts, a family of glycoproteins [111], in the promotion of osteoblastic bone metastases in prostate cancer [112]. They found that promotion of Wnt activity (by blocking the Wnt antagonist DKK-1), led to enhanced osteoblastic bone metastases in typically osteolytic PC-3 prostate cancer cells [112]. These results suggest that the involvement of DKK-1 dictates whether bone metastases are osteoblastic or osteolytic, and once again emphasize the importance of the bone microenvironment.

Cancer cell secreted IL-1, IL-6, and IL-11 have also been found to increase osteoclast activation. IL-6 is a pleiotropic cytokine that is naturally expressed by osteoblasts in low quantities. IL-6 receptors are found on osteoclasts and when stimulated, cause osteoclast differentiation and bone resorption [113]. There is a correlation of poor prognosis with increased IL-6 expression and metastatic breast cancer. IL-6 additionally has been implicated with increased breast cancer cell migration [114–116]. IL-1 is also a potent stimulator of osteoclast activation. To explore the notion that increased bone turnover attracts metastatic cancer cells, Sasaki et al. increased bone resorption by injecting recombinant IL-1β locally over the calvaria of nude mice [117]. Four weeks after cancer cell inoculation, osteolytic metastatic cancer cells were found in the calvariae of IL-1 treated mice. None were seen in the control. IL-11 is an additional key player in osteoclast activation. It has been reported that IL-11 mediates the actions of IL-1 on osteoclast development [118]; however, IL-11 has independent effects on osteoclast activity [119]. IL-11, IL-1, and IL-6 have all been found to be involved in an interacting cascade of cytokines which play a large part in osteoclast development and activity. Increased osteoclast activity subsequently creates a bone microenvironment that favors cancer cell metastasis, growth, and development. IL-1 contributes to the production of IL-11 and IL-6 [118]. IL-6 and IL-11 production are also regulated by IL-1, growth factors such as PDGF, IGF-1, and TGF-β, vitamin D, PTHrP, and PTH [119, 120].

11 Bone matrix is fertile soil for metastatic cancer cells

During bone deposition, osteoblasts secrete a variety of growth factors, such as IGF, TGF-β, FGF, and BMPs, that become incorporated into the bone matrix [121]. As bone resorption occurs, these factors are released into the bone microenvironment, making it an attractive place for cancer cells to metastasize and grow [122]. TGF-β released from the bone, in particular, has been found to stimulate the expression of CTGF, IL-11, and PTHrP by cancer cells [42, 123]. These factors are involved in tumor metastasis to bone and subsequently promote additional bone resorption, leading to the release of more growth factors and further preferential tumor metastasis to bone. Growth factors released during bone remodeling and present in the bone microenvironment may be chemoattractive molecules for the cancer cells. Orr et al. and Mundy et al. using a Boyden Chamber assay both demonstrated that the release of growth factors during bone resorption stimulated the chemotaxis of cancer cells [124, 125]. Additionally, cytokines have been implicated in cancer cell chemotaxis to bone. The SDF-1/CXCR4 axis is a ubiquitous chemotaxis mechanism in normal biology and is used for directed migration of a variety of immune and hematopoetic cells [126–129]. Jung et al. found that SDF-1 is secreted by osteoblasts, and that certain factors, namely IL-1β, PDGF-BB, VEGF, tumor necrosis factor-alpha (TNF-α), and PTH, act on osteoblasts to increase SDF-1 production [130]. Consequently, many of these cytokines play a role in increasing osteoclast activity during bone resorption [119, 120]. Furthermore, the results of this study suggested that osteoblast secretion of SDF-1 may be a chemotactic mechanism for stem cell homing. It goes without saying that the SDF-1/CXCR4 axis may be involved in cancer cell chemoattraction as well. In fact, Muller et al., among others [131, 132], explored the idea that metastatic breast cancer cells were responsive to gradients of chemokines [133]. CXCR4 was found to be highly expressed on metastatic breast cancer cells, and its ligand, SDF-1 was found to be highly expressed in organs to which cancer cells preferentially metastasizes (such as bone) [133]. Treatment with a neutralizing antibody to CXCR4 suppressed bone metastatic breast cancer [133]. Sun et al. conducted a similar study using prostate cancer as a model and found comparable results [134]. Once in bone, cancer cells become tethered by integrins and cell adhesion molecules as previously described [135, 136].

Current models suggest that chemokines and cytokines produced by breast cancer cells are key to breast cancer cell metastasis [92–94, 137]. Elevated levels of IL-8 production by human breast cancer cells have been correlated with increased bone metastasis *in vivo* and with stimulation of osteoclast differentiation and bone resorption [92, 94]. Tumor-derived IL-1, IL-6, and IL-11, insulin-growth factor-II, TNF-α, and a variety of other factors can also contribute to osteoclast activation and bone destruction [98, 138].

While breast cancer cells undoubtedly play an important role in breast cancer metastasis to the bone, data have shown that osteoblasts can be directed by the breast cancer cells to produce several inflammatory cytokines that have been implicated in osteoclast activation as well as breast cancer cell migration and survival [93, 139–143]. (Table 1 gives a brief summary of some relevant cytokines and their sources in the bone.) Kinder et al. demonstrated that osteoblasts undergo an inflammatory stress response in the presence of human metastatic breast cancer cells and produce elevated levels of IL-6, human IL-8 (murine KC, MIP-2), and MCP-1 [144]. These cytokines are known to attract, differentiate, and activate osteoclasts; thus co-opting osteoblasts into creating a bone microenvironment that exacerbates bone loss [144]. Similar findings were seen with murine osteoblasts and primary calvarial osteoblasts [144]. These results support the idea that cancer metastases create a unique niche in the bone microenvironment by co-opting normal cells of the bone to favor tumor growth and development.

Furthermore, Mastro and colleagues have preliminary *in vivo* evidence that osteoblasts themselves in the bone naturally produce cytokines that may be chemoattractants for metastatic breast cancer cells. In particular, they showed that metaphyses of bone cleared of bone marrow produced chemokines and cytokines that were different from those in the diaphysis (shaft). Prominent among these were KC (present only in the metaphyses), MIP-2 (murine homolog to human IL-8), and MCP-1 (Fig. 2) (Bussard and Mastro, 2007, unpublished data).

These cytokines were strongly observed in cultures of the bone metaphysis alone and not found in cultures of bone marrow from the metaphysis (Bussard and Mastro, 2007, unpublished data). This observation suggests that the cytokines were specifically produced by the cells of the bone (i.e. osteoblasts) and not the stromal cells. Murine IL-6, KC, and MIP-2 located in femur metaphyses were also found to be increased in the presence of human metastatic breast cancer cells compared with femur metaphyses from control mice (Bussard and Mastro, 2007, unpublished data). Finally, a novel experiment was conducted to monitor and quantify the initial stages (arrival, localization, and initial colonization) of breast cancer cell trafficking in the bone [59]. The DNA from femurs of mice inoculated with MDA-MB-435^{GFP} cells via intracardiac injection were isolated at various times, purified, and subjected to quantitative PCR for a human gene, HERV-1, and the number of breast cancer cells calculated. Femurs were separated into metaphyses and diaphyses. Results indicated that breast cancer cells preferentially migrated within days directly to the distal then proximal metaphyses. Few were found in the diaphyses [59]. These results additionally support the idea that metastatic breast cancer cells may follow a gradient of chemoattractant cytokines as well as suggests the importance of the local bone microenvironment.

In addition to IL-6 and IL-8, KC and MCP-1 are osteoblast-derived cytokines that greatly increase in response to metastatic breast cancer cells (Bussard and Mastro, 2007, unpublished data). MCP-1, a member of the CC chemokine family, is naturally produced by osteoblasts [96]. It regulates bone resorption by stimulating the migration of common monocyte-osteoclast progenitor cells from the blood or the bone marrow to the bone. MCP-1 concentrations are increased in metastatic cell lines, and it is associated with angiogenesis and increased cancer cell survival [145–147]. KC is another member of the CXC chemokine family with homology to IL-8 [148]. KC stimulates angiogenesis and is involved in neutrophil chemotaxis and activation [148, 149]. KC is also expressed by osteoblasts [149].

In addition to directing osteoblasts to secrete cytokines which alter the bone microenvironment, cancer cells affect the bone building cells in other ways as well. Mercer et al. demonstrated that culturing mouse osteoblasts with the conditioned medium from a human metastatic breast cancer cell line inhibited expression of osteoblast differentiation and blocked osteoblast ability to mineralize bone matrix [45]. This *in vitro* observation was confirmed in a mouse study [59]. Since osteoblasts do not differentiate properly in the presence of breast cancer cells, it is possible that the

Table 1 Source of several important chemokines and cytokines in the bone microenvironment in the presence of metastatic breast cancer cells

	Osteoblasts	Bone matrix	Breast cancer cells	Other cells in the bone microenvironment
IL-6	[153, 154]	–	[138, 155]	Bone Marrow Stromal Cells [156], Monocytes, Macrophages [157], and Osteoclasts [158]
IL-8	[155, 159]	–	[94, 155, 160]	Osteoclasts [155, 161], Bone Marrow Stromal Cells [159], Macrophages [162], Endothelial Cells [162]
PTHrP	–	–	[91, 94, 155]	–
TGFβ	[121, 155]	[155, 163]	[155]	Bone Marrow Stromal Cells [164], Endothelial Cells [165]

Many cells in the metastatic bone environment produce cytokines and chemokines. The cell sources of several important ones are indicated. The dash indicates that we were unable to find evidence from the literature or in our laboratory that the molecule was produced in the indicated cell type.

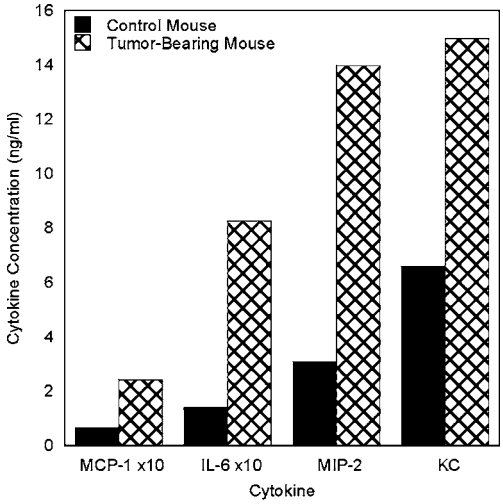

Fig. 2 Cytokine expression of murine femur metaphyses ex-vivo following intracardiac inoculation. MDA-MB-231^{GFP} cells (3×10^5 cells) were inoculated into the left cardiac ventricle of 4–6 week old athymic, female mice. Control mice were untreated. Mice were euthanized at 4 weeks and femurs harvested. The bone marrow was removed and the femur metaphyses were fractionated. Isolated metasphyseal bone pieces were crushed and cultured. Media were collected and tested after 24 h. Murine MCP-1 cytokine production was quantified using ELISAs. Murine IL-6, MIP-2, and KC were quantified using a Bio-Rad Bio-Plex™ murine cytokine quantification assay. Shown is a representative experiment. MCP-1 and IL-6 concentrations were multiplied by 10 in order to be shown on the same graph as MIP-2 and KC

cancer cells may alter the overall protein secretion profile of osteoblasts. This alteration may involve preventing osteoblasts from producing the differentiation proteins necessary for developing into mature, bone-depositing cells, as well as inducing osteoblast production of cytokines that could contribute to progression of bone metastasis, increase activation of osteoclasts, and contribute to the formation of osteolytic lesions.

12 Conclusions

Clearly, the organ microenvironment is extremely influential in cancer cell metastasis to a specific location. Crosstalk between the cancer cell "seed" and the target organ microenvironment "soil" will determine if the cancer cell metastasizes to a specific site and if that microenvironment supports growth and proliferation of the metastatic cancer cell. Only then will the metastatic cancer cell population flourish. Bone provides an especially attractive site for a variety of reasons. Metabolically active areas of bone are well-vascularized with a system that allows various cells to easily enter and exit. The normal remodeling process provides chemotactic and growth factors that attract cancer cells and support them once in place. The bone matrix contains a rich storehouse of growth factors such as TGF-β that are released during bone turnover. Resident cancer cells thrive in the rich cocktail of released cytokines. Finally, both osteoblast and octeoclast activities can be modulated by cancer cells to their advantage. The release of characteristic sets of cytokines by the bone matrix of an osteolytic lesion or osteoblastic lesion (e.g. MCP-1, IL-6, IL-8) will facilitate the chemoattraction and survival of metastatic cancer cells. Understanding the mechanisms behind these events will aid in the development of therapeutics to combat specific metastases and manipulate their target organ microenvironments. While the origin of metastatic variants remains unclear, is it certain that the target organ microenvironment contributes greatly to their metastasis.

13 Unanswered questions

Many unanswered questions remain. One of the most critical is to determine a 'metastatic signature' for the primary tumor which would indicate the possibility of metastasis. However, not all tumor cells that arrive in the bone, even from the same primary tumor, will remain or grow there. Dormant metastases in the bone remain a mystery. It is known that individual cells or micrometastases can be found in patients with no evidence of metastasis [150]. These individuals may never exhibit bone metastasis. On the other hand, bone micrometastases can remain dormant for years in spite of the rich microenvironment. What event triggers that cell to begin to grow?

14 Future studies

It is difficult to study bone metastases and the tumor microenvironment for many reasons. (1) The marrow space is relatively inaccessible. (2) It is also a complex space containing not only bone cells, osteoblasts and osteoclasts, but also hematopoietic cells and transient immune cells. Cell lines, particularly osteoblasts, have been developed that recapitulate in culture the stages of osteoblast differentiation. However, these lines have limitations when compared to intact bone.

We have recently developed a specialized bioreactor that allows extended-term culture of osteoblasts. The cells have been grown uninterrupted for up to 10 months. They proliferate and form a multilayer (>6 cell layers) of mature osteoblasts that begin to mineralize and form macroscopic bone chips [151]. By 10 months the morphology of the cells resembles osteocytes. We have inoculated human metastatic breast cancer cells, MDA-MB-231^{GFP}, into these chambers and have seen by microscopy that the cells adhere, grow, and move through the cell layers, mimicking *in vivo* migration and invasion [152]. We have evidence

that the osteoblasts likewise undergo a stress response and produce increased amounts of IL-6, for example. While the bioreactor has been used to study osteoblast-cancer cell interactions, it will allow introduction of other cell types, e.g. macrophages, lymphocytes. Thus, the bioreactor promises to be a useful 3-D culture system to study and to manipulate the bone-tumor microenvironment.

Acknowledgments KMB was supported by a predoctoral traineeship from the U.S. Army Medical and Materiel Research Command Breast Cancer Program (W81XWH-06-1-0363). The authors' work was supported by was supported by the U.S. Army Medical and Material Research Command Breast Cancer Program; (DAMD 17-02-1-0358 and W81XWH-06-1-0432 to AMM,); National Foundation for Cancer Research, Center for Metastasis Research; The Susan G. Komen Breast Cancer Foundation, BCTR104406; The American Institute of Cancer Research, #06A027-REV2; The authors thank Richard Ball of the Immunomodulation Core, Penn State GCRC (work supported by NIHM01RR10732) for technical advice regarding ELISAs.

References

1. Rubens, R. D., & Mundy, G. R. (2000). *Cancer and the skeleton*. London: Martin Dunitz.
2. Price, J. E. (2004). *The breast comprehensive management of benign and malignant disorders* pp. 537–557. St. Louis: Saunders.
3. Mundy, G. R. (2002). Metastasis to bone: Causes, consequences and therapeutic opportunities. *Nature Reviews. Cancer*, *2*, 584–593.
4. Chambers, A. F., Groom, A. C., & MacDonald, I. C. (2002). Dissemination and growth of cancer cells in metastatic sites. *Nature Reviews. Cancer*, *2*, 563–572.
5. Batson, O. V. (1942). *Annals of Internal Medicine*, *16*, 38–45.
6. Marks, S. C., & Odgren, P. R. (2002). Structure and development of the skeleton. In J. P. Bilezikian, L. G. Raisz, & G. A. Rodan (Eds.) *Principles of bone biology* (vol. 1 (pp. 3–15). New York: Academic.
7. Hancox, N. M. (1972). *Biology of bone*. Cambridge: University Press.
8. Baron, R. (2003). General principles of bone biology. In M. J. Favus (Ed.) *Primer on the metabolic bone diseases and disorders of mineral metabolism* (pp. 1–8). Washington, D.C.: American Society for Bone and Mineral Research.
9. Alberts, B., Johnson, A., Lewis, J., Raff, M., Roberts, K., & Walter, P. (2002). *Molecular biology of the cell* p. 1308. New York: Garland Science.
10. Guise, T. A., & Mundy, G. R. (1998). Cancer and bone. *Endocrine Reviews*, *19*, 18–54.
11. Price, J. S., Oyajobi, B. O., & Russell, R. G. (1994). The cell biology of bone growth. *European Journal of Clinical Nutrition*, *48*(Suppl 1), S131–S149.
12. Minguell, J. J., Erices, A., & Conget, P. (2001). Mesenchymal stem cells. *Experimental Biology and Medicine*, *226*, 507–520.
13. Kanis, J. A., & McCloskey, E. V. (1997). Bone turnover and biochemical markers in malignancy. *Cancer*, *80*, 1538–1545.
14. Gartner, L. P., & Hiatt, J. L. (1997). *Color textbook of histology.* Philadelphia: Saunders.
15. Baron, R. (2003). General principles of bone biology. In J. B. Lian, & S. R. Goldring (Eds.) *Primer on the metabolic bone diseases and disorders of mineral metabolism*. Washington, D.C: American Society for Bone and Mineral Research.
16. Takahashi, N., Udagawa, N., Takami, M., & Suda, T. (2002). Cells of bone: Osteoclast generation. In J. P. Bilezikian, L. G. Raisz, & G. A. Rodan (Eds.) *Principles of bone biology* (vol. 1 (pp. 109–126). San Diego: Academic.
17. Michigami, T., Shimizu, N., Williams, P. J., Miewolna, M., Dallas, S. L., Mundy, G. R., et al. (2000). Cell–cell contact between marrow stromal cells and myeloma cells via VCAM-1 and α4B1 integrin enhances production of osteoclast-stimulating activity. *Blood*, *96*, 1953–1960.
18. Iyengar, P., Combs, T. P., Shah, S. J., Gouon-Evans, V., Pollard, J. W., Albanese, C., et al. (2003). Adipocyte-secreted factors synergistically promote mammary tumorigenesis through induction of anti-apoptotic transcriptional programs and proto-oncogene stabilization. *Oncogene*, *22*, 6408–6423.
19. Maurin, A. C., Chavassieux, P. M., Frappart, L., Delmas, P., Serre, C.-M., & Meunier, P. J. (2000). Influence of mature adipocytes on osteoblast proliferation in human primary cocultures. *Bone*, *26*, 485–489.
20. Maeda, T., Alexander, C. M., & Friedl, A. (2004). Induction of syndecan-1 expression in stromal fibroblasts promotes proliferation of human breast cancer cells. *Cancer Research*, *64*, 612–621.
21. Saad, S., Gottlieb, D. J., Bradstock, K. F., Overall, C. M., & Bendall, L. J. (2002). Cancer cell-associated fibronectin induces release of matrix metalloproteinase-2 from normal fibroblasts. *Cancer Research*, *62*, 283–289.
22. Lau, Y. S., Sabokbar, A., Giele, H., Cerundolo, V., Hofstetter, W., & Athanasou, N. A. (2006). Malignant melanoma and bone resorption. *British Journal of Cancer*, *94*, 1496–1503.
23. Chavez-Macgregor, M., Aviles-Salas, A., Green, D., Fuentes-Alburo, A., Gomez-Ruiz, C., & Aguayo, A. (2005). Angiogenesis in the bone marrow of patients with breast cancer. *Clinical Cancer Research*, *11*, 5396–5400.
24. Eberhardt, C., Gray, P. W., & Tjoelker, L. W. (1997). Human lysophosphatidic acid acyltransferase: cDNA cloning, expression, and localization to chromosome 9q34.3. *Journal of Biological Chemistry*, *272*, 20299–20305.
25. Boucharaba, A., Serre, C. M., Gres, S., Saulnier-Blache, J. S., Bordet, J. C., Guglielmi, J., et al. (2004). Platelet-derived lysophosphatidic acid supports the progression of osteolytic bone metastases in breast cancer. *Journal of Clinical Investigation*, *114*, 1714–1725.
26. Lapumbo, J. S., Talmage, K. E., Massari, J. B., La Jeunesse, C. M., Flick, M. J., Kombrinck, K. W., et al. (2005). Platelets and fibrin(ogen) increase metastatic potential by impeding natural killer cell-mediated elimination of tumor cells. *Blood*, *105*, 178–185.
27. Walsh, M. C., Kim, N., Kadono, Y., Rho, J., Lee, S. Y., Lorenzo, J., et al. (2006). Osteoimmunology: Interplay between the immune system and bone metabolism. In W. E. Paul, C. G. Fathman, & L. H. Glimcher (Eds.) *Annual review of immunology* (vol. 24 (pp. 33–63). Palo Alto: Annual Reviews.
28. Sroato, I., Grano, N., Brunetti, G., Colucci, S., Mussa, A., & Bertetto, O. (2005). Mechanisms of spontaneous osteoclastogenesis in cancer with bone involvement. *FASEB Journal*, *19*, 228–230.
29. Fournier, P. G., Chirgwin, J. M., & Guise, T. A. (2006). New insights into the role of T cells in the vicious cycle of bone metastases. *Current Opinion in Rheumatology*, *18*, 396–404.
30. Coussens, L. M., & Werb, Z. (2002). Inflammation and cancer. *Nature*, *420*, 860–867.
31. Brigati, C., Noonan, D. N., Albini, A., & Benelli, R. (2002). Tumors and inflammatory infiltrates: Friends or foes? *Clinical & Experimental Metastasis*, *19*, 247–258.
32. Schoppmann, S. F., Birner, P., Stockl, J., Kalt, R., Ullrich, R., Caucig, C., et al. (2002). Tumor-associated macrophages express lymphatic endothelial growth factors and are related to peritu-

moral lymphangiogenesis. *American Journal of Pathology*, *161*, 947–956.
33. Torisu, H., Ono, M., Kiryu, H., Furue, M., Ohmoto, Y., Nakayama, J., et al. (2000). Macrophage infiltration correlates with tumor stage and angiogenesis in human malignant melanoma: Possible involvement of TNF-α and IL-1α. *International Journal of Cancer*, *85*, 182–188.
34. Jonjic, N., Peri, G., Bernasconi, S., Sciacca, F. L., Colotta, F., Pelicci, P., et al. (1992). Expression of adhesion molecules and chemotactic cytokines in cultured human mesothelial cells. *Journal of Experimental Medicine*, *176*, 1165–1174.
35. Paget, S. (1889). The distribution of secondary growths in cancer of the breast. *Cancer and Metastasis Reviews*, *8*, 98–101.
36. Roodman, G. D. (2004). Mechanisms of bone metastasis. *New England Journal of Medicine*, *350*, 1655–1664.
37. Roodman, G. D. (2001). Biology of osteoclast activation in cancer. *Journal of Clinical Oncology*, *19*, 3562–3571.
38. Yoneda, T. (1996). Mechanisms of preferential metastasis of breast cancer to bone. *Journal of Clinical Oncology*, *9*, 103–109.
39. Powles, T., Paterson, S., Kanis, J. A., McCloskey, E. V., Ashley, S., Tidy, A., et al. (2002). Randomized, placebo-controlled trial of clodronate in patients with primary operable breast cancer. *Journal of Clinical Oncology*, *20*, 3219–3224.
40. Sasaki, A., Boyce, B. F., Story, B., Wright, K. R., Chapman, M., Boyce, R., et al. (1995). Bisphosphonate risedronate reduces metastatic human breast cancer cells and bone metastases development. *Journal of Clinical Investigation*, *103*, 197–206.
41. Guise, T. A., Yin, J. J., Taylor, S. D., Kumagai, Y., Dallas, M. R., Boyce, B. F., et al. (1996). Evidence for a causal role of parathyroid-hormone-related protein in the pathogenesis of human breast cancer-mediated osteolysis. *Journal of Clinical Investigation*, *98*, 1544–1549.
42. Yin, J.-J., Selander, K., Chirgwin, J. M., Dallas, M. R., Grubbs, B. G., Wieser, R., et al. (1999). TGF-β signaling blockade inhibits PTHrP secretion by breast cancer cells and bone metastases development. *Journal of Clinical Investigation*, *103*, 197–206.
43. Mastro, A. M., Gay, C. V., Welch, D. R., Donahue, H. J., Jewell, J., Mercer, R., et al. (2004). Breast cancer cells induce osteoblast apoptosis: a possible contributor to bone degradation. *Journal of Cell Biology*, *91*, 265–276.
44. Mastro, A. M., Gay, C. V., & Welch, D. R. (2003). The skeleton as a unique environment for breast cancer cells. *Clinical & Experimental Metastasis*, *20*, 275–284.
45. Mercer, R., Miyasaka, C., & Mastro, A. M. (2004). Metastatic breast cancer cells suppress osteoblast adhesion and differentiation. *Clinical & Experimental Metastasis*, *21*, 427–435.
46. Guise, T. A., Yin, J. J., & Mohammad, K. S. (2003). Role of endothelin-1 in osteoblastic bone metastases. *Cancer*, *97*, 779–784.
47. Yin, J. J., Mohammad, K. S., Käkönen, S. M., Harris, S., Wu-Wong, J. R., Wessale, J. L., et al. (2003). A causal role for endothelin-1 in the pathogenesis of osteoblastic bone metastases. *Proceedings of the National Academy of Sciences*, *100*, 10954–10959.
48. Kasperk, C. H., Borcsok, I., Schairer, H. U., Schneider, U., Nawroth, P. P., Niethard, F. U., et al. (1997). Endothelin-1 is a potent regulator of human bone cell metabolism *in vitro*. *Calcified Tissue International*, *60*, 368–374.
49. Nelson, J. B., Hedican, S. P., George, D. J., Reddi, A. H., Piantadosi, S., Eisenberger, M. A., et al. (1995). Identification of endothelin-1 in the pathophysiology of metastatic adenocarcinoma of the prostate. *Nature Medicine*, *1*, 944–949.
50. Yi, B., Williams, P. J., Niewolna, M., Wang, Y., & Yoneda, T. (2002). Tumor-derived platelet-derived growth factor-BB plays a critical role in osteosclerotic bone metastasis in an animal model of human breast cancer. *Cancer Research*, *62*, 917–923.
51. Hiraga, T., Williams, P. J., & Mundy, G. R. (2001). The bisphosphonate ibandronate promotes apoptosis in MDA-MB-231 human breast cancer cells in bone metastases. *Cancer Research*, *61*, 4418–4424.
52. Delmas, P. D., Demiaux, B., Malaval, L., Chapuy, M. C., Edouard, C., & Meunier, P. J. (1986). Serum bone gamma carboxyglutamic acid-containing protein in primary hyperthyroidism and in malignant hypercalcemia. *Journal of Clinical Investigation*, *77*, 985–991.
53. Kukreja, S. C., Rosol, T. J., Shevrin, D. H., & York, P. A. (1998). Quantitative bone histomorphometry in nude mice bearing a human squamous cell lung cancer. *Journal of Bone and Mineral Research*, *3*, 341–346.
54. Stewart, A. F., Vignery, A., Silverglate, A., Ravin, N. D., Livolsi, V., Broadus, A. E., et al. (1982). Quantitative bone histomorphology in humoral hypercalcemia of malignancy: Uncoupling of bone cell activity. *Journal of Clinical Endocrinology and Metabolism*, *55*, 219–227.
55. Taube, T., Elomaa, I., Blomqvist, C., Benton, N. C., & Kanis, J. A. (1994). Histomorphometric evidence for osteoclast-mediated bone resorption in metastatic breast cancer. *Bone*, *15*, 161–166.
56. Galasko, C. S. (1982). Mechanisms of lytic and blastic metastatic disease of bone. *Clinica Ortopedica*, *169*, 20–27.
57. Martin, T. J., & Moseley, J. M. (2000). Mechanisms in the skeletal complications of breast cancer. *Endocrine Related Cancer*, *7*, 271–284.
58. Mundy, G. R., & Guise, T. A. (2000). Pathophysiology of bone metastasis. In R. D. Rubens, & G. R. Mundy (Eds.) *Cancer and the skeleton* (pp. 43–64). London: Martin Dunitz Ltd.
59. Phadke, P. A., Mercer, R. R., Harms, J. F., Jia, Y., Kappes, J. C., Frost, A. R., et al. (2006). Kinetics of metastatic breast cancer cell trafficking in bone. *Clinical Cancer Research*, *12*, 1431–1440.
60. Everts, V., Delaisse, J. M., Korper, W., Jansen, D. C., Tigchelaar-Gutter, W., Saftig, P., et al. (2002). The bone lining cell: Its role in cleaning Howship's lacunae and initiating bone formation. *Journal of Bone and Mineral Research*, *17*, 77–90.
61. Glinsky, V. V. (2006). Intravascular cell-to-cell adhesive interactions and bone metastasis. *Cancer and Metastasis Reviews*, *25*, 531–540.
62. Sasaki, A., Boyce, B. F., Story, B., Wright, K. R., Chapman, M., Boyce, R., et al. (1995). Bisphosphonate risedronate reduces metastatic human breast cancer burden in bone in nude mice. *Cancer Research*, *55*, 3551–3557.
63. Mazo, I. B., & von Andrian, U. H. (1999). Adhesion and homing of blood-borne cells in bone marrow microvessels. *Journal of Leukocyte Biology*, *66*, 25–32.
64. Buckwalter, J. A. (1995). Pharmacological treatment of soft-tissue injuries. *Journal of Bone and Joint Surgery. American Volume*, *77*, 1902–1914.
65. Schnitzer, J. E., McKinstry, P., Light, T. R., & Ogden, J. A. (1982). Quantitation of regional chondro-osseous circulation in canine tibia and femur. *American Journal of Physiology*, *242*, H365–H375.
66. Stephenson, R. B. (1989). The splanchnic circulation. In H. D. Patton, A. F. Fuchs, B. Hille, A. M. Scher, & R. Steiner (Eds.) *Textbook of physiology* (pp. 911–923). Philadelphia: Saunders.
67. Mastro, A. M., Gay, C. V., & Welch, D. R. (2003). The skeleton as a unique environment for breast cancer cells. *Clinical & Experimental Metastasis*, *20*, 275–284.
68. Makuch, L. A., Sosnoski, D. M., & Gay, C. V. (2006). Osteoblast-conditioned media influence the expression of E-selectin on bone-derived vascular endothelial cells. *Journal of Cellular Biochemistry*, *98*, 1221–1229.
69. Lehr, J. E., & Pienta, K. J. (1998). Preferential adhesion of prostate cancer cells to a human bone marrow endothelial cell line. *Journal of the National Cancer Institute*, *90*, 118–123.

70. Scott, L. J., Clarke, N. W., George, N. J., Shanks, J. H., Testa, N. G., & Lang, S. H. (2001). Interactions of human prostatic epithelial cells with bone marrow endothelium: Binding and invasion. *British Journal of Cancer*, *84*, 1417–1423.
71. Glinsky, V. V., Glinsky, G. V., Rittenhouse-Olson, K., Huflejt, M. E., Glinskii, O. V., Deutscher, S. L., et al. (2001). The role of Thomsen–Friedenreich antigen in adhesion of human breast and prostate cancer cells to the endothelium. *Cancer Research*, *61*, 4851–4857.
72. Glinsky, V. V., Huflejt, M. E., Glinsky, G. V., Deutscher, S. L., & Quinn, T. P. (2000). Effects of Thomsen–Friedenreich antigen-specific peptide P-30 on beta-galactoside-mediated homotypic aggregation and adhesion to the endothelium of MDA-MB-435 human breast carcinoma cells. *Cancer Research*, *60*, 2584–2588.
73. McEver, R. P. (1997). Selectin-carbohydrate interactions during inflammation and metastasis. *Glycoconjugate Journal*, *14*, 585–591.
74. Cooper, C. R., Bhatia, J. K., Muenchen, H. J., McLean, L., Hayasaka, S., Taylor, J., et al. (2002). The regulation of prostate cancer cell adhesion to human bone marrow endothelial cell monolayers by androgen dihydrotestosterone and cytokines. *Clinical & Experimental Metastasis*, *19*, 25–33.
75. Glinskii, O. V., Turk, J. R., Pienta, K. J., Huxley, V. H., & Glinsky, V. V. (2004). Evidence of porcine and human endothelium activation by cancer-associated carbohydrates expressed on glycoproteins and tumour cells. *Journal of Physiology*, *554*, 89–99.
76. Krause, T., & Turner, G. A. (1999). Are selectins involved in metastasis? *Clinical & Experimental Metastasis*, *17*, 183–192.
77. Khaldoyanidi, S. K., Glinsky, V. V., Sikora, L., Glinskii, A. B., Mossine, V. V., Quinn, T. P., et al. (2003). MDA-MB-435 human breast carcinoma cell homo- and heterotypic adhesion under flow conditions is mediated in part by Thomsen–Friedenreich antigen-galectin-3 interactions. *Journal of Biological Chemistry*, *278*, 4127–4134.
78. Jacobsen, K., Kravitz, J., Kincade, P. W., & Osmond, D. G. (1996). Adhesion receptors on bone marrow stromal cells: *in vivo* expression of vascular cell adhesion molecule-1 by reticular cells and sinusoidal endothelium in normal and gamma-irradiated mice. *Blood*, *87*, 73–82.
79. Pecheur, I., Peyruchaud, O., Serre, C. M., Guglielmi, J., Voland, C., Bourre, F., et al. (2002). Integrin alpha(v)beta3 expression confers on tumor cells a greater propensity to metastasize to bone. *FASEB Journal*, *16*, 1266–1268.
80. Faccio, R., Grano, M., Colucci, S., Zallone, A. Z., Quaranta, V., & Pelletier, A. J. (1998). Activation of alphav beta3 integrin on human osteoclast-like cells stimulates adhesion and migration in response to osteopontin. *Biochemical and Biophysical Research Communications*, *249*, 522–525.
81. Carron, C. P., Meyer, D. M., Engleman, V. W., Rico, J. G., Ruminski, P. G., Ornberg, R. L., et al. (2000). Peptidomimetic antagonists of alphavbeta3 inhibit bone resorption by inhibiting osteoclast bone resorptive activity, not osteoclast adhesion to bone. *Journal of Endocrinology*, *165*, 587–598.
82. Liapis, H., Flath, A., & Kitazawa, S. (1996). Integrin alpha V beta 3 expression by bone-residing breast cancer metastases. *Diagnostic Molecular Pathology*, *5*, 127–135.
83. Chellaiah, M., Kizer, N., Silva, M., Alvarez, U., Kwiatkowski, D., & Hruska, K. A. (2000). Gelsolin deficiency blocks podosome assembly and produces increased bone mass and strength. *Journal of Cell Biology*, *148*, 665–678.
84. Harms, J. F., Welch, D. R., Samant, R. S., Shevde, L. A., Miele, M. E., Babu, G. R., et al. (2003). A small molecule antagonist of the alpha v beta 3 integrin suppresses MDA-MB-435 skeletal metastasis. *Clinical & Experimental Metastasis*, *21*, 119–128.
85. Horton, M. A., Nesbitt, S. A., Bennett, J. H., & Stenbeck, G. (2002). Integrins and other cell surface attachment molecules of bone cells. In J. P. Bilezikian, L. G. Raisz, & G. A. Rodan (Eds.) *Principles of bone biology* (vol. 1 (pp. 265–286). San Diego: Academic.
86. Rodan, G. A. (2003). The development and function of the skeleton and bone metastases. *Cancer*, *97*, 726–732.
87. Kikuchi, T., Matsuguchi, T., Tsuboi, N., Mitani, A., Tanaka, S., Matsuoka, M., et al. (2001). Gene expression of osteoclast differentiation factor is induced by lipopolysaccharide in mouse osteoblasts via Toll-like receptors. *Journal of Immunology*, *166*, 3574–3579.
88. Fritz, E., Jacobs, J., Glant, T., & Roebuck, K. (2005). Chemokine IL-8 induction by particulate wear debris in osteoblasts is mediated by NF-kappaB. *Journal of Orthopaedic Research*, *23*, 1249–1257.
89. Lisignoli, G., Toneguzzi, S., Grassi, F., Piacentini, A., Tschon, M., Cristino, S., et al. (2002). Different chemokines are expressed in human arthritic bone biopsies: IFN-gamma and IL-6 differently modulate IL-8, MCP-1 and rantes production by arthritic osteoblasts. *Cytokine*, *20*, 231–238.
90. Fritz, E., Glant, T., Vermes, C., Jacobs, J., & Roebuck, K. (2005). Chemokine gene activation in human bone marrow-derived osteoblasts following exposure to particulate wear debris. *Journal of Biomedical Materials Research A*, *77*, 192–201.
91. Guise, T. A., Yin, J. J., Taylor, S. D., Kumagai, Y., Dallas, M., Boyce, B. F., et al. (1996). Evidence for a causal role of parathyroid hormone-related protein in the pathogenesis of human breast-cancer-mediated osteolysis. *Journal of Clinical Investigation*, *98*, 1544–1549.
92. Bendre, M., Montague, D. C., Peery, T., Akel, N. S., Gaddy, D., & Suva, L. J. (2003). Interleukin-8 stimulation of osteoclastogenesis and bone resorption is a mechanism for the increased osteolysis of metastatic bone disease. *Bone*, *33*, 28–37.
93. Bendre, M., Gaddy, D., Nicholas, R. W., & Suva, L. J. (2003). Breast cancer metastasis to bone. *Clinical Orthopaedics and Related Research*, *415S*, S39–S45.
94. Bendre, M., Gaddy-Kurten, D., Foote-Mon, T., Akel, N. S., Skinner, R. A., Nicholas, R. W., et al. (2002). Expression of interleukin 8 and not parathyroid hormone-related protein by human breast cancer cells correlates with bone metastasis *in vivo*. *Cancer Research*, *62*, 5571–5579.
95. Henderson, M. A., Danks, J. A., Slavin, J. L., Bryrnes, G. B., Choong, P. F. M., Spillane, J. B., et al. (2006). Parathyroid hormone-related protein localization in breast cancers predict improved prognosis. *Cancer Research*, *66*, 2250–2256.
96. Horowitz, M. C., & Lorenzo, J. A. (2002). *Principles of bone biology*. San Diego: Academic.
97. Graves, D. T., Jiang, Y., & Valente, A. J. (1999). The expression of monocyte chemoattractant protein-1 and other chemokines by osteoblasts. *Frontiers in Bioscience*, *4*, 571–580.
98. Guise, T. A., & Chirgwin, J. M. (2003). Transforming growth factor-beta in osteolytic breast cancer bone metastases. *Clinical Orthopaedics and Related Research*, *4155*, 532–538.
99. Dovio, A., Sartori, M. L., Masera, R. G., Peretti, L., Perotti, L., & Angeli, A. (2004). Effects of physiological concentrations of steriod hormones and interleukin-11 on basal and stimulated production of interleukin-8 by human osteoblast-like cells with different functional profiles. *Clinical and Experimental Rheumatology*, *22*, 79–84.
100. Kundu, N., Yang, Q., Dorsey, R., & Fulton, A. M. (2001). Increased cyclooxygenase-2 (COX-2) expression and activity in a murine model of metastatic breast cancer. *International Journal of Cancer*, *94*, 681–686.
101. Liu, C. H., Chang, S.-H., Narko, K., Trifan, O. C., Wu, M.-T., Smith, E., et al. (2001). Overexpression of cyclooxygenase-2 is sufficient to induce tumorigenesis in transgenic mice. *Journal of Biological Chemistry*, *276*, 18563–18569.
102. Ristimaki, A., Sivula, A., Lundin, J., Lundin, M., Salminen, T., Haglund, C., et al. (2002). Prognostic significance of elevated

cycloozygenase-2 expression in breast cancer. *Cancer Research*, *62*, 632–635.
103. Rozic, J. G., Chakraborty, C., & Lala, P. K. (2001). Cyclo-oxygenase inhibitors retard murine mammary tumor progression by reducing tumor cell migration, invasiveness and angiogenesis. *International Journal of Cancer*, *93*, 497–506.
104. Witters, L. M., Crispino, J., Fraterrigo, T., Green, J., Lipton, A. (2003). Effects of the combination of docetaxel, zoledronic acid, and a COX-2 inhibitor on the growth of human breast cancer cell line. *American Journal of Clinical Oncology*, *26*.
105. Davies, G., Salter, J., Hills, M., Martin, L. A., Sacks, N., & Dowsett, M. (2003). Correlation between cyclooxygenase-2 expression and angiogenesis in human breast cancer. *Clinical Cancer Research*, *9*, 2651–2656.
106. Denkert, C., Winzer, K. J., Muller, B. M., Weichert, W., Pest, S., Kobel, M., et al. (2003). Elevated expression of cyclooxygenase-2 is a negative prognostic factor for disease free survival and overall survival in patients with breast carcinoma. *Cancer*, *97*, 2978–2987.
107. Singh, B., Berry, J. A., Vincent, L. E., & Lucci, A.(2006). Involvement of IL-8 in COX-2-mediated bone metastases from breast cancer. *Journal of Surgical Research*.
108. Benoy, I. H., Salgado, R., Van Dam, P., Geboers, K., Van Marck, E., Scharpe, S., et al. (2004). Increased serum interleukin-8 in patients with early and metastatic breast cancer correlates with early dissemination and survival. *Clinical Cancer Research*, *10*, 7157–7162.
109. Li, X., Pilbeam, C. C., Pan, L., Breyer, R. M., & Raisz, L. G. (2002). Effects of prostaglandin E_2 on gene expression in primary osteoblastic cells from prostaglandin receptor knockout mice. *Bone*, *30*, 567–573.
110. Hiraga, T., Myoui, A., Choi, M. E., Yoshikawa, H., & Yoneda, T. (2006). Stimulation of cyclooxygenase-2 expression by bone-derived transforming growth factor-β enhances bone metastases in breast cancer. *Cancer Research*, *66*, 2067–2073.
111. Westendorf, J. J., Kahler, R. A., & Schroeder, T. M. (2004). Wnt signaling in osteoblasts and bone diseases. *Gene*, *341*, 19–39.
112. Hall, C. L., Bafico, A., Dai, J., Aaronson, S. A., & Keller, E. T. (2005). Prostate cancer cells promote osteoblastic bone metastases through Wnts. *Cancer Research*, *65*, 7554–7560.
113. Manolagas, S. C. (1995). Role of cytokines in bone resorption. *Bone*, *17*, 63S–67S.
114. Morinaga, Y., Fujita, N., Ohishi, K., & Tsurot, T. (1997). Stimulation of interleukin-11 production from osteoclast-like cells by transforming growth factor-beta and tumor cell factors. *International Journal of Cancer*, *71*, 422–428.
115. Zhang, G. J., & Adachi, I. (1999). Serum interleukin-6 levels correlate to tumor progression and prognosis in metastatic breast carcinoma. *Anticancer Research*, *19*, 1427–1432.
116. Yoneda, T., Sasaki, A., & Mundy, G. R. (1994). Osteolytic bone metastasis in breast cancer. *Breast Cancer Research and Treatment*, *32*, 273–284.
117. Sasaki, A., Williams, P., Mundy, G. R., & Yoneda, T. (1994). Osteolysis and tumor growth are enhanced in sites of increased bone turnover *in vivo*. *Journal of Bone and Mineral Research*, *9*, S294.
118. Manolagas, S. C. (1995). Role of cytokines in bone resorption. *Bone*, *17*, 63S–67S.
119. Girasole, G., Passeri, G., Jilka, R. L., & Monolagas, S. C. (1994). Interleukin-11: A new cytokine critical for osteoclast development. *Journal of Clinical Investigation*, *93*, 1516–1524.
120. Manolagas, S. C., Jilka, R. L., Girasole, G., Passeri, G., & Bellido, T. (1994). Estrogens, cytokines, and the pathophysiology of osteoporosis. In P. O. Kohler (Ed.) *Current opinion in endocrinology and diabetes* (pp. 275–281). Philadelphia: Current Science.
121. Hauschka, P. V., Mavrakos, A. E., Iafrati, M. D., Doleman, S. E., & Klagsburn, M. (1986). Growth factors in bone matrix. Isolation of multiple types by affinity chromatography on heparin-Sepharose. *Journal of Biological Chemistry*, *261*, 12665–12674.
122. Pfeilschifter, J., & Mundy, G. R. (1987). Modulation of transforming growth factor beta activity in bone cultures by osteotropic hormones. *Proceedings of the National Academy of Sciences*, *84*, 2024–2028.
123. Kang, Y., Siegel, P. M., Shu, W., Drobnjak, M., Kakonen, S. M., Cordon-Cardo, C., et al. (2003). A multigenic program mediating breast cancer metastasis to bone. *Cancer Research*, *3*, 537–549.
124. Mundy, G. R., DeMartino, S., & Rowe, D. W. (1981). Collagen and collagen fragments are chemotactic for tumor cells. *Journal of Clinical Investigation*, *68*, 1102–1105.
125. Orr, F. W., Varani, J., Gondek, M. D., Ward, P. A., & Mundy, G. R. (1979). Chemotactic response of tumor cells to productions of resorbing bone. *Science*, *203*, 176–179.
126. Zou, Y.-R., Kottmann, A. H., Kuroda, M., Tainwchi, I., & Littman, D. R. (1998). Function of the chemokine receptor CXCR4 in hematopoiesis and in cerebellar development. *Nature*, *393*, 595–599.
127. Nagasawa, T., Hirota, S., Tachibana, K., Takakura, N., Nishikawa, S., Kitamura, Y., et al. (1996). Defects of B-cell lymphopoiesis and bone marrow myelopoiesis in mice lacking the CXC chemokine PBSF/SDF-1. *Nature*, *382*, 635–638.
128. Bluel, C. C., Fuhlbrigge, R. C., Casanovas, J. M., Aiuiti, A., & Springer, T. A. (1996). Highly efficacious lymphocyte chemo-attractant, stromal cell-derived factor 1 (SDF-1). *Journal of Experimental Medicine*, *184*, 1101–1109.
129. D'Apuzzo, M., Rolink, A., Loetscher, M., Hoxie, J. A., Clark-Lewis, I., Melchers, F., et al. (1997). The chemokine SDF-1, stromal cell-derived factor-1, attracts early stage B cell precursors via the chemokine receptor CXCR4. *European Journal of Immunology*, *27*, 1788–1793.
130. Jung, Y., Wang, J., Schneider, A., Sun, Y.-X., Koh-Paige, A. J., Osman, N. I., et al. (2006). Regulation of SDF-1 (CXCL12) production by osteoblasts; a possible mechanism for stem cell homing. *Bone*, *38*, 497–508.
131. Wang, J., Wang, J., Sun, Y.-X., Song, W., Nor, J. E., Wang, C. Y., et al. (2005). Diverse signaling pathways through the SDF-1/CXCR4 chemokine axis in prostate cancer cell lines leads to altered patterns of cytokine secretion and angiogenesis. *Cellular Signalling*, *17*, 1578–1592.
132. Luker, K. E., & Luker, G. D. (2005). Functions of CXCL12 and CXCR4 in breast cancer. *Cancer Letters*.
133. Muller, A., Homey, B., Soto, H., Ge, N., Catron, D., Buchanan, M. E., et al. (2001). Involvement of chemokine receptors in breast cancer metastasis. *Nature*, *410*, 50–56.
134. Sun, Y.-X., Schneider, A., Jung, Y., Wang, J., Dai, J., Wang, J., et al. (2005). Skeletal localization and neutralization of the SDF-1 (CXCL12)/CXCR4 axis blocks prostate cancer metastasis and growth in osseous sites *in vivo*. *Journal of Bone and Mineral Research*, *20*, 318–329.
135. Siclari, V. A., Guise, T. A., & Chirgwin, J. M. (2006). Molecular interactions between breast cancer cells and the bone microenvironment drive skeletal metastases. *Cancer and Metastasis Reviews*, *25*, 621–633.
136. Yoneda, T. (2000). Cellular and molecular basis of preferential metastasis of breast cancer to bone. *Journal of Orthopaedic Science*, *5*, 75–81.
137. Guise, T. A. (2000). Molecular mechanisms of osteolytic bone metastases. *Cancer*, *88*, 2892–2898.
138. Pederson, L., Winding, B., Foged, N. T., Spelsberg, T. C., & Oursler, M. J. (1999). Identification of breast cancer cell line-derived paracrine factors that stimulate osteoclast activity. *Cancer Research*, *59*, 5849–5855.
139. Badache, A., & Hynes, N. E. (2001). Interleukin 6 inhibits proliferation and, in cooperation with an epidermal growth factor

receptor autocrine loop, increases migration of T47D breast cancer cells. *Cancer Research*, *61*, 383–391.
140. Kotake, S., Sato, K., Kim, K. J., Takahashi, N., Udagawa, N., Nakamura, I., et al. (1996). Interleukin-6 and soluble interleukin-6 receptors in the synovial fluids from rheumatoid arthritis patients are responsible for osteoclast-like cell formation. *Journal of Bone and Mineral Research*, *11*, 88–95.
141. Scapini, P., Morini, M., Tecchio, C., Minghelli, S., Di Carlo, E., Tanghetti, E., et al. (2004). CXCL1/macrophage inflammatory protein-2-induced angiogenesis *in vivo* is mediated by neutrophil-derived vascular endothelial growth factor-A. *Journal of Immunology*, *172*, 5034–5040.
142. Goede, V., Brogelli, L., Ziche, M., & Augustin, H. G. (1999). Induction of inflammatory angiogenesis by monocyte chemoattractant protein-1. *International Journal of Cancer*, *82*, 765–770.
143. Fitzgerald, K. A., O'Neill, L. A. J., Gearing, A. J. H., & Callard, R. E. (2001). *The cytokine facts book*. New York: Academic.
144. Kinder, M. , Chislock, E. M., Bussard, K. M., Shuman, L. A., & Mastro, A. M. (2007). Metastatic breast cancer induces an osteoblast inflammatory response. *Experimental Cell Research*, Oct. 4 (in press).
145. Neumark, E., Cohn, M. A., Lukanidin, E., Witz, I. P., & Ben-Baruch, A. (2002). Possible co-regulation of genes associated with enhanced progression of mammary adenocarcinomas. *Immunology Letters*, *82*, 111–121.
146. Neumark, E., Sagi-Assif, O., Shalmon, B., Ben-Baruch, A., & Witz, I. P. (2003). Progression of mouse mammary tumors: MCP-1-TNF-alpha cross regulatory pathway and clonal expression of promalignancy and antimalignancy factors. *International Journal of Cancer*, *106*, 879–886.
147. Ueno, T., Toi, M., Saji, J., Muta, M., Bando, H., Kuroi, K., et al. (2000). Significance of macrophage chemoattractant protein-1 in macrophage recruitment, angiogenesis, and survival in human breast cancer. *Clinical Cancer Research*, *6*, 3282–3289.
148. Mukaida, N., Ketlunsky, S. A., & Matsushima, K. (2003). *The cytokine handbook*. Amsterdam: Academic.
149. Bischoff, D. S., Zhu, J. H., Makhijani, N. S., & Yamaguchi, D. T. (2005). KC chemokine expression by TGF-B in C3H10T1/2 cells induced towards osteoblasts. *Biochemical and Biophysical Research Communications*, *326*, 364–370.
150. Wolfle, U., Muller, V., & Pantel, K. (2006). Disseminated tumor cells in breast cancer: detection, characterization and clinical relevance. *Future Oncology*, *2*, 553–561.
151. Dhurjati, R., Liu, X., Gay, C. V., Mastro, A. M., & Vogler, E. A. (2006). Extended-term culture of bone cells in a compartmentalized bioreactor. *Tissue Engineering*, *12*, 3045–3054.
152. Dhurjati, R., Shuman, L. A., Krishnan, V., Mastro, A. M., Gay, C. V., & Vogler, E. A. (2006). Compartmentalized bioreactor: *In vitro* model for osteobiology and osteopathology. *28th Annual Meeting of the American Society for Bone and Mineral Research*, *21*, 349.
153. Deyama, Y., Takeyama, S., Suzuki, K., Yoshimura, Y., Nishikata, M., & Matsumoto, A. (2001). Inactivation of NF-KB involved in osteoblast development through interleukin-6. *Biochemical and Biophysical Research Communications*, *282*, 1080–1084.
154. Ishimi, Y., Miyaura, C., Jin, C. H., Akatsu, T., Abe, E., Nakamura, Y., et al. (1990). IL-6 is produced by osteoblasts and induces bone resorption. *Journal of Immunology*, *145*, 3297–3303.
155. Bendre, M., Gaddy, D., Nicholas, R. W., & Suva, L. J. (2003). Breast cancer metastasis to bone: It is not all about PTHrP. *Clinical Orthopaedics and Related Research*, *415S*, S39–S45.
156. Girasole, G., Jilka, R. L., Passeri, G., Boswell, S., Boder, G., Williams, D. C., et al. (1992). 17 beta-estradiol inhibits interleukin-6 production by bone marrow-derived stromal cells and osteoblasts *in vitro*: A potential mechanism for the antiosteoporotic effect of estrogens. *Journal of Clinical Investigation*, *89*, 883–891.
157. Linkhart, T. A., Linkhart, S. G., MacCharles, D. C., Long, D. L., & Strong, D. D. (1991). Interleukin-6 messenger RNA expression and interleukin-6 protein secretion in cells isolated from normal human bone. *Journal of Bone and Mineral Research*, *6*, 1285–1294.
158. O'Keefe, R. J., Teot, L. A., Singh, D., Puzas, J. E., Rosier, R. N., & Hicks, D. G. (1997). Osteoclasts constitutively express regulators of bone resorption: An immunohistochemical and in situ hybridization study. *Laboratory Investigation*, *76*, 457–465.
159. Chaudhary, L. R., & Avioli, L. V. (1994). Dexamethasone regulates IL-1 beta and TNF-alpha-induced interleukin-8 production in human bone marrow stromal and osteoblast-like cells. *Calcified Tissue International*, *55*, 16–20.
160. Bendre, M. S., Margulies, A. G., Walser, B., Akel, N. S., Bhattacharrya, S., Skinner, R. A., et al. (2005). Tumor-derived interleukin-8 stimulates osteolysis independent of the receptor activator of nuclear factor-kappaB ligand pathway. *Cancer Research*, *65*, 11001–11009.
161. Rothe, L., Collin-Osdoby, P., Chen, Y., Sunyer, T., Chaudhary, L., Tsay, A., et al. (1998). Human osteoclasts and osteoclast-like cells synthesize and release high basal and inflammatory stimulated levels of the potent chemokine interleukin-8. *Endocrinology*, *139*, 4353–4363.
162. Sozzani, S., Locati, M., Allavena, P., Van Damme, J., & Mantovani, A. (1996). Chemokines: A superfamily of chemotactic cytokines. *International Journal of Clinical & Laboratory Research*, *26*, 69–82.
163. Lipton, A. (2000). Bisphosphonates and breast carcinoma: Present and future. *Cancer*, *88*, 3033–3037.
164. Oslen, N. J., Gu, X., & Kovacs, W. J. (2001). Bone marrow stromal cells mediate androgenic suppression of B lymphocyte development. *Journal of Clinical Investigation*, *108*, 1697–1704.
165. Schultz-Cherry, S., Ribeiro, S., Gentry, L., & Murphy-Ullrich, J. E. (1994). Thrombospondin binds and activates the small and large forms of latent transforming growth factor-beta in a chemically defined system. *Journal of Biological Chemistry*, *269*, 26775–26782.

BMB Departmental Poster Session Abstract: Crossover 2005 Poster

The Interaction of Metastatic Breast Cancer Cells with Osteoblasts

Karen M. Bussard, Laurie A. Shuman, Robyn R. Mercer, Pushkar A. Phadke, Shakira M. Nelson, Jennifer L. Jewell, Elizabeth M. Chislock, Michelle Kinder, Danny R. Welch, Carol V. Gay, and Andrea M. Mastro.

Breast cancer frequently metastasizes to the bone. In a cancer-free environment in the adult, the skeleton continuously undergoes remodeling. Bone-resorbing osteoclasts excavate erosion cavities and bone-depositing osteoblasts synthesize new bone matrix. Usually, there is a precise balance between osteoblasts and osteoclasts with no net bone gain or loss. However, when metastatic breast cancer cells (BC) invade the bone, this balance is disrupted. BC indirectly activate osteoclasts, resulting in osteolytic lesions that cause bone pain and fractures. Current therapies which utilize bisphosphonate drugs to block osteoclast activity are not curative. Osteolytic lesion progression is slowed, but the lesions do not heal. Evidence suggests BC alter osteoblast properties including decreased proliferation, altered adhesion, and loss of differentiation capabilities. To study how BC affect osteoblasts, hFOB1.19 or MC3T3-E1 cells, immature osteoblast lines that can be made to differentiate *in vitro,* were cultured with human (h) BC or their conditioned medium (CM). hFOB1.19 apoptosis was increased in the presence of hBC. MC3T3-E1 alkaline phosphatase (ALP) activity and mineralization were blocked and mRNA expression for bone sialoprotein (BSP) and osteocalcin (OCN) were not expressed. Treatment of BC CM with a neutralizing agent to transforming growth factor β (TGFβ) restored mRNA expression of ALP, BSP, and OCN. hBC CM also altered osteoblast morphology and adhesion. Restoration to actin stress fiber and focal adhesion plaque formation occurred when platelet derived growth factor, insulin-like growth factor, and TGFβ were neutralized in the hBC CM. *In vivo* kinetic studies indicate that hBC quickly migrate to and spread in the bone diaphysis and cause a decrease in osteoblast and osteoclast number. MC3T3-E1 osteoblasts also undergo an inflammatory stress response and produce cytokines which may be chemoattractants for hBC. Our studies indicate that osteoblasts as well as osteoclasts are responsible for bone loss and are appropriate therapeutic targets.

AACR Abstract 2006
Applicant: Karen M. Bussard

Kinetics of metastatic breast cancer cell trafficking in bone

Breast cancer has a high propensity for bone colonization. When present in the bone microenvironment, metastatic breast cancer cells induce osteolysis by increasing bone resorbing osteoclast activity and decreasing bone depositing osteoblast activity. Most *in-vivo* studies have focused on the later stages of bone metastasis, where breast cancer cells characteristically colonize the ends of long bones in humans. While this localization is of significant clinical importance, little is understood about early bone metastastic events including cell arrival, localization, and initial cancer cell colonization, which may be of importance in therapeutic intervention.

MDA-MB-435 human breast cancer cells engineered to contain green fluorescent protein were injected into the left ventricle of female athymic mice, thereby minimizing first-pass filtration through pulmonary capillaries and allowing a maximal number of cells to reach the bone. Mice were then euthanized at times from 1 hr to 6 wks, and femurs isolated and analyzed by fluorescent microscopy, immunohistochemistry, real-time polymerase chain reaction, flow cytometry, and histomorphometry.

As early as 1 hr post-injection, single tumor cells could be detected throughout the bone, with the majority (~90%) found in the distal metaphyses as opposed to the diaphysis. Tumor cells remained in a single cell state in bone ends for up to 72 hrs indicating a lack of tumor cell proliferation. Solitary cells in the diaphysis were rarely detected beyond 24 hrs. Numerous foci (2-10 cells) were observed at 1 wk, and by 2 wks, fewer but larger foci (≥50 cells) were seen. By 4 wks, most bones had a single large mass (either originating from a single colony or coalescing foci) which extended into the diaphysis by 4-6 wks. While little change (<20%) was seen in osteoblast or osteoclast number at 2 wks, by 4-6 wks, the number of osteoblasts was drastically reduced (to 8% of control), with osteoclast numbers being modestly reduced (to ~60% of control). These data confirm previous *in-vitro* evidence that suggest breast cancer cells induce osteoblast apoptosis and impede osteoblast replacement.

This is the first *in vivo* study to describe the kinetics of breast cancer cells at the earliest time after arrival in the femur (a common site of metastatic breast cancer cell colonization). It also supports *in vivo* our recent *in vitro* studies that indicated osteoblasts, in the presence of breast cancer cells, undergo increased apoptosis and are prevented from differentiating. Since skeletal structural integrity is integral to survival and quality of life, comprehensive treatment of bone metastases must restore bone matrix deposition as well as limit osteolysis.

Supported by the U.S. Army Medical Research and Materiel Command (DAMD-17-02-1-0541, DAMD-17-03-01-0584, and DAMD-17-02-1-0358), the University of Alabama Breast SPORE (P50-CA89019), and the National Foundation for Cancer Research and the PA Dept. of Health (CA87728).

Authors: Karen M. Bussard, Pushkar A. Phadke, Robyn R. Mercer, John F. Harms, Yijiang Jia, John C. Kappes, Andra R. Frost, Jennifer L. Jewell, Shakira Nelson, Cynthia Moore, Carol V. Gay, Danny R. Welch, and Andrea M. Mastro, The University of Alabama at Birmingham, Birmingham, AL and The Pennsylvania State University, University Park, PA

Title: A Classic Set of Osteoblast-Derived Inflammatory Cytokines is Produced in Response to Bone Metastatic Breast Cancer

Authors: Karen M. Bussard[1*], Elizabeth M. Chislock[1*], Michelle Kinder[1*], Carol V. Gay[1], and Andrea M. Mastro[1]. *Authors contributed equally to this work, [1]The Pennsylvania State University, University Park, PA

Breast cancer frequently metastasizes to bone and disrupts the balance between bone resorbing osteoclasts and bone depositing osteoblasts. During metastatic breast cancer cells invasion, osteoclasts are indirectly activated to degrade bone and osteoblasts cease to deposit new bone. Current therapies which utilize bisphosphonates to block osteoclast function are not curative. While osteolytic lesion progression is slowed, the lesions do not heal. Presently, the mechanism by which this disease occurs is unclear.

We previously reported that osteoblasts no longer produce non-collagenous bone matrix proteins. The focus of this project was to determine how osteoblast-derived cytokine production was altered in response to metastatic breast cancer cells or their conditioned medium (CM).

Alterations in osteoblast-derived cytokine production were examined using Raybio® species-specific cytokine arrays and quantified with standard ELISAs. Preliminary in–vitro experiments utilized hFOB 1.19 human fetal osteoblasts. Subsequent experiments were performed using MC3T3-E1 murine osteoblasts incubated with breast cancer cell CM. In addition, femurs from untreated or cancer bearing female athymic mice inoculated by intracardiac injection with MDA-MB-231 human metastatic breast cancer cells were assayed at various times for the presence of inflammatory cytokines. Murine femurs were harvested, minced, and incubated for 24 hours in culture medium.

Incubation of osteoblast cell lines with metastatic breast cancer CM led to enhanced expression of osteoblast inflammatory stress molecules KC, IL-6, MIP-2, and MCP-1. Cultures of metaphyses of long bones cleared of bone marrow from untreated mice expressed cytokines different from those in the diaphysis (predominantly KC, MIP-2, and MCP-1). Cultures of femurs from cancer bearing animals showed elevated levels of these inflammatory cytokines.

These results suggest metastatic breast cancer cells induce osteoblasts to undergo a stress response and produce inflammatory cytokines. Additionally, cytokines were specifically produced by cells of the bone and not marrow stromal cells. From these results, we believe osteoblast-derived factors are as integral, if not more important, than breast cancer-derived factors in modifying the metastatic environment. Furthermore, inflammatory cytokines produced by osteoblasts may attract and activate osteoclasts, thereby supporting a favorable bone microenvironment for metastatic breast cancer cells. By identifying alterations in osteoblast-derived cytokines specific to the presence of metastatic breast cancer cells, it may be possible to block or disrupt these factors through the use of targeted drugs.

Supported by Sigma Xi, The Pennsylvania State University President's Fund for Research, National Foundation for Cancer Research Center for Metastasis Research, and U.S. Army Medical Research and Materiel Command W81XWH-06-1-0363.

Osteoblast-Derived Inflammatory Cytokines are Produced in Response to Human Metastatic Breast Cancer Cells

Breast cancer frequently metastasizes to bone. Although the precise mechanism underlying this preferential metastasis is unknown, bone likely provides a hospitable environment that attracts breast cancer cells and allows them to colonize and grow. Metastatic breast cancer cells induce osteoclast bone resorption, halt osteoblast bone deposition, and profoundly alter osteoblast properties. Current models suggest that chemokines and cytokines produced by breast cancer cells are key to understanding breast cancer metastasis. While cancer-derived cytokines may play an important role, we have evidence that *osteoblasts* can be directed by metastatic breast cancer cells to produce inflammatory cytokines that may be chemoattractants for both osteoclasts and cancer cells, as well as growth or maintenance factors for the cancer cells.

MC3T3-E1 murine osteoblasts (OB) were grown to different stages of differentiation (growth: 4 days, early differentiation: 10 days, and late differentiation: 20 days) and were treated for 24 hours with conditioned media (CM) from human metastatic breast cancer (BC) MDA-MB-231 cell variants (parental MDA-MB-231W, parental MDA-MB-231PY, bone-seeking MDA-MB-231BO, or brain-seeking MDA-MB-231BR). OB media was replaced with BC CM at 0, 10, 25, or 50%. Twenty-four hrs later, the culture media was collected and subjected to RayBio® mouse cytokine arrays and species-specific ELISAs to quantify OB-derived cytokines produced in response to human BC cells.

A RayBio® cytokine antibody array showed that BC CM treatment increased OB-derived inflammatory cytokine secretion. The increase in IL-6 levels was particularly notable. As quantitated by ELISAs, OB-derived IL-6 at day 4 doubled from control values when OBs were treated with MDA-MB-231BR CM. For days 10 and 20, OB-derived IL-6 was increased at least 10 fold over control values. Noteworthy increases in OB-derived IL-6 included greater than 80 fold increases from control values with the addition of 50% MDA-MB-231BR CM on day 10 and 50% MDA-MB-231PY CM on day 20. In summary, OB-derived IL-6 production increased in a dose-dependent manner with the addition of all types of BC CM at all points. Maximum induction of OB-derived IL-6 secretion occurred in more differentiated cells.

Literature suggests that IL-6 has numerous functions that could contribute to BC cell metastases to bone. These functions include effects on OBs, osteoclasts (OC), and BC cells. This study implicates OBs as an important source of IL-6 in the vicious cycle of BC bone metastasis. Comprehensive treatment of bone metastases must consider OBs, OCs, and BC cells in order to restore bone matrix deposition and limit osteolysis.

Supported by the U.S. Army Medical Research and Materiel Command (W81XWH-06-1-0363, W81XWH-06-1-0432), Susan G. Komen Breast Cancer Foundation (BCTR0601044), and National Foundation for Cancer Research, Center for Metastasis Research.

Authors: Karen M. Bussard and Andrea M. Mastro, The Pennsylvania State University, University Park, PA

Osteoblasts Naturally Produce Cytokines that Influence the Tumor Microenvironment in Bone Metastastic Breast Cancer, Karen M. Bussard* and Andrea M. Mastro, The Pennsylvania State University, University Park, PA, 16802

Breast cancer has a high propensity for bone colonization and specifically metastasizes to the ends of long bones in humans. Although the precise mechanism underlying preferential metastasis is unknown, it is likely that the bone (femur metaphyses) provides a hospitable environment that both attracts breast cancer cells and allows them to colonize and grow.

Bone remodeling begins when bone resorbing osteoclasts excavate an erosion cavity in the matrix. Next, bone depositing osteoblasts migrate to the cavity and synthesize layers of osteoid matrix that form new bone. Bone metastatic breast cancer cells disrupt the balance between osteoblasts and osteoclasts. Metastatic breast cancer cells induce osteoclast bone resorption, halt osteoblast deposition, and profoundly alter osteoblast properties. Current models implicate chemokines and cytokines produced by breast cancer cells as keys to understanding breast cancer cell metastasis. While cancer-derived cytokines undoubtedlyportant role, we have evidence that *osteoblasts* can be directed by metastatic breast cancer cells to produce inflammatory cytokines that may be chemoattractants, growth, or maintenance factors for the cancer cells as well as for osteoclasts.

We hypothesize that *osteoblast*-derived cytokines are increased in the presence of metastatic breast cancer cells and act as chemoattractants, growth, and maintenance factors for them. To further investigate these phenomanae, the current study was carried out **1) to determine how *osteoblast*-derived inflammatory cytokine production by MC3T3-E1 osteoblasts is altered in response to conditioned medium of bone metastatic MDA-MB-231 breast cancer cell variants.** The cytokine response of MC3T3-E1 murine osteoblasts to human metastatic breast cancer conditioned medium was examined using Raybio® murine cytokine arrays and quantified with either murine ELISAs or Bio-rad Bio-plex™ murine cytokine assays. Osteoblasts were cultured *in-vitro* for 4 (growth), 10 (early differentiation), and 20 days (late differentiation) and treated with either 0, 10, 25, or 50% conditioned media from human non-metastatic cells (hTERT-HME1 or MDA-MB-231BRMS) or human metastatic breast cancer MDA-MB-231 cell variants (parental MDA-231W, parental MDA-231PY, bone-seeking MDA-231BO, or brain-seeking MDA-231BR). Twenty-four hours later, culture supernatants were collected and quantified.

Cultured MC3T3-E1 osteoblasts increased production of IL-6, MCP-1, and VEGF in the presence of metastatic breast cancer cell conditioned media as determined by a Raybio® murine cytokine screen. An increase in murine KC was detected using a Bio-rad Bio-plex™ murine cytokine assay. KC, MCP-1, and IL-6 were secreted in a dose-response manner with increasing conditioned medium treatment. The largest induction of osteoblast-derived cytokine production occurred in 20 day old osteoblasts (late differentiation). Treatment with the conditioned medium of a MDA-231 bone-seeking variant further enhanced osteoblast cytokine secretion at day 20. Furthermore, osteoblast-derived MCP-1 expression varied dramatically with conditioned media treatment. MCP-1 expression was not detected in osteoblasts treated with conditioned media from non-metastatic human mammary epithelial cells, but was significantly

increased in osteoblasts treated with metastatic breast cancer conditioned media. Collectively, these results suggest that osteoblasts undergo an inflammatory response in the presence of metastatic breast cancer cell conditioned medium.

In addition, we sought **2) to determine how bone-derived inflammatory cytokine production is altered in response to breast cancer cells *in vivo*.** Femurs from either control or mice inoculated via intracardiac injection with metastatic breast cancer cells were assayed *ex vivo* for breast cancer cell trafficking patterns and inflammatory cytokine production using quantitative PCR and species-specific antibody arrays respectively. The metaphyses (ends) of femurs cleared of bone marrow expressed a different pattern of cytokines than the diaphysis (shaft). In particular, it was found that metaphyses of bone in normal mice cleared of bone marrow produced substantial amounts of KC, MIP-2, and MCP-1. In mice inoculated with MDA-MB-231W human metastatic breast cancer cells, the breast cancer cells preferentially trafficked to the metaphyses of the bone as opposed to the diaphysis, where concentrations of MCP-1, IL-6, MIP-2, and KC increased significantly from control values as determined by standard ELISAs and Bio-rad Bio-plex™ murine cytokine assays. Taken together, these results suggest that metastatic cancer cells are attracted to cytokines naturally secreted by osteoblasts that are concentrated in the ends of the femur.

In summary, we propose that metastatic breast cancer cells are attracted to cytokines naturally produced by osteoblasts. Once in the bone microenvironment, metastatic breast cancer cells induce osteoblasts to undergo a stress response, increasing osteoblast production of these chemotactic inflammatory cytokines.

Supported by the U.S. Army Medical Research and Materiel Command (W81XWH-06-1-0363, W81XWH-06-1-0432), Susan G. Komen Breast Cancer Foundation (BCTR0601044), and National Foundation for Cancer Research, Center for Metastasis Research.

AACR 2008 Abstract
Author: Karen Bussard

Osteoblast-Derived Cytokines are Major Mediators in Facilitating in Bone Metastatic Breast Cancer

Breast cancer (BC), with its predilection for bone metastases, is the second leading cause of cancer deaths in American women. While the mechanism for directional metastasis is unknown, the bone microenvironment likely provides a fertile soil for metastatic BC cells. Besides affecting osteoblast (OB) and osteoclast (OC) properties, we have evidence that metastatic BC cells further create a unique bone niche by co-opting *osteoblasts* to increase production of inflammatory cytokines that may be chemoattractants, growth, or maintenance factors for cancer cells or OCs.

MC3T3-E1 murine OBs were grown to various stages of maturity: 4 (growth), 10 (early differentiation), and 20 days (late differentiation) and incubated with conditioned medium (CM) from human metastatic BC MDA-MB-231 cell variants (parental MDA-231W, parental MDA-231PY, bone-seeking MDA-231BO, or brain-seeking MDA-231BR). Culture supernatants were assayed for cytokine expression with species-specific Bio-Rad Bio-Plex™ cytokine arrays. Also, femurs from mice inoculated via intracardic injection with MDA-231-GFP BC cells were assayed *ex vivo* for cytokine production.

MC3T3-E1 murine OBs treated with human metastatic BC CM produced increased amounts of murine IL-6, VEGF, MIP-2 (human IL-8), KC (human GRO-α), and MCP-1 with the largest induction seen in 20 day old OBs. The human metastatic BC cell variants themselves produced a similar array of cytokines: IL-6, VEGF, IL-8, and GRO-α. However, the human metastatic BC cell variants produced only very small amounts of MCP-1. Monocyte chemoattractant protein-1 (MCP-1) is associated with angiogenesis and increased cancer cell survival. MCP-1 also regulates bone resorption by stimulating the migration of monocyte-osteoclast progenitor cells to the bone.

These same cytokines were detected *ex vivo* in femurs of mice bearing human metastatic bone metastases. It is known that MDA-231 BC cells preferentially traffic to the metaphyseal ends of long bones. We found that metaphyses of femurs cleared of bone marrow expressed cytokines different from those in the diaphysis. Furthermore, concentrations of IL-6, VEGF, KC, MIP-2, and MCP-1 increased significantly in cancer-bearing mice compared to non-cancer-bearing mice.

Overall, these data suggest that OBs are an important source of cytokines, specifically MCP-1, in BC bone metastasis. The nature of this cytokine panel suggests their importance for the attraction and activation of OCs leading to increased bone resorption in bone metastatic BC. Thus, these findings clearly implicate the bone microenvironment and cancer cell manipulation thereof in facilitating metastatic tumor cell colonization and survival.

Supported by the U.S. Army Medical Research and Materiel Command (W81XWH-06-1-0363, W81XWH-06-1-0432), Susan G. Komen Breast Cancer Foundation (BCTR0601044), and National Foundation for Cancer Research, Center for Metastasis Research.

Authors: Karen M. Bussard and Andrea M. Mastro, The Pennsylvania State University, University Park, PA

Era of Hope 2008 Abstract
Author: Karen Bussard

The Role of Osteoblast-Derived Cytokines in Bone Metastatic Breast Cancer

Breast cancer is the second leading cause of cancer deaths among American women. In late stages of the disease, breast cancer preferentially metastasizes to the bone. While the mechanism for directional metastasis is unknown, the bone microenvironment likely provides a fertile soil for metastatic breast cancer cells. In addition to affecting osteoblast and osteoclast properties, we have evidence that metastatic breast cancer cells create a unique bone microenvironment by co-opting *osteoblasts* to increase their production of inflammatory cytokines. These cytokines may be chemoattractants, growth, or maintenance factors for cancer cells as well as osteoclasts.

MC3T3-E1 murine osteoblasts were grown to 4 (growth), 10 (early differentiation), and 20 days (late differentiation), and incubated with cells or conditioned medium from human metastatic BC MDA-MB-231 variants (parental MDA-231W, parental MDA-231PY, bone-seeking MDA-231BO, or brain-seeking MDA-231BR). Culture supernatants were assayed for cytokine expression with species-specific Bio-Rad Bio-Plex™ cytokine arrays. In addition, femurs from mice inoculated via intracardic injection with MDA-231-GFP (parental), MDA-231-PY-GFP (parental), MDA-231-BO-GFP (bone-seeking), or MDA-231-BRMS-GFP (metastasis suppressed) cells or control were assayed *ex vivo* for cancer cell migration and cytokine production.

MC3T3-E1 murine osteoblasts treated with human metastatic breast cancer conditioned medium produced increased amounts of murine IL-6, VEGF, MIP-2, KC, and MCP-1 with the largest induction seen in 20 day osteoblasts treated with bone-seeking conditioned medium. The human metastatic breast cancer cells themselves produced a similar array of cytokines: IL-6, VEGF, IL-8, and GRO-α with one exception, they produced only small quantities of MCP-1, an important cytokine in angiogenesis, cancer cell survival, and monocyte-osteoclast progenitor cell migration to bone. Indirect transwell co-cultures led to similar results.

The same cytokines were detected *ex vivo* in femurs of mice bearing human metastatic bone metastases. The metaphyseal ends of long bones, an area of preferential breast cancer cell trafficking, expressed cytokines different from those of the diaphysis. We found that concentrations of IL-6, VEGF, KC, MIP-2, and MCP-1 increased significantly in cancer-bearing mice compared to non-cancer-bearing mice.

Overall, these data suggest that osteoblasts are an important source of cytokines, specifically MCP-1, in breast cancer bone metastasis. These cytokines are known to attract and activate osteoclasts leading to increased bone resorption in bone metastatic breast cancer. Thus, these findings clearly implicate the bone microenvironment and cancer cell manipulation thereof in facilitating metastatic tumor cell colonization and survival.

Supported by the U.S. Army Medical Research and Materiel Command (W81XWH-06-1-0363, W81XWH-06-1-0432), Susan G. Komen Breast Cancer Foundation (BCTR0601044), and National Foundation for Cancer Research, Center for Metastasis Research.

Authors: Karen M. Bussard and Andrea M. Mastro, The Pennsylvania State University, University Park, PA

KAREN M. BUSSARD, M.S., Ph.D.
CRTA Post-Doctoral Fellow
5377 Partners Court
Frederick, MD 21703
Work: (301) 451-3765

EDUCATION

The Pennsylvania State University, University Park, PA
Ph.D. in Pathobiology 2004-2008
Ph.D. G.P.A. 3.95
Ph.D. thesis entitled "The Role of Osteoblast-Derived Inflammatory Cytokines in Bone Metastatic Breast Cancer"

The Pennsylvania State University, Hershey, PA
M.S. in Biomedical Engineering 2000-2002
Master's thesis entitled "Interactions of Model Biomaterials and Enzymes in Contact Activation of the Blood Plasma Coagulation Cascade"

Fairleigh Dickinson University, Madison, NJ
B.S. in Biology / minor in Chemistry 1995-1999
Honor's thesis entitled "Sports Injuries: How They Occur, Methods of Treatment, and Ways of Prevention"

WORK EXPERIENCE

Cancer Research Training Award Post-Doctoral Fellow 2008-present
The Mammary Biology and Tumorigenesis Laboratory, Center for Cancer Research, National Cancer Institute, The National Institutes of Health
Advisor: Gilbert H. Smith, Ph.D., Chief, Section for Mammary Stem Cell Biology
• Investigate the influence of the mammary gland microenvironment on the reprogramming of cancer cells.
• Perform microdissections, cell and fragment implantation into the mammary glands of athymic nude mice.
• Develop and perform protocols and analysis.
• Supervise, educate, and orient assistants in performance of protocols.

Graduate Research Assistant 8/2004-9/2008
The Pennsylvania State University, University Park, Pennsylvania
Advisor: Andrea M. Mastro, Ph.D., Professor of Microbiology and Cell Biology
• Investigate the influence of osteoblast-dervied inflammatory cytokines on metastatic breast cancer cells.
• Perform intracardiac inoculations on athymic nude mice.
• Study and quantify the trafficking of breast cancer cells throughout long bones.
• Develop and perform protocols and analysis.
• Supervise, educate, and orient students in performance of protocols.

Research Support Associate/Graduate Research Assistant 8/2000 – 8/2004
The Pennsylvania State University, College of Medicine, Hershey, Pennsylvania
Advisor: Christopher A. Siedlecki, Ph.D,. Assistant Professor of Surgery and Bioengineering
• Study adhesion of blood coagulation factors to biomaterials with Atomic Force Microscope.
• Investigate the clotting mechanisms of human plasma in response to biomaterials.
• Analyze bovine blood of Left Ventricular Assist Device and Total Artificial Heart recipient research calves with the Thromboelastograph Hemostasis Analyzer (TEG).
• Develop and perform protocols and analysis.
• Supervise, educate, and orient assistant in performance of protocols.

Laboratory Technician II 10/1999 – 8/2000
University of Maryland Medical System, Baltimore, Maryland
• Blood Bank Technician assisting Medical Technologists in their work.
• Issue and perform ABO checks on blood products, receive, record, and sort blood specimens.
• Assist physicians in clinical decision making on product administration.
• Irradiate and thaw blood products.
• Cancer Center Platelet Laboratory Technician assisting physicians in clinical decision making of product administration and providing patients with platelets.

Laboratory Technician 10/1997 – 5/1999
Severn Trent Laboratories, Whippany, New Jersey
• Inorganics Laboratory Technician testing samples for Biochemical Oxygen Demand (BOD), Phenol distillation and reading, Alkalinity, Toxicity Characteristic Leaching Procedure (TCLP), ZHE tumbling and leaching, Total Suspended Solids (TSS), Total Dissolved Solids (TDS), Total Solids (TS), Reactivity, Cyanide, Specific Gravity, and Ignitability.
• Made reagents necessary for and calibrated instruments used for each test.

PROFESSIONAL MEMBERSHIPS

2002-2003	Society for Biomaterials
2003	American Society for Artificial Internal Organs
2005-present	Sigma Xi, The Scientific Research Society
2005-present	American Association for Cancer Research
2005-present	Women in Cancer Research (WICR)

PUBLICATIONS

2001 Siedlecki, CA, **Bussard, KM**, Vogler, EA. "FXII interactions with biomaterial surfaces." American Society for Artificial Internal Organs Journal. 47: (2), 170.

2005 Zhuo, R, Miller, R, **Bussard, KM**, Siedlecki, CA, Vogler, EA. "Procoagulant Stimulus Processing by the Intrinsic Pathway of Blood Plasma Coagulation." Biomaterials. 26: (16), 2965.

2005 Guo, Z, **Bussard, KM**, Chatterjee, K, Miller, R, Vogler, EA, Siedlecki, CA. "Mathematical Modeling of Material- Induced Blood Plasma Coagulation." Biomaterials. 27: (5), 796.

2006 Phadke, PA, Mercer, RR, Harms JF, Jia, Y, Kappes, JC, Frost, AR, Jewell, JL, **Bussard, KM,** Nelson, S, Moore, C, Gay, CV, Mastro, AM, Welch, DR. "Kinetics of Metastatic Breast Cancer Cell Trafficking in Bone." Clinical Cancer Research. 12: (5) 1431.

2008 Kinder, M, Chislock, EM, **Bussard, KM**, Shuman, LA, Mastro, AM. Metastatic Breast Cancer Induces an Osteoblast Inflammatory Response. Experimental Cell Research. 314: (1), 173.

2008 **Bussard, KM**, Gay, CV, Mastro, AM. The Microenvironment in Metastasis: What is Special About Bone? Cancer Metastasis Reviews. 27: (1), 41.

2009 **Bussard, KM**, Okita, N, Sharkey, N, Neuberger, T, Webb, A, Mastro, AM. IL-6, MCP-1, and VEGF are Localized the in Bone Microenvironment of Metastatic Breast Cancer-Bearing Mice. Submitted to Cancer Cell.

2009 **Bussard, KM**, Mastro, AM. Osteoblast-derived Cytokines Facilitate Bone Metastatic Breast Cancer. (working title) Manuscript in preparation.

ORAL PRESENTATIONS

2008 **Bussard, KM**, Mastro, AM. "Osteoblast-Derived Cytokines are Major Mediators in Facilitating Bone Metastatic Breast Cancer." Presented at the American Association for Cancer Research Annual Meeting's Tumor Biology Minisymposium, April 12-16, 2008.

2006 **Bussard, KM,** Phadke, PA, Mercer, RR, Harms JF, Jia, Y, Kappes, JC, Frost, AR, Jewell, JL, Nelson, S, Moore, C, Gay, CV, Mastro, AM, Welch, DR. "Kinetics of Metastatic Breast Cancer Cell Trafficking in Bone." Presented at the American Association for Cancer Research Annual Meeting's Tumor Biology Minisymposium, April 1-5, 2006.

POSTER PRESENTATIONS

2002 **Bussard, KM**, Vogler, EA, Siedlecki, CA. "Effective Production of FXIIa and Thrombin by Model Biomaterials." Proceedings of the IEEE 28th Annual Northeast Bioengineering Conference, 02CH37342, April 20-21, 2002

2002 **Bussard, KM**, Vogler, EA, Siedlecki, CA. "Effective Enzyme Production of FXIIa and Thrombin by Model Biomaterials." Transactions of the 28th Annual Society for Biomaterials Conference, Volume XXV, April 24-27, 2002.

2003 **Bussard, KM**, Trivedi, SH, Vogler, EA, Siedlecki, CA. "Surface Acceleration of Blood Plasma Coagulation." Transactions of the 29th Annual Society for Biomaterials Conference, Volume XXVI, April 30-May 3, 2003.

2003 **Bussard, KM**, Zapanta, CM, Rosenberg, G, Pae, WE, Siedlecki, CA. "Thromboelastograph Evaluation of Bovine Blood." American Society for Artificial Internal Organs Journal 49: (2) 222. Presented at the Annual ASAIO-ISAO Joint Conference, June 19-21, 2003.

2005 **Bussard, KM,** Shuman, LS, Mercer, RR, Phadke, PA, Nelson, SM, Jewell, JL, Chislock, EM, Kinder, M, Welch, DR, Gay, CV, Mastro, AM. "The Interaction of Metastatic Breast Cancer Cells with Osteoblasts." Presented at the CrossOver 2005 Meeting sponsored by The Huck Institutes of The Life Sciences and The Materials Research Institute, The Pennsylvania State University, October 13-14, 2005.

2006 **Bussard, KM,** Chislock, EM, Kinder, M, Gay, CV, Mastro, AM. "A Classic Set of Osteoblast-Derived Inflammatory Cytokines is Produced in Response to Bone Metastatic Breast Cancer." The 11 th International Congress of the Metastasis Research Society, Tokushima, Japan, September 3-6, 2006.

2007 **Bussard, KM**, Mastro, AM. "Osteoblast-derived Inflammatory Cytokines are Produced in Response to Human Metastatic Breast Cancer Cells." The 100th Annual American Association for Cancer Research Annual Meeting, Los Angeles, CA, April 14-18, 2007. Proceedings of the 97th Annual Meeting for American Association for Cancer Research, Volume 48.

2007 **Bussard, KM**, Mastro, AM. "Osteoblasts Naturally Produce Cytokines that Influence the Tumor Microenvironment in Bone Metastatic Breast Cancer." Skeletal Complications of Malignancy V, The Paget Foundation. October 25-27, 2007.

2008 **Bussard, KM**, Mastro, AM. "The Role of Osteoblast-Derived Cytokines in Bone Metastatic Breast Cancer." Era of Hope Meeting, Baltimore, MD, June 25-28, 2008.

AWARDS AND HONORS

- American Association for Cancer Research – Scholar-In-Training Award: 2008
- The Pennsylvania State University College of Agricultural Sciences Travel Award: 2008.
- American Association for Cancer Research – Edward A. Smuckler "Pathobiology of Cancer" Workshop selected attendee. Snowmass, CO: July 15-22, 2007.
- American Association for Cancer Research – Women in Cancer Research Brigid G. Leventhal Scholar Award in Cancer Research: 2006.
- Department of Defense Predoctoral Traineeship Award in Breast Cancer (Fellowship): 2006-2009.
- The Pennsylvania Space Grant Consortium NASA Space Grant Fellowship: 2005-2007, 2007-2009.
- Sigma Xi Grants-in-Aid of Research: 2005-2006.
- Chancellor's List Publication: Inaugural Edition (2005), 2006.
- Honorable Mention for Student Travel and Professional Development Award, Society for Biomaterials: 2002.
- FDU Outstanding Academic Excellence Award in Biology: May 1999.
- FDU James A. Griffo Award for Academic Excellence and Athletic Achievement during college career: May 1999.
- FDU University Honors Program: 1995-1999 (Senior thesis entitled "Sports Injuries: How they occur, Methods of Treatment, and Ways of Prevention" presented April 30, 1999).
- FDU Presidential Scholar (Full Academic Tuition Scholarship): 1995-1999.
- Who's Who of Students in American Colleges and Universities Publication: 1995-1999.
- The National Dean's List Publication: 1995-1999.